Canada

DRYING PAPER BY IMPINGING JETS OF SUPERHEATED STEAM:
DRYING RATES AND THERMODYNAMIC CYCLES

by

Jean-François Bond

A Thesis submitted to the Faculty of Graduate Studies
and Research in partial fulfillment of the
requirements for the degree of
Doctor of Philosophy

Department of Chemical Engineering
McGill University
Montréal   October 1991

Canada

1. For science there is no longer any money; the observatory has gone to complete rack and ruin. 2. The astronomy professor begs the government for funds, but in vain. 3. In uttermost desperation he resolves to take up astrology.

4. As astrologer he casts horoscopes for war profiteers. 5. His prophesies are soon in much demand; he makes lots of money. 6. Now the professor has the funds to renovate himself and the observatory; the newest and best instruments are procured.

ABSTRACT

Drying of paper by impinging jets of superheated steam was studied in an apparatus which closely simulates conditions for a potential industrial impingement dryer.

Drying was found to consist in a constant rate period, followed by a falling rate period where the drying rate decreases linearly with moisture content. The relation found between the constant rate and Reynolds number and temperature of the jet is consistent with a previous correlation for air impingement heat transfer, suitably modified for conditions in a steam environment. For a given mass flux, steam drying is slower than air drying below an *inversion temperature* of 175 ^{o}C and faster above. The specific blower power for steam drying is much lower than for air drying at temperatures in the industrial range.

Equilibrium moisture content measurements showed that complete drying can be obtained at steam temperatures only slightly above the boiling point. Expressions for the critical moisture content in impingement drying in steam and in air were obtained. In steam drying, the falling rate period was found to be determined more by internal transport resistance than by adsorption of water on the fibers.

A new arrangement for drying paper, in which the first half of the drying is done by a conventional dryer to which steam is supplied from a steam impingement dryer handling the second half, was analyzed. In regions with low electricity cost, recirculation of steam around the impingement dryer circuit by a mechanical fan is much more economical than by a thermocompressor. However, this advantage is only marginal where electricity cost is high. The overall performance is optimized by using the highest temperature and lowest jet velocity possible. The drying cycle proposed is a realistic and attractive means to increase drying capacity and reduce energy consumption.

i

RESUME

Le séchage du papier par jets de vapeur surchauffée a fait l'objet d'une étude expérimentale dans un appareil simulant les conditions d'un sécheur à vapeur industriel potentiel.

Le séchage du papier comporte une période à taux constant, suivie d'une période à taux décroissant, pendant laquelle le taux de séchage décroît linéairement avec la teneur en eau. La relation entre le taux de séchage constant et le nombre de Reynolds et la température du jet est conforme à une corrélation développée précédemment décrivant le transfert de chaleur par jets d'air, adaptée pour les conditions d'une atmosphère de vapeur. Pour un débit massique donné, le séchage par vapeur est moins rapide que le séchage par l'air sous la *température d'inversion*, qui est de 175 °C, et plus rapide au dessus de celle-ci. Aux températures d'usage industriel, la puissance de ventilation spécifique est beaucoup moins élevée pour la vapeur que pour l'air.

Des mesures de teneur en eau à l'équilibre ont démontré qu'on peut obtenir un séchage complet par la vapeur à une température à peine supérieure au point d'ébullition. On a obtenu des expressions décrivant la teneur en eau critique pour le séchage par jets de vapeur et d'air. Pour le séchage par vapeur, les caractéristiques du séchage à taux décroissant dépendent plus de la résistance interne au transport de chaleur et de masse, que de l'adsorption de l'eau sur les fibres.

On propose un nouveau procédé pour le séchage du papier, dans lequel la première portion du séchage est faite dans un sécheur conventionnel et la seconde dans un sécheur à jets de vapeur surchauffée, la vapeur requise pour la première portion étant fournie par la seconde. Dans les régions où le coût de l'électricité est peu élevé, il est beaucoup plus économique d'utiliser un ventilateur mécanique qu'un thermocompresseur pour la recirculation de la vapeur. Cependant, cet avantage est marginal là où le coût de l'électricité est élevé. Le rendement du procédé est optimisé en utilisant une température aussi élevée, et une vitesse de jet aussi basse, que possible. Le procédé proposé est une méthode réaliste et efficace d'augmenter la capacité de production et de réduire la consommation énergétique.

ii

ACKNOWLEDGEMENTS

TABLE OF CONTENTS

LIST OF FIGURES

LIST OF TABLES

NOMENCLATURE

A	Surface area, m^2; A_i impingement surface area; A_s paper sheet area; A_t venturi throat area
B	Basis weight of dry paper, g/m^2; B_h blowing parameter, equation 1.10
b	A constant
Bi	Biot number; Bi_h heat transfer, Bi_m mass transfer Biot number
C_d	Nozzle discharge coefficient
C_p	Specific heat capacity, kJ/kg-K; C_{pa}, C_{pf}, C_{ps}, C_{pw} C_{py} dry air, dry fiber, steam, water and moist air heat capacities
C_v	Venturi flow coefficient
D	Nozzle or orifice diameter, m; D_f fiber diameter; D_p pore diameter
D	Moisture diffusivity, m^2/s
E_a	Activation energy, cal/gmole
E_e	Total equivalent energy consumption, kg steam/kg water evaporated;
E_t	Total energy consumption, kJ/kg water evaporated
F	Overall geometrical heat transfer factor, equation 1.1
f	Open area ratio: area ratio of jet nozzle to impingement surface
H	Nozzle-to-web spacing, m
h	Convective heat transfer coefficient, W/m^2-K; $h^{\bullet}$, heat transfer coefficient in the absence of mass transfer; specific enthalpy, kJ/kg
Δh_a	Heat of adsorption of water on fibers, kJ/kg

Δh_v	Latent heat of vaporization of water, kJ/kg
J	Water removal rate, kg/h; J_c, conventional dryer; J_i, impingement dryer; J_t, total
K	Geometrical heat transfer factor, equation 1.2
k	Thermal conductivity, W/m-K; k_a, k_f, k_p, k_s, k_w dry air, dry fiber, moist paper, steam and water thermal conductivities
k_g	Mass transfer coefficient, kg/m^2-s
M	Molecular weight, kg/kgmole
M_c	Mass flow rate of steam to the conventional dryer, kg/h
M_{con1}	Mass flow rate of condensate to first desuperheater, kg/h
M_{con2}	Mass flow rate of condensate to second desuperheater, kg/h
M_e	Mass flow rate of exhaust steam from the impingement dryer, kg/h
M_j	Mass flow rate of steam to the impingement dryer, kg/h
M_{Te}	Mass flow rate of thermocompressor exhaust steam, kg/h
M_{Ti}	Mass flow rate of induced steam to thermocompressor, kg/h
M_{Tm}	Mass flow rate of motive steam to thermocompressor, kg/h
m	Slope of the R - X curve, equation 2.8, kg/m^2-h; mole fraction, mole of component/mole of mixture
N	Mass flux, kg/m^2-h
n	Property ratio exponent
Nu	Nusselt number
P	Absolute pressure, kPa; P_c, conventional dryer operating pressure; P_j, impinging jet stagnation pressure; P_{sat}, saturation pressure; P_t, thermocompressor motive steam pressure; P_v, vapor pressure
ΔP	Pressure drop, kPa

P_b Blower power, W/m^2

Pr   Prandtl number

Q   Heat flow, kJ/h; Q_i heat transfer in impingement dryer

R   Drying rate, $kg/h\text{-}m^2$; R_c, constant drying rate; R_{con}, condensation rate; R_{ev}, evaporation rate; R_f, falling drying rate; $\bar{R}_i$ average impingement drying rate

$\mathbb{R}$ Gas constant, J/gmole-K

r   Capillary radius, m

Re   Reynolds number; Re_j, impinging jet Reynolds number

Sc   Schmidt number

Sh   Sherwood number

T   Temperature, ^oK unless otherwise indicated; T_a, air; $T_{a.s}$, adiabatic saturation; T_{inv}, inversion; T_j, jet; T_o, base; T_s, surface; T_{sat} saturation, $T_{w.b.}$, wet bulb temperatures; T_b, boiling point at atmospheric pressure

ΔT Temperature driving force, K

t   Time, s

t_p Paper sheet thickness, μm

u   Velocity, m/s

W   Work, kJ/h; W_c, compressor work; W_F, fan work; sheet weight, g; W_n, width of slot nozzle, m; W_d dry sheet weight

w   Specific work, kJ/kg water; w_c compressor work; w_F fan work

X   Paper moisture content, kg/kg dry fiber; X_b, X_i, X_f, X_c, X_{eq}, X_o, breakout, initial, final, critical, equilibrium and saturation moisture contents; X_{ii} initial moisture content for impingement drying; X_{ic} initial moisture content for impingement drying in the constant rate period; X_{if} initial

	moisture content for impingement drying in the falling rate period
x	Distance from the impingement surface, m
x	Steam quality
Y	Air humidity, kg/kg dry air; Y_i, Y_o at the inlet and exit of the sheet respectively; Y_s at saturation
ΔY	Humidity driving force, kg/kg dry air

Greek letters

α	Thermal diffusivity, m^2/s; Chance's cross-flow interference factor, equation 1.11
γ	Ratio of specific heats, C_p/C_v
ε	Work-to-heat value ratio, equation 5.1; porosity
η	Isentropic efficiency
κ	Dryer steam consumption index, mass ratio of steam consumed per unit water evaporated
μ	Dynamic viscosity, Pa-s
ν	Kinematic viscosity, m^2/s
ρ	Density, kg/m^3; ρ_a, air density; ρ_b, bulk density; ρ_f, fiber density
σ	Standard deviation
ϕ	Vapor pressure ratio, equation 4.1

Subscripts and superscripts

a	Air

a.s.	Adiabatic saturation
atm	Atmospheric
b	Boiler
c	Compressor
con	Condensate
c.p.	Constant property
d	Dry
e	Dryer exhaust
est	Estimated
F	Fan
f	Saturated liquid state; film conditions; fiber
g	Saturated vapor state
I	Impingement
J	Jet conditions
l	Limiting
m	Water vapor-air mixture
n.c.	Natural convection
s	Superheater
sat	Saturated state
Te	Thermocompressor exhaust stream
Ti	Thermocompressor induced stream
Tm	Thermocompressor motive stream
t	Target value; throttling valve
v	Vapor
v.c.	Vena contracta
w	Water, wet
w.b.	Wet bulb

1   Desuperheater #1

2   Desuperheater #2

1/3   1/3 rule reference conditions, equations 1.8 and 1.9

∞   Free stream conditions

CHAPTER 1

INTRODUCTION

1.1 OLD AND NEW TECHNOLOGIES FOR DRYING PAPER

Papermaking consists in forming an aqueous pulp of wood fibers into a sheet, pressing this sheet to approximately 150 % moisture per dry fiber weight, then drying to 7 - 8% moisture. The North American production of 88 million tonnes of paper per year (Lockwood-Post, 1990) requires the removal of about 125 million tons of water in the dryer section.

Generally (table 1.1), current industrial practice is to dry paper

DRYER TYPE	APPLICATION					
	Pulp	Tissue	Paper	Board	Coating	TOTAL
Dryer cylinder		15	95	95	35	82.3
Impingement	70		2	2	50	7.6
Yankee		70				4.2
Infrared			3	3	15	2.8
Through dryer		15				0.9
Flash	15					1.1
Vacuum	15					1.1
TOTAL	100	100	100	100	100	100

Table 1.1 - Dryer distribution in the U. S. pulp and paper industry, percent (adapted from McConnell, 1980).

by passing the sheet over a series of cylinders heated internally by steam, in an atmosphere of air, shown schematically in figure 1.1:
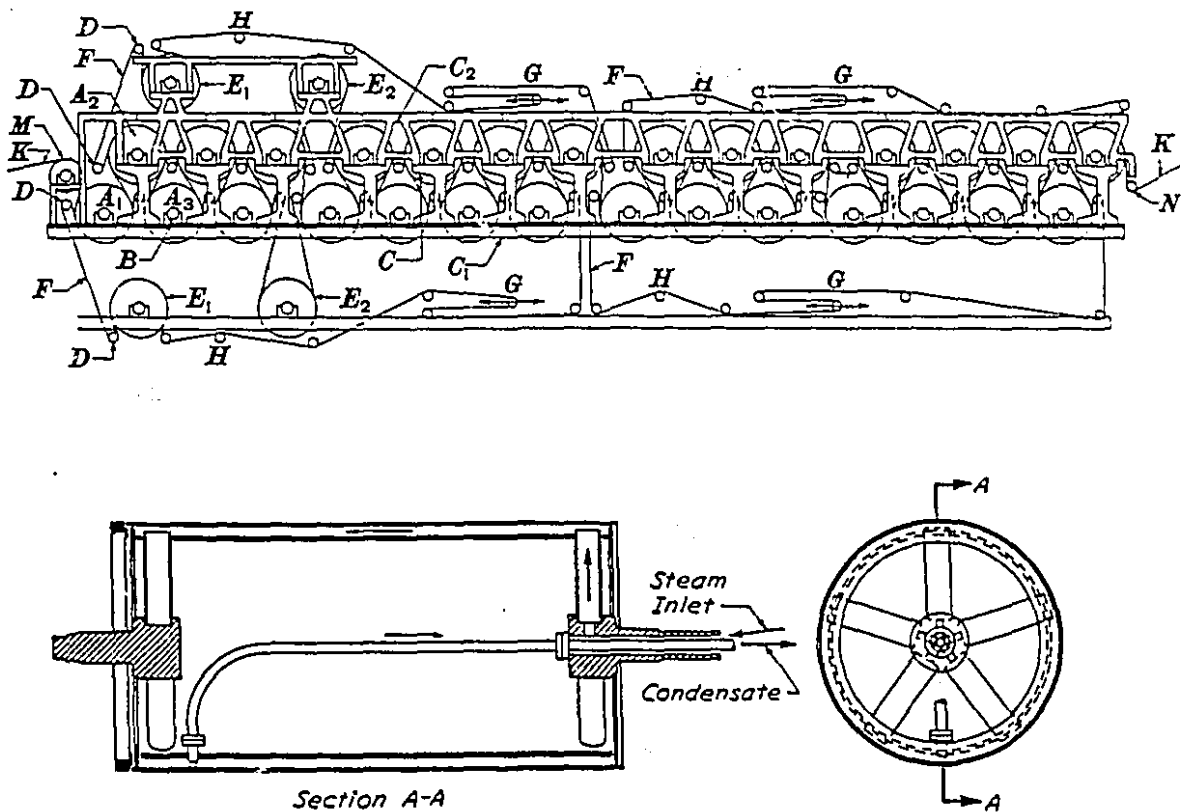
Figure 1.1 - Conventional dryer section and dryer cylinder.

The conventional drum dryer, characterized by a low drying rate (average value: 15 kg/m^2-h) and high energy consumption (average value: 1.5 kg steam used / kg water evaporated, Sayegh et al., 1986), is not of the standard of modern engineering performance. The fact that, in many mills, production capacity is dryer-limited, and the annual energy consumption of 65 million barrels of oil for paper drying in North America, highlight the need for more efficient drying techniques.

In the early 1970's, research at the Pulp and Paper Research Institute of Canada on a novel process combining the action of impinging air jets and suction across the permeable sheet (Burgess et al., 1972a,

2

1972b), figure 1.2, demonstrated the feasibility of an average drying
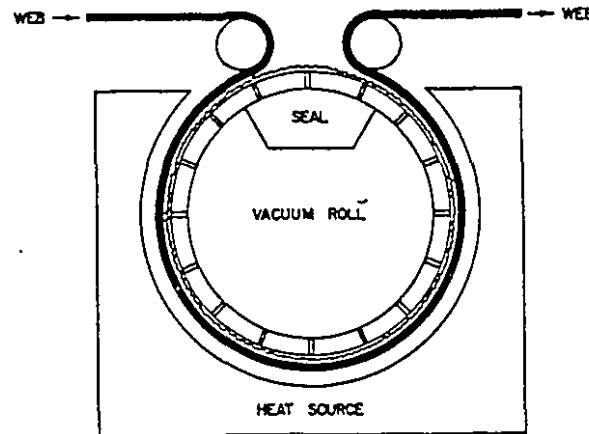
Figure 1.2 - Schematic view of PAPRIDRYER.

rate of 150 kg/m^2-h, over ten times conventional dryer performance. Unfortunately, since drying in this *Papridryer* takes place in an air atmosphere, energy consumption is not lower than that of the conventional dryer, as it is not possible to efficiently recover the heat content of the exhaust stream in either case. As the higher drying rate of the Papridryer was not sufficient alone to convince papermakers to abandon proven technology, its development was dropped.

More recently, the Institute of Paper Chemistry (Sprague, 1985) developed a process whereby drying occurs by passing the sheet in a high pressure nip underneath a roll heated to very high temperature. Very high water removal rates are achieved in this so-called *impulse dryer*, shown schematically in figure 1.3. Initial tests on a static press at IPC, confirmed by experimentation on a dynamic apparatus at the Pulp & Paper Research Institute of Canada (Poirier and Sparkes, 1991), revealed an energy efficiency (rate of water removal × enthalpy of evaporation / heat flux) greater than one, indicating water removal in the liquid
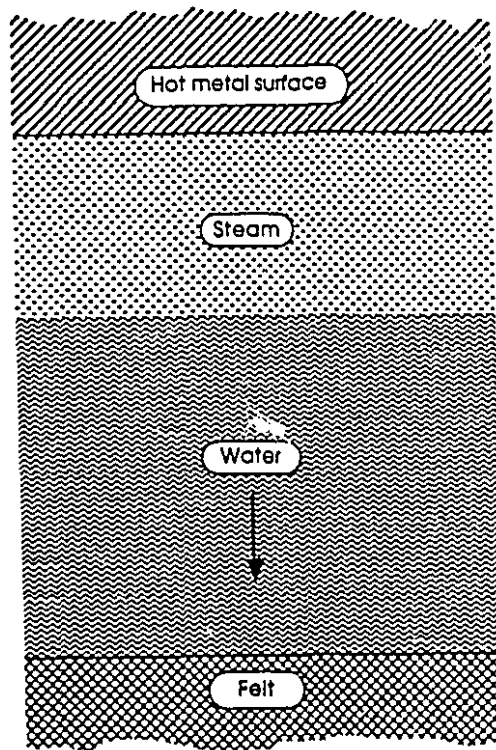
Figure 1.3 - Schematic view of impulse drying process

state. It was postulated that a steam film formed at the web / roll interface pushes moisture through the wet fiber matrix. Important problems, however, remain with impulse drying: a tendency towards sheet delamination, the difficulty of supplying the high heat fluxes required, and the inability to dry paper completely. Despite its attractive energy efficiency, the impulse dryer is a technique of limited scope and with numerous problems to be resolved prior to becoming an industrial technology.

Since the early 1980's, researchers in the Chemical Engineering Department of McGill University have been investigating the drying of paper under impinging jets of superheated steam. This technique shows great promise, on the three following fronts:

a) DRYING RATE. Compared to conduction drying, very high heat

4

transfer rates can be reached by impinging jets, and because of the better transport properties of steam at high temperature, higher heat transfer coefficients are possible in steam than in air. Drying rates over an order of magnitude higher than those of conventional dryers can be obtained, potentially leading to important capital costs savings and large increases in production capacity;

b) ENERGY EFFICIENCY. Since, in superheated steam drying, the outlet stream consists of steam alone, its heat content can be completely recovered and the net energy expenditure for drying can be reduced to zero in principle. Furthermore, as a superheated steam drying process is simultaneously a steam generation process, capital costs of steam production in the paper mill may be reduced;

c) PAPER PROPERTIES. The higher sheet temperature and oxygen-free environment of steam drying produce stronger paper. The preliminary tests of Cui *et al.* (1985) and David (1987), followed by Poirier's (1991) extensive study, show important strength improvements for superheated steam dried paper, compared to conventionally dried, establishing the potential of superheated steam drying as a technique for enhancing paper properties.

1.2 OUTLINE OF THE THESIS

The goal of this thesis is to characterize the drying of paper under impinging jets of superheated steam by measuring the drying rate in conditions of industrial relevance and by analyzing specific cycles for implementing superheated steam drying in the paper mill. It is hoped that the present thesis will serve as the necessary step between the conceptual design studies which have been the focus of most of the

earlier work, and pilot plant scale trials which must precede the implementation of superheated steam drying of paper on an industrial scale.

A brief literature review completes this introductory chapter. The apparatus for simulating conditions in a hypothetical industrial dryer, and the experimental procedures, are described in chapter two. Chapter three presents the results for constant drying rate under impinging jets of superheated steam and of air, comparing and contrasting the drying performance of the two fluids. Characteristics of the falling rate period, and measurements of the equilibrium moisture content of paper in superheated steam, are given in chapter four. In chapter five, two combined superheated steam impingement – conventional drying cycles are proposed and are shown to be superior to a previously suggested cycle with energy recovery by means of an open-cycle heat pump. The findings of the study are summarized, and recommendations for future work are presented, in chapter 6.

1.3   LITERATURE REVIEW

1.3.1 Studies on Superheated Steam Drying of Paper

The use of superheated steam for drying bulk materials was introduced at the beginning of this century (Hausbrand, 1908) and has found limited but very successful application in drying such diverse materials as coal, lumber, hog fuel and wood pulp.

Dungler (1952) has patented a dryer in which steam jets impinge on both sides of a sheet of fibrous material, through a permeable fabric. However, he seems not to have realized the potential of this process for energy recovery, as he proposed that the water evaporated in the dryer

6

simply be vented to the ambient atmosphere. The proposed dryer did not result in an industrial application.

All the known research on using superheated steam to dry paper has been done at McGill University. Cui and Mujumdar (1984) presented a model for a combined impingement-conduction dryer using superheated steam as the drying medium, essentially a Yankee dryer running on superheated steam. The model predicted a net energy consumption of 700 kJ/kg water evaporated and a typical drying rate of 260 kg/m^2-h for a well-designed dryer with recycling of the exhaust steam by thermocompression, compared to 6000 kJ/kg water evaporated and 200 kg/m^2-h drying rates for Yankee dryers.

The first measurement of the rate of drying paper in superheated steam was made by Cui *et al.* (*op. cit.*). They made preliminary measurements of the constant drying rate in a laboratory-scale steam impingement dryer in the following ranges of conditions:

steam temperature: 190 – 230 °C

jet velocity: 50 – 100 m/s

jet pressure: 100 – 200 kPa abs.

Drying rate was found to increase nearly linearly with these parameters. The sheet temperature was measured to be that of saturated steam at the jet pressure.

Loo and Mujumdar (1984) made a first attempt at modeling superheated steam drying of paper with impingement and flow through, using Crotogino and Allenger's (1979) approach of linearly combining the impingement and through drying contributions. The impingement part was

treated by equating the heat flux with the energy required for evaporating the water, using the heat transfer correlations of Saad (1980) and Das (1982) for slot jets and Chance (1974) for round jets, and taking into account the heat of adsorption determined experimentally by Prahl (1968). In the absence of experimental data, the through drying side was treated by assuming that the exhausted steam was saturated. The latter assumption appears to be invalidated by the finding of O. Polat (1989) of unsaturated exit air in through drying of paper. Thus Loo & Mujumdar's prediction must be considered to be of qualitative importance only.

Beeby and Potter (1986) recently reviewed superheated steam drying, with primary focus on bulk solids drying applications. The direct contact superheated steam drying process consists in a heat-up period, a constant-rate drying period and a falling rate period. Each of these was contrasted to its equivalent for air or for conduction drying. Important differences are the condensation on the solid surface during the heat-up period and the elevated surface temperature during the constant-rate period.

1.3.2 Heat and Mass Transfer Under Impinging Jets

1.3.2.1 Effect of geometry

In their critical review of design correlations for heat and mass transfer under impinging jets, Obot *et al.* (1980) noted that the heat transfer coefficient is sensitive to the nozzle shape (ASME-contoured nozzle vs. sharp-edged orifice), length-to-diameter ratio and extent of confinement, and recommended using the average exit plane velocity and the nozzle diameter to define the Reynolds number. Reduced correlations,

8

computed in this manner from the studies of Gardon and Cobonpue (1963), Allander (1961), Hilgeroth (1965), Glaser (1962), Krötzsch (1968) and Martin (1977) agreed within ± 15 %. Martin's correlation was recommended for arrays of circular orifices:

$$\frac{Nu}{Pr^{0.42}} = \frac{h\,D}{k\,Pr^{0.42}} = K\,(H/D,f)\,\sqrt{f}\;\frac{1\;-\;2.2\;\sqrt{f}}{1\;+\;0.2\;(H/D\;-\;6)\;\sqrt{f}}\;Re^{2/3}$$

$$= F\,(H/D,\;f)\,Re^{2/3} \tag{1.1}$$

where the geometrical dependence factor is

$$K\,(H/D,f) = \left[\,1\;+\;\left[\frac{H/D}{0.6\,/\sqrt{f}}\right]^{6}\,\right]^{-0.05} \tag{1.2}$$

The correlation is deemed to be valid in the Reynolds number range $2 \times 10^{3} \le Re \le 10^{5}$, with Re defined as

$$Re = \frac{\overline{u}_{j}\,d_{v.c.}}{\nu_{f}} \tag{1.3}$$

where $\overline{u}_{j}$ is the mean velocity at the jet exit plane, $d_{v.c.}$ the vena contracta diameter, and ν_{f} the kinematic viscosity at the film temperature $T_{f} = (T_{j} + T_{b})\,/\,2$.

1.3.2.2 Effect of variable fluid properties

In the present study, absolute temperature varies between the

nozzle exit and the sheet surface by a ratio as high as two; over this range, thermal conductivity and viscosity vary by approximately the same ratio (cf. appendix 4). Clearly, conditions used to define the physical properties are very important.

Kays and Crawford (1980) restate the long established practice that the heat transfer rate in a variable property flow can be obtained from the constant property solution either by evaluating all properties in the non-dimensional groups (Nu, Re, Pr) at a *reference temperature*, with a value intermediate between the surface and the free stream, or by multiplying the Nusselt number obtained with all properties evaluated at the free stream temperature by a *property ratio*. For gases, since properties vary as a power of the absolute temperature, the property ratio is simply the temperature ratio raised to a characteristic power; for laminar flow at a two-dimensional stagnation point, Kays and Crawford obtained

$$\frac{Nu}{Nu_{c.p.}} = \left[\frac{T_{\infty}}{T_s} \right]^n \qquad (1.4)$$

where n = -0.10 for the fluid cooling the surface, -0.07 for the fluid heating the surface.

The recommendation of Martin (*op. cit.*) to evaluate physical properties at the film temperature is not based on a critical evaluation of this aspect as the data with which it was obtained were for low ΔT, of the order of a few tens of degrees only.

Das *et al.* (1985) correlated their measurements of heat transfer from a hot turbulent air jet to a cool surface under large temperature

differences by the property ratio expression:

$$Nu_j = a \, Re_j^{\;b} \, (H/W_n)^c \, (T_j/T_s)^d \, Pr_j^{\;1/3} \qquad (1.5)$$

where a is a geometrical heat transfer factor, $b \cong 0.55$, $c \cong -0.08$, $d \cong -0.11$. They pointed out the necessity to be quite explicit as to the basis used. To avoid any ambiguity, temperature dependence of the heat transfer coefficient $h \equiv q \, / \, (T_j - T_s)$ can be formulated explicitly as

$$h = \frac{k_j \, Nu_j}{W_n} = \frac{k_j}{W_n} \, a \, Re_j^{\;b} \left[\frac{H}{W_n}\right]^c \left[\frac{T_j}{T_s}\right]^d Pr_j^{\;1/3} \qquad (1.6)$$

$$= \frac{k_j}{W_n} \, a \left[\frac{\bar{u}_j \, W_n}{\nu_j}\right]^b \left[\frac{H}{W_n}\right]^c \left[\frac{T_j}{T_s}\right]^d Pr_j^{\;1/3} \qquad (1.7)$$

Since the temperature sensitivity of thermal conductivity and viscosity is much higher for steam than air, the above equation may not properly describe the effect of temperature-dependent fluid properties in superheated steam drying.

The only studies on the influence of the temperature dependence of fluid properties in superheated steam heat transfer are due to Chow and Chung (1983a, 1983b). For evaporation of water into a laminar flat plate boundary layer of steam or air, they obtained a numerical solution of the similarity equations of the boundary layer. For air in the temperature range $150 \, ^\circ C \leq T_\infty \leq 500 \, ^\circ C$ and for steam in the temperature range $150 \, ^\circ C \leq T_\infty \leq 300 \, ^\circ C$, the evaporation rates from the solution,

taking into account the variation in fluid properties, agreed very well with those from the solution taking constant fluid properties evaluated at the 1/3 rule reference conditions:

$$T_{1/3} \equiv T_s + 1/3 \ (\ T_\infty - T_s \ ) \qquad (1.8)$$

$$m_{a,1/3} \equiv m_{a,a.s.} + 1/3 \ (\ m_{a,\infty} - m_{a,a.s.}) \qquad (1.9)$$

the latter equation applying to air only. However, for steam above 300 ^{o}C, the agreement was unsatisfactory.

Haji and Chow (1988) measured evaporation rate into a turbulent stream of superheated steam at up to 200 ^{o}C over a flat plate, and found good agreement with an expression derived from an empirical Nusselt number correlation for such boundary layer flow, with all thermophysical properties evaluated at the 1/3 reference temperature. However, such treatment may not be valid for the turbulent jet heat transfer at the very high temperature differences of the present study, as a flat plate boundary layer is very much thicker than that of a turbulent jet.

1.3.2.3 Effect of transpiration

Unidirectional mass transfer away from a solid surface reduces convective heat transfer rate to that surface by increasing the boundary layer thickness and reducing the temperature gradient. Numerous authors (Chow and Chung, *op. cit.*, Kast, 1982) suggest that the heat transfer rate be corrected by a factor derived analytically for Couette flow:

$$\frac{h}{h^\bullet} = \frac{\ln(1 + B_h)}{B_h} \qquad (1.10)$$

where $h^\bullet$ is the heat transfer coefficient in the absence of mass transfer, and the blowing parameter $B_h \equiv \bar{C}_{ps}(T_\infty - T_s) / \Delta h_v$.

1.3.2.4 Effect of cross-flow interference

Chance (*op. cit.*) studied the effect of cross-flow interference by constraining the flow to exit through only one side of a square enclosure between an impingement surface and a nozzle array, monitoring the decrease in the local heat transfer coefficient in the direction of cross-flow due to mixing between the fresh impinging gas and the spent exhaust gas. The reduction of local heat transfer coefficient was described by a *cross-flow interference factor*:

$$\alpha = 1.0 - 0.236 \frac{f \, L_i}{D} \qquad (1.11)$$

where f is the open area ratio, D the nozzle diameter and L_i the distance from the closed edge of the array (i.e. the starting point for cross-flow) to the position, denoted by index i, at which the heat transfer rate is measured. Nusselt number decreases linearly with distance from the starting point for cross-flow. The cross-flow interference factor is usually very close to one for well-designed impinging jet arrays.

13

1.3.3 Comparison of Steam and Air as Drying Fluids

Early experimental studies (Wenzel & White, 1951, Chu *et al.*, 1953) established the existence, for equal mass flux of the drying fluid, of an *inversion temperature* below which steam drying is slower than air drying, and faster above. However, only recently was the reason for an inversion temperature clarified, and its value measured under a variety of conditions.

Chow and Chung (1983a) solved numerically the equations governing evaporation of water into a laminar boundary layer of steam, air or steam-air mixtures over a completely wet flat plate. An inversion temperature of about 250 ^{o}C was found. The existence of the inversion temperature was explained by the interplay between higher heat transfer coefficients for steam drying and the wet surface temperature depression in air drying. At low drying fluid temperature, the heat transfer driving potential is higher in air because the evaporating surface is at the wet bulb temperature, whereas in steam it is at the boiling point. With the drying fluid at high temperature, the difference in driving potential is less significant and the more favorable transport properties of steam (higher Prandtl number and conductivity) become dominant.

Chow and Chung (1983b) later extended their study to a turbulent boundary layer and predicted an inversion temperature of 190 ^{o}C, which agreed fairly well with the value of 175 ^{o}C found experimentally by Yoshida and Hyodo (1970) .

Theoretical studies of flow over a stretching surface (Al-Taleb *et al.*, 1987) and co-current liquid and gas flow (Hasan *et al.*, 1986), as well as the alumina drying experiments of Ramamurthy (1991) have come to

14

similar conclusions.

Faber et al. (1986) compared water removal rates from porous alumina particles by steam and air in a laboratory-scale fluidized bed dryer, in the temperature range 100 °C $\leq$ T $\leq$ 250 °C. In fluidized bed drying, the drying medium leaves in thermal equilibrium with the bed. Hence water removal rate does not depend on the transport properties, but only on the heat content of the inlet stream. On this basis, an inversion temperature is predicted by the equation:

$$C_{pa} (T_{inv} - T_{w.b.}) = C_{ps} (T_{inv} - T_b) \qquad (1.12)$$

where T_{inv}, $T_{w.b.}$ and T_b are the inversion, wet bulb and boiling point temperatures, respectively, and C_{pa} and C_{ps} are the specific heat at constant pressure of air and steam, respectively. Solving this equation gives T_{inv} = 160 °C, in excellent agreement with the data.

Shibata (1990) found that the drying of a sphere of coarse sintered glass beads in superheated steam consists in a constant rate period, followed by a nearly linear falling rate period. The onset of the falling rate period is signaled by the appearance of dry spots on the surface of the sphere. For the very low intensity drying conditions studied ($R_c \cong 1$ kg/m^2-h), the critical moisture content increases mildly with constant drying rate, both in steam and air. For equal constant drying rate, the critical moisture content is higher in air than in superheated steam. The drying rate decrease during the falling rate period is successfully modeled by taking into account the heat transfer resistance of a dry layer between the surface of the sphere and the receding evaporation front.

15

1.3.4 Kinetics of Paper Drying

The question of what happens within a paper sheet during drying was investigated experimentally by Lee and Hinds. They obtained temperature and moisture concentration profiles across a six-ply sheet of kraft paper drying over a hot plate (temperature 105 °C) with its surface exposed to dry air at 45 °C, conditions simulating the environment of a drum dryer. Drying was characterized by a short heat-up period, followed by a constant rate drying period and finally, a falling rate period. Drying proceeded at a constant rate so long as liquid diffusion due to a capillary pressure gradient sufficed to keep the bottom of the sheet wet. Past this point, a layer of dry fibers formed in the immediate vicinity of the hot surface and the drying rate fell as a result of the increasing heat transfer resistance of this dry layer.

Clearly, the different boundary conditions of contact and impingement drying lead to sharply contrasting transport behavior. For drying of capillary-porous bodies, with initial and boundary conditions similar to those encountered in impingement drying, Suzuki *et al.* (1977), Endo *et al.* (1977), and Shishido *et al.* (1985) found that the evolution of the local moisture content profile is governed by the diffusion equation within the body:

$$\frac{\partial X}{\partial t} = \frac{\partial}{\partial x} \left[D \frac{\partial X}{\partial x} \right] \qquad (1.13)$$

where D is the moisture diffusivity in paper, subject to the boundary conditions of moisture flux at the exposed surface equal to the drying rate and zero flux at the bottom of the sheet:

16

$$D \frac{\partial X}{\partial x} = R \qquad @ \ x = 0$$

$$\text{(1.14)}$$

$$\frac{\partial X}{\partial x} = 0 \qquad @ \ x = t_p$$

Drying occurs at a constant rate, determined by conditions in the external boundary layer, as long as the surface moisture content is higher than zero. When this point is reached ($X = 0$ @ $x = 0$), the evaporation front recedes from the impingement surface and the drying rate falls.

Keey (1978) remarks that this receding plane model provides a simple, yet physically realistic picture of the way porous solids dry, and reports that while some authors have considered critical moisture content to be a constant property of the material, their original data show clearly that it actually depends on the drying conditions. Transport phenomena theory indicates that critical moisture content cannot be simply a material property. For moisture diffusivity independent of temperature and moisture content, Suzuki *et al.* obtained an approximate solution to the diffusion equation by assuming a parabolic moisture profile. The critical moisture content was found to be

$$X_c = \frac{1}{3} \frac{R_c \ t_p}{\rho_b \ D} \qquad \text{for } N \le 2 \quad \text{(1.15)}$$
$$\text{(low intensity)}$$

$$X_c = \left[1 - \frac{2}{3 \ N} \right] X_o \qquad \text{for } N > 2 \quad \text{(1.16)}$$
$$\text{(high intensity)}$$

where

$$N \equiv \frac{R_c \, t_p}{\rho_b \, X_o \, D} \qquad (1.17)$$

called the *drying intensity*, is the ratio of internal moisture to external vapor transport resistances. In the above equation, X_o, the *saturation moisture content*, i. e. the moisture content when all pores are completely filled with water, can be taken, for paper, to be related to the porosity by:

$$X_o = \frac{\varepsilon \, \rho_w}{(1 - \varepsilon) \, \rho_f} \qquad (1.18)$$

Suzuki *et al.* further showed that the critical moisture content expressions, equations 1.15 and 1.16, agree very well with the values determined numerically from the exact solution of the partial differential equation, within their respective range of applicability.

The diffusivity of moisture in paper is expected to depend on moisture content and temperature. For slow diffusion in kraft paper in the very low moisture content range, $0 \le X \le 0.07$, in the temperature range $20 \le T \le 85$ °C, Lin (1990, 1991) obtained the following expression from Ast's (1966) data:

$$D = D_o \exp (0.5 \, X) \exp \left\{ \frac{E_a}{R} \left[\frac{1}{T_o} - \frac{1}{T} \right] \right\} \qquad (1.19)$$

where $\quad D_o$ = 2.616 × 10^{-6} cm^2/s $\qquad$ (base diffusivity)

$\qquad\qquad E_a$ = 16 050 cal/gmole $\qquad$ (activation energy)

$\qquad\qquad T_o$ = 298 °K $\qquad$ (base temperature).

As the time scale in Lin's work is many days, and the moisture content very low, it is uncertain whether this diffusivity expression is valid for the very fast drying studied here, especially when one considers that Luikov's (1978) research indicates a wide variety of patterns of behavior for the moisture diffusivity of capillary-porous bodies.

For variable diffusivity, the diffusion equation becomes non-linear and an analytical solution is not possible. Comparison of an approximate solution (based on a parabolic moisture profile) with the numerical solution for a moisture diffusivity depending exponentially on moisture content led Suzuki *et al.* to suggest that the drying intensity N_o, based on the dry material diffusivity, is suitable to describe slow drying of a material with a variable moisture diffusivity. In this case, the critical moisture content is given by

$$X_c = \frac{1}{3} \frac{R_c t_p}{\rho_b D_o} \qquad (1.20)$$

1.3.5 Superheated Steam Drying Cycles

While practically all studies of superheated steam drying note its potential for very low energy consumption, few have proposed how to implement steam drying for energy recovery. Luthi (1981) has proposed a cycle in which most of the latent heat of the exhausted steam is recovered by means of an open-cycle heat pump. An embodiment of this

cycle has been successfully implemented on the pilot-plant scale for clay drying in Great Britain (Heaton and Benstead, 1984). Luthi's cycle is analyzed in detail in chapter 5.

A steam dryer for wood pulp or hog fuel has been operating successfully in Rockhammar, Sweden, (Svensson, 1980, 1981), since 1978. Low pressure steam is used to transport the wet material along the tube side of a heat exchanger. The pulp is heated by high pressure steam on the shell side. The process is a net producer of steam in an amount equal to the water removed from the pulp. The generated steam is used as process steam in other parts of the mill. The exhausted steam is reported to be of high purity: no problems in particulate content or in condensing it have arisen. As no significant degradation of steam is encountered when mixing it intimately with pulp fibers, by extension there should be little problem from contacting with paper. Note, however, that sealing this bulk material dryer is much easier than a sheet dryer: the possibility of fouling due to leakage of air into the dryer, which is present in steam drying of paper, does not arise in pulp drying.

Faber et al. (1986) describe an industrial application of superheated steam drying to carbon pellet drying. The dryer, essentially a plug-flow fluidized bed, has been operating in South Africa without any difficulties since 1985. The generated steam is used to preheat the feed. The installed cost of this steam dryer is about 40 % less than that estimated for a conventional air dryer of the same capacity. The air dryer would have had to operate at below 125 $^{\circ}$C to avoid combustion of the charcoal, whereas the non-oxidizing steam atmosphere allows operation at 300 $^{\circ}$C.

Stubbing (1990) has patented in Great Britain the process, previously suggested by Choudhury and Chance (1975), of converting a conventional paper dryer into an "airless" steam dryer by making the hood airtight and compressing the exhaust steam mechanically to 3 bar gauge pressure. A cost-benefit analysis showed a simple payback period of two years. The main costs are operating and purchase costs of the compressors and the cost of sealing and insulating the hood. Two commercially available mechanical compressors, with a capacity of 10 tonnes/hour, were suggested for steam production and recycling. The economic analysis, however, did not take into account the important reduction in drying rate per unit area of drying cylinder which is bound to occur as the sheet temperature is increased from the adiabatic saturation temperature in air drying (approximately 45-70 $^{\circ}$C) to the atmospheric boiling point of water in steam drying. Furthermore, sealing such a large dryer from air infiltration poses formidable problems.

A techno-economic analysis of the conversion of a Yankee dryer to operate with superheated steam has been made by Thompson *et al.* (1991). For the steam generated by the dryer, their design investigated the alternatives of mechanical and thermocompression to 3 atmospheres, a typical value for the low pressure steam supply in paper mills. This analysis indicated a strong economic incentive for conversion to superheated steam as the drying medium and identified the remaining technical problems, which appear solvable.

1.3.6 Summary

Previous studies of drying of paper by impinging jets of superheated steam have established the industrial potential of this

technique, but the drying rate must be measured under conditions of industrial relevance before a pilot-plant can be built with confidence.

While heat and mass transfer under impinging jets have been extensively studied, no reliable means of accounting for the temperature dependence of thermophysical properties is available for superheated steam impingement drying.

Comparison of steam and air drying rates under equivalent conditions in a single apparatus are needed to ascertain the improvements resulting from switching from air to steam drying.

Transport phenomena within a sheet material with known diffusivity drying under impinging jets are well understood. However, the complexity of interaction between water and the porous fiber network in paper may lead to substantially different behavior. The transport behavior in fast drying in a steam environment is unknown and must be determined experimentally to characterize the falling rate period.

Practical means of implementing superheated steam drying for energy recovery in the paper mill requires analysis.

CHAPTER 2

APPARATUS AND EXPERIMENTAL PROCEDURE

2.1 Experimental strategy

The prime objective of the experimental design was to determine the effect of jet flow rate, temperature, basis weight and type of pulp on the drying rate of a sheet of paper under impinging jets of superheated steam or air. Since it is planned to extend the present investigation to drying in superheated steam with impingement and flow through (SWIFT drying), a secondary objective was to provide for future study with through flow.

To ensure direct industrial relevance for the measured drying rates, the principle guiding the experimental design was to try to replicate conditions in a hypothetical industrial-scale SWIFT dryer. In such a dryer, the flow field encountered by the paper sheet would be a superposition of the following elements:

1- Impinging jets with a nozzle exit velocity of the order of 100 m/s;

2- Impingement surface moving under these jets, with a velocity of the order of 1000 m/min;

3- Flow through the sheet, from a pressure drop of the order of 20 kPa.

Ideally, all three elements should be incorporated into the apparatus, but motion of the sheet presents a major drawback. In order to achieve complete drying in a single pass, the sheet residence time needs to be that corresponding to complete drying. Thus if the sheet were to move at a speed typical of an industrial dryer, no scaling down

to a laboratory-scale apparatus would be possible. Moreover, as the effect of impingement surface motion on heat transfer rates has recently been intensively studied by S. Polat and Douglas (1990) and S. Polat *et al.* (1991a, 1991b), the effect of surface motion on transfer rates is now well documented. Therefore the effect of surface motion was not included, simplifying the design to the batch drying of stationary, circular paper sheets inside a drying chamber.

No technique is currently available to determine continuously the moisture content of a sheet drying in an atmosphere of superheated steam. The technique adopted to measure drying rate consisted in performing, for each drying condition, a series of identical batch drying experiments with variable residence time, determining the final sheet moisture content gravimetrically. The drying rate was determined as the slope of the moisture content - residence time data.

2.2 Drying chamber

A cross-section of the stainless steel drying chamber is shown in figure 2.1. Superheated steam or air jets from a multiple orifice plate with a triangular pattern, with a temperature of up to 500 ^{o}C, impinged on the surface of the paper sheet. The impinging fluid, along with evaporated water, exhausted to a spray condenser through openings in the four corners of the drying chamber. The drying chamber pressure was nominally atmospheric. The nozzle plate was agitated horizontally by means of a motor-driven slider crank mechanism to help achieve uniform heat transfer across the paper surface. To limit the variations of local heat transfer rate, the jet open area ratio used was substantially higher than the value of 1.5 % reported by Martin (*op. cit.*) to maximize
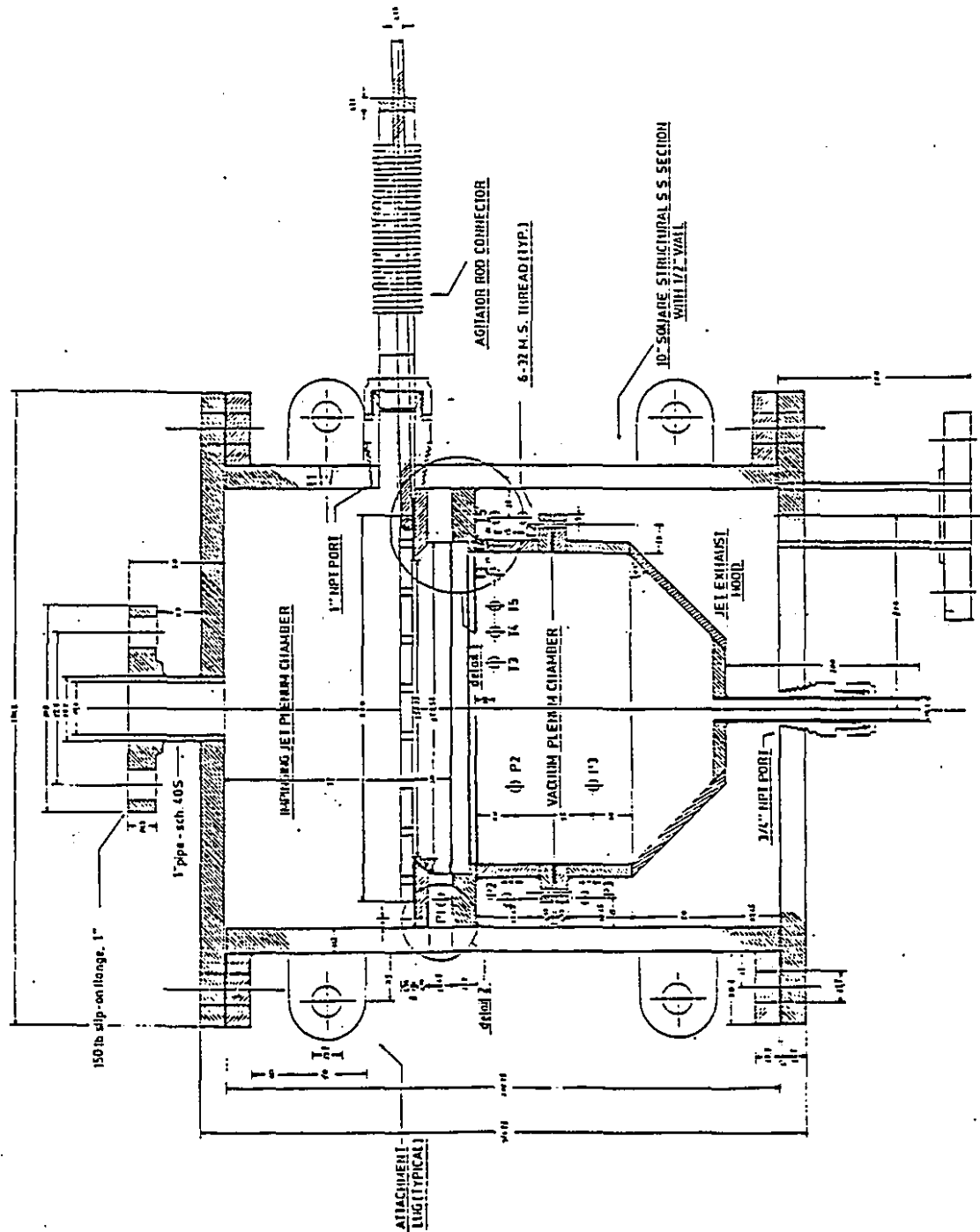
Figure 2.1 - Cross-sectional view of SWIFT drying chamber

25

the heat transfer rate for a given blower power.

A clamping ring was used to fasten the paper sheet to a sample holder, figure 2.2, consisting of a circular disk covered with a glass plate to minimize conduction from the bottom of the sheet.
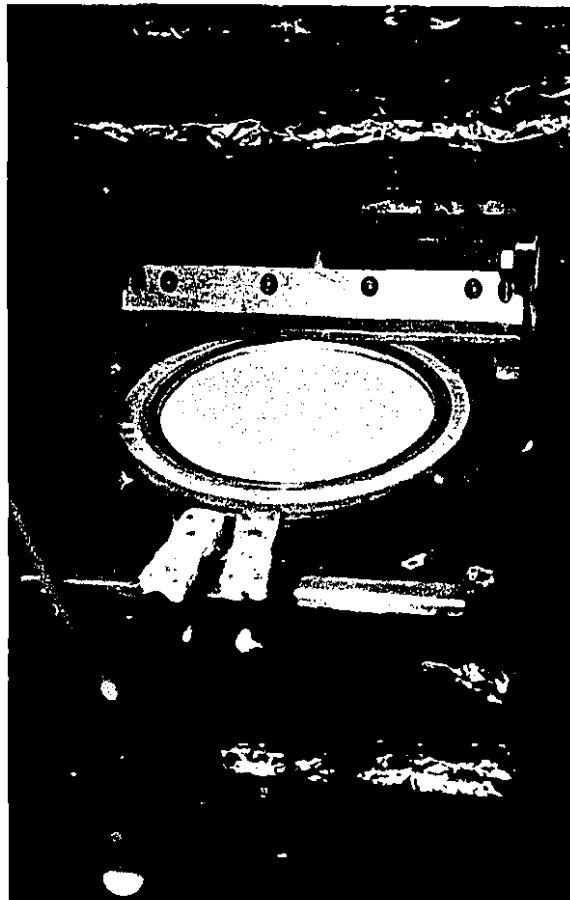
Figure 2.2 - Drying chamber and paper sheet on sample holder.

The sheet was moved in and out of the drying chamber by means of a fast-acting, computer-controlled pneumatic cylinder.

The characteristics of the SWIFT drying apparatus are as follows:

Air temperature: 20 to 450 $^\circ$C
Steam temperature: 100 to 500 $^\circ$C
Drying chamber pressure (nominal): Atmospheric
Jet Reynolds number: 500 to 12000
Jet velocity: 0 to 120 m/s
Pressure difference across sheet: 0 to 50 kPa

Nozzle-to-web distance: 23 mm
Nozzle diameter: 4 mm
Nozzle plate thickness: 6.35 mm
Open-area ratio: 4.1 %
Nozzle plate agitation frequency: 7 Hz

Weight of sample holder: 455 g
Weight of dry sheet: 0.5 to 2.5 g
Sheet diameter: 160.35 mm
Drying chamber material: stainless steel 316
Sheet residence time: 1 to 100 s

Table 2.1 – Characteristics of SWIFT drying apparatus

2.3 Auxiliary equipment

In addition to the drying chamber, the apparatus comprised equipment to feed steam or air, to condense the exhausted steam and for measurement and control. The air and steam supply pressure was 790 kPa abs. The air was essentially dry, as evidenced by its measured dew point of -30 $^\circ$C. The complete experimental facility is shown on a photograph, figure 2.3, and schematically on the flow diagram, figure 2.4.

The drying fluid went through a pressure regulator to a 15 kW electrical superheater, to a throttling valve and a venturi flow meter, then into the drying chamber. The impingement exhaust fluid exited the drying chamber to a second venturi before going to the condenser. To

provide for future extension to the study of SWIFT drying, a water jet
exhauster provided a vacuum source for through flow. Through flow rate
was determined by measuring the pressure drop across a calibrated
screen. The degree of vacuum was controlled by a back-pressure regulator
consisting of two fast-acting, computer-controlled solenoid valves.

PRESSURE
REGULATOR SUPERHEATER

CONDENSER   DRYING
                             CHAMBER
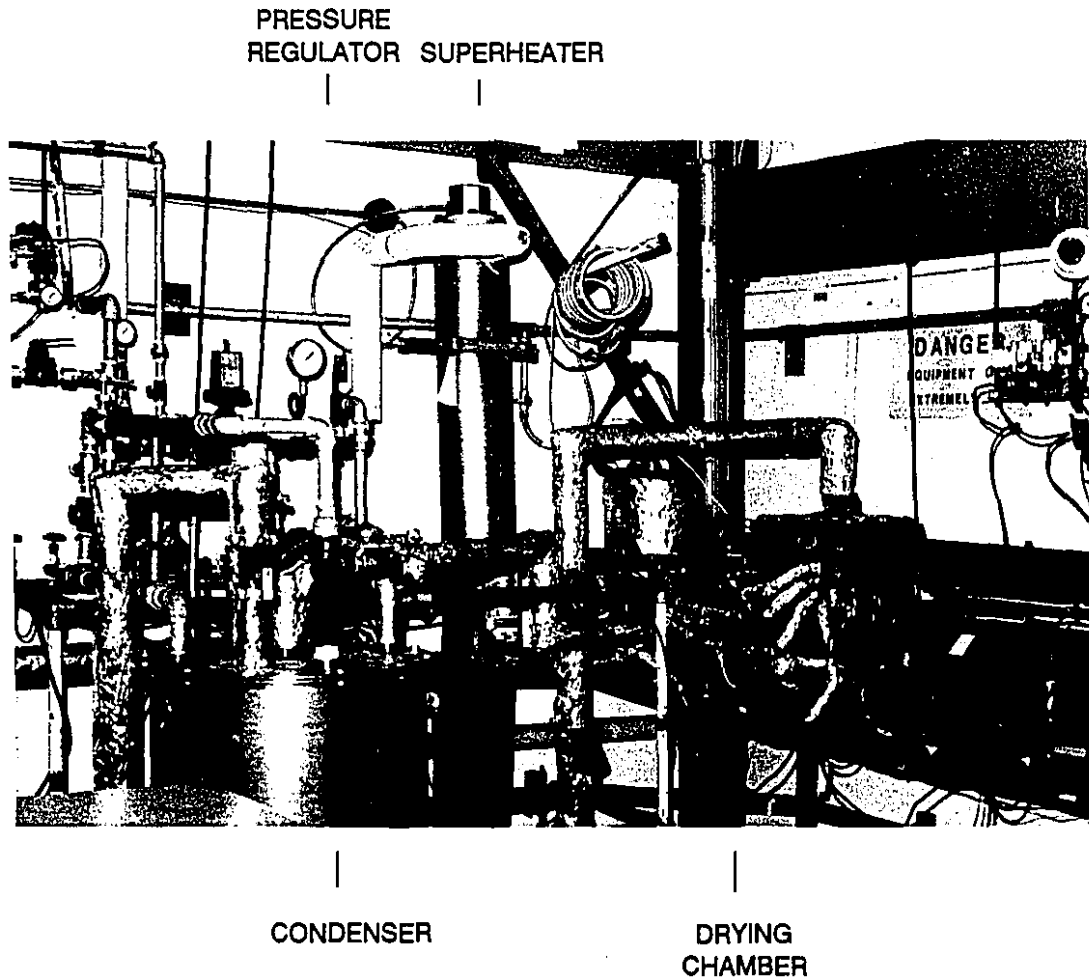
Figure 2.3 SWIFT drying apparatus.
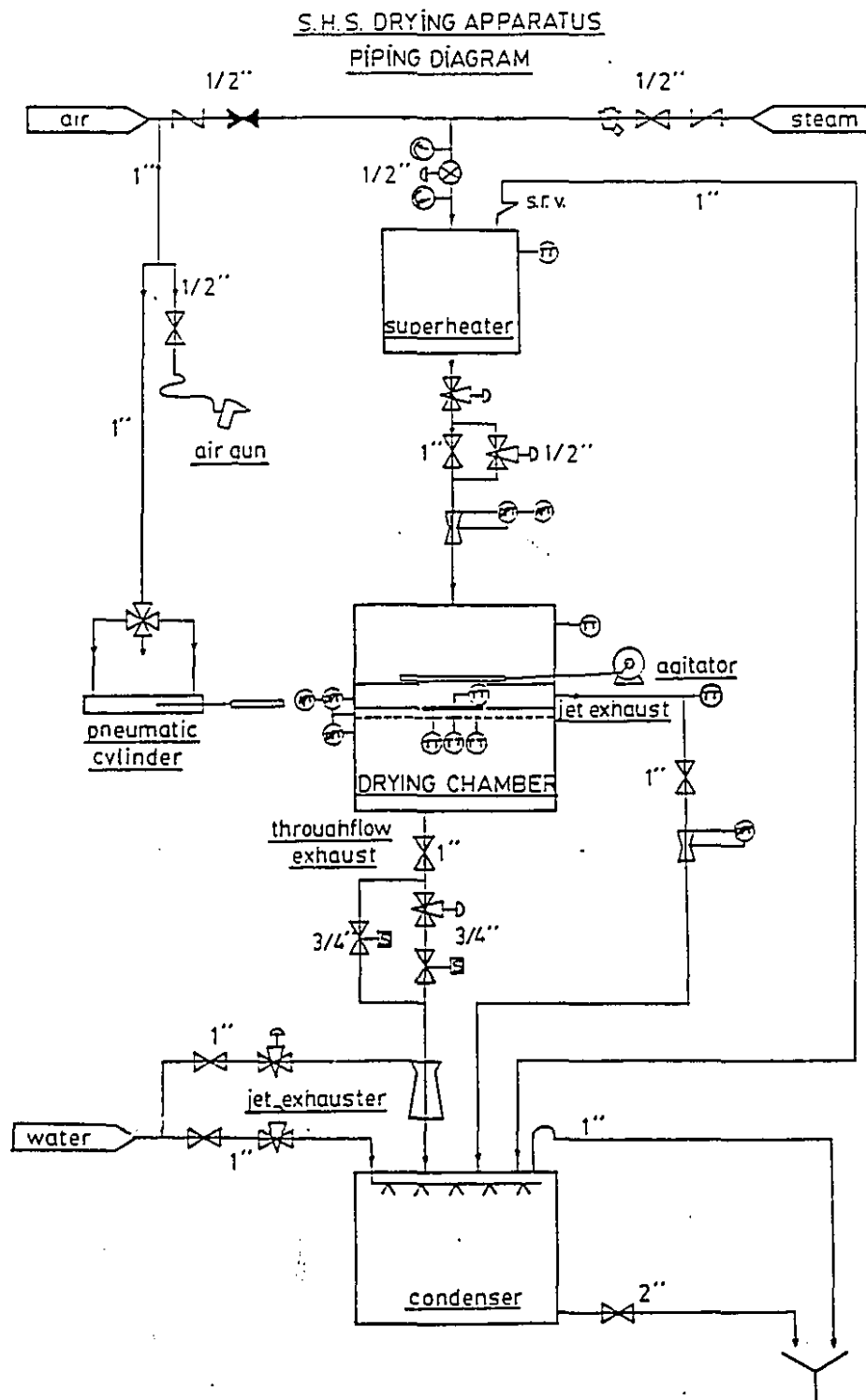
Figure 2.4 Flow diagram of SWIFT drying apparatus

2.4 Instrumentation

A complete instrumentation system monitored temperatures, pressures and flow rates.

K-type thermocouples measured temperature at the outlet of the superheater, in the plenum chamber, in the exhaust line, at the bottom of the paper sheet and, for a few experiments, at the top of the sheet. A bare thermocouple (wire diameter: 75 μm) monitored sheet bottom temperature; its junction was sandwiched between the sheet and the glass surface of the sample holder, at a location 2 cm away from the edge of the sheet. The response time of the thermocouple under these conditions is estimated to be a few milliseconds. Since the junction diameter was about the thickness of the sheet, the measured temperature is only an approximation of the temperature at the bottom of the sheet during drying.

Flow rates were measured in the impinging jet inlet and exhaust lines by means of venturi meters (Preso model #V100-65). The impingement mass flow rate was determined from the venturi equation:

$$M_j = \frac{C_v}{\sqrt{1 - (D_t/D_i)^4}} \, A_t \, \sqrt{2 \, \rho \, \Delta P} \qquad (2.1)$$

Using the perfect gas law, this equation can be rewritten:

$$M_j = b \, \sqrt{\frac{M}{R}} \, \sqrt{\frac{P \, \Delta P}{T}} \qquad (2.2)$$

where   b, which is $\sqrt{2}$ times the throat area times the venturi

30

discharge coefficient, was given by the manufacturer to be 5.426×10^{-1} m^2;

M is the molecular weight of the gas;

R is the universal gas constant;

P is the absolute pressure at the venturi inlet;

ΔP is the venturi inlet-to-throat pressure drop;

T is the temperature at the venturi.

The average jet exit velocity was obtained from:

$$\bar{u}_j = \frac{M_j}{\rho_j \, A_1 \, f} \tag{2.3}$$

where ρ_j, the jet density, was taken to be $P_j \, M / R \, T_j$, with P_j and T_j the plenum chamber absolute pressure and temperature, respectively;

A_1, the impingement surface, was 1.93×10^{-2} m^2;

f, the nozzle plate open area ratio, was 4.1 %.

Flow through a square-edged round orifice forms a vena contracta, but reexpands to the full orifice diameter for orifices with the present aspect ratio L/D = 6.35 mm / 4 mm = 1.59 (King and Brater, 1963). Therefore, the velocity profile was taken to be flat at the orifice exit, and the average exit velocity and orifice diameter were used to define the jet Reynolds number:

$$Re_j \equiv \frac{\bar{u}_j \, D}{\nu_j} \tag{2.4}$$

Piezoresistive pressure transducers (Omega PX series) measured pressures for flow rate determination as well as the absolute pressure

on the sheet surface. These transducers were immersed in a constant
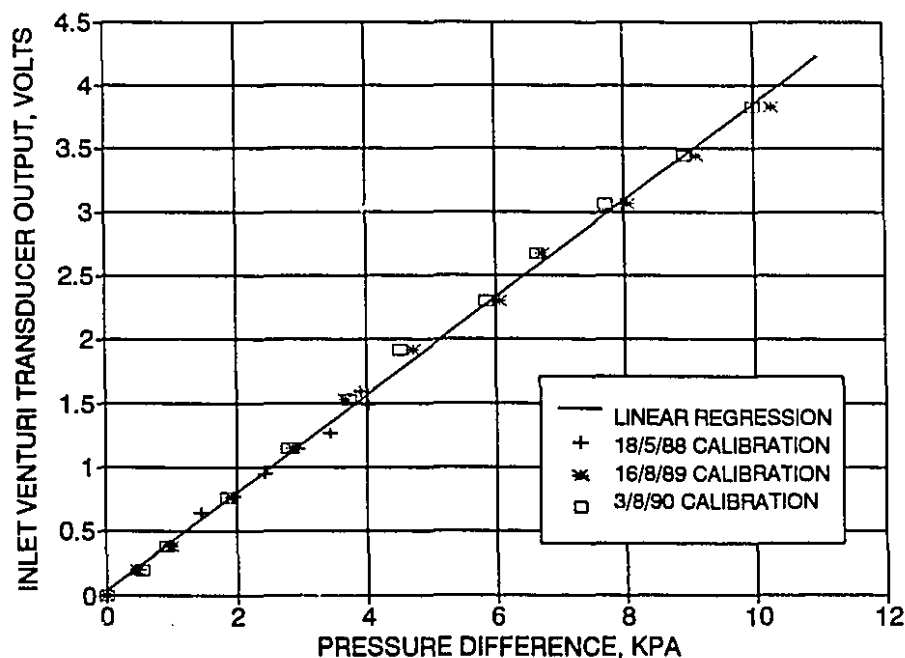
Figure 2.5 Calibration of inlet venturi pressure transducer

temperature oil bath at 115 °C, a temperature below their maximum
operating value of 125 °C, yet high enough to prevent the degradation of
accuracy from steam condensation in the pressure measurement lines. The
calibration of the pressure transducer for jet flow rate measurement,
determined three times during the course of the project using a mercury
manometer, was found to be stable, figure 2.5. A linear regression on
the combined results of the three calibrations has a standard error
equal to 3 % of the mean. Results of a linear regression of the output
voltage vs. pressure difference data were incorporated into the flow
monitoring and control program after each calibration. The standard
error from the three calibrations averaged 0.1 kPa. All other pressure
transducers were calibrated once and were found to perform within the
manufacturer's specifications.

2.5 Data acquisition and process control

Data acquisition and process control were performed by a high performance board (Data Translation Model DT 2801-A) connected to an IBM-PC-XT-compatible computer. The board had sixteen 12-bit analog input channels and sixteen digital input-output lines. The complete set of instruments was scanned at a frequency varying between 5 Hz for the slowest experiments (residence time between 50 and 100 seconds) and 50 Hz for the fastest ones (residence time less than 10 seconds).

During an experiment, raw digital data were acquired and moved to a RAM array in the computer's memory using direct memory access (DMA). The array was stored on disk at the end of the experiment. The digital data were converted to physical quantities using a data processing program written in QUICKBASIC, and these were stored in a QUATTRO PRO worksheet for analysis and display.

The digital output capabilities of the board were used to operate the pneumatic cylinder for sheet insertion and removal. The superheater and the back-pressure regulating valves were also operated by the board in closed-loop control circuits.

2.6 Paper sheet characteristics

The experiments were done with never-dried, circular handsheets (diameter: 160.35 mm) prepared in a standard sheet-making machine, according to CCPA Standard C4 (CPPA, 1950). Most experiments were done with unbleached kraft pulp from black spruce, with 48% yield, 698 Canadian Standard Freeness, and Kappa number 30, from the pilot plant of the Pulp and Paper Research Institute of Canada in Pointe-Claire, Quebec. A substantial number were done with black spruce

thermomechanical pulp (TMP), with 164 Canadian Standard Freeness, from the Donohue Normick mill in Amos, Quebec. A few additional experiments were done with rewetted commercial towel paper, comprising 35-45% softwood kraft, 30-35% CTMP and 20-35% broke, with approximately 1% per weight of wet strength resins.

The sheet thickness was measured after drying on a standard caliper gauge for a statistically significant sample of sheets. The thickness-basis weight results are reported in figure 2.6. The sheet bulk is 2.71 cm^3/g for kraft, 4.47 cm^3/g for TMP and 6.73 cm^3/g for towel paper.
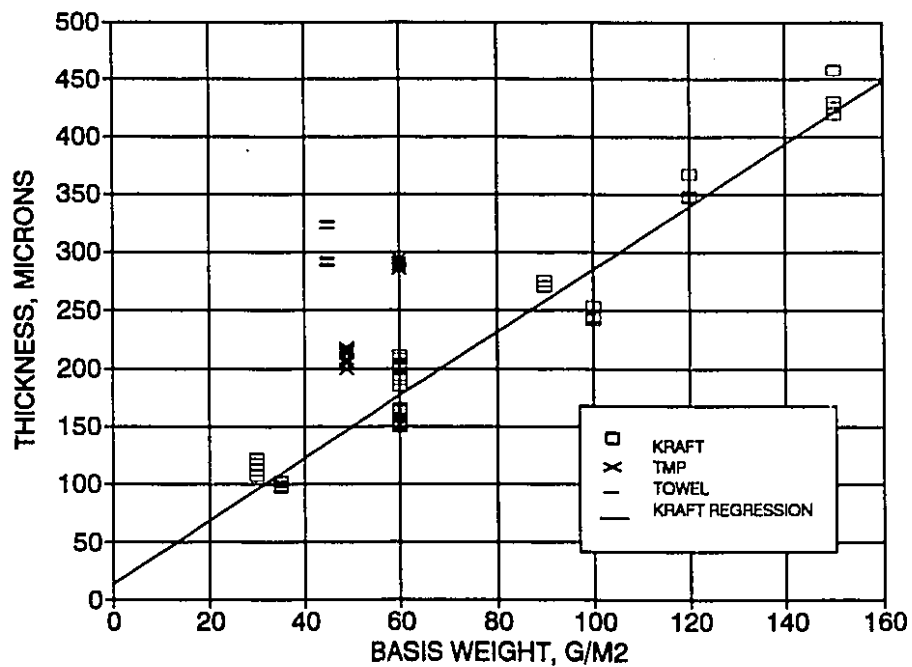
Figure 2.6 Sheet thickness-basis weight relation.

2.7 Experimental procedure

The evolution of sheet moisture content was determined by performing, for each set of experimental conditions, a series of identical runs with residence time as the only variable. The drying rate was measured in 79 conditions, with typically 12 residence times per condition. A total of 1047 paper sheets were dried. A complete inventory of the experimental conditions is included as appendix 1.

The experimental procedure comprised the following steps:

1) The apparatus was readied for the desired drying conditions. Air was used during the warming-up stage of the steam drying runs to prevent condensation. Steady state was reached after about two hours.

2) The sample holder and lid weights were recorded. A wet sheet was clamped on the sample holder. The sample holder/paper sheet assembly was weighed. The moisture content of the wet sheet was then estimated as

$$X = \frac{\text{weight of water}}{\text{weight of fiber}} \qquad (2.5)$$

The wet sheet was then allowed to dry slowly on the balance, until the desired initial moisture content, X_i, was reached. For most experiments, this was $X_i = 1.6$; some experiments, particularly with lower basis weight sheets with a lower water retention capacity, were done with $X_i = 1.0$.

3) Upon reaching the desired initial moisture content, the sample holder was covered with a leakproof lid and moved into its slot on the drying chamber. The lid was then removed and the experiment triggered 1-2 seconds thereafter from the computer keyboard.

4) The sheet was inserted into the drying chamber by means of a computer-controlled pneumatic cylinder. The nozzle plate was agitated

during the experiment.

5) After the target residence time, the sheet was withdrawn from the drying chamber; the sample holder was immediately covered with the lid and taken to the balance to measure the final moisture content. The moisture-free fibre weight was determined by further drying the sheet in a microwave oven for five minutes. By tests on ten sheets, the dry fibre weight thus determined was found equal to that measured after letting the microwave-dried sheet rehumidify at room temperature, then drying in a standard oven at 105 $^\circ$C for 12 hours.

2.8 Demonstration results

2.8.1 Introduction

Demonstration results are shown here to introduce the phenomena at play and to establish the validity and repeatability of the experimental procedure.

The conditions for the demonstration results were:

> Jet temperature T_J = 350 $^\circ$C
> Jet Reynolds number Re_J = 2000
> Pulp type: Unbleached kraft
> Basis weight B: 60 g/m^2
> Initial moisture content X_i = 1.0

2.8.2 Evolution of moisture content

The evolution of moisture content for these sets of drying runs is shown in figures 2.7 and 2.8 for air and steam, respectively. Air drying is characterized by a constant rate period and a falling rate period. Steam drying begins with a rapid and significant condensation period

36
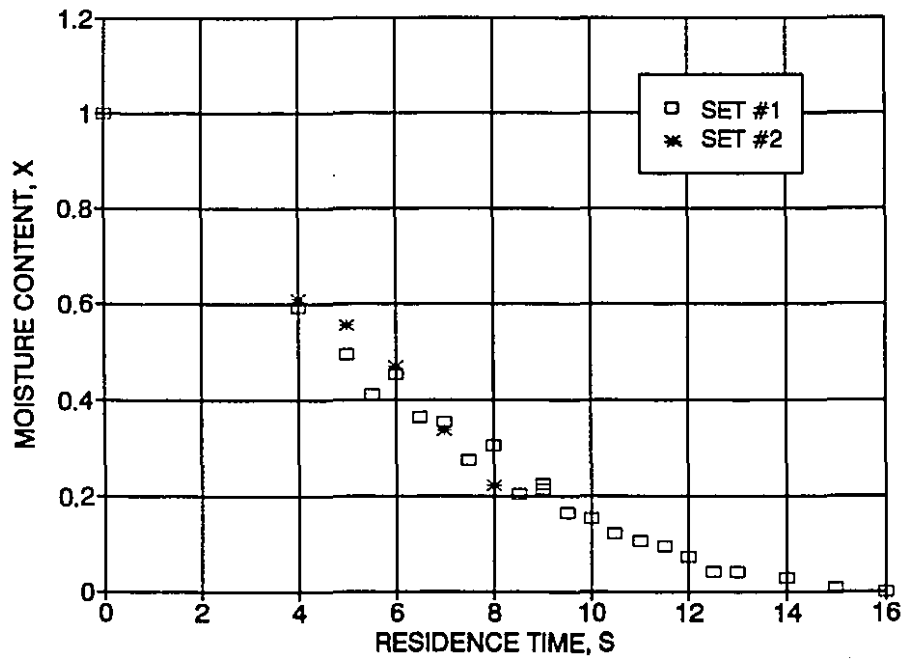
Figure 2.7 Moisture content-residence time relation in air drying
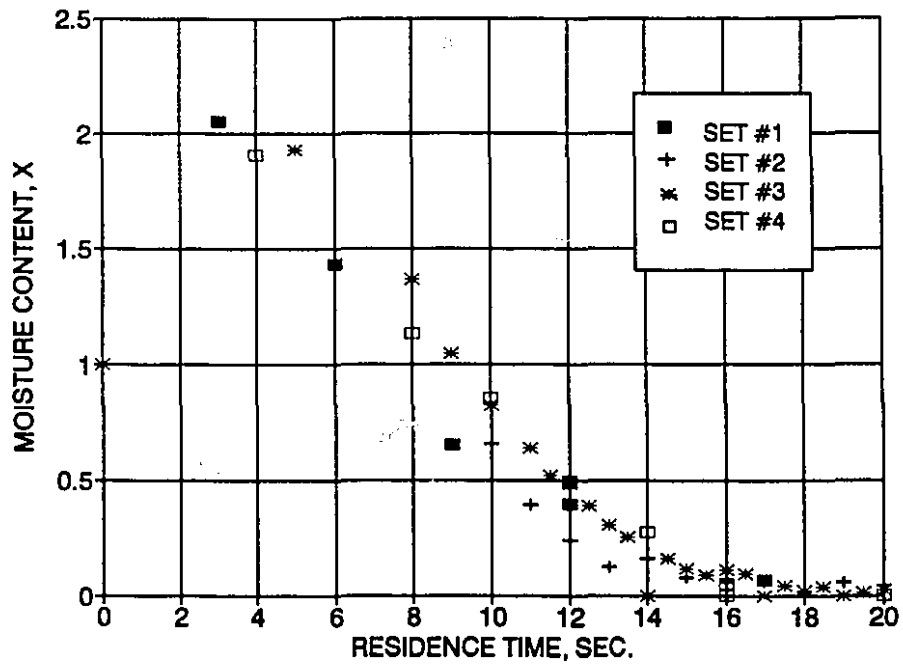
Figure 2.8 - Moisture content-residence time relation in steam drying

during which the cool wet sheet is heated to 100 °C, then a long constant rate drying period, finally a falling rate period. It is shown (appendix 3) that most of the condensation is due to heat conduction through the bottom of the sheet. This condensation, specific to the laboratory apparatus, would not occur in an industrial impingement steam dryer.

For these four series of runs done many months apart, the regression coefficient of the derived composite linear-exponential expression (section 2.9) was 0.986. This high consistency establishes the very good repeatability of the experiments, considering the large number of factors affecting the drying rate and the number of sources of experimental error (appendix 2).

2.8.3 Evolution of sheet temperature

The evolution of sheet temperature is shown in figures 2.9 and 2.10 for steam and air drying, respectively.

For steam, the bottom of the wet sheet is initially at about the adiabatic saturation temperature corresponding to room temperature ($T_{a.s.} = 6$ °C for dry air). After insertion in the drying chamber, the temperature quickly rises to 100 °C and remains there as evaporation proceeds, until the thermocouple is no longer surrounded by free water, at which point it suddenly rises from 100 °C. Comparison with figure 2.8 shows that this breakout point occurs shortly before drying is complete. The temperature rises steadily from this point on, but does not reach the jet temperature because of the cooling effect of the sample holder, the bottom of which is in contact with liquid water droplets at 100 °C (appendix 3).
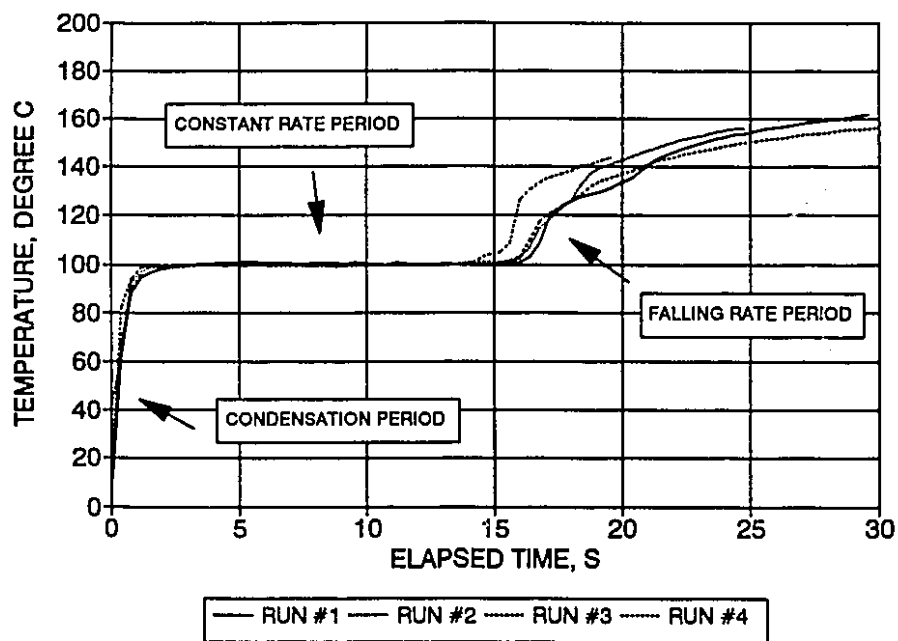
Figure 2.9 Sheet bottom temperature in steam drying
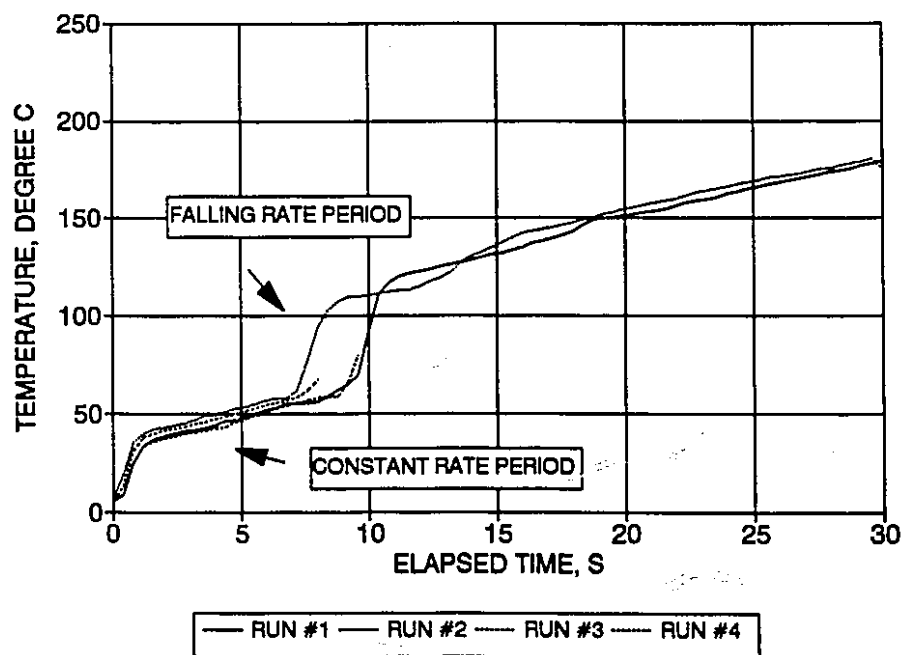
Figure 2.10 Sheet bottom temperature in air drying

For air drying, the evolution of sheet temperature is qualitatively the same as for steam drying, but the constant rate period temperature is about the adiabatic saturation temperature ($T_{a.s.}$ = 57 $^{\circ}$C for dry air at 350 $^{\circ}$C).

2.8.4 Flow rates, temperatures and pressures

The evolution of inlet and outlet flow rates and temperatures for a typical steam drying experiment are shown as figure 2.11. After a short disturbance at the moment of sheet insertion, inlet and outlet flow rates were constant. The outlet flow rate was about 6 % lower than the inlet flow rate, owing to leaks through the slot for sample insertion. Although the drying chamber temperature control was disabled during an experiment to permit data acquisition, the plenum chamber temperature remained constant. The exhaust temperature, initially 20 degrees lower
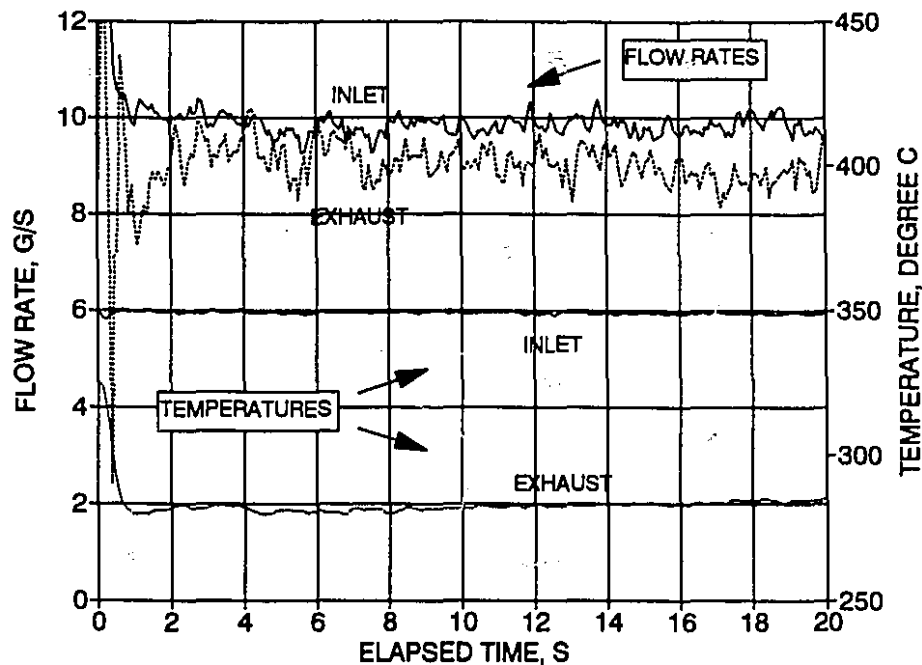
Figure 2.11 Flow rates and temperatures in steam drying

than the plenum temperature due to heat loss through the section of walls between the plenum and the exhaust ports, dropped suddenly when the sheet and sample holder at room temperature were inserted, slowly returning towards its original value.

Pressure in the drying chamber between the nozzle plate and the sheet was constant at slightly above one atmosphere, typically 105 kPa in steam drying, 110 kPa in air drying. The pressure was somewhat lower with steam, due to the effect of exhaust steam condensation.

2.9 Drying rate calculation

2.9.1. Statistical treatment of batch drying data

Drying rates were obtained from the measured moisture content-time data by a statistical procedure adapted from Petersen (1986). Expressions for the moisture content evolution during the constant rate and the falling rate periods are supplied. Values of the parameters in those expressions which best match the observed data are determined using non-linear regression, subject to the constraints that the two expressions have the same value and the same slope at their point of intersection.

For the constant rate period, the drying rate equation

$$R = -B \ \frac{dX}{dt} = R_c \qquad (2.6)$$

is integrated to yield

$$X = X_1 - \frac{R_c \ t}{B} \qquad (2.7)$$

For the falling rate period, the drying rate is taken to be directly proportional to moisture content (article 4.3):

$$R = -B \frac{dX}{dt} = mX + b \qquad (2.8)$$

Integrating this equation gives

$$X = k_1 \exp\left[- \frac{m}{B} t\right] - \frac{b}{m} \qquad (2.9)$$

where k_1 is an arbitrary constant.

From the equality of drying rates at the critical moisture content X_c at time t_c, $b = R_c - m X_c$. Hence equation 2.8 can be rewritten:

$$R = R_c + m (X - X_c) \qquad (2.10)$$

The critical time t_c can be expressed in terms of the critical moisture content X_c using equation 2.7:

$$t_c = \frac{B}{R_c} (X_1 - X_c) \qquad (2.11)$$

Substituting from 2.10 and 2.11 into 2.9,

$$X_c = k_1 \exp\left[\frac{-m}{R_c}(X_1 - X_c) \right] - \frac{R_c}{m} + X_c \qquad (2.12)$$

$$\therefore \ k_1 = \frac{R_c / m}{\exp\left[\frac{-m}{R_c} (X_1 - X_c)\right]} \qquad (2.13)$$

Substituting from equations 2.13 and 2.10 into equation 2.9 and rearranging yields:

42

$$X = X_c - \frac{R_c}{m} \left\{ 1 - \exp\left[\frac{m}{R_c} (X_i - X_c) \right] \exp\left[\frac{-m\, t}{B} \right] \right\} \qquad (2.14)$$

The two moisture content evolution expressions,

$$X > X_c : \qquad X = X_i - \frac{R_c\, t}{B} \qquad (2.7)$$

$$0 \leq X \leq X_c :$$

$$X = X_c - \frac{R_c}{m} \left\{ 1 - \exp\left[\frac{m}{R_c} (X_i - X_c) \right] \exp\left[\frac{-m\, t}{B} \right] \right\} \qquad (2.14)$$

contain four parameters:

X_i, the X-intercept of the X vs. t plot of a series of drying runs, can be considered as the initial moisture content of an experiment in which drying began immediately at the constant rate period;

R_c is the constant drying rate;

X_c is the critical moisture content, the point of transition between the constant and falling rate periods;

m is the slope of the drying rate-moisture content curve, a measure of the additional resistance to heat and mass transfer within the sheet during the falling rate period.

The drying rate parameters were estimated by a non-linear regression routine from SYSTAT (Wilkinson, 1989), a commercial statistical software package. The procedure, using the SIMPLEX

algorithm, with a convergence criterion of 0.001 in the relative parameter changes, usually converged within 50 iterations.

2.9.2 Correction for the effect of initial moisture content variation

The accuracy of the final moisture contents measured, and therefore, of the drying rates, was limited by several sources of experimental error (appendix 2). One of these, the variation in initial moisture content caused by a variation in sheet basis weight, could be systematically corrected.

In experiments with never-dried sheets, the dry sheet weight was unknown prior to performing the experiment: it was *estimated* from the concentration of the pulp suspension, the volume used, and the experimentally estimated retention factor. These factors introduce a corresponding uncertainty in the initial moisture content of the sheet. This correction is illustrated for a dry sheet weight estimated to be $W_{d,t}$ = 1.000 g and a target initial moisture content of $X_{i,t}$ = 1.500. The wet sheet is clamped on the sample holder and allowed to dry on the balance until reaching a wet sheet weight of

$$W_{d,t} \ (1 + X_{i,t}) = 1.000 \ (\ 1 + 1.500) = 2.500 \ g \qquad (2.15)$$

at which time the sample holder is covered and the experiment started. If the actual dry sheet weight were subsequently determined to be 1.030 g, the actual initial moisture content is not 1.500 but rather

$$\frac{\text{wet sheet weight} - \text{actual dry sheet weight}}{\text{actual dry sheet weight}} = \frac{2.500 - 1.030}{1.030} = 1.427 \qquad (2.16)$$

44

i. e. 0.073 less than the target value.

To investigate the variation in the dry weight of sheets made using a handsheet-making machine, the distribution of sheet dry weights was measured for two batches of sheets dried overnight in an oven at 105 °C, table 2.2:

PULP TYPE	NUMBER OF SHEETS IN SAMPLE	TARGET WEIGHT, g	MEAN WEIGHT $\bar{W}_d$, g	STANDARD DEVIATION, σ, g	$\dfrac{\sigma}{\bar{W}_d}$, %
Kraft	19	1.212	1.247	0.030	2.5
T.M.P.	10	1.212	1.196	0.049	4.1

Table 2.2 - Distribution of dry sheet weight in two batches

The variation is caused by the difficulty in pouring exactly the right amount of pulp suspension into the handsheet-making machine, by variable retention of the fibers on the screen and inhomogeneous concentration of the fibers in the suspension.

The relationship between the variations in basis weight and initial moisture content can be obtained from equation 2.15 as follows:

$$W_w = W_{d,t} (1 + X_{i,t}) = (W_{d,t} + \Delta W_d) (1 + X_{i,t} + \Delta X_i) \qquad (2.17)$$

Expanding this expression, dropping the second order term $\Delta W_d \Delta X_i$ and rearranging gives:

$$\frac{\Delta W_d}{W_{d,t}} = \frac{\Delta B}{B_t} = \frac{- \Delta X_i}{1 + X_{i,t}} \qquad (2.18)$$

After the experiment, the sheet was dried for five minutes in a microwave oven, allowing determination of the *actual* dry sheet weight W_d, final moisture content X_f and, retrospectively, initial moisture content X_i from the above equation. The variation in initial moisture content provokes a deviation in final moisture content from the value which would be measured in its absence, which in turn induces an error in the evaluation of the drying rate. Since it possible to measure the variation in the initial moisture content of the sheet ΔX_i, this effect is corrected for by estimating the deviation which it produces in the final moisture content, ΔX_f, and subtracting this from the measured value.

For the constant rate period, the moisture content evolves according to equation 2.7, and the final moisture content is measured to be

$$X_{f'} = X_{i'} + \int_0^{t'} \frac{dX}{dt}\ dt = (X_{i,t} + \Delta X_i) - \frac{R\ t'}{B_t + \Delta B'} \qquad (2.19)$$

The final moisture content which would have been measured in the absence of these variations is

$$X_{f',t} = X_{i,t} - \frac{R\ t'}{B_t} \qquad (2.20)$$

Therefore, the variation produces a deviation equal to

$$\Delta X_f = X_{f'} - X_f = \Delta X_{1'} - R \ t' \left[\frac{1}{B_t + \Delta B'} - \frac{1}{B_t} \right] \qquad (2.21)$$

$$= \frac{- \Delta B' \ (1 + X_{1,t})}{B_t} - R \ t' \left[\frac{1}{B_t + \Delta B'} - \frac{1}{B_t} \right] \qquad (2.22)$$

$$\text{Now,} \qquad \frac{1}{B_t + \Delta B'} = B_t^{-1} \left[1 + \frac{\Delta B'}{B_t} \right]^{-1} \qquad (2.23)$$

$$= B_t^{-1} \left[1 - \frac{\Delta B'}{B_t} + \left[\frac{\Delta B'}{B_t} \right]^2 \ldots \right] \cong B_t^{-1} \left[1 - \frac{\Delta B'}{B_t} \right]^{-1}$$

$$(2.24)$$

$$\therefore \Delta X_f \cong \frac{- \Delta B' \ (1 + X_{1,t})}{B_t} - R \ t' \left[\frac{1}{B_t} - \frac{\Delta B'}{B_t^2} - \frac{1}{B_t} \right] \qquad (2.25)$$

$$= - \frac{\Delta B'}{B_t} \left[(1 + X_{1,t}) - \frac{R \ t'}{B_t} \right] \qquad (2.26)$$

47

$$\Delta X_f \cong - \frac{\Delta B'}{B_t} \left[1 + X_{f'} \right] \qquad (2.27)$$

For an experiment ending in the falling rate period, the moisture content evolves according equation 2.14 and, for a sheet of basis weight $B + \Delta B$ and initial moisture content $X_1 + \Delta X_1$:

$$X_{f'} = X_c - \frac{R_c}{m} \left[1 - \exp\left[\frac{m}{R_c} (X_1 + \Delta X_1 - X_c) \right] \exp\left[\frac{-m\,t}{B + \Delta B} \right] \right] \qquad (2.28)$$

$\Delta X_{f'}$, the difference between $X_{f'}$ (equation 2.28) and X_f (equation 2.14) is

$$- \frac{R_c}{m} \left\{ - \exp\left[\frac{m}{R_c} (X_1 + \Delta X_1 - X_c) \right] \exp\left[\frac{-m\,t}{B + \Delta B} \right] \right\} \qquad (2.29)$$

$$+ \exp\left[\frac{m}{R_c} (X_1 - X_c) \right] \exp\left[\frac{-m\,t}{B} \right] \right\}$$

Using, once again, the approximation

$$\frac{-m\,t}{B + \Delta B} \cong \frac{-m\,t}{B} \left[1 - \frac{\Delta B}{B} \right] \qquad (2.30)$$

$$\Delta X_f = \frac{R_c}{m} \left\{ \exp\left[\frac{m}{R_c}(X_i - X_c)\right] \exp\left[\frac{m \Delta X_i}{R_c}\right] \exp\left[\frac{-mt}{B}\right] \exp\left[\frac{m t \Delta B}{B^2}\right] \right.$$

$$\left. - \exp\left[\frac{m}{R_c}(X_i - X_c)\right] \exp\left[\frac{-m t}{B}\right] \right\}$$

(2.31)

$$= \frac{R_c}{m} \left\{ \exp\left[\frac{m}{R_c}(X_i - X_c)\right] \exp\left[\frac{-mt}{B}\right] \right.$$

(2.32)

$$\left. * \left[\exp\left[\frac{m \Delta X_i}{R_c}\right] \exp\left[\frac{m t \Delta B}{B^2}\right] - 1 \right] \right\}$$

$$\boxed{\Delta X_f = \left[(X_f - X_c) + \frac{R_c}{m}\right]\left[\exp\left[\frac{m \Delta X_i}{R_c}\right] \exp\left[\frac{m t \Delta B}{B^2}\right] - 1\right]}$$ (2.33)

2.9.3 Summary of the calculation method

From the foregoing analysis, a suitable procedure to account for the effect of the variation in initial moisture content, is as follows:

1- The parameters X_i, R_c, X_c and m were estimated from a least squares regression of the raw data;

2- The final moisture content data were corrected by the deviation formulas, equations 2.27 and 2.33, for the constant rate and the falling rate period;

3- The parameters X_i, R_c, X_c and m were estimated anew from the corrected data.

In principle, this procedure should be performed iteratively until the parameter estimates converge. However, an iterative correction on one set of data revealed no significant change in the parameter estimates beyond the first iteration. Consequently, only one cycle of the procedure was performed in the processing of all subsequent data sets. The drying rate calculation procedure is summarized in the flowsheet, figure 2.12:
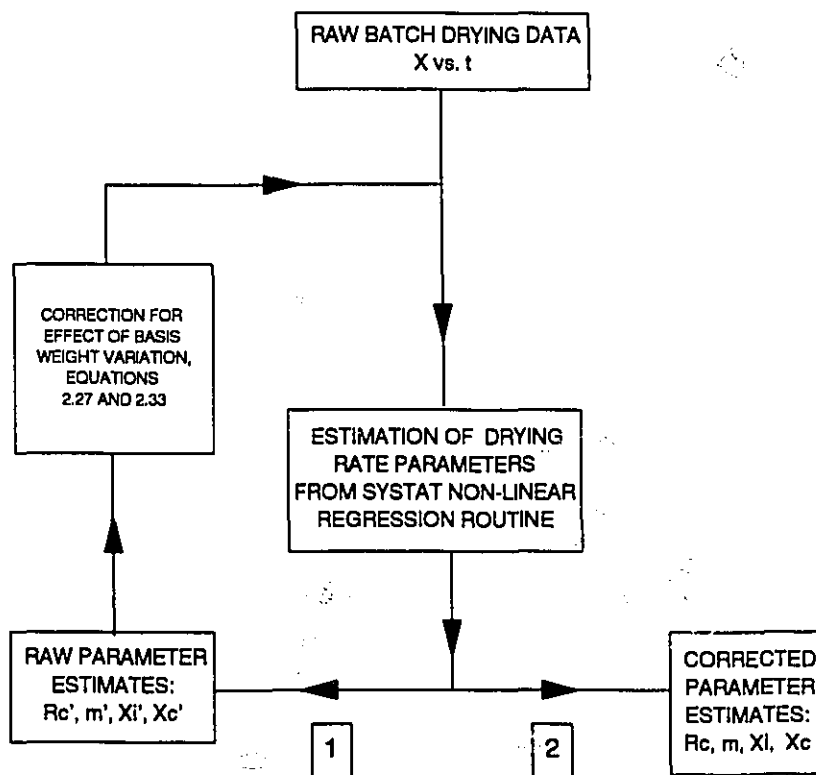
Figure 2.12 Flowsheet of the drying rate calculation procedure

CHAPTER 3

CONSTANT RATE DRYING

3.1 STEAM DRYING

3.1.1 Mechanism of constant rate impingement steam drying

It is well known that in impingement air drying, drying occurs initially at a constant rate as the driving forces and transport coefficients for heat and mass transfer all remain constant, as long as the surface is entirely wet with free water. By contrast, in superheated steam drying, there is no concentration gradient, and mass transfer takes place by bulk flow of vapor, rather than Fick's law diffusion. To understand why such drying occurs at a constant rate, and what factors determine this rate, the kinetics of evaporation of liquid water into its pure vapor must be examined.

In a closed, thermally insulated vessel containing liquid water in equilibrium with pure water vapor at temperature T_v, liquid molecules are continually crossing the phase boundary into the vapor phase, and vice versa. The condition for equilibrium is that the rates of these two processes, evaporation and condensation, be equal. The rate, which depends on the molecular velocity distribution in the liquid and gas phase, is derived from the kinetic theory of gases to be

$$R_{ev} = R_{con} = P_v \sqrt{\frac{M}{2 \pi R T_v}} \qquad (3.1)$$

where P_v is the pressure in the vapor phase (the saturation vapor pressure), R the gas constant and M the molecular weight of water.

If heat is transferred from a hot source, as occurs, for example,

51

in superheated steam drying, the liquid surface temperature may be raised above the equilibrium value. As liquid water is incompressible, the velocity distribution of the liquid molecules depends only on temperature. Thus the above kinetic equation still describes the rate of transfer into the gas phase, but the rate of condensation from the gas phase is, in principle, changed. The net rate of evaporation is given by the modified Hertz-Knudsen equation (Maa, 1967, 1970):

$$R = R_{ev} - R_{con} = P_l \sqrt{\frac{M}{2 \pi R T_l}} - \Gamma P_v \sqrt{\frac{M}{2 \pi R T_v}} \qquad (3.2)$$

where T_l and T_v are the temperatures on the liquid and gas side of the phase boundary, P_l is the saturation pressure at T_l, P_v is the ambient gas pressure and Γ is a factor which corrects the condensation rate for the effect of the net velocity of vapor away from the phase boundary. This correction factor was derived by Schrage (1953) to be

$$\Gamma = \exp\left[- \frac{M}{2 R T_v} u^2 \right] - \qquad (3.3)$$

$$\sqrt{\frac{\pi M}{2 R T_v}} \; u \; erfc\left[\sqrt{\frac{M}{2 R T_v}} \; u \right]$$

where u is the average velocity of vapor molecules away from the phase boundary. The above evaporation rate and correction factor equations were verified experimentally by Maa for evaporation or condensation of water and p-cymene.

A simple relationship between drying rate and liquid surface

temperature in superheated steam drying can be obtained from the above evaporation rate equation if a few simplifying assumptions are made. For evaporation rates of the order of those reached in this study, the effect of the net vapor flux away from the phase boundary may be safely neglected, i. e. Γ may be taken equal to 1 as its exact value is 0.99992898 for an evaporation rate of 100 kg/ m^2-h at 100 $^\circ$C. Determination of evaporation rate from equation 3.2 depends then on relating (P_v, T_v) to (P_1, T_1).

The relationship between saturation pressure and temperature in the vicinity of the atmospheric boiling point is obtained when the Clausius-Clapeyron equation,

$$\frac{dP_{sat}}{dT_{sat}} = \frac{M\ P_{sat}\ \Delta h_v}{\mathbb{R}\ T^2} \tag{3.4}$$

is integrated to yield

$$\ln P_{sat} = \frac{-\ M\ \Delta h_v}{\mathbb{R}\ T_{sat}} + C \tag{3.5}$$

At the atmospheric boiling point of water T_b, we have $P_{sat} = P_{atm}$. Hence

$$C = \ln P_{atm} + \frac{M\ \Delta h_v}{\mathbb{R}\ T_b} \tag{3.6}$$

$$\therefore \ln \frac{P_{sat}}{P_{atm}} = \frac{M\ \Delta h_v}{\mathbb{R}} \left[\frac{1}{T_b} - \frac{1}{T_{sat}} \right] \tag{3.7}$$

$$\frac{P_{sat}}{P_{atm}} = \exp\left\{\frac{-M\,\Delta h_v}{R}\left[\frac{1}{T_{sat}} - \frac{1}{T_b}\right]\right\} \qquad (3.8)$$

For small deviations around T_b, letting $T_{sat} = T_b + \Delta T$, we have

$$\frac{P_{sat}}{P_{atm}} = \exp\left\{\frac{-M\,\Delta h_v}{R}\left[\frac{1}{T_b + \Delta T} - \frac{1}{T_b}\right]\right\} \qquad (3.9)$$

Expanding the term $1 / (T_b + \Delta T)$ as a power series and dropping higher order terms, we obtain

$$\frac{P_{sat}}{P_{atm}} = \exp\left\{\frac{-M\,\Delta h_v}{R}\left[\frac{1}{T_b} - \frac{\Delta T}{T_b^2} - \frac{1}{T_b}\right]\right\} \qquad (3.10)$$

and finally

$$P_{sat} = P_{atm}\,\exp\left\{\frac{M\,\Delta h_v\,\Delta T}{R\,T_b^2}\right\} \qquad (3.11)$$

Setting $T_l \cong T_v$ and $P_v = P_{atm}$ for drying in pure steam at atmospheric pressure, and substituting the above expression for saturation vapor pressure into the evaporation rate equation, we obtain

$$R = P_{atm}\,\sqrt{\frac{M}{2\,\pi\,R\,T_l}}\,\left[\exp\left\{\frac{M\,\Delta h_v\,\Delta T}{R\,T_b^2}\right\} - 1\right] \qquad (3.12)$$

This expression has the value $R = 1.24 \times 10^4$ kg/m^2-h at $T_1 = 101$ °C. This analysis establishes that only an extremely small elevation in liquid surface temperature above the saturation temperature is required to bring about a very large evaporation rate, thereby confirming what was postulated by early workers in superheated steam drying (Wenzel & White, 1951, Chu *et al.*, 1953).

Hence in constant rate drying of paper by impinging jets of superheated steam, where the drying rate is of the order of 100 kg/m^2-h, the evaporation surface temperature is equal to the boiling point for all practical purposes. This close approach is confirmed by thermocouple measurements of temperature at the bottom of the sheet, figure 2.9. The temperature field assumes the shape described in figure 3.1:
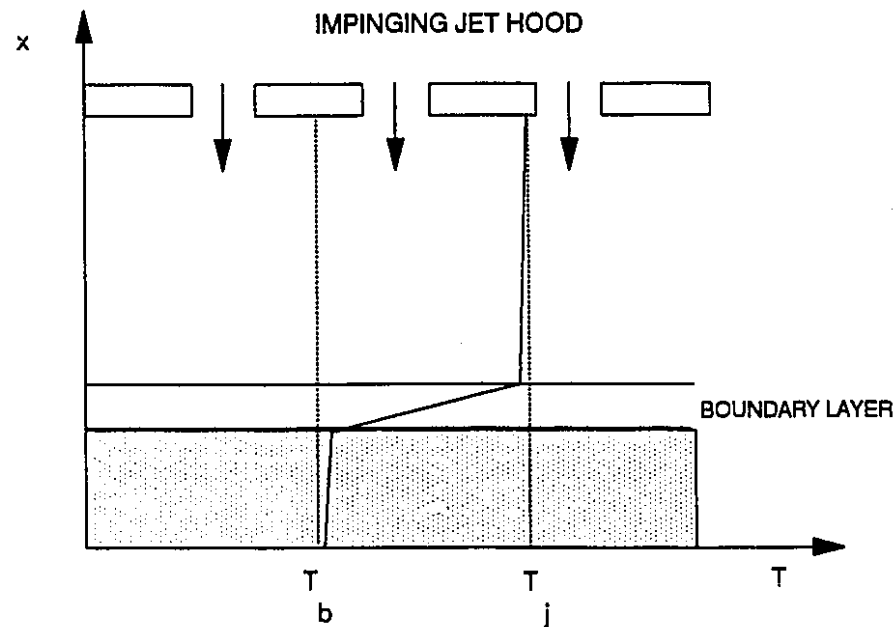
Figure 3.1 - Temperature field during the constant rate period.

As the temperature of the evaporation surface is practically equal to the boiling point, the mass transfer kinetic expression, equation

3.12, is not required to relate the drying rate to measurable variables. The drying rate is controlled by the rate of heat transfer from the impinging jets to the constant temperature surface at T_b. Predicting the drying rate is then reduced to predicting the impinging jet heat transfer coefficient, from which the drying rate is simply obtained as

$$R_{cs} = \frac{h \ (\ T_J \ - \ T_b \ )}{\Delta \ h_v} \tag{3.13}$$

In this section, the results of experiments to investigate the effect of jet flow rate, jet temperature, pulp type and basis weight will be reported, and an overall correlation for the constant drying rate of impingement steam drying of paper will be developed.

3.1.2 Effect of jet flow rate

Current industrial practice for the impinging jet hoods of Yankee dryers is $10,000 \leq Re_J \leq 30,000$. To investigate the effect of jet flow rate on drying rate, kraft paper, $B = 60 \ g/m^2$, was dried in superheated steam at $150 \ ^oC$ and $350 \ ^oC$ in the Reynolds number ranges $2000 \leq Re_J \leq 12000$ ($150 \ ^oC$), $500 \leq Re_J \leq 5000$ ($350 \ ^oC$). The lower bound was set by the ability to accurately measure the flow rate. At $T_J = 350 \ ^oC$, the upper bound was set by the steam superheater capacity. At $T_J = 150 \ ^oC$, since the steam supply line temperature was $156 \ ^oC$ (saturated steam at 790 kPa abs.), it was possible to increase the jet Reynolds number well above the maximum investigated value of 12 000 without superheating. However, at $Re_J = 16 \ 000$ ($u_J = 108.2 \ m/sec$), the drying rate could not be measured as the wet sheet was shredded due to

the intense surface shear stress.

At T_j = 350 °C the results, figure 3.2, are best correlated by distinguishing two flow regimes, for Re_j below and above 1500. Best fit straight line regression gives:

$$\begin{cases} \text{for } Re_j < 1500: & R_{cs} = 1.67 \; Re_j^{0.44} \quad (R^2=0.9984) \\ \text{for } 1500 \leq Re_j \leq 5000: & R_{cs} = 0.275 \; Re_j^{0.69} \quad (R^2=0.9998) \end{cases}$$

At T_j = 150 °C,

for all Re_j: $\qquad R_{cs} = 0.0582 \; Re_j^{0.62} (R^2=0.9989)$
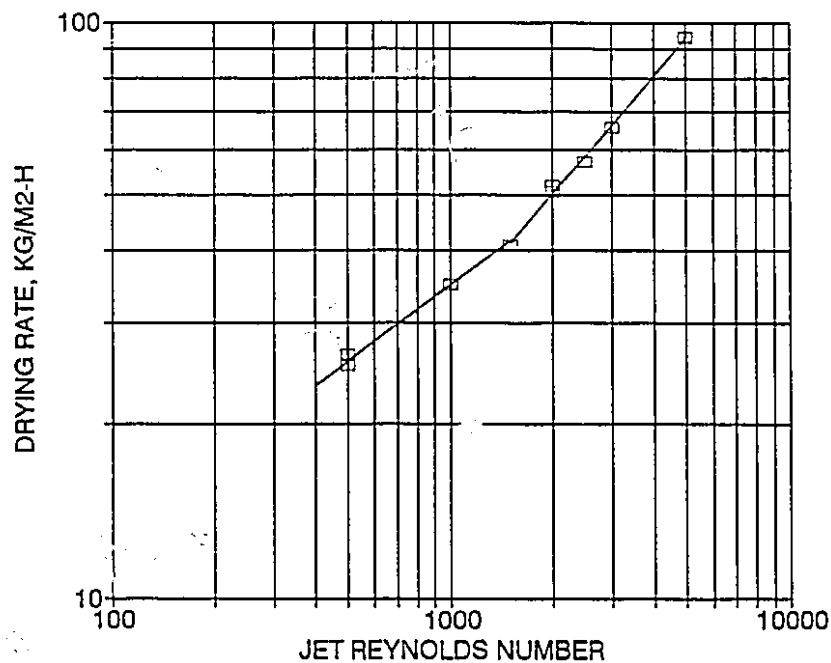
Figure 3.2 - Effect of jet Reynolds number on drying rate: T_j = 350 °C.

The transition at Re_j = 1500 probably indicates change from laminar

to turbulent flow. Mujumdar (1987) estimates the critical Reynolds number for transition from laminar to turbulent flow under impinging jets to be between 1000 and 2000. Kercher and Tabakoff (1969) also noted the existence of a transition point in measurements on an array of circular orifices, but found it to be between 3000 and 4000. The different values of the transition point may be due to the fact that transition depends not only on Re_j but also on the specific geometry and exhaust conditions.

PROPOSED CORRELATION

By forcing the regression exponent to be 1/2, the value accepted for laminar jets, for $Re_j < 1500$ and 2/3, the value proposed by Martin, for $Re_j \geq 1500$, the following regression equations are obtained:

For $Re_j \geq 1500$, $T_j = 150^\circ$ C: $R_{cs} = 0.0389\ Re_j^{2/3}$ $(R^2 = 0.9984)$

$$(3.14)$$

For $Re_j \geq 1500$, $T_j = 350^\circ$ C: $R_{cs} = 0.3187\ Re_j^{2/3}$ $(R^2 = 0.9997)$

$$(3.15)$$

For $Re_j < 1500$, $T_j = 350\ ^\circ$C: $R_{cs} = 1.097\ Re_j^{1/2}$ $(R^2 = 0.9946)$

$$(3.16)$$

Because these expressions fit the results nearly as well as the best fit equations, they are the preferred form and are plotted with the data as figure 3.3.
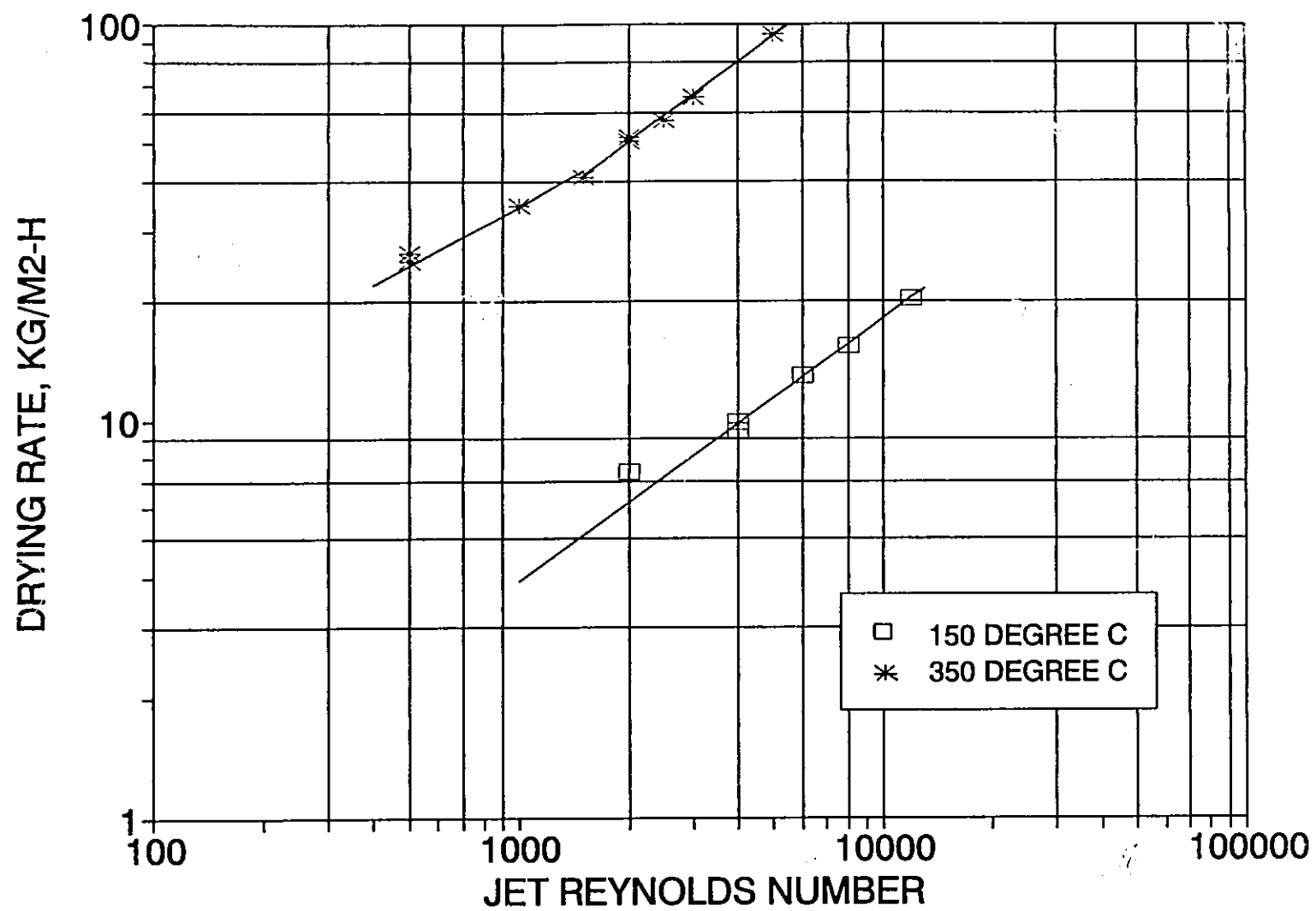
Figure 3.3 Effect of jet Reynolds number on drying rate.

3.1.3 Effect of jet temperature

In high temperature steam drying of paper, the absolute temperature varies between the nozzle exit and the paper surface by a ratio as high as two to one. Thermal conductivity and absolute viscosity vary over this temperature range by approximately the same ratio (appendix 4). Some deviation from linearity in the R_{cs} versus T_j relation at constant Re_j is expected due to the variation in fluid properties across the boundary layer, and to the reduction in heat transfer rate due to evaporation at the boundary layer surface.

The influence of steam jet temperature on drying rate was investigated by drying kraft paper of basis weight 60 g/m^2 at Re_j = 2000 and 150 ^{o}C $\leq T_j \leq$ 465 ^{o}C. The constant drying rate, determined from equation 3.13, can be expressed as

$$R_{cs} = \frac{h \; (geometry, \; C_{ps}, \; Re, \; Pr, \; k) \; \Delta T}{\Delta h_v} \qquad (3.17)$$

Martin's (1977) correlation of the heat transfer rate under an array of round impinging jets, equation 1.1, is expressed in terms of dimensionless geometrical and fluid property groups, properly determined from dimensional analysis. Therefore, the influence of geometry in superheated steam impingement heat transfer can be trusted to follow the pattern found in Martin's study, even though the source heat transfer data were obtained from impinging air jets only. In addition, since the jet conditions are a boundary condition on this system, and since, for turbulent impinging jets, the development of turbulent eddies occurs mostly in the free jet and stagnation flow regions, where temperature is practically equal to the jet exit plane temperature, the flow must be

characterized by the Reynolds number measured at jet exit conditions, Re_j. Thus, equation 3.17 can be rewritten

$$R_{cs} = \left\{ R_1(k, C_{ps}, Pr, \Delta T, \Delta h_v) \right\} \left\{ \frac{F(H/D, f) Re_j^{2/3}}{D} \right\} \quad (3.18)$$

in which R_1 groups all the temperature-dependent factors, followed by the flow and geometric factors. Therefore, the results are presented in figure 3.4 as the effect of jet temperature on the temperature-dependent component of drying rate, R_1:

$$R_1(T) \equiv \frac{R_{cs} D}{F \left[\frac{H}{D}, f \right] Re_j^{2/3}} \quad (3.19)$$

The temperature effects are thus separated from the geometrical and fluid dynamic effects. The results of the experiments described in article 3.1.2, for $Re_j > 1500$, are also included in this figure.

PROPOSED CORRELATION

To show explicitly the effect of variable fluid properties and of evaporation on the drying rate, equation 3.13 can be written

$$R_{cs} = h_j^* \left[\frac{h^*}{h_j^*} \right] \left[\frac{h}{h^*} \right] \frac{(T_j - T_b)}{\Delta h_v} \quad (3.20)$$

where h is the actual heat transfer coefficient in this variable property flow with evaporation, h^* the heat transfer coefficient
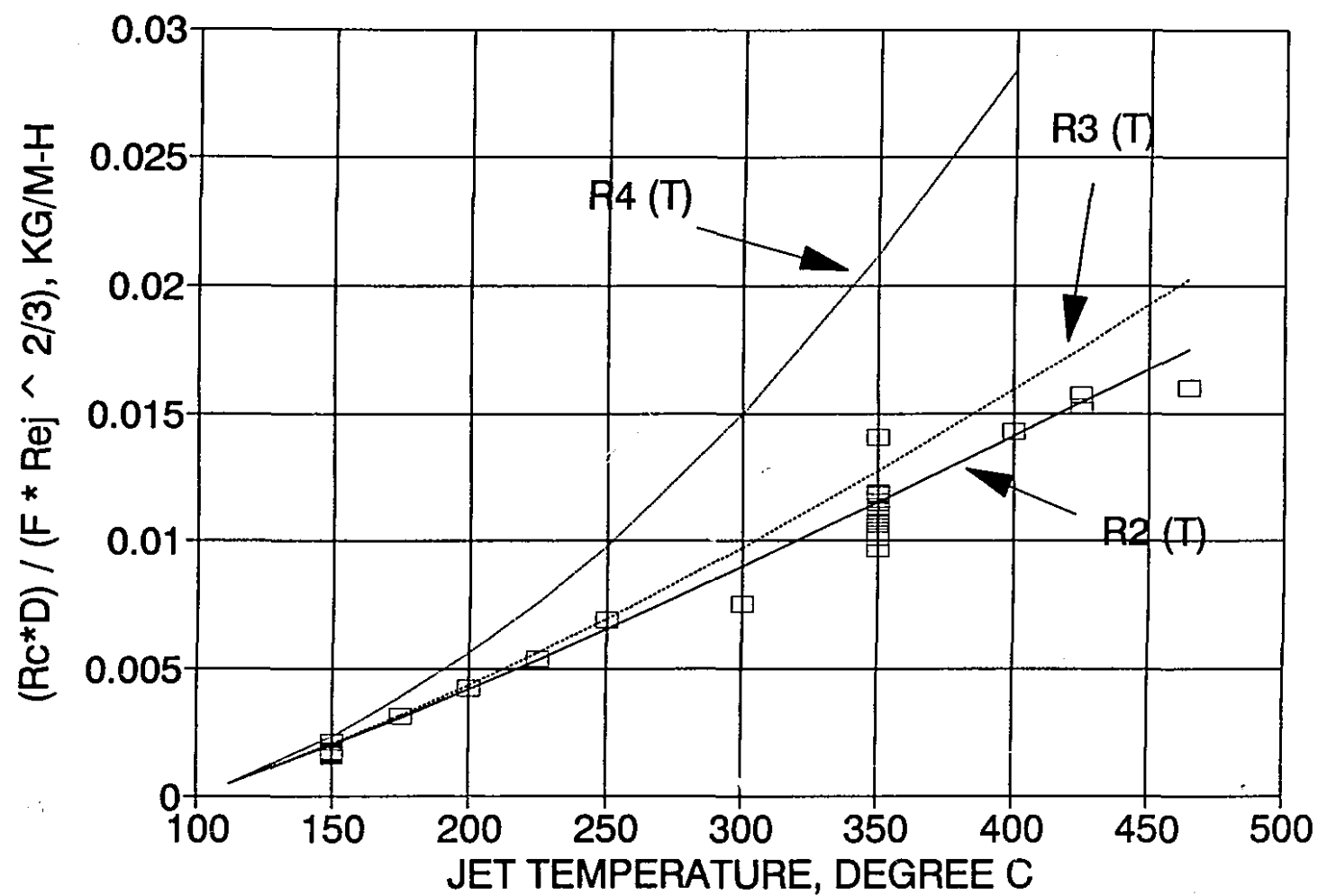
Figure 3.4 Effect of jet temperature on constant drying rate with superheated steam. Experimental data: R1 (T). Predicted rates: R2 (T) – R4 (T).

applicable in this variable property flow if there were no evaporation, and $h_j^\bullet$ the heat transfer coefficient applicable at jet conditions, in the absence of fluid property variation or evaporation. Numerous authors (Chow and Chung, 1983a, 1983b, Martin, 1977, Kays and Crawford, 1980) suggest the Couette flow approximation correction factor to account for the effect of evaporation on the heat transfer rate, i.e.

$$\left[\frac{h}{h^\bullet} \right] = \frac{\ln(1 + B_h)}{B_h} = \frac{\ln\left[1 + \dfrac{C_{ps,f}(T_J - T_b)}{\Delta h_v} \right]}{\dfrac{C_{ps,f}(T_J - T_b)}{\Delta h_v}} \tag{3.21}$$

In the above equation, Δh_v is evaluated at T_b, the evaporation surface temperature. It is uncertain on theoretical grounds, at what temperature C_{ps} should be evaluated. However, as C_{ps} increases only slowly with temperature, e. g. by only 10% between 100 $^\circ$C and 500 $^\circ$C, and as the effect of its variation tends to be canceled by its simultaneous presence in the numerator of the logarithmic factor and in the denominator, this question is of very little practical relevance. For $T_J = 500$ $^\circ$C, the correction factor with C_{ps} evaluated at T_J is only 1.4% higher than at T_b. C_{ps} is evaluated here at the film temperature. Substituting this into equation 3.20 gives

$$R_{cs} = h_j^* \left[\frac{h^*}{h_j^*} \right] \frac{\ln\left[1 + \frac{C_{ps,f}(T_j - T_b)}{\Delta h_v} \right]}{C_{ps,f}} \qquad (3.22)$$

In the absence of an established correlation for the temperature dependence of physical properties in superheated steam impingement heat transfer, the *property ratio* approach (section 1.3.2.2) was applied in the manner suggested by Kays and Crawford (1980) and Das *et al.* (1985). The property ratio was taken as

$$\left(\frac{h^*}{h_j^*} \right) = \left(\frac{T_j}{T_b} \right)^{n_s} \qquad (3.23)$$

The exponent n_s, determined from non-linear regression, was equal to -0.77. The results, presented in figure 3.4 as

$$R_2(T) \equiv k_j \, Pr_j^{0.42} \left[\frac{T_j}{T_b} \right]^{-0.77} \frac{\ln\left[1 + \frac{C_{ps,f}(T_j - T_b)}{\Delta h_v} \right]}{C_{ps,f}} \qquad (3.24)$$

fit the data with a regression coefficient of 0.958.

To illustrate the sensitivity of the predicted heat transfer rate to the transpiration correction, figure 3.4 also shows the expression resulting from dropping the transpiration correction from equation 3.24, i. e.:

$$R_3(T) \equiv k_J \, Pr_J^{0.42} \left[\frac{T_J}{T_b} \right]^{-0.77} \frac{(T_J - T_b)}{\Delta h_v} \qquad (3.25)$$

This expression is seen to overpredict the drying rate by 16% at 465 °C.

Also shown is the expression obtained by evaluating all physical properties (including those in the Reynolds number) at the 1/3 rule reference temperature, following the work of Chow and Chung (article 1.3.3), i. e.:

$$R_4(T) \equiv k_{1/3} \, Pr_{1/3}^{0.42} \left[\frac{\nu_J}{\nu_{1/3}} \right] \frac{\ln \left[1 + \frac{C_{ps,f}(T_J - T_b)}{\Delta h_v} \right]}{C_{ps,f}} \qquad (3.26)$$

This expression overpredicts the drying rate significantly at all temperatures, indicating that the results of the flat-plate boundary layer analysis of these authors cannot be extrapolated to the situation of an impinging jet. If it had been necessary, prior to the present work, to make the best estimate possible of the rate of drying paper under high temperature jets of superheated steam, that estimate would have incorporated R_4 (T) as the temperature dependent component of an equation for predicting drying rate, as this expression incorporates the best estimate known for the effect of evaporation on heat transfer rate and uses the method of treating temperature dependent physical properties recommended by a study of drying with superheated steam. The fact that, for a jet temperature of 400 °C, such a prediction would have overestimated by 100 % the actual drying rate found here, is a measure

of the necessity of making the experimental measurements of the present
investigation for industrial modelling of this new process.

3.1.4 Effect of basis weight and type of pulp

Experiments were done to investigate the effect of basis weight and
type of pulp on the drying rate. Table 3.1 shows the comparison of
drying rates in pairs of experiments done under identical jet
temperature and Reynolds number, with different basis weights and/or
pulp types. No significant effect of the basis weight or pulp type is
observed. This confirms that the rate-determining step for constant rate
drying is the resistance to heat transfer in the boundary layer above
the wet surface of the sheet.

PULP TYPE	BASIS WEIGHT (G/M^2)	JET REYNOLDS NUMBER	JET TEMPERATURE (°C)	DRYING RATE (KG/M^2-H)
TISSUE	35	2000	350	42.2
TISSUE	100	2000	350	41.9
KRAFT	60	2000	350	35.6
KRAFT	100	2000	350	36.3
TMP	48.8	2000	425	56.3
TMP	60	2000	425	58.0
KRAFT	60	2000	150	6.4
TMP	48.8	2000	150	7.8

Table 3.1 - Effect of paper type and basis weight on drying rate.

66

In drying paper made of a TMP black spruce pulp, it was found that boiling either within or below the sheet caused formation of a steam pocket which lifted the sheet off the surface of the sample holder by as much as 10 mm. To prevent this phenomenon, which alters the heat transfer conditions, 5 cm long slits, 1 cm apart, were cut across the the wet sheet, providing an outlet for steam evolved beneath the sheet. The drying rates listed in table 3.1 were obtained using this technique. The problem of lifting of the sheet did not occur in air, and indicates that, for industrial impingement steam drying of TMP paper, special means of bonding the sheet firmly to the roll, such as higher sheet tension, adhesives or a porous roll, may be necessary.

3.1.5 Overall correlation for impingement steam drying rate

By combining equations 3.19 and 3.24, and taking into account the fact that the drying rate was observed to be proportional to $Re_j^{1/2}$ for $Re_j < 1500$ and to $Re_j^{2/3}$ above, the following expressions are obtained to correlate all drying rate results:

For $Re_j < 1500$,

$$R_{cs} = 3.38 \ k_j \ Pr_j^{0.42} \left[\frac{T_j}{T_b} \right]^{-0.77} \frac{F \ (H/D, \ f)}{D} \ Re_j^{1/2} \ \frac{\ln \left[1 + \frac{C_{ps,f} \ (T_j - T_b)}{\Delta h_v} \right]}{C_{ps,f}}$$

$$(3.27)$$

For $Re_j > 1500$,

$$R_{cs} = k_j \ Pr_j^{0.42} \left[\frac{T_j}{T_b} \right]^{-0.77} \frac{F \ (H/D, \ f) \ Re_j^{2/3}}{D} \ \frac{\ln \left[1 + \frac{C_{p\,,f} \ (T_j - T_b)}{\Delta h_v} \right]}{C_{p\,,f}}$$

$$(3.28)$$

The factor $3.38 = 1500^{2/3-1/2}$ in equation 3.27 arises from the requirement that the two expressions be equal at $Re_j = 1500$.

Figure 3.5 shows the agreement between the experimental results and the above drying rate expressions. The standard error is 12% of the mean value. This figure includes a number of experiments in addition to those shown in figures 3.3 and 3.4 and table 3.1, performed under conditions which do not correspond to those categories. A complete listing of impingement drying experiments is included as Appendix 1.

The measurements of Cui et al. (1985), in an apparatus with a different geometry (H = 13 mm, D = 3 mm, f = 1.77%), under the limited range of conditions 60 m/s < u_j ≤ 100 m/s at T_j = 220 °C (4800 < Re_j ≤ 7900) and 190 < T_j < 230 °C at u_j = 77 m/s (5900 < Re_j ≤ 7000), are seen on figure 3.5 to be also well described by equation 3.28. Cui et al. correlated their data using Chance's (1974) expression for the Nusselt number, and evaluating all properties at the jet temperature, without accounting for the temperature dependence of fluid properties. While their results are well correlated by equation 3.28, it is not possible to compare the validity their approach with that of equation 3.28 outside the relatively narrow range of conditions of this previous study.
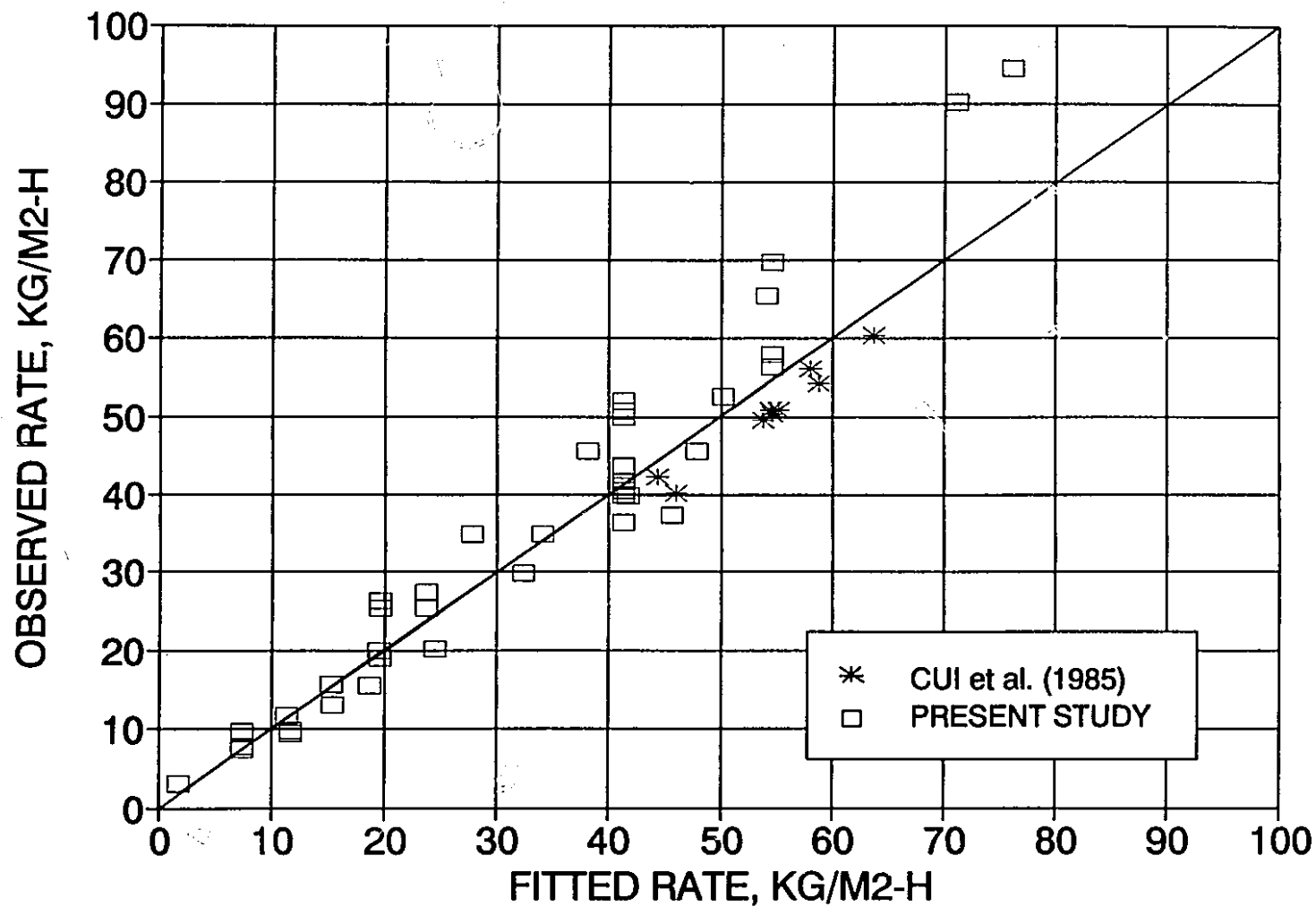
Figure 3.5 Constant drying rate with impinging jets of superheated steam: measurements and correlation.

Thus the drying rate during the constant rate period of superheated steam drying is successfully described by using Martin's correlation for heat transfer from an array of impinging jets, suitably modified for laminar flow below Re_j = 1500, evaluating thermal conductivity at the film temperature and the jet Reynolds number at the jet temperature, and incorporating the Couette flow approximation correction factor to account for the effect of evaporation on mass transfer.

3.2 AIR DRYING

3.2.1 Mechanism of constant rate air drying

Drying paper by turbulent impinging jets of air involves countercurrent transfer of heat, as a result of temperature difference, and mass, as a result of concentration difference. After a short heating-up period, the dry air – wet paper system comes to an equilibrium in which water is removed at a constant rate, as the driving potentials and conductances for heat and mass transfer remain constant. This equilibrium continues until internal water transport no longer suffices to keep the surface completely wetted, at which point the falling rate period begins.

Determining the constant drying rate involves solving simultaneously the heat and mass transfer equations:

$$R_{ca} = \frac{h \ (T_j - T_s)}{\Delta h_v} \tag{3.29}$$

$$R_{ca} = k_g \ (Y_s - Y_j) \tag{3.30}$$

Equations 3.29 and 3.30 yield a simple relationship between the humidity and temperature differences:

$$(T_j - T_s) = \frac{k_g \, \Delta h_v}{h} (Y_s - Y_j) \qquad (3.31)$$

The specific case of simultaneous heat and mass transfer for the air-water system leads to the Lewis (1922) relation:

$$\frac{h}{k_g} = C_{py} \qquad (3.32)$$

Substituting this relation into equation 3.31 yields

$$C_{py} (T_j - T_s) = (Y_s - Y_j) \, \Delta h_v \qquad (3.33)$$

the relationship between the dry bulb and adiabatic saturation temperatures. This relationship yields a considerable simplification in the analysis, as one may compute the drying rate from the heat transfer equation alone, with surface temperature set equal to the adiabatic saturation temperature, a system property available from psychrometric charts. Thus the drying rate becomes:

$$R_{ca} = \frac{h \, (T_j - T_{a.s.})}{\Delta h_v} \qquad (3.34)$$

There is uncertainty concerning the value of the heat transfer

coefficient because of the lack of data for simultaneous heat and mass transfer under turbulent impinging jets at large temperature differences. As in steam drying, air properties change significantly from the nozzle exit to the paper surface. In addition, fluid property variations arise due to concentration changes across the boundary layer. Furthermore, a decrease in heat transfer coefficient is expected because of evaporation at the impingement surface. The results of Das *et al.* under turbulent air jets with large temperature differences are not directly applicable to the present case, as they were obtained with pure heat transfer. Neither is Martin's correlation reliable for the present case as the source data were obtained under small temperature differences.

In the absence of reliable correlations, drying experiments were performed under turbulent impinging jets of air in the range of jet temperature and Reynolds numbers, $20\ ^{\circ}C \leq T_j \leq 400\ ^{\circ}C$, $1500 \leq Re_j \leq 8000$.

3.2.2 Evaporation surface temperature

To determine whether the Lewis relation applies in drying under high temperature turbulent impinging air jets, the sheet temperature was measured by a 75-μm diameter thermocouple sandwiched between the bottom of the sheet and the glass surface of the sample holder. The sheet bottom temperature was determined as the average value of readings during the constant rate period plateau, figure 2.10. Because the thermal conduction resistance across the sheet is small during this period, the sheet bottom temperature closely approaches that of the evaporation surface.

72

In figure 3.6, the sheet bottom temperature, and the adiabatic saturation temperature for dry air determined from the solution of equation 3.33 with fluid properties as given in appendix 4, are plotted versus the jet temperature. Sheet temperature is close to the adiabatic saturation temperature up to T_j = 200 °C, falling slightly lower at higher values of T_j, due to heat loss to the sample holder, as detailed in appendix 3. From this reasonable agreement, it is concluded that the Lewis relation applies satisfactorily for the case of drying under turbulent impinging air jets.
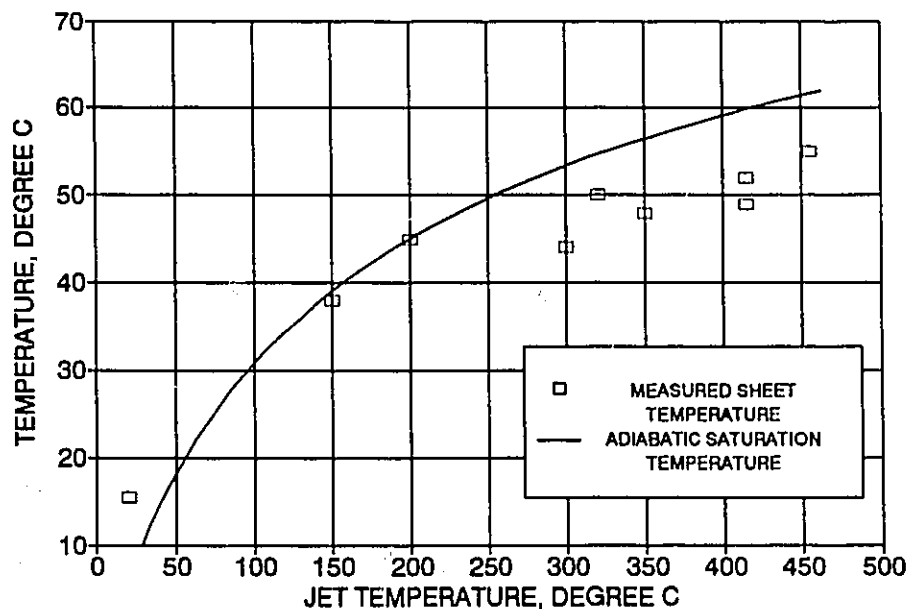
Figure 3.6 - Sheet bottom temperature during the constant rate
period of air drying.

3.2.3 Effect of jet temperature

The effect of jet temperature was investigated by drying kraft

paper, with basis weight 60 g/m^2, in air at three Reynolds numbers:

$$\text{For } Re_j = 2000: \quad 20 \text{ }^{\circ}C \leq T_j \leq 400 \text{ }^{\circ}C$$

$$\text{For } Re_j = 4000: \quad 20 \text{ }^{\circ}C \leq T_j \leq 350 \text{ }^{\circ}C$$

$$\text{For } Re_j = 8000: \quad 20 \text{ }^{\circ}C \leq T_j \leq 150 \text{ }^{\circ}C$$

A numerical simulation of heat transfer in the sample holder, described in detail in appendix 3, showed that the measured air drying rate is substantially lowered by transient conduction heat losses from the sheet to the sample holder. A correction factor was defined as the ratio of the adiabatic heat flux to the evaporation front (that which would occur in the absence of conduction heat loss) to the net heat flux (that which takes conduction heat losses into account). By multiplying the observed drying rate by this correction factor, a drying rate corrected for the effect of conduction heat losses was obtained. (In steam drying, heat loss to the sample holder considerably increased the duration and amount of condensation at the beginning of an experiment, but no such drying rate correction was necessary because this transient phenomenon was dissipated when the constant rate period began.)

Although the temperature dependence of drying rate cannot be obtained from existing correlations, the geometric and Reynolds number dependences found by Martin should apply to the present situation. Therefore, the experimental results are presented in figure 3.7 as $R_1 (T) = (R_{ca} D) / F (H/D, f) Re_j^{2/3})$, as for steam drying, figure 3.4. The validity of this approach is supported by the fact that the results for the three Reynolds numbers collapse on a single curve.
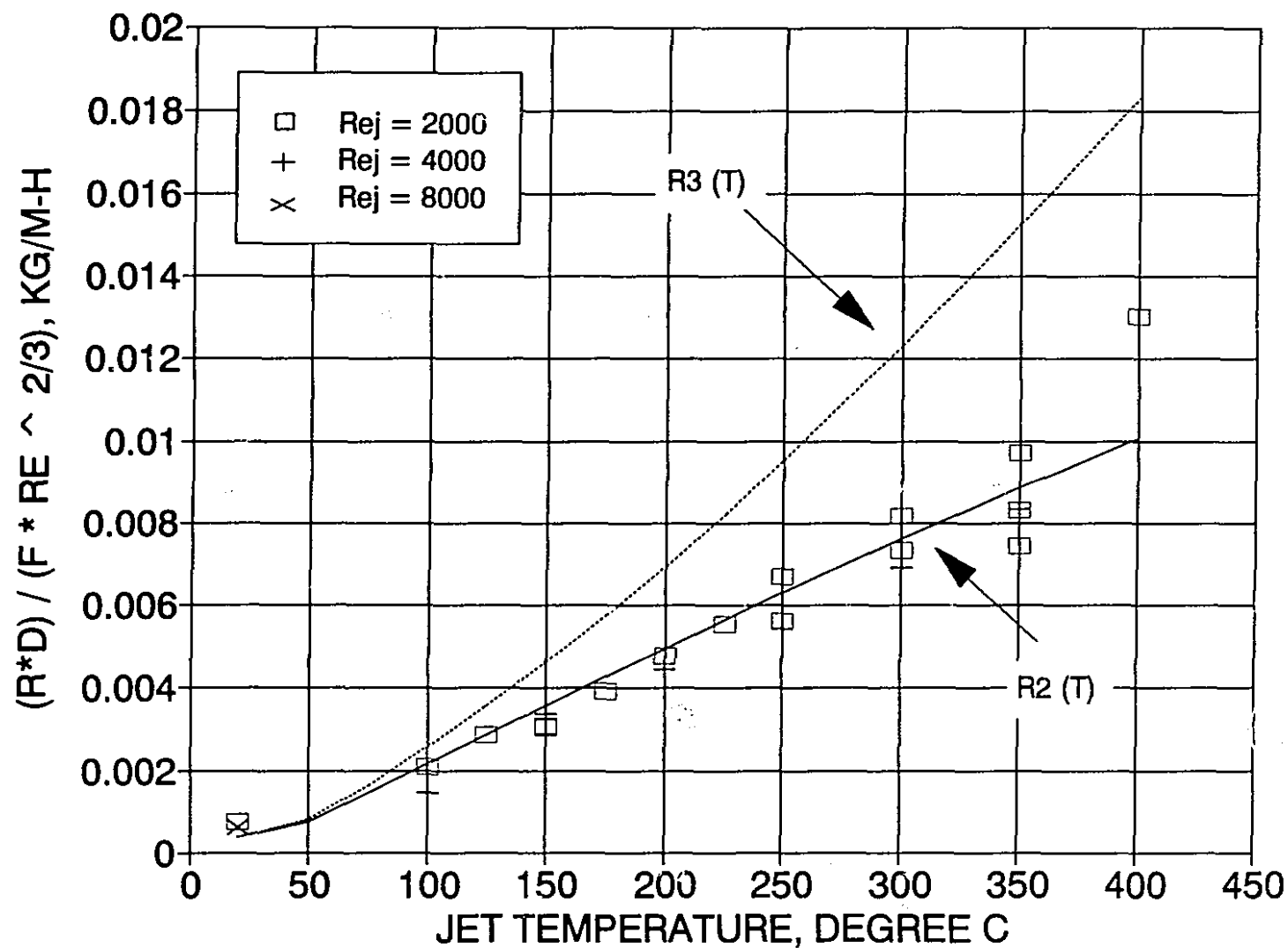
Figure 3.7   Effect of jet temperature on constant drying rate with air.
Corrected experimental data: R1 (T). Predicted rates: R2 (T) – R3 (T).

PROPOSED CORRELATION

As for steam drying, the experimental results were correlated by accounting for the fluid property variation by the property ratio method, and accounting for the effect of evaporation by the Couette flow approximation correction factor, with the latent heat of evaporation now evaluated at the adiabatic saturation temperature:

$$R_2(T) \equiv k_j \, Pr_j^{0.42} \left[\frac{T_j}{T_{a.s.}} \right]^{-0.96} \frac{\ln \left[1 + \frac{C_{ps,f}(T_j - T_{a.s.})}{\Delta h_v} \right]}{C_{ps,f}} \qquad (3.35)$$

Figure 3.7 shows the agreement between this expression and the experimental results, with a regression coefficient of 0.90. Also shown for comparison is the expression

$$R_3(T) = k_j \, Pr_j^{0.42} \left[\frac{T_j}{T_{a.s.}} \right]^{-0.11} \frac{\ln \left[1 + \frac{C_{ps,f}(T_j - T_{a.s.})}{\Delta h_v} \right]}{C_{ps,f}}$$

$$(3.36)$$

in which all properties are computed at the jet temperature and the result is multiplied by the property ratio $(T_j / T_{a.s.})^{-0.11}$ determined by Das *et al.* for pure heat transfer at high values of ΔT. The large variation between these expressions illustrates the sensitivity of the predicted heat transfer rate to the temperature and composition dependence of the fluid properties.

The different values of the exponent of the jet-to-surface temperature ratios in the property ratio expressions, equation 3.24, 3.35 and 3.36, shown here in table 3.2, are readily explained by differences in the nature of each process. In pure heat transfer under

PROCESS	PROPERTY RATIO EXPONENT, n
Pure heat transfer with impinging air jets (Das *et al.*, 1985):	-0.11
Constant rate drying by impinging jets of superheated steam (present study):	-0.77
Constant rate drying by impinging jets of air (present study):	-0.96

Table 3.2   Property ratio exponents in transport processes under impinging jets with large temperature differences.

impinging air jets, only the temperature difference across the boundary layer reduces the heat transfer coefficient compared to its constant property value at the jet temperature. In drying by impinging jets of superheated steam, the effect of property variation is stronger because of the higher temperature sensitivity of thermal conductivity for steam than for air, appendix 4. The strongest influence is seen in combined heat and mass transfer under impinging air jets, as both temperature and composition change due to the intense flux of cool water vapor at the bottom of the boundary layer.

The complete expression for the constant drying rate under impinging jets of air is:

$$R_{ca} = k_j \, Pr_j^{0.42} \left[\frac{T_j}{T_{a.s.}} \right]^{-0.96} \frac{F\,(H/D,\ f)}{D} \, Re_j^{2/3} \, \frac{\ln \left[1 + \dfrac{C_{ps,f}(T_j - T_{a.s.})}{\Delta h_v} \right]}{C_{ps,f}}$$

$$\text{(3.37)}$$

3.3 COMPARISON BETWEEN STEAM AND AIR DRYING

3.3.1 Inversion temperature

Standard practice has been to compare air and steam drying rates on the basis of equal mass flux, a quantity whose value can be determined without ambiguity regardless of fluid property variations. By formulating the drying rate expressions, equations 3.28 and 3.37, in terms of the impinging jet mass flux

$$N_j = \frac{f \, \mu_j \, Re_j}{D} \qquad\qquad \text{(3.38)}$$

and grouping all temperature-dependent properties on one side, the following expressions are obtained for steam and air, respectively:

$$R'_{cs} \equiv \frac{R_{cs} \, D^{1/3}}{F(H/D,\ f)} \left[\frac{f}{N_{js}} \right]^{2/3} = \frac{k_{s,j} \, Pr_{s,j}^{0.42}}{\mu_{s,j}^{2/3}} \left[\frac{T_j}{T_b} \right]^{-0.77} \frac{\ln \left[1 + \dfrac{C_{ps,f}\,(T_j - T_b)}{\Delta h_v} \right]}{C_{ps,f}}$$

$$\text{(3.39)}$$

$$R'_{ca} \equiv \frac{R_{ca}\, D^{1/3}}{F(H/D,\ f)} \left[\frac{f}{N_{ja}}\right]^{2/3} = \frac{k_{a,J}\, Pr_{a,J}^{0.42}}{\mu_{a,J}^{2/3}} \left(\frac{T_J}{T_{a.s.}}\right)^{-0.96} \frac{\ln\left[1 + \dfrac{C_{ps,f}(T_J - T_{a.s.})}{\Delta h_v}\right]}{C_{ps,f}}$$

<div align="right">(3.40)</div>

The subscripts s, for steam and a, for air, have been added to the fluid properties at this stage, to avoid possible confusion. Only the turbulent ($Re_J > 1500$) expression is considered for steam drying, as it is of more practical importance.

The significance of these expressions, plotted versus temperature in figure 3.8, is easily understood by considering the ratio of equations 3.39 and 3.40:

$$\frac{R'_{cs}}{R'_{ca}} = \frac{\dfrac{R_{cs}\, D^{1/3}}{F(H/D,\ f)}\left[\dfrac{f}{N_{js}}\right]^{2/3}}{\dfrac{R_{ca}\, D^{1/3}}{F(H/D,\ f)}\left[\dfrac{f}{N_{ja}}\right]^{2/3}}$$

<div align="right">(3.41)</div>

For a steam and an air dryer with the same geometry (H, D, f) and with the same mass flux ($N_{js} = N_{ja}$), the ratio of two points at the same temperature on figure 3.8, R'_{cs}/R'_{ca}, is equal to the ratio of the constant drying rates, R_{cs}/R_{ca}. This is true for any mass flux and any dryer geometry to which Martin's correlation applies, including, for instance, that determined by Martin to be optimal as it maximizes the
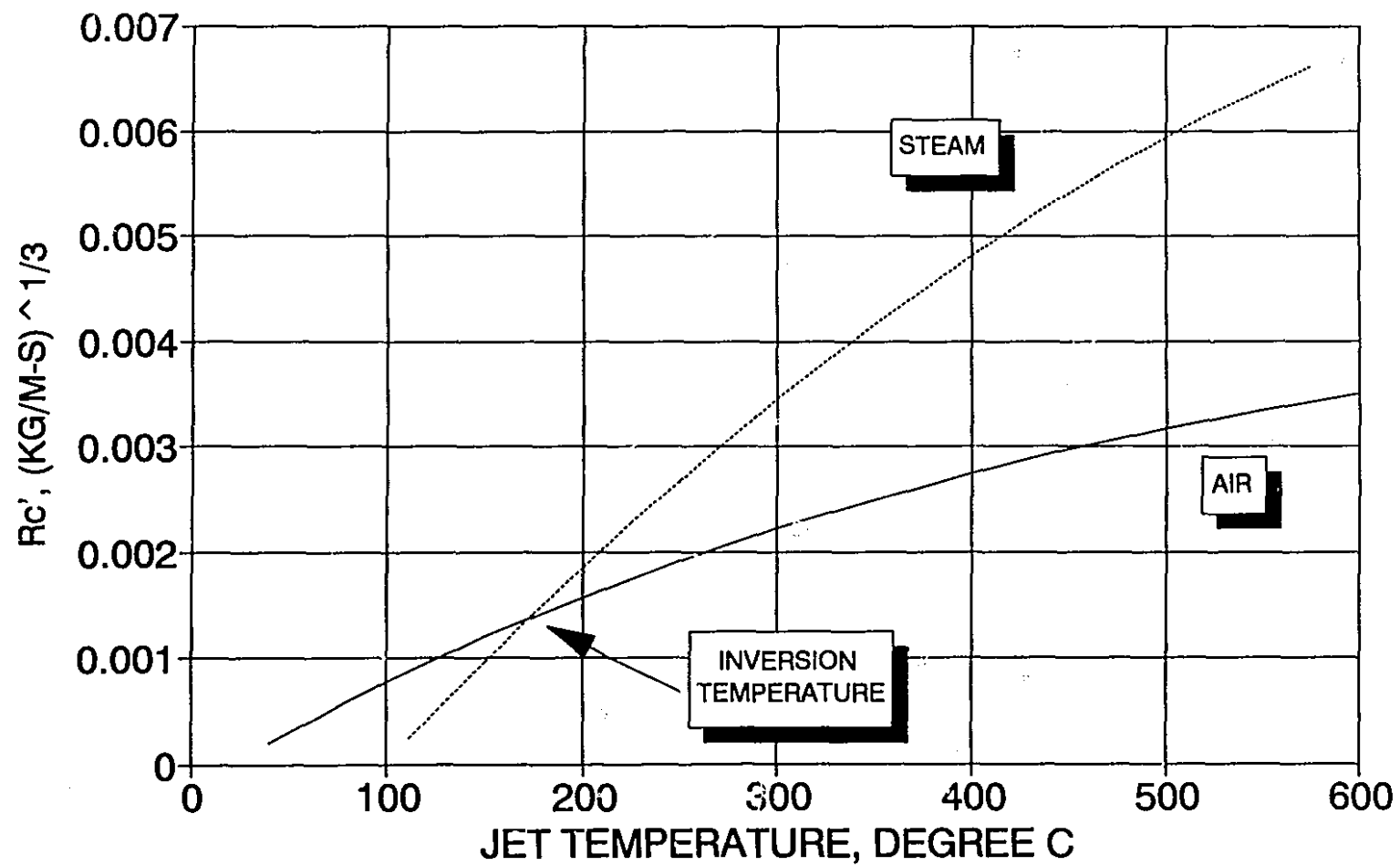
Figure 3.8   Effect of jet temperature on drying rate in superheated steam and air, at equal mass flux of the drying fluid.

heat transfer rate per unit blower power (H/D = 5.43, f =1.5%).

The comparison shows that for equal mass fluxes of steam and air in a given dryer geometry, drying rate is lower in steam than air below a given point, called the *inversion temperature*, and higher above. The inversion temperature arises because of the interplay between two competing factors. For a given jet temperature, the temperature difference, ΔT, is higher with air than with steam, $(T_j - T_{a.s.})$ versus $(T_j - T_b)$; however, the heat transfer coefficient, being proportional to $k\, Pr^{0.42}/\mu^{2/3}$, is higher with steam. At jet temperatures around the boiling point, the difference in ΔT dominates, making the air drying rate higher. As jet temperature increases, however, the difference in ΔT becomes relatively smaller, and the steam drying rate is higher due to the higher h. The experimentally determined value of 175 $^{\circ}$C is at the low end of the range obtained in other measurements or calculations of the inversion temperature, as can be seen in table 3.3:

AUTHOR	TYPE OF STUDY	DESCRIPTION	FLOW REGIME	INVERSION TEMPERATURE ($^{\circ}$C)
Al-Taleb et al. [1987]	Theoretical	Flow over a stretching surface	Laminar	225
Chow and Chung [1983a]	Theoretical	Flow over a flat plate	Laminar	250
Hasan et al. [1986]	Theoretical	Co-current liquid and gas flows	Laminar	230 - 260
Ramamurthy [1991]	Experimental	Drying of Al_2O_3 by impinging jets	Laminar	218 - 230
Haji and Chow [1988]	Experimental	Flow over a flat plate	Turbulent	190
Yoshida and Hyodo [1970]	Experimental	Flow over a flat plate enclosed by a duct	Turbulent	160 - 175
Present study	Experimental	Drying of paper by impinging jets	Turbulent	175

Table 3.3 - Determinations of inversion temperature

In equations 3.39 and 3.40, the dynamic viscosity appears in the denominator at the power of the Reynolds number dependence of the Nusselt number. As this power is higher in turbulent flow (Nu $\propto$ Re$^{2/3}$) than in the laminar case (Nu $\propto$ Re$^{1/2}$), the impact of the lower viscosity of steam is stronger in turbulent than in laminar flow, explaining why the inversion temperature is lower in turbulent flow.

An inversion temperature is also observed in fluidized bed drying using air or superheated steam, in which thermodynamic equilibrium is reached at the bed exit. Faber *et al.* (1985) and Sheikholeslami (1990) have measured its value to be about 160 °C. This "thermodynamic" inversion temperature, arising from the equality of the drying potentials, equation 1.12, is quite different from the "kinetic" inversion temperature measured in the studies described in table 3.3, which depends on the transport properties. The closeness of the values of the two inversion temperatures is coincidental.

3.3.2 Blower power

For the design of industrial impingement dryers, an economic basis for comparing steam and air drying rates is that of equal blower power per unit heat transfer area. While the total energy (as heat and work) which must be added to the drying fluid per unit water evaporated is the same for steam and air, comparison on the basis of equal blower power is warranted by the fact that one unit of work is generally costlier than one unit of heat (cf. table 5.1). Blower power is the pressure generated by the blower times the volumetric flow rate. Equating the blower pressure to the pressure drop across the nozzle, i. e., neglecting other pressure losses, the blower power per unit area is

$$P_b = (c_d \frac{1}{2} \rho_j u_j^2) (u_j f) \qquad (3.42)$$

By formulating the drying rate expressions, equations 3.28 and 3.37, in terms of the blower power and grouping all temperature-dependent properties on one side, the following expressions

are obtained for steam and air, respectively:

$$R''_{cs} \equiv \frac{R_{cs} D^{1/3}}{F(H/D, \ f)} \left[\frac{c_d \ f}{P_{bs}} \right]^{2/9}$$

(3.43)

$$= 2^{2/9} \frac{\rho_{s,j}^{4/9}}{\mu_{s,j}^{2/3}} \ k_{s,j} \ Pr_{s,j}^{0.42} \left[\frac{T_j}{T_b} \right]^{-0.77} \frac{\ln \left[1 + \frac{C_{ps,f} \ (T_j - T_b)}{\Delta h_v} \right]}{C_{ps,f}}$$

$$R''_{ca} \equiv \frac{R_{ca} D^{1/3}}{F(H/D, \ f)} \left[\frac{c_d \ f}{P_{ba}} \right]^{2/9}$$

(3.44)

$$= 2^{2/9} \frac{\rho_{a,j}^{4/9}}{\mu_{a,j}^{2/3}} \ k_{a,j} \ Pr_{a,j}^{0.42} \left[\frac{T_j}{T_{a.s.}} \right]^{-0.96} \frac{\ln \left[1 + \frac{C_{ps,f} (T_j - T_{a.s.})}{\Delta h_v} \right]}{C_{ps,f}}$$

In a manner similar to figure 3.8, the ratio of two points at the same temperature on figure 3.9, R''_{cs}/R''_{ca}, is equal to the ratio of the constant drying rates, R_{cs}/R_{ca} in a steam and an air impingement dryer with the same blower power per unit area and the same geometry. The comparison shows a behavior similar to that observed for the constant mass flux comparison. In the temperature range of greatest industrial
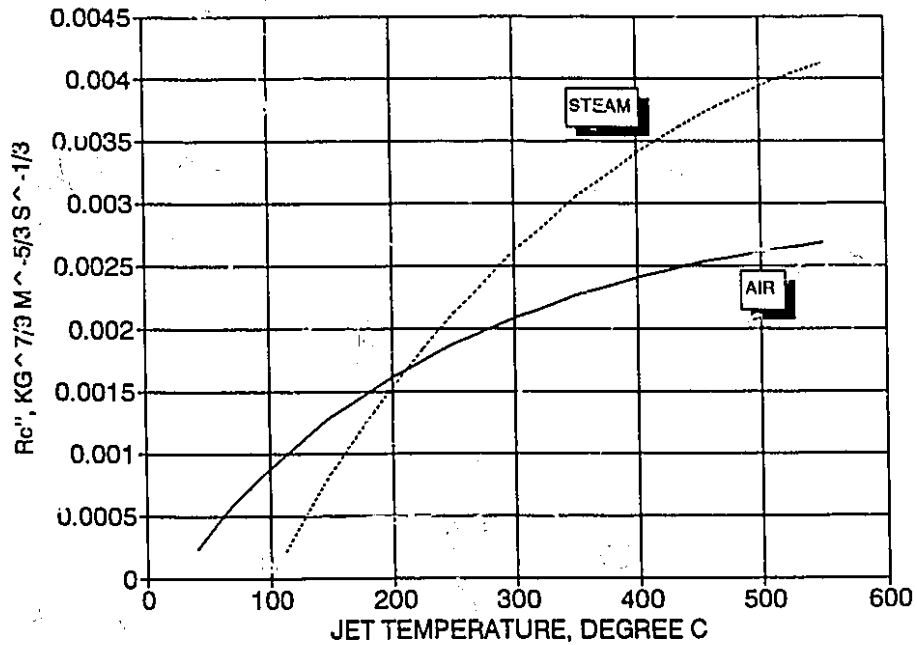
Figure 3.9 - Effect of jet temperature on drying rate in superheated
steam and air, for equal blower power.

interest, say, 300 °C - 500 °C, the drying rate is 30 to 50% higher in

steam than in air for equal blower power in a given dryer geometry.

Because one important potential application of impingement steam

drying of paper is the conversion of Yankee tissue dryers from air to

steam operation, it is interesting to compare the blower power required

to obtain a given drying rate with the two fluids. Transforming

equations 3.43 and 3.44 to obtain p_b explicitly, the following

expressions for specific blower power are obtained for steam and air:

$$p'_{bs} \equiv \frac{P_{bs}}{c_d \, f} \left[\frac{F(H/D, \, f)}{R_s \, D^{1/3}} \right]^{9/2} \qquad (3.45)$$

$$p'_{ba} \equiv \frac{P_{ba}}{c_d \ f} \left[\frac{F(H/D, \ f)}{R_a \ D^{1/3}} \right]^{9/2} \tag{3.46}$$

In a manner similar to figures 3.8 and 3.9, the ratio of two points at the same temperature on figure 3.10, p'_{bs}/p'_{ba}, is equal to the ratio of the blower power per unit area, p_{bs}/p_{ba} in a steam and an air impingement dryer with the same constant drying rate and the same geometry. The comparison shows that for equal drying rates in a given dryer geometry, the blower power required for steam drying is only of 36 % that required with air at 300 $^{\circ}$C and only 15 % at 500 $^{\circ}$C. Considerable blower power savings are possible in drying with superheated steam, compared to air.

3.4 CONCLUSION

Study of the kinetics of evaporation of liquid water into its pure vapor shows that the evaporation surface remains practically at the boiling point during the constant rate period of superheated steam impingement drying. Therefore, the constant drying rate is determined solely by the rate of heat transfer from the impinging jets. This rate is successfully described by a standard correlation for impinging jet heat transfer, with steam properties evaluated at the jet temperature, incorporating the Couette flow approximation correction factor to account for evaporation, and using a property ratio to account for the variation of fluid properties. In impingement air drying, the evaporation surface is at the adiabatic saturation temperature. The constant drying rate is described by a correlation similar to that for
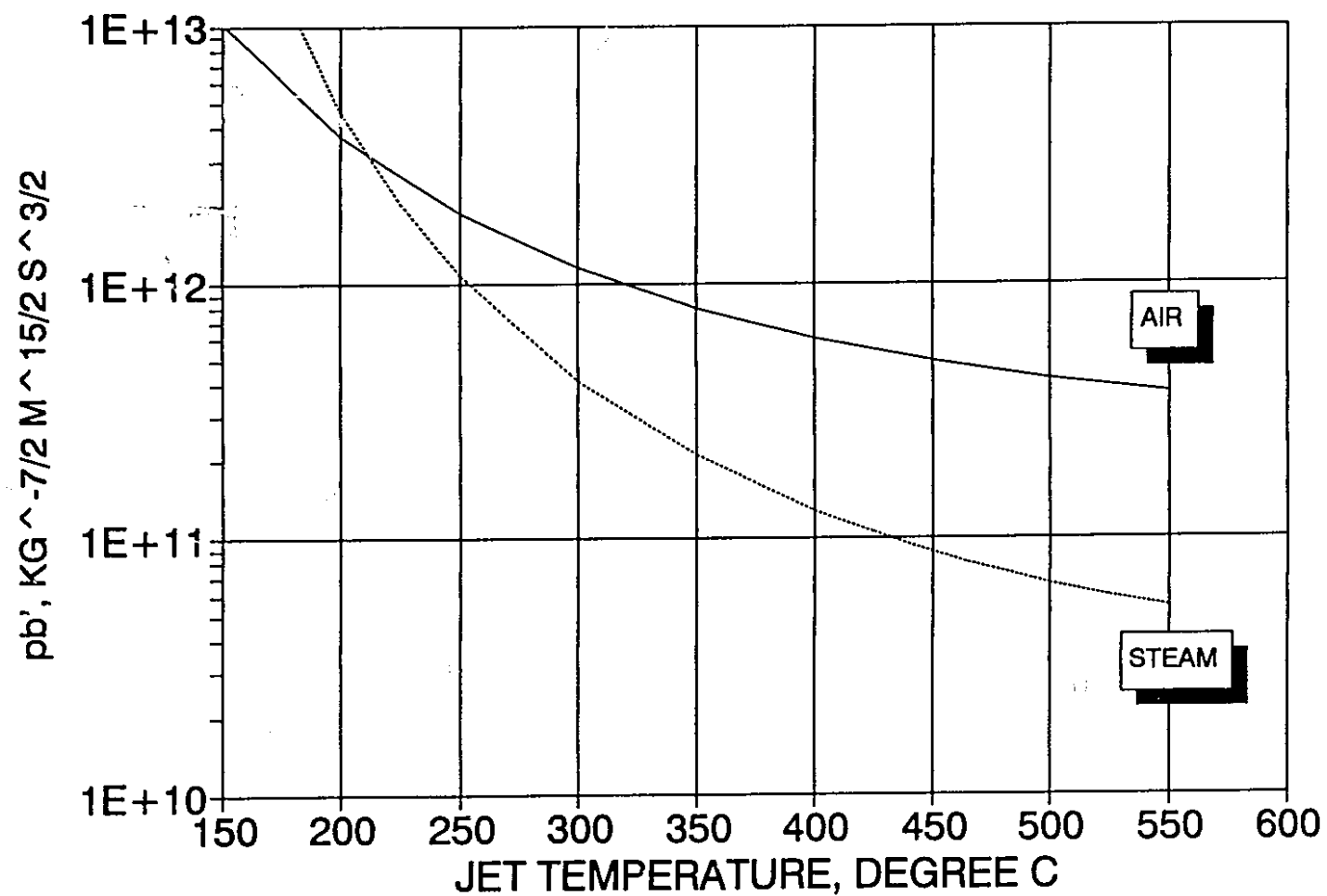
Figure 3.10   Effect of jet temperature on specific blower power
for steam and air impingement drying

steam drying, but the influence of the variation of fluid properties is stronger due to the intense flux of cool water vapor at the bottom of the boundary layer.

The higher drying rate for impingement drying in superheated steam above the inversion temperature of about 175 °C, translates into smaller dryers than for operation with air as the drying medium. The lower blower power for impingement drying in superheated steam translates into reduced operating cost relative to air as the drying medium. These advantages are now quantitatively determined for the constant rate segment of an impingement dryer, a major component in impingement drying of paper. Analysis of the falling rate period, to complete this perspective of paper drying, follows next.

CHAPTER 4

FALLING RATE DRYING

4.1 Introduction

As is generally observed in drying, a falling rate period follows the constant rate period when drying paper by impinging jets of superheated steam. Below a certain moisture content, the drying rate is no longer controlled solely by external transport in the boundary layer: resistance to internal transport within the sheet becomes important and as a result, the drying rate decreases significantly. For superheated steam drying of paper to be suitable industrially, the final moisture content attainable should be acceptably low, and the drying rate during the falling rate period acceptably high. The falling rate period of superheated steam drying of paper was therefore investigated experimentally from this perspective.

Two hypotheses can be formulated to explain the existence of the falling rate period. The first is additional resistance to heat and mass transfer within the sheet as the evaporation front recedes from the surface. The second is a decrease in the equilibrium vapor pressure due to adsorption of water on the fibres. This chapter describes measurements made to identify the role played by each phenomenon, both in steam and in air drying under an array of impinging jets, so as to characterize the falling rate period.

Theoretical work on drying of sheet materials under conditions similar to those of impingement drying (section 1.3.4), especially by Suzuki et al. (1977), gives some insight into the possible mechanisms. Initially, diffusion of liquid moisture through the porous sheet

89

suffices to keep the sheet surface wet, and evaporation takes place at a constant rate. As drying proceeds, the local moisture content gradients diminish, and therefore, so does the moisture flux. The critical condition is reached when the moisture content at the sheet surface falls to zero. From that point on, the evaporation front recedes beneath the surface of the sheet. The drying rate decreases as a result of the additional resistance to heat and vapor transfer of the dry layer between the sheet surface and the evaporation front. The position of this front depends both on the evaporation rate and on the rate of moisture diffusion.

From this existing theoretical analysis, it appears that the falling rate period of impingement steam drying is a highly complex process, involving moisture transport within the sheet, vapor transport from the evaporation front to the sheet surface and from there across the external boundary layer to the exhaust stream, with coupled spatial and temporal variations of temperature, moisture content and all transport coefficients.

4.2 Equilibrium moisture content and adsorption energy

4.2.1 Fiber-water interactions

Water is held inside the fiber mat by the following mechanisms, listed in order of decreasing bond strength (British Paper and Board Industry Federation, 1978):

a) Monolayer adsorption on the cellulose surface by hydrogen bonding;

b) Multilayer adsorption near the cellulose surface by Van der Waals bonding;

c) Capillary adsorption in micropores inside the fiber wall;

d) Capillary adsorption in macropores between the fibers;

e) Capillary adsorption in the lumen.

At the beginning of drying, the fibres are thought to be saturated with water, with additional water held in the pores between the fibres. For unbleached kraft pulp from black spruce similar to that used in the present study, O. Polat (1989) measured the fiber saturation point to be between 0.71 and 0.82 by the solute exclusion technique, and for the black spruce thermomechanical pulp used, Nanri (1991) measured the water retention value to be 1.00 by the centrifugation technique.

To properly model falling rate drying, it would be useful to know the proportion of water held by each of the abovementioned mechanisms as drying proceeds. Such information is only partly available at the present time. Kershaw (1980) reports that monomolecularly held water amounts to 1 to 2 % of the dry fiber weight, that a sizable amount is absorbed and adsorbed in the lumen, that 25 % is inside the fiber wall, the rest being in the pores between the fibers. It should also be noted that water in the lumen, while more weakly bound than interfiber water, is in fact harder to remove as most of it must diffuse through the fiber wall during drying.

4.2.2 Equilibrium moisture content below the atmospheric boiling point

Prahl (1968) measured the desorption isotherms of kraft pine pulp for $0 \leq X \leq 0.40$ in the range $20 \,^{\circ}C \leq T \leq 80 \,^{\circ}C$, the range of sheet temperature during the constant rate period of air drying. The measurements were done in an initially evacuated chamber containing only

water vapor in equilibrium with moist paper. Experiments done in an air atmosphere with relative humidity controlled by saturated salt solutions gave identical results for equal water vapor pressure, confirming that the presence of air does not affect the equilibrium of the system. Prahl's data were reexamined to try to identify the relationship between the vapor pressure, moisture content and temperature. Upon testing a number of forms of this relationship, the best new correlation of Prahl's results is found to be:

$$\phi \equiv \frac{P_v}{P_{sat}} = \exp\left[\frac{-M\ f\ (X,\ T)}{\mathbb{R}\ T}\right] =$$

$$\exp\left[\frac{-M\ \{\ 1\ -\ \alpha\ (T\ -\ 293.2)\}\ \exp\ (\beta\ -\ \gamma\ X)}{\mathbb{R}\ T}\right]$$

(4.1)

where $\alpha = 0.005974$,

$\beta = 6.5776$,

$\gamma = 24.0851$.
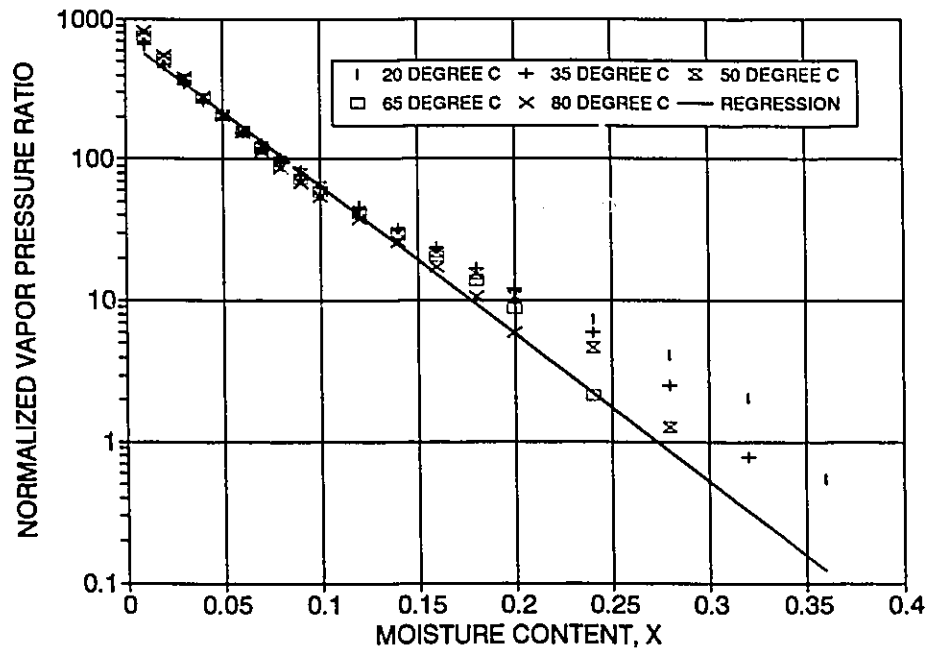
Figure 4.1 Comparison of Prahl's measurements and equation 4.1.

The agreement between this equation and Prahl's data is shown in figure 4.1, where the normalized vapor pressure ratio is - R T ln ϕ / M (1 - α (T - 293.2)), with a regression coefficient of 0.994.

An expression for the heat of adsorption can be obtained from the above equation by considering the Clausius-Clapeyron equation applied to the paper fibre - adsorbed water - water vapor system:

$$\frac{\partial (\ln \phi)}{\partial T} = \frac{\partial (\ln P_v)}{\partial T} - \frac{\partial (\ln P_{sat})}{\partial T} = \frac{M \, \Delta h_a}{R \, T^2} \qquad (4.2)$$

Substituting from equation 4.1 into 4.2 gives

$$\frac{\Delta h_a}{T^2} = \frac{\partial}{\partial T} \left[\frac{- f(X, T)}{T} \right] =$$

(4.3)

$$\frac{-1}{T} \frac{\partial f(X, T)}{\partial T} + \frac{f(X, T)}{T^2}$$

$$\Delta h_a = (1 + 293.2 \, \alpha) \, \exp(\beta - \gamma X) \qquad (4.4)$$

Letting $(1 + 293.2 \, \alpha) = \exp \delta$ finally gives

$$\Delta h_a = \exp(\delta + \beta - \gamma X) = \exp(7.59 - 24.085 \, X) \qquad (4.5)$$

This equation is nearly identical to that obtained by Crotogino and Allenger (1979) by regression of the values tabulated in Prahl's thesis:

$$\Delta h_a = \exp(7.2 - 17.3 \, X) \qquad (4.6)$$

However, as Prahl obtained adsorption energies from his vapor pressure measurements by a graphical procedure involving a visual fit of the data plotted on semilog paper, equation 4.6 does not represent his measurements as accurately as equation 4.5, obtained by a purely numerical procedure on the original data. At $X = 0.08$, a normal final moisture content for drying paper, equation 4.5 gives $\Delta h_a = 288$ kJ/kg, 12.8% of Δh_v at the atmospheric boiling point.

4.2.3 Equilibrium moisture content in superheated steam.

The desorption equilibrium moisture content of kraft and TMP paper was measured in superheated steam as a function of temperature by leaving the sheet in the drying chamber for a sufficient time under a high jet flow rate. The experimental conditions for these measurements were as follows:

Paper type: from unbleached kraft black spruce pulp, of basis weight 60 g/m^2; from thermomechanical black spruce pulp of basis weight 48.8 g/m^2;

Residence time: 4 hours;

Drying chamber pressure: 107 kPa abs.;

Jet Reynolds number: 5000.

For kraft paper, surprisingly, the equilibrium moisture content is practically zero (within the experimental error of 0.01) at a temperature as low as 103 $^{\circ}$C, i.e. the lowest temperature that could be achieved and maintained in the drying chamber. This temperature is only 1.6 degrees above the saturation temperature of 101.4 $^{\circ}$C corresponding to the drying chamber pressure. For paper made of TMP pulp, figure 4.2 shows that the equilibrium moisture content decreases regularly with increasing temperature, from 0.123 at 103 $^{\circ}$C, to practically 0 at 109 $^{\circ}$C.
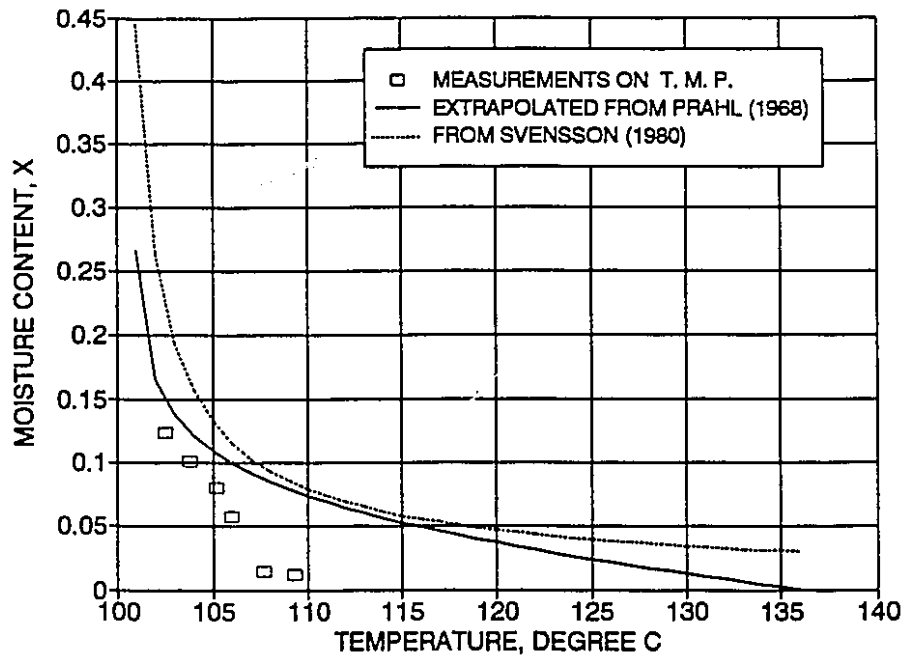
Figure 4.2 - Equilibrium moisture content in superheated
steam.

The higher equilibrium moisture content in TMP than in kraft paper is in agreement with previous findings for equilibrium moisture content in air at room temperature (Attwood, 1972, Brandon, 1981). This behavior was attributed to a larger proportion of components more hygroscopic than pure crystalline cellulose in TMP, possibly lignin and more importantly hemicellulose (Britt, 1964).

As the equilibrium condition for the paper-steam system is that the vapor pressure of the bound moisture equals atmospheric pressure, one can set $P_v = P_{atm}$ in equation 4.1 for Prahl's results, to obtain an expression for the dependence of the equilibrium moisture content on sheet temperature:

$$\ln\left[\frac{P_{atm}}{P_{sat}(T)}\right] = \ln(P_{atm}) - \ln(P_{sat}(T)) = \frac{-M\,\{1-\alpha(T - 293.2)\}\,\exp(\beta - \gamma\,X_{eq})}{RT}$$

$$(4.7)$$

$$X_{eq} = \frac{1}{\gamma}\left\{\beta - \ln\left[\frac{RT\,(\ln P_{sat}(T) - \ln(P_{atm}))}{M\,\{1 - \alpha(T - 293.2)\}}\right]\right\} \qquad (4.8)$$

In figure 4.2, the equilibrium moisture contents, extrapolated in this way from Prahl's measurements for kraft pine pulp for temperatures below the atmospheric boiling point, are seen to agree with those reported by Svensson (1980) for wood pulp, but are substantially higher than the values measured here for TMP in superheated steam. Svensson makes no mention of the type of pulp or of his measurement technique. The above comparison in figure 4.2 indicates that the adsorption energy of water is substantially lower above the boiling point than below. It should be recalled however that the estimate from Prahl's work is based on measurements made over the temperature range 20 °C - 80 °C, i. e. substantially below the present temperatures of over 100 °C, and that Svensson's results, given without documentation, are therefore of unknown reliability. From a practical point of view, the experimental findings indicate that complete drying of paper is possible with steam at quite low superheat. This conclusion will be confirmed subsequently.

4.3 Falling rate drying experiments

4.3.1 Basis of analysis of falling rate period

Keey (1978) notes that a linear relationship between the drying rate and moisture content is often used to describe the falling rate period. Wenzel and White (1951) and Chu *et al.* (1959) observed such a linear falling rate period following the constant rate period when drying a bed of sand in a parallel flow dryer with superheated steam. Luikov separates six types of drying curves in the falling rate period, according to the nature of the material being dried, and reports linear behavior for paper or thin cardboard (Strumillo and Kudra, 1986).

In the absence of any previous work on the falling rate period of superheated steam drying of paper, it was thought best to base the analysis of the falling rate period on the approach suggested by the work of these previous authors. Therefore, the falling rate period was assumed to be suitably described by a linear relationship between drying rate and moisture content, figures 4.3a, 4.3b. This hypothesis was then checked with the experimental data.
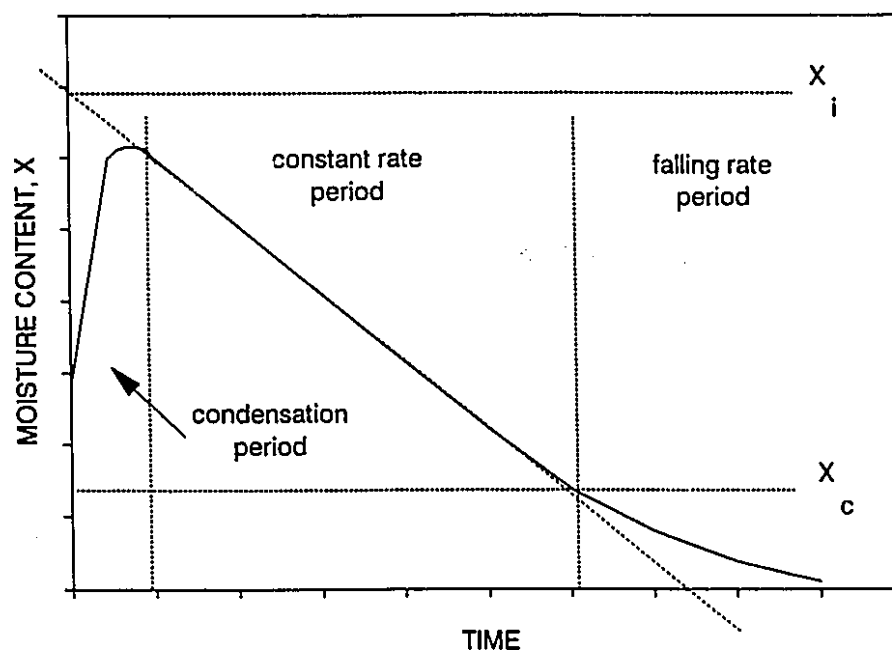
Figure 4.3a - Evolution of moisture content
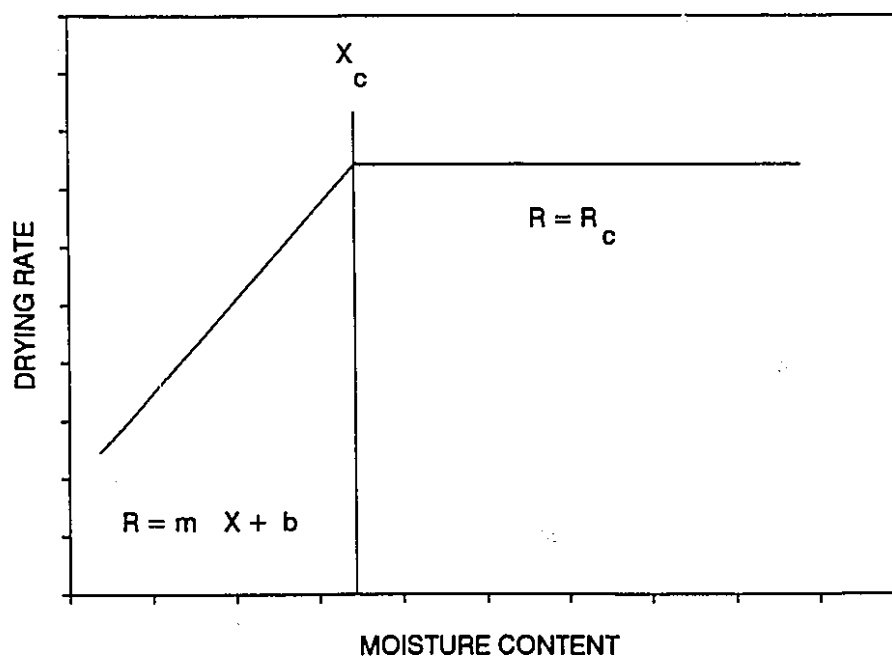
Figure 4.3b - Constant and falling rate periods

It is shown in section 2.9 that a linear falling drying rate leads to the following expressions for moisture content as a function of time:

Constant rate period $(X > X_c)$:

$$X = X_i - \frac{R_c\, t}{B} \tag{4.9}$$

Falling rate period $(0 \leq X \leq X_c)$:

$$X = X_c - \frac{R_c}{m}\left\{ 1 - \exp\left[\frac{m}{R_c}(X_i - X_c) \right] \exp\left[\frac{-m\, t}{B} \right] \right\} \tag{4.10}$$

where

X_i, the X-intercept of the $X - t$ plot, can be considered as the initial moisture content of an experiment in which drying would begin immediately at the constant rate, as illustrated in figure 4.3a;

R_c is the constant drying rate;

X_c is the critical moisture content, the point of transition between the constant and falling rate periods;

m is the slope of the drying rate – moisture content curve during the falling rate period.

The parameters X_i, R_c, X_c and m were evaluated by a non-linear least squares regression routine (Wilkinson, 1988). The regression coefficient averaged 0.993. The high value of the regression coefficient supports the basic hypothesis that, in superheated steam impingement drying of paper, the drying rate decreases linearly with moisture

content during the falling rate period.

The approach taken subsequently is to relate the critical moisture content, X_c, and the slope of the falling drying rate curve, m, to the relevant experimental variables in terms of the phenomena known to affect falling rate drying.

4.3.2 Experimental conditions and evolution of sheet temperature and moisture content

The critical moisture content and slope of the falling rate period were measured for kraft paper in air and in steam under a constant jet Reynolds number of 2000. The following basis weight and jet temperature range were investigated:

$$150 \leq T_j \leq 450 \ ^\circ C, \ \text{in } 100 \ ^\circ C \text{ increments, for } B = 60 \ g/m^2;$$
$$60 \leq B \leq 150 \ g/m^2, \ \text{in } 30 \ g/m^2 \text{ increments, for } T_j = 350 \ ^\circ C.$$

A few additional experiments were done with towel paper and with paper made from a thermomechanical pulp. The complete description of these additional experiments is found in the inventory of drying experiments, appendix 1.

Figure 4.4 shows the evolution of moisture content and sheet top and bottom temperatures in steam drying of 48.8 g/m^2 paper made from TMP, of initial moisture content 1.6 g water/g fiber, dried at a jet temperature of 350 $^\circ C$, with a jet Reynolds number of 2000. The fitted composite expression for the evolution of moisture content, equations 4.9 and 4.10, with parameters determined as described in section 2.9, is seen to agree very well with the experimental data: for this series of

experiments, the regression coefficient is 0.995. This success in fitting the data with equations 4.9 - 4.10 supports the hypothesis made at the outset that drying is characterized by a constant rate period, followed by a falling rate period during which the drying rate varies linearly with moisture content.
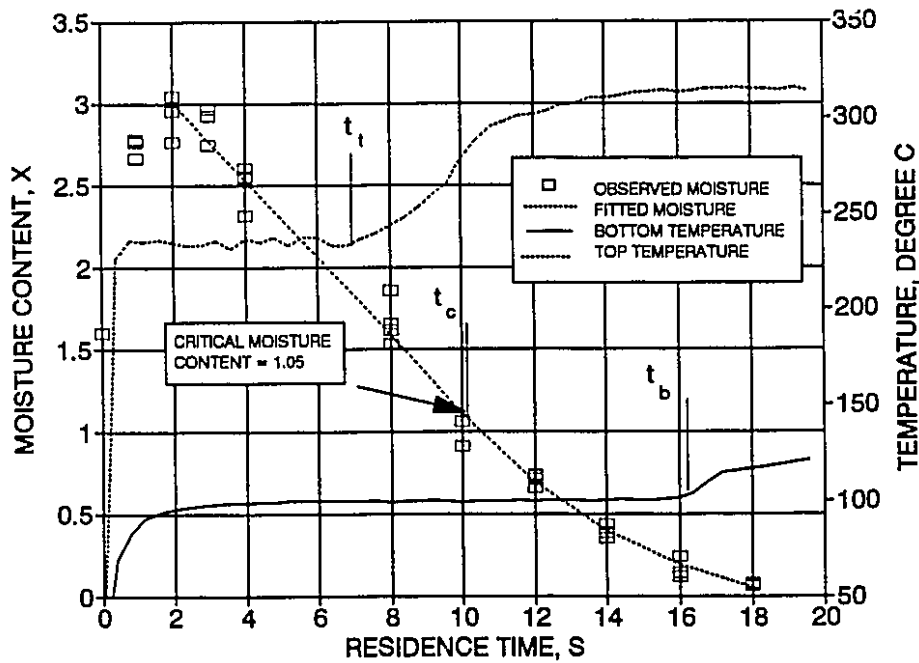
Figure 4.4 - Evolution of sheet temperature and moisture content.
48.8 g/m^2 TMP, T_j = 350 °C, Re_j = 2000, t_p = 200 μm.

In the absence of a direct measurement of the moisture distribution within the sheet during drying, the temperature traces provide clues as to the evolution of local moisture content. The temperatures at the top and bottom of the sheet were measured by bare, 75 μm wire diameter thermocouples. At the top, steady contact was ensured by bending the wires so as to force the bead against the sheet by springing action. The

temperature at the top of the sheet rises quickly to a steady value, figure 4.4. The top of this thermocouple bead is immersed in boundary layer steam, the bottom is in contact with moisture on the surface of the sheet. The measured temperature, about 240 $^{\circ}$C, is therefore intermediate between that of the jet, 350 $^{\circ}$C, and of the wet paper, 100 $^{\circ}$C. At time t_t, this temperature starts to increase, indicating drying of the top surface. Shortly afterwards, at the critical time t_c, as determined by regression of the moisture – time data, the falling rate drying period starts. At the support plate side, the thermocouple is sandwiched between the glass plate and the paper sheet. The thermocouple bead has only point contact with the glass surface, with most of the bead surface in contact with the bottom of the paper. The measured temperature remains constant at the atmospheric boiling point until time t_b when it rises due to drying of the bottom surface.

These observations of sheet temperature are consistent with the concept of an evaporation zone, first located at the top surface of the sheet during the constant rate period, then receding towards the bottom surface, as illustrated in figure 4.5. The fact that the backing plate surface temperature starts to increase at a non-zero moisture content, $X_b \cong 0.2$ at time t_b, is evidence that the evaporation occurs in a layer of finite thickness. Such behavior is generally observed in drying of capillary-porous bodies (Strumillo and Kudra, *op. cit.*).
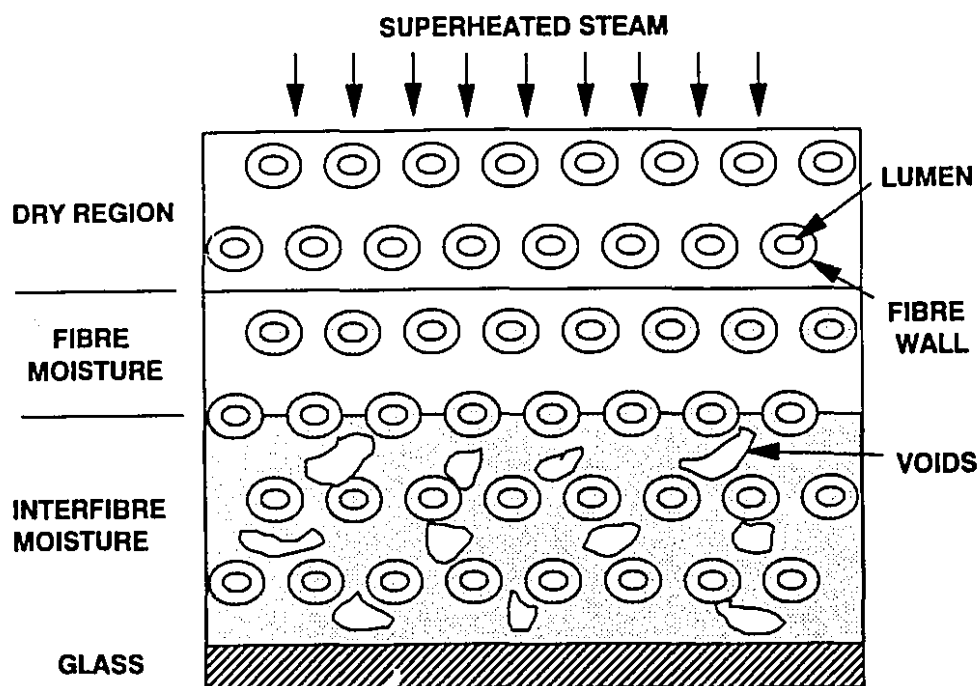
Figure 4.5   Moisture distribution within the sheet during the
falling rate period of superheated steam impingement drying.

4.3.3 Critical moisture content

The critical moisture content for impingement drying of paper was found to vary between 0.6 and 1.6 in steam, and between 0.2 and 1.5 in air drying, depending on the operating conditions. While the average value of critical moisture content is close to the fiber saturation point, 0.72 - 0.81, and water retention value, 1.00, determined by O. Polat and Nanri, respectively, the wide variability shows that critical moisture content is not a material property, as was sometimes assumed in earlier work on drying of solids (Keey, 1972).

Critical moisture content may be related to the drying intensity N, according to the theoretical development of Suzuki *et al.* (1977), section 1.3.4. For the typical experimental conditions of this study:

$$R_c = 40 \text{ kg } / \text{ m}^2\text{-h};$$

$$t_p = 150 \ \mu\text{m} \ (\text{for } B = 48.8 \text{ g/m}^2)$$

$$\varepsilon = 2/3 \ (\text{typical value for kraft paper, Polat, 1989})$$

$$\rho_b = 0.4 \text{ g/cm}^3$$

the drying intensity based on the dry paper diffusivity calculated at 100 $^\circ$C using Lin's (*op. cit.*) formula, equation 1.19, is $N_o = 0.051$. For such *low intensity* drying, equation 1.20 would predict a critical moisture content of 0.024, much lower than the range of values observed. Hence, if the analysis of Suzuki *et al.* is applicable to the present situation, it appears that the effective diffusivity for movement of moisture under fast drying conditions provided by impinging jets is lower than that obtained by Lin's correlation of slow drying at very low moisture contents.

An attempt was made to correlate the data by expressions of the form suggested by equations 1.15, 1.16 and 1.19. Estimations of the parameters D_o and E_a by a non-linear regression routine did not result in satisfactory regressions for either the low (equation 1.15) or high intensity (equation 1.16) case.

The most satisfactory correlation was obtained by relating critical moisture content directly to the value of drying rate for the constant drying rate period. For impingement steam drying, figure 4.6 shows that the data are reasonably represented by the expression

$$X_c = 0.373 \ R_c^{0.265} \tag{4.11}$$

105

with a regression coefficient of 0.93. The increase of critical moisture content with constant drying rate is in agreement with Shibata's measurements of drying of a sintered sphere of glass beads by laminar flow of superheated steam in a tube.

Adding a constant term to the regression, i. e. $X_c = a + b\ R_c^c$, does not result in a significant increase of the regression coefficient, indicating that the critical moisture content approaches zero at zero constant drying rate. This is indeed expected for the present system, as it was shown in figure 4.2 that water is only slightly bound to TMP fibers and not measurably so for kraft fibers.

For air drying, figure 4.7, there is a slightly better agreement between the data and the regression equation:
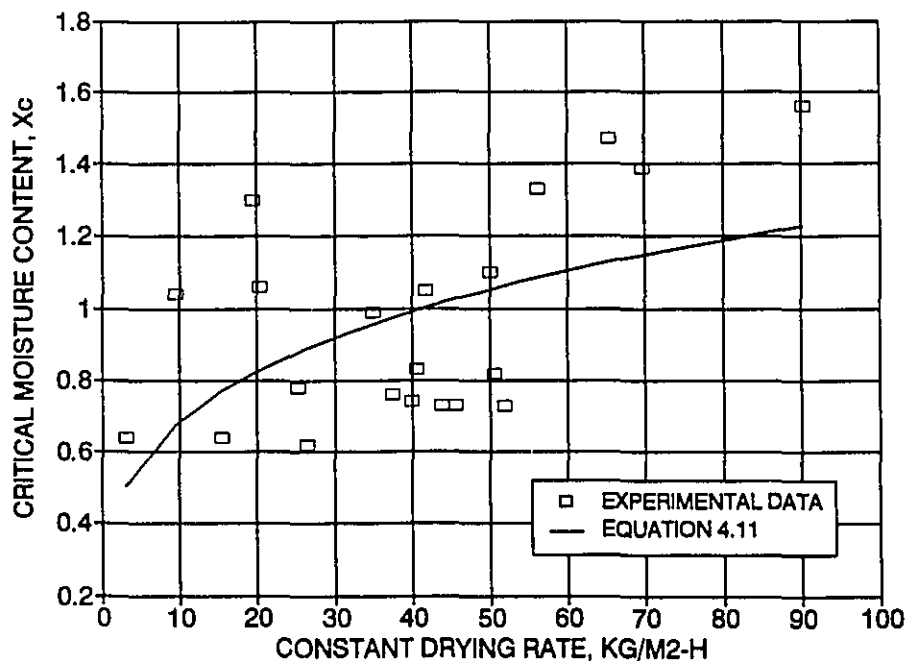
Figure 4.6 - Critical moisture content for impingement drying in superheated steam.

$$X_c = 0.114 + 4.08 \times 10^{-3} R_c^{1.5} \qquad (4.12)$$

with a regression coefficient of 0.95. Comparison of equations 4.11 and 4.12 shows that the critical moisture content is much more sensitive to the constant drying rate in air than in steam drying. This suggests that
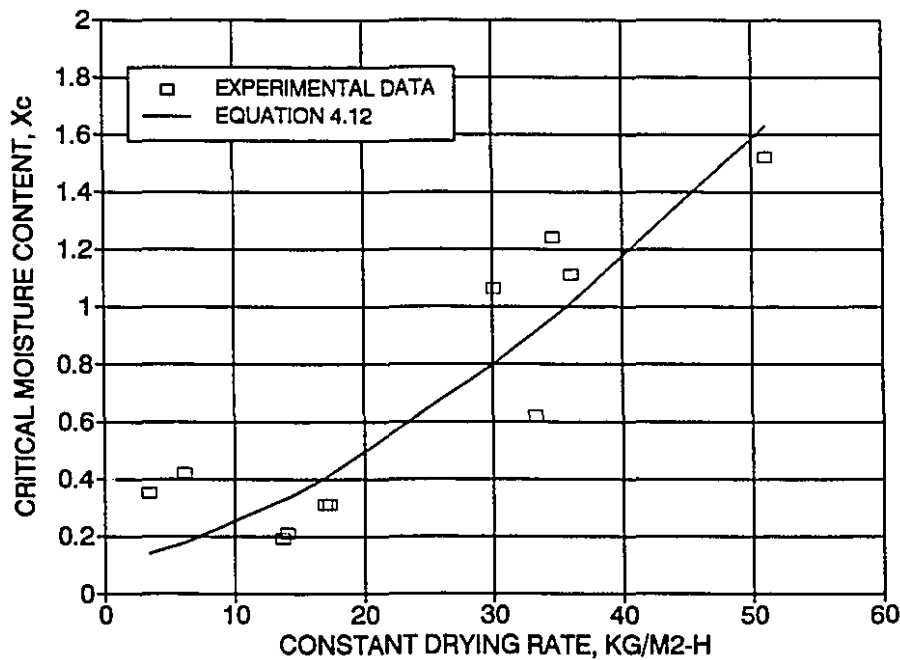
Figure 4.7 - Critical moisture content for impingement drying in air.

the drying mechanism during the falling rate period is different in steam than in air.

For steam and air, the possibility that critical moisture content is dependent on basis weight was examined by fitting the data to regression equations of the form

$$X_c = k_1 R_c^{k_2} B^{k_3} \qquad (4.13)$$

where k_1, k_2 and k_3 are constants. However, regression coefficients

obtained with this form were not significantly higher than those of equations 4.11 and 4.12. This does not necessarily mean that there was no correlation between critical moisture content and basis weight: one may have existed and may have been too weak to be detected. The trend, indicated by equations 4.9 and 4.10, that critical moisture content increases with constant drying rate, is consistent with Suzuki *et al.*'s (*op. cit.*) analysis of moisture diffusion within the sheet, equations 1.15 and 1.16. However, the dependence has power law behavior, rather than the linear behavior of these equations. The increase of critical moisture content with sheet thickness, also predicted by these equations, is not observed.

4.3.4 Slope of the falling rate period

When the evaporation front recedes into the paper sheet, additional heat and mass transfer resistances in the region between the evaporation front and the exposed surface of the sheet lead to a decrease in drying rate. For drying of a sphere of coarse glass beads suspended in a tube inside which there was laminar flow of superheated steam, Shibata (*op. cit.*) explained the drying rate decrease observed purely in terms of heat transfer resistance. However, for paper, at the typical conditions given in section 4.3.3, the heat transfer Biot number, the ratio of internal resistance to conduction to external resistance to convection, based on the extreme condition of conduction through the entire thickness of the dry sheet,

$$Bi_h \equiv \frac{h\ t_p}{k_p} = \frac{R_c\ \Delta h_v\ t_p}{(T_J - T_b)\ k_p} \quad , \qquad\qquad (4.14)$$

is 0.12 when the thermal conductivity of dry paper, 0.127 W / m ^{o}C (Kerekes, 1980), is used. Such a low Biot number indicates that the internal conduction resistance is minimal and that mass transfer, not heat transfer, limits the falling rate period. Lin (*op. cit.*) also argues that mass transfer rather than heat transfer is rate-limiting, in his model of slow drying of kraft paper. Thus in steam and in air drying, it appears that temperature is nearly uniform across the sheet thickness during the falling rate period. In superheated steam drying, this value must be higher than the boiling point.

For impingement steam drying, the slope, m, of the falling rate period is correlated (regression coefficient of 0.904) by the equation

$$m = 3.028\ R_c^{0.495}\ B^{0.198} \qquad\qquad (4.15)$$

as can be seen in Figure 4.8.
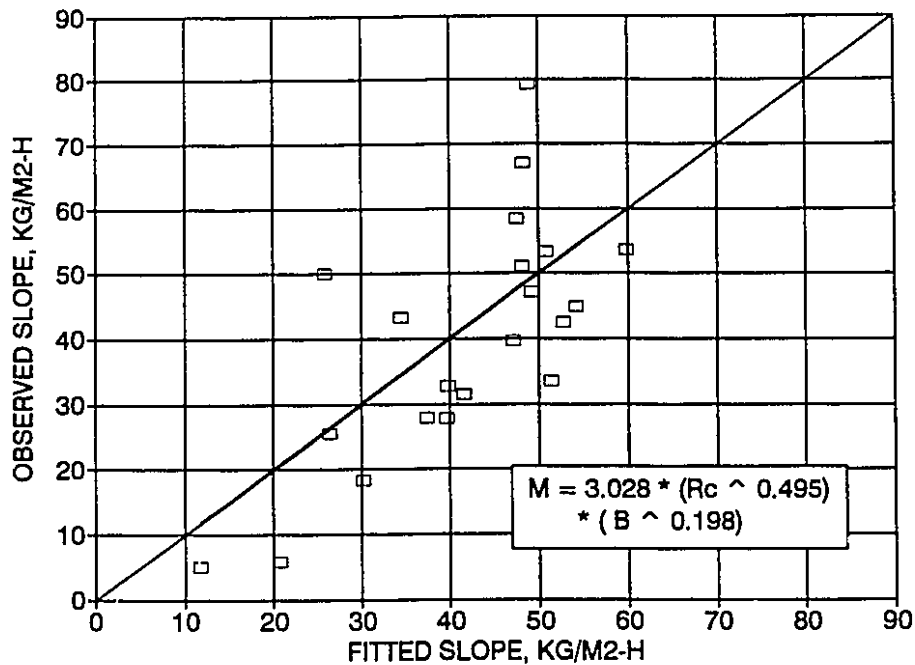
Figure 4.8 - Slope of the falling rate period in superheated
steam drying.

For air drying, non-linear regression does not produce a statistically significant correlation. For most experiments, m is about 40 kg/m^2-h. However in some experiments, especially at low temperature, m is considerably smaller. The experiments were not extended to a more complete determination of the air drying parameters as air drying was not the basic objective of the present study.

4.4 Complete drying rate - moisture content histories for superheated steam impingement drying

To summarize the results of this investigation on drying paper by impinging jets of superheated steam, complete drying rate - moisture content histories, figures 4.9 - 4.15, were generated for a representative set of conditions from the correlation equations:

$$X > X_c : \qquad R = R_c \qquad\qquad (2.6)$$

$$0 \le X < X_c : \qquad R = R_c + m\,(X - X_c) \qquad (2.11)$$

$$R_c = k_j\,Pr_j^{0.42} \left[\frac{T_j}{T_b}\right]^{-0.77} \frac{F\,(H/D,\ f)}{D}\,Re_j^{2/3}\,\frac{\ln\left[1 + \dfrac{C_{ps,f}\,(T_j - T_b)}{\Delta h_v}\right]}{C_{ps,f}}$$

$$(3.28)$$

$$X_c = 0.373\,R_c^{0.265} \qquad\qquad (4.11)$$

$$m = 3.028\,R_c^{0.495}\,B^{0.198} \qquad (4.12)$$

Table 4.1 Correlation equations for drying paper by impinging
jets of superheated steam.

Each figure shows R calculated from the above equations, t corresponding
to each moisture content calculated from equations 4.9 and 4.10 with
drying rates obtained from the correlation, and t vs. X experimental
data for the specified conditions. For 60 g/m^2 Kraft paper, figure 4.9
represents a low ΔT, low Re_j condition, figure 4.10 a high ΔT, low Re_j
condition, figure 4.11 a low ΔT, high Re_j condition, figure 4.12 a high
ΔT , high Re_j condition. For $T_j = 350\ ^\circ C$ and $Re_j = 2000$, figure 4.13 is
for a medium B Kraft paper, figure 4.14 for a high B Kraft paper, and
figure 4.15 a low B TMP paper.

Figure #	Jet temperature T_j, $^{\circ}$C	Jet Reynolds number Re_j	Paper type	Basis weight B, g/m^2
4.9	150	2000	Kraft	60
4.10	435	2000	Kraft	60
4.11	150	12000	Kraft	60
4.12	350	4000	Tissue	60
4.13	350	2000	Kraft	60
4.14	350	2000	Kraft	150
4.15	350	2000	TMP	48.8

Table 4.2 – Experimental conditions for complete drying rate – moisture content curves, figures 4.9 – 4.15.

The generally good agreement between the experimental and generated X vs. t curves testify to the trustworthiness of the correlation equations, considering the difficulty of the experimental procedures, the wide range of conditions, and the absence of any previous measurements in this field.
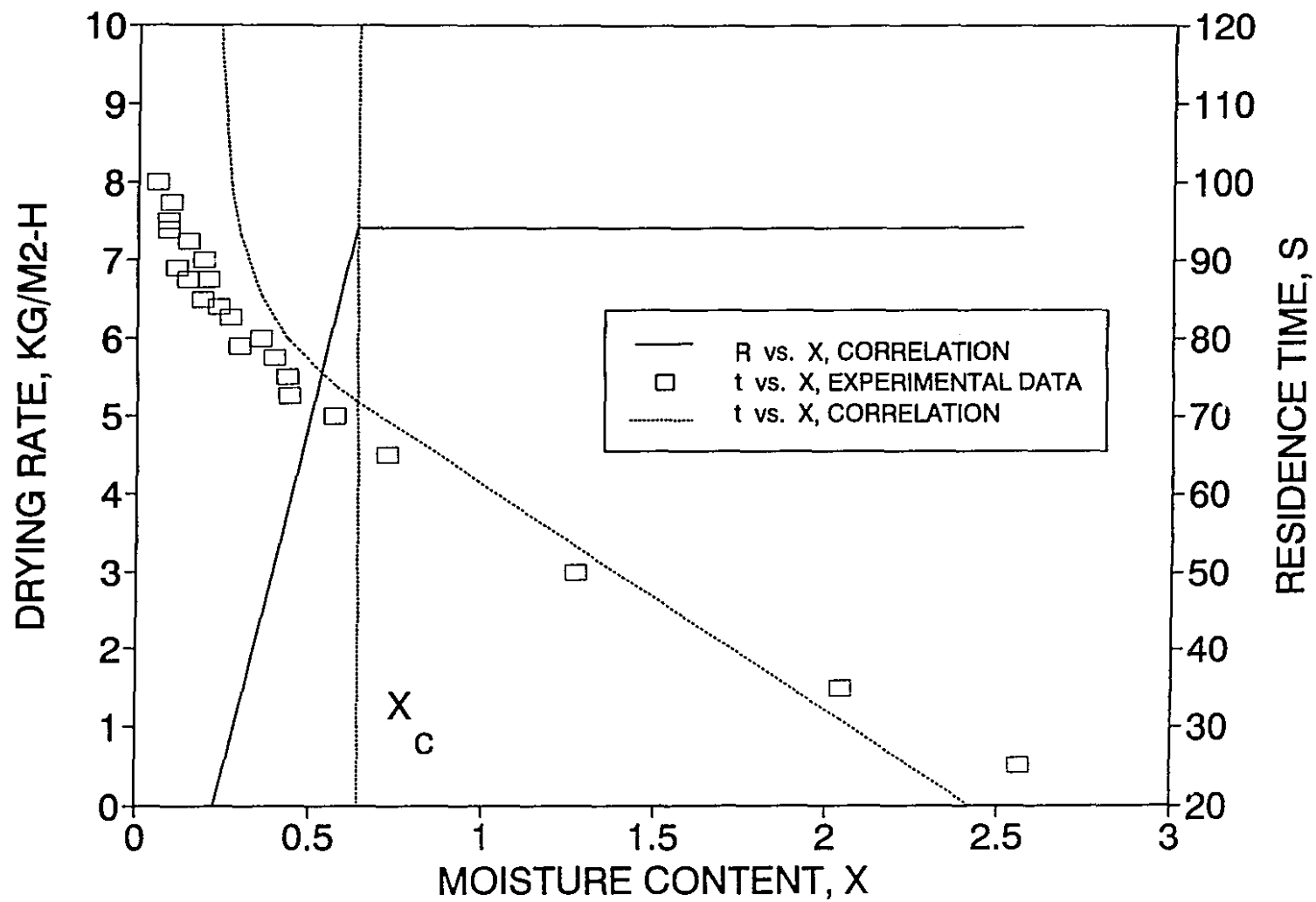
Figure 4.9 – Drying rate and moisture content in superheated steam impingement drying.
Tj = 150 degree C, Rej = 2000, Kraft paper, B = 60 g/m2.
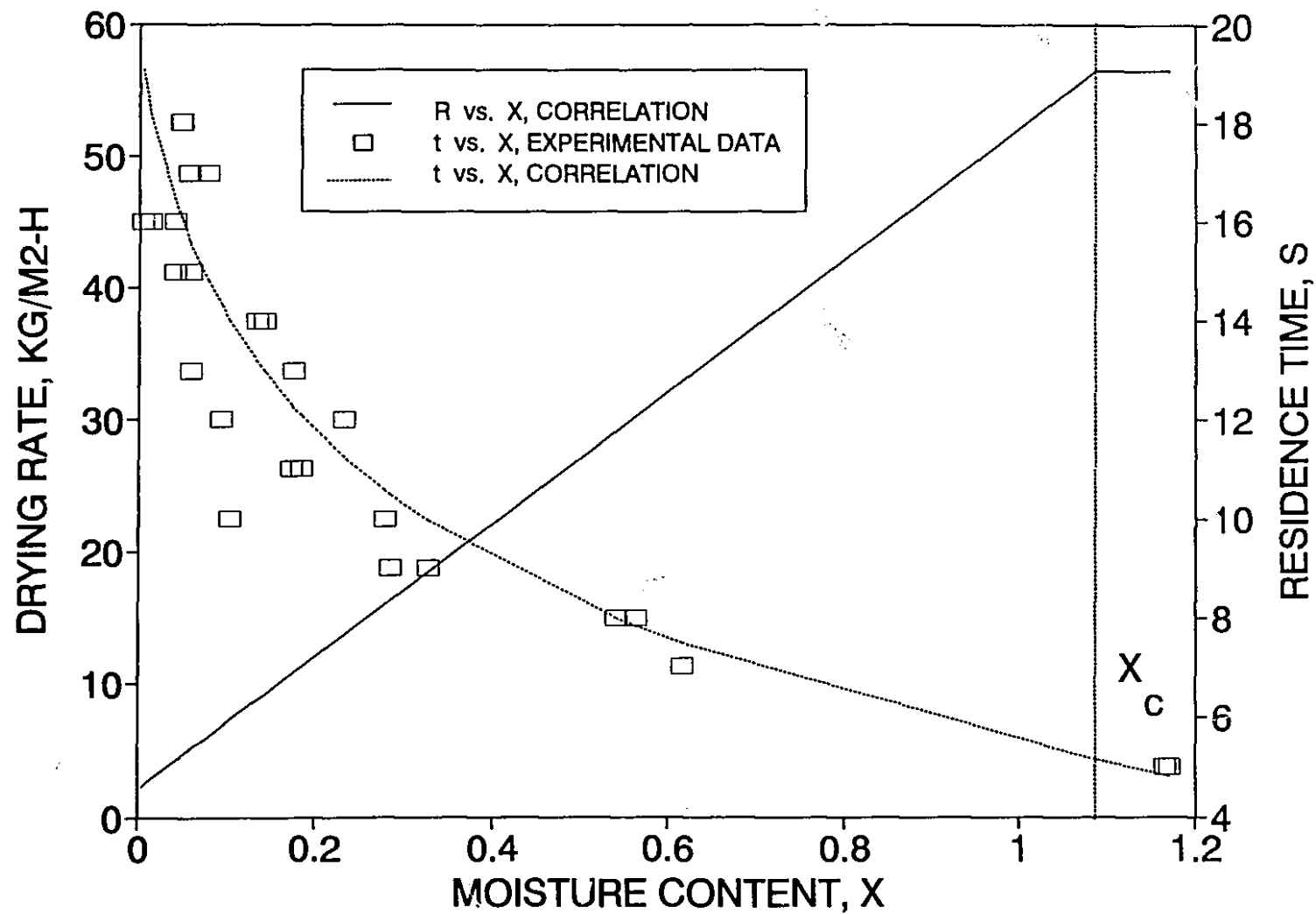
Figure 4.10 – Drying rate and moisture content in superheated steam impingement drying. Tj = 435 degree C, Rej = 2000, Kraft paper, B = 60 g/m2.
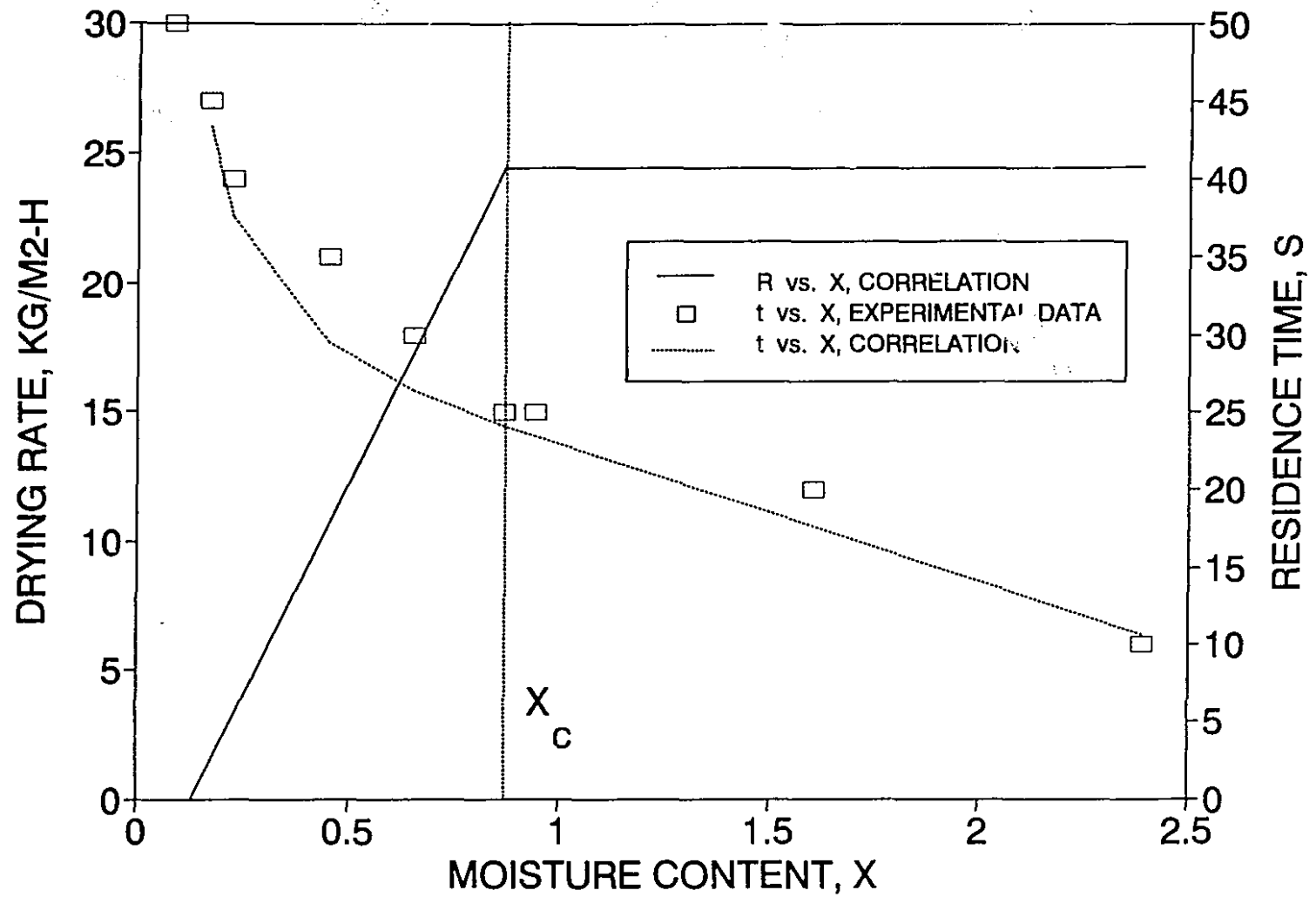
Figure 4.11 – Drying rate and moisture content in superheated steam impingement drying.
Tj = 150 degree C, Rej = 12000, Kraft paper, B = 60 g/m2.
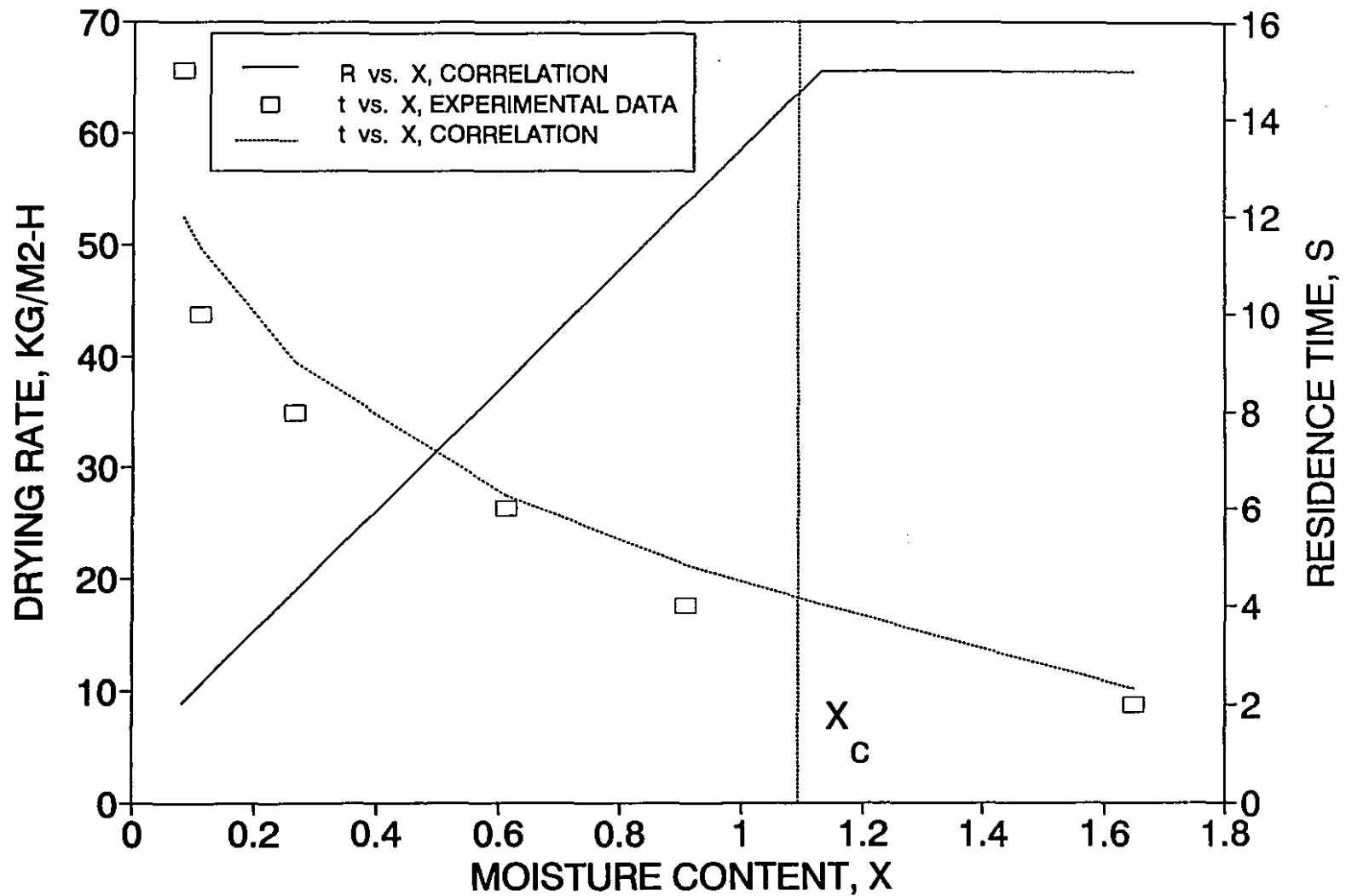
Figure 4.12 – Drying rate and moisture content in superheated steam impingement drying. Tj = 350 degree C, Rej = 4000, Tissue paper, B = 60 g/m2.
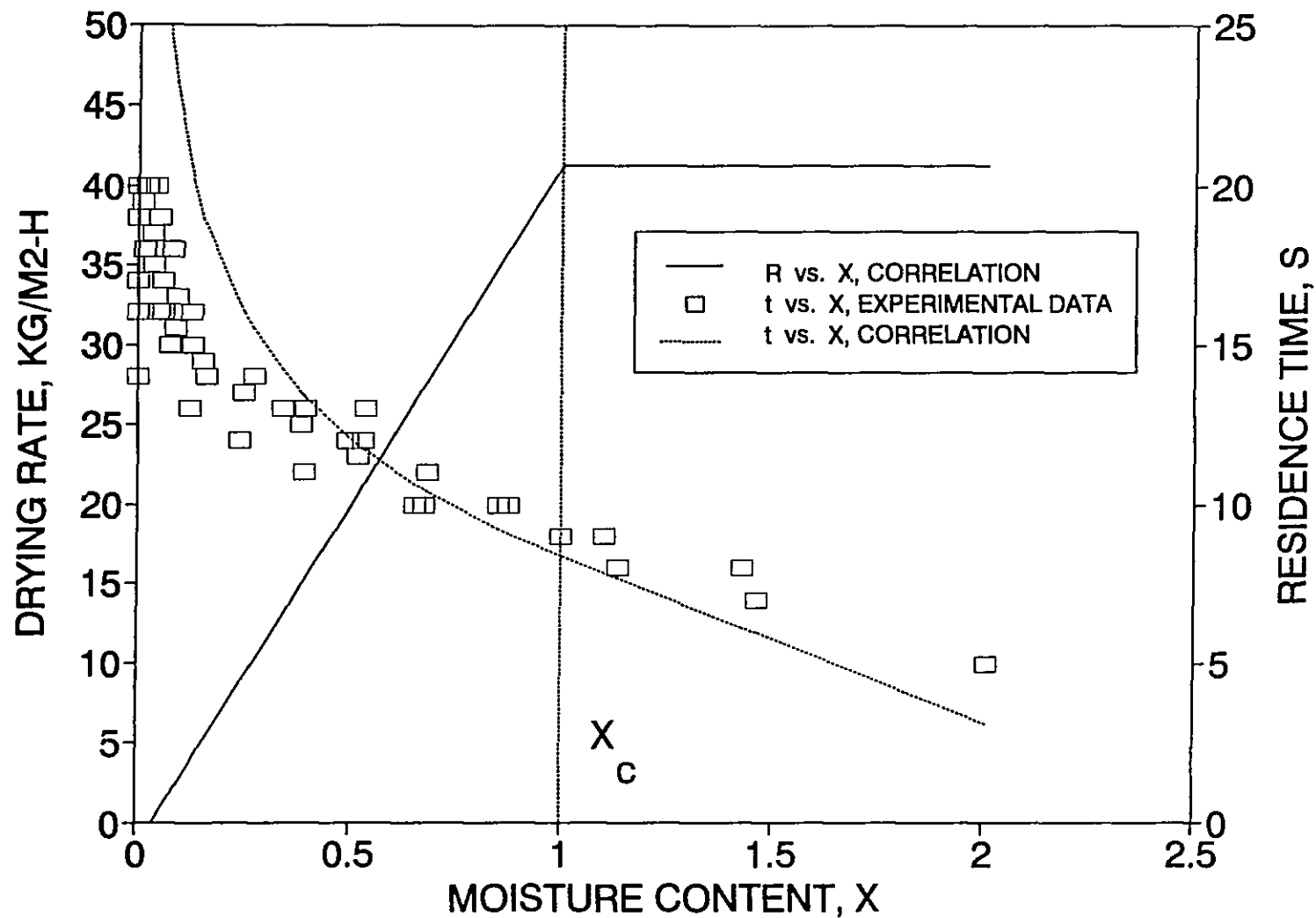
Figure 4.13 — Drying rate and moisture content in superheated steam impingement drying. Tj = 350 degree C, Rej = 2000, Kraft paper, B = 60 g/m2.
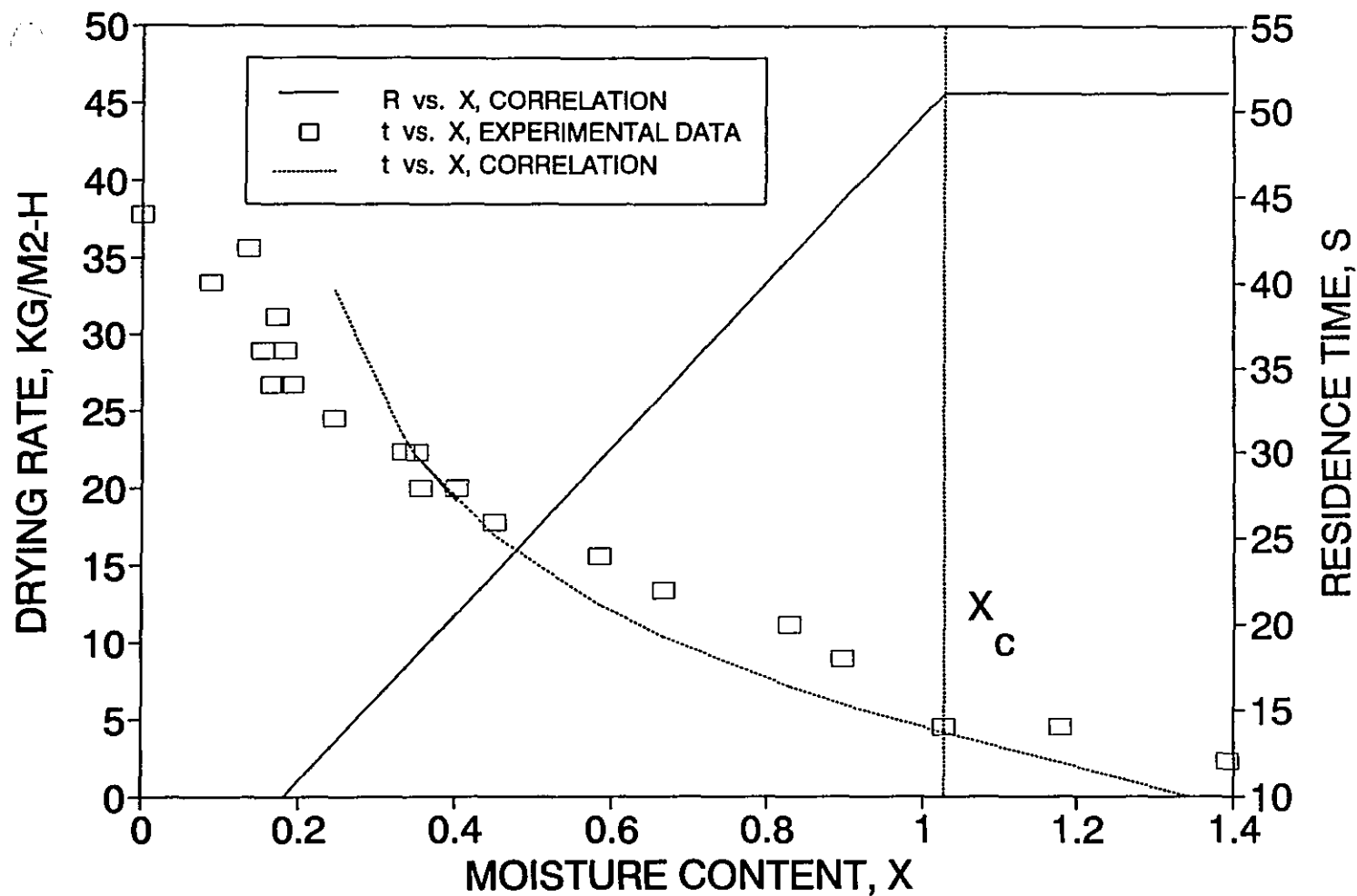
Figure 4.14 – Drying rate and moisture content in superheated steam impingement drying.
Tj = 350 degree C, Rej = 2000, Kraft paper, B = 150 g/m2.
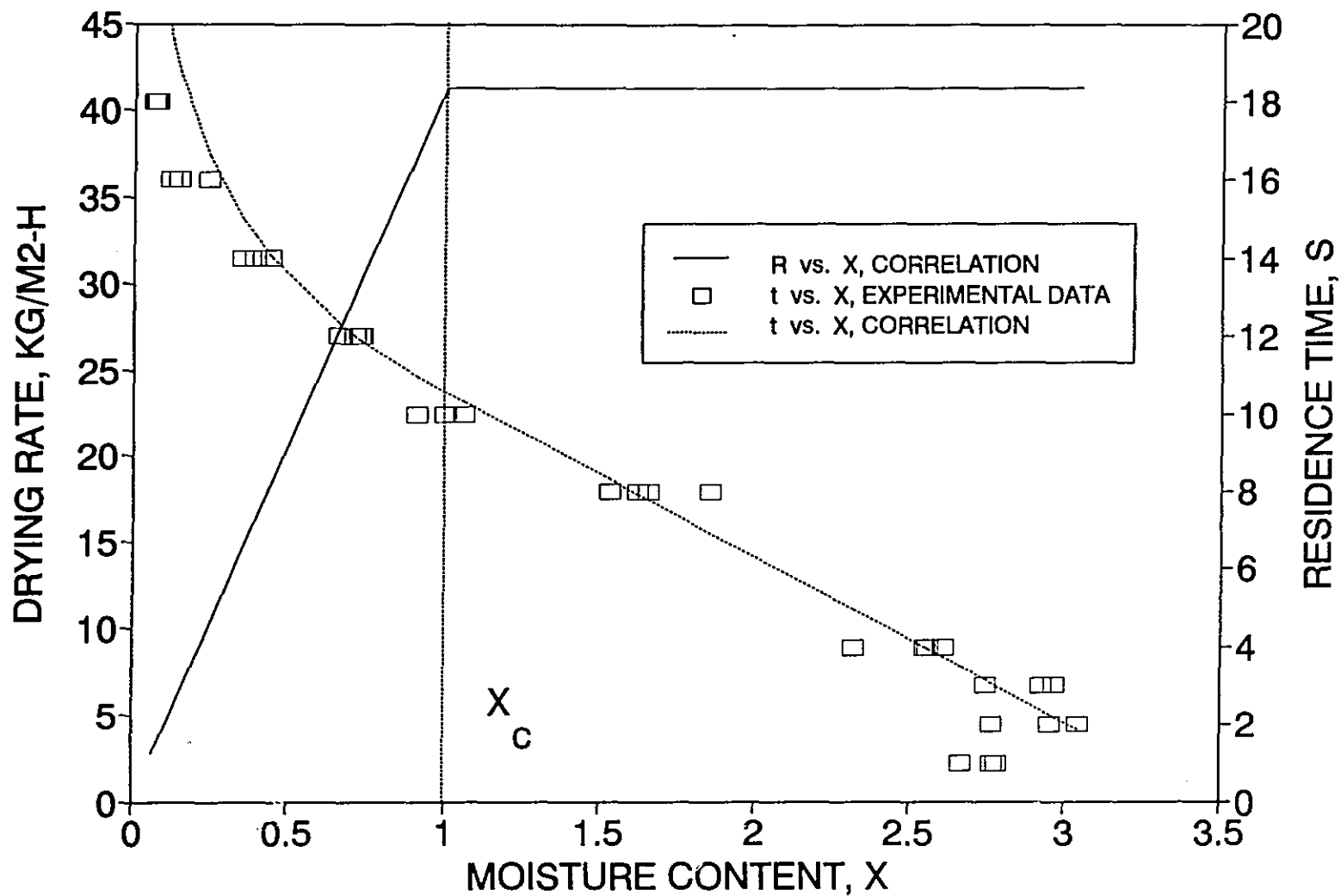
Figure 4.15 – Drying rate and moisture content in superheated steam impingement drying.
Tj = 350 degree C, Rej = 2000, TMP paper, B = 48.8 g/m2.

4.5 Conclusion

The equilibrium moisture content of paper in superheated steam measured here is much lower than the values calculated from extrapolation of Prahl's measurements made at lower temperatures. Hence the falling rate period in superheated steam is controlled only by internal transport resistance, whereas in air drying it is also affected by adsorption of water on the fibers. Complete drying of paper is possible in superheated steam at very low levels of superheat.

For superheated steam and air impingement drying, the critical moisture content increases with the constant drying rate. The rate of increase with constant drying rate is higher in air than in superheated steam. The increase of critical moisture content with constant drying rate is consistent with expressions obtained from Suzuki *et al.*'s approximate analysis of moisture diffusion within the sheet. However, neither the form of the dependence, nor the magnitude of the critical moisture content, agree with the predictions of this model. This indicates a complexity of transport processes specific to drying of paper by impinging jets of superheated steam.

Correlation equations for the constant and falling rate periods are shown to agree generally well with experimental measurements under a wide range of jet temperatures, flow rates, basis weight and type of paper. The results of this laboratory-scale investigation can therefore be applied with confidence for the design of an industrial superheated steam impingement dryer.

CHAPTER 5

THERMODYNAMIC CYCLES FOR SUPERHEATED STEAM DRYING OF PAPER.

5.1 INTRODUCTION AND METHODOLOGY

When paper is dried in pure superheated steam, the drying process is a net producer of steam at a rate equal to the rate of water removal from the wet sheet. If the exhausted steam is reused in another part of the paper mill, the energy supplied as heat and work for drying can be completely recovered in principle. Previous studies on superheated steam drying of paper, e. g. Cui *et al.*(1985) and Loo *et al.* (1984), have demonstrated large energy savings if the exhaust steam can be fully utilized. These studies, however, did not address the crucial question of the end use of the exhaust steam. In the present study, three cycles will be presented for implementing superheated steam drying of paper, for which the end use of the exhausted steam is to further dry paper in a conventional cylinder dryer. These cycles are *self-contained* in that the steam consumption for the part of the drying done conventionally equals the steam production from the part effected by a superheated steam dryer. As these cycles can be analyzed without reference to other processes in the paper mill, their performance is a realistic estimate of the potential of this technology for reducing energy consumption.

The most obvious use for the steam exhausted from a superheated steam dryer is to condense it in the drying cylinders of a conventional dryer section. Operating experience with a superheated steam pulp dryer in Sweden (Svensson, 1980, 1981) and with a TMP steam recovery system in the United States (Blumberg, 1983) indicates that steam contamination is minimal when steam is intimately mixed with moist paper fibers. Hence it

is probable that steam exhausted from an impingement steam dryer can be condensed directly in conventional dryer cylinders. Air infiltration into the steam circuit can probably be prevented by using a proper sealing arrangement and operating the dryer under slight positive pressure.

This chapter therefore analyzes combined drying cycles, in which one part of the drying is done by conventional steam-heated cylinders, while the rest is done by a superheated steam impingement dryer. The steam required by the former section is exactly balanced by steam production in the latter. Since conventional dryers operate most efficiently at high paper moisture content, when drying occurs in the constant rate period, it appears sensible to do the first part of the drying conventionally and the second one with superheated steam, rather than vice-versa. In the first cycle analyzed, steam is recirculated around the impingement dryer circuit by a fan, the exhaust steam being desuperheated and compressed to a pressure appropriate for condensation in the conventional drying cylinders. In the second cycle, recirculation of impingement drying steam is achieved by a thermocompressor, eliminating the capital cost and power consumption of the recirculating fan. In the third cycle, energy recovery is by means of an integrated open-cycle heat pump.

Both capital expenditure and energy consumption are relevant to the economic evaluation of any new drying process. Specific considerations of capital cost are beyond the scope of the present study, but the high drying rates of impingement steam drying, documented in chapters 3 and 4, indicate potential for reduction in equipment cost. Here the focus is on determining the relationship between the energy consumption (the

most important factor affecting operating costs) and the drying rate (the most important factor affecting capital costs) in each of these three cycles.

In conventional paper dryers, energy is supplied in the form of the latent heat of steam generated by combustion of spent pulping liquor, biomass or fossil fuel. The energy consumption is usually expressed as the mass ratio of steam required per unit water removed from the sheet. By contrast, in a combined steam impingement-conventional dryer arrangement, a significant portion of the total energy required for drying is supplied as work to recirculate the steam around the impingement dryer circuit and to compress the exhaust steam to the conventional dryer section. Energy consumption as heat and work must therefore be distinguished, because an energy unit of heat and work have different economic value, as indicated by table 5.1:

LOCATION	ELECTRICITY-TO-HEAVY OIL PRICE RATIO	ELECTRICITY-TO-NATURAL GAS PRICE RATIO
ATLANTIC CANADA	3.13	2.70
QUEBEC	1.79	1.64
ONTARIO	2.08	2.17
ALBERTA	2.17	4.35
UNITED STATES	8.27	4.43

Table 5.1 - Ratio of electricity-to-fuel price in the industrial sector, 1987. References: National Energy Board (1988), Statistical Abstract of the United States (1989).

To take into account relative energy prices, and to allow direct performance comparisons with conventional dryer sections, it is useful to define an *equivalent energy consumption* as

$$E_e \equiv \frac{Q + \varepsilon \, W}{J_t \, \Delta h_v} \qquad (5.1)$$

where Q and W are the rates of heat and work energy consumption, J_t is the total rate of water removal, Δh_v is the heat of evaporation of water, and ε is a *work-to-heat value ratio*, for which table 5.1 gives representative values relative to fossil fuels.

In this chapter, the expression for the steam impingement drying rate will first be introduced. The temperature decrease and pressure drop across the impingement dryer will then be calculated. Next, the water removal rate in the cycle considered as a whole will be related to the impingement drying rate. Finally, expressions for heat, work and equivalent energy consumption will be derived as a function of the total water removal rate and the results of a computer simulation of the process will be presented.

Because the analyses presented here neglect minor considerations, such as heat loss from the impingement hood and seals, pressure drop in piping, and the potential reduction in paper machine drive power, the performance figures calculated are to be taken as an indication, rather than an accurate prediction.

5.2 STEAM IMPINGEMENT-CONVENTIONAL CYCLE WITH RECIRCULATION BY A FAN

5.2.1 Cycle description

Figure 5.1 shows the proposed combined steam

124

COMPRESSOR

FAN

SUPERHEATER

DESUPERHEATERS

FUEL

PUMP

CONVENTIONAL DRYER SECTION

STEAM IMPINGEMENT DRYER
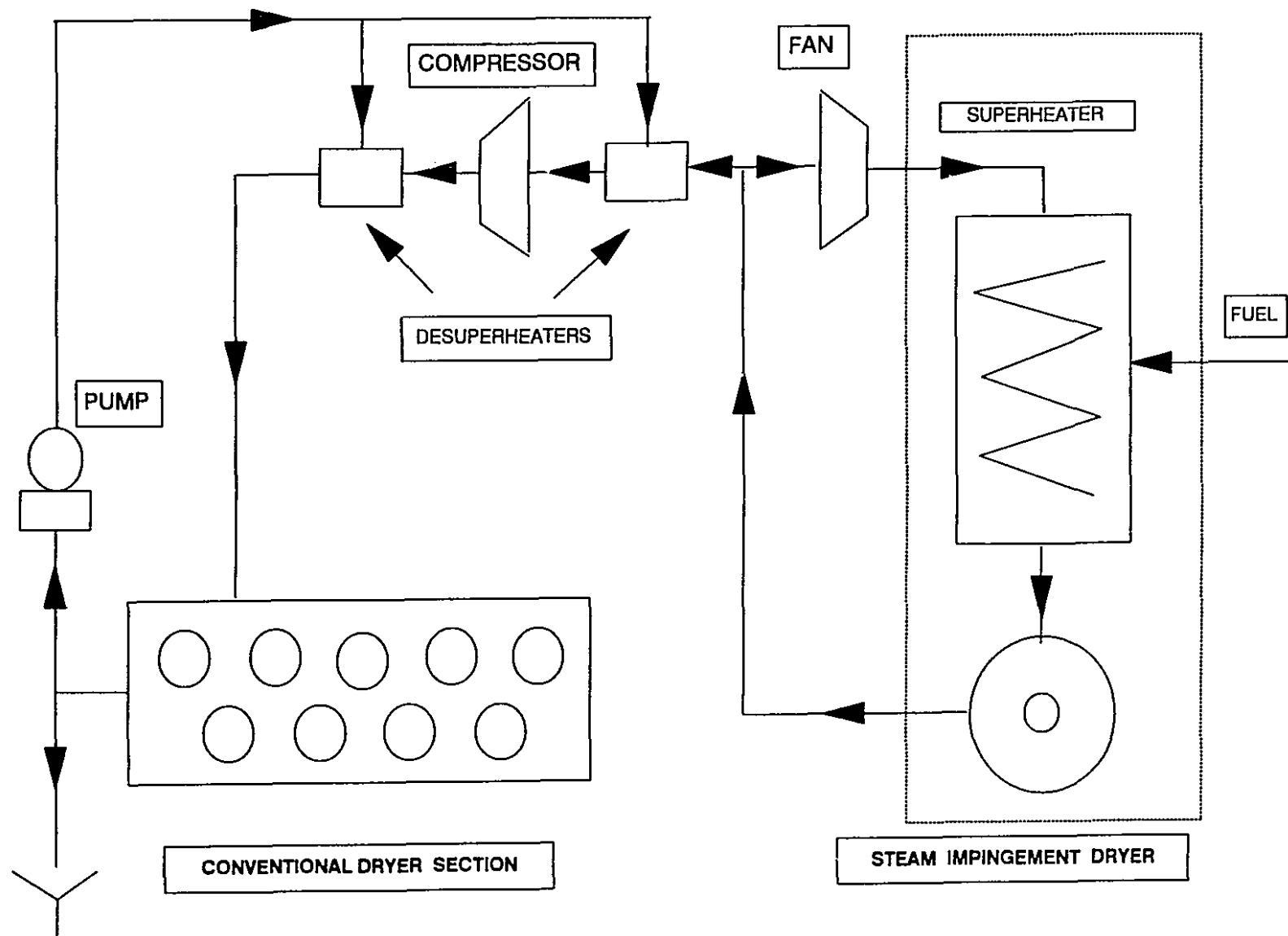
Figure 5.1 – Combined steam impingement-conventional dryer cycle with recirculation by a fan

impingement - conventional cycle with recirculation by a fan. The impingement dryer is operated at atmospheric pressure, to avoid the cost and operational hazards of operation under pressure. As conventional drying cylinders perform erratically with superheated steam (Gavelin, 1973), the steam exhausted from the impingement dryer must first be desuperheated by mixing with condensate. Compressor work per unit mass steam is minimized by desuperheating prior to compression (Becker and Zakak, 1985), as the advantageous effect of temperature decrease more than offsets the increase in compressor work from the addition of condensate.

5.2.2 Average impingement drying rate

As described in chapters 3 and 4, drying paper by impinging jets of superheated steam consists in a constant rate period, followed by a falling rate period. When a steam impingement dryer is used after a conventional dryer section, as in the present cycle, a large part, or possibly all of the drying is in the falling rate period. To evaluate the average impingement drying rate, two situations, illustrated in figure 5.2, must be considered:
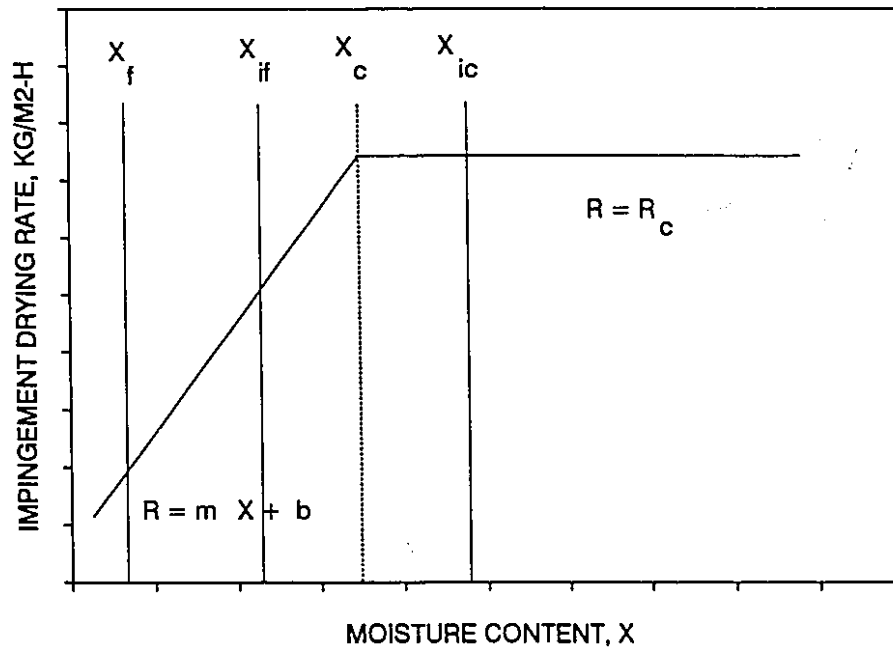
Figure 5.2 Impingement drying rate - moisture content relation

The initial moisture content for impingement steam drying may either be in the falling rate period, X_{if}, or in the constant rate period, X_{ic}. For drying entirely in the falling rate period, the average drying rate between the initial and final moisture contents, X_{if} and X_f, is found as follows:

$$\bar{R}_1 = -B \frac{(X_f - X_{if})}{(t_{X_f} - t_{X_{if}})} \tag{5.2}$$

The relationship between elapsed time t and moisture content X is obtained by equation 4.10:

$$t = \frac{B}{m} \left\{ \frac{m}{R_c} (X_1 - X_c) - \ln \left[1 + \frac{m}{R_c} (X - X_c) \right] \right\} \qquad (5.3)$$

This gives:

$$(t_{X_f} - t_{X_{1f}}) = \frac{B}{m} \left\{ -\ln \left[1 + \frac{m}{R_c} (X_f - X_c) \right] + \ln \left[1 + \frac{m}{R_c} (X_{1f} - X_c) \right] \right\}$$

$$= \frac{B}{m} \ln \left\{ \frac{\left[1 + \frac{m}{R_c} (X_{1f} - X_c) \right]}{\left[1 + \frac{m}{R_c} (X_f - X_c) \right]} \right\} \qquad (5.4)$$

Substituting this into equation 5.2 and rearranging gives:

$$\bar{R}_1 = \frac{m (X_{1f} - X_f)}{\ln \left\{ \frac{\left[1 + \frac{m}{R_c} (X_f - X_c) \right]}{\left[1 + \frac{m}{R_c} (X_{1f} - X_c) \right]} \right\}} \qquad (5.5)$$

If however drying begins in the constant rate period at X_{1c}, the average drying rate is

$$\bar{R}_1 = -B \left[\frac{(X_{1c} - X_c) + (X_c - X_f)}{(t_{X_{1c}} - t_{X_c}) + (t_{X_c} - t_{X_f})} \right] \qquad (5.6)$$

128

The time elapsed in the constant rate period is $-B (X_{1c} - X_c) / R_c$, and the time elapsed in the falling rate period is found by substituting X_c for X_{1f} in equation 5.4. Therefore, the average drying rate is

$$\bar{R}_1 = -B \left[\frac{(X_{1c} - X_f)}{\dfrac{- B (X_{1c} - X_c)}{R_c} + \dfrac{B}{m} \ln \left[1 + \dfrac{m}{R_c} (X_f - X_c) \right]} \right] \quad (5.7)$$

which simplifies to

$$\bar{R}_1 = \left[\frac{(X_{1c} - X_f)}{\dfrac{(X_{1c} - X_c)}{R_c} - \dfrac{1}{m} \ln \left[1 + \dfrac{m}{R_c} (X_f - X_c) \right]} \right] \quad (5.8)$$

In the present cycle, one unit of water exhausted from the superheated steam impingement dryer is desuperheated by mixing with condensate, then condensed in a conventional dryer section. With the approximation that the fractional amount of liquid water used for desuperheating may be neglected, one unit of water exhausted from the impingement dryer results in further removal of $1/\kappa$ unit of water in the conventional section, where κ, the steam consumption index, is the mass of steam consumed per unit mass water evaporated in that section. Therefore, a fraction equal to $1/(1+1/\kappa)$ of the total water removal occurs in the superheated steam impingement dryer. Hence the initial moisture content at the entrance of the superheated steam impingement dryer is

$$X_{11} = X_f + \frac{1}{1 + 1/\kappa} \; (X_1 - X_f) \qquad\qquad (5.9)$$

This value for X_{11}, and correlation equations for R_c, X_c and m given in table 4.1, are used to determine the average impingement drying rate using equation 5.5 or 5.8.

5.2.3 Temperature decrease and pressure drop across an impingement steam dryer

a) Temperature decrease of steam

With the assumptions that:

i- Radiation and conduction heat losses are neglected;

ii- The change in sensible heat of the water and fiber across the dryer are neglected; water is removed in the saturated liquid state;

iii- The heat of adsorption of bound water is neglected;

an enthalpy balance for a dryer with an impingement surface A_1 and
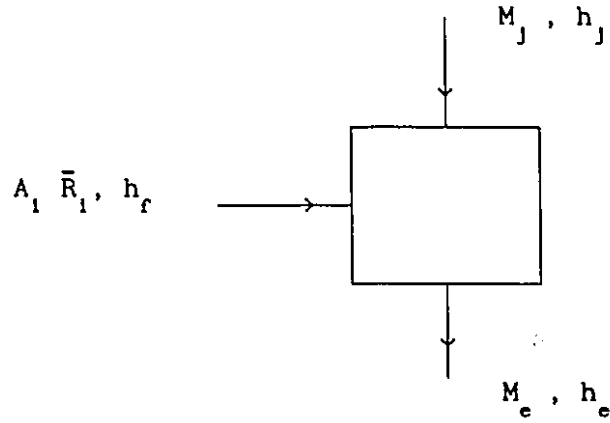
Figure 5.3 - Streams around an impingement steam dryer

an average drying rate R_1, figure 5.3, gives:

$$M_J \, h_J + A_1 \bar{R}_1 \, h_f = M_e \, h_e \qquad (5.10)$$

Treating superheated steam as a perfect gas, we have

$$M_J \, [h_g + \bar{C}_{ps}(T_J - T_b)] + A_1 \bar{R}_1 \, h_f =$$

$$(M_J + A_1 \bar{R}_1) \, [h_g + \bar{C}_{ps}(T_e - T_b)] \qquad (5.11)$$

which yields

$$\frac{T_J - T_e}{T_e - T_b} = \frac{A_1 \bar{R}_1}{M_J} \left[1 + \frac{\Delta h_v}{\bar{C}_{ps}(T_e - T_b)} \right] \qquad (5.12)$$

Substituting into the above equation the jet mass flow rate

$$M_j = \frac{A_i f \mu_j Re_j}{D} \qquad (5.13)$$

gives

$$\frac{T_j - T_e}{T_e - T_b} = \frac{\bar{R}_i D}{f \mu_j Re_j} \left[1 + \frac{\Delta h_v}{\bar{C}_{ps} (T_e - T_b)} \right] \qquad (5.14)$$

Upon rearranging, the exhaust temperature is found to be

$$T_e = \frac{1}{1 + \dfrac{\bar{R}_i D}{f \mu_j Re_j}} \left[T_j + \frac{\bar{R}_i D}{f \mu_j Re_j} \left(T_b - \frac{\Delta h_v}{\bar{C}_{ps}} \right) \right] \qquad (5.15)$$

b) Pressure drop

The pressure drop across the impingement dryer nozzles is:

$$\Delta P = \frac{1}{2} \frac{\rho_j u^2}{C_d^2} \qquad (5.16)$$

where the nozzle discharge coefficient $C_d \cong 0.80$ (Obot *et al.*, 1980). The Reynolds number dependence of ΔP is given by:

$$\Delta P = \frac{1}{2 \rho_j C_d^2 D^2} \mu_j^2 Re_j^2 = \frac{1}{2} \left(\frac{\mu_j}{C_d D} \right)^2 \frac{\mathbb{R} T_j}{M P_j} Re_j^2 \qquad (5.17)$$

Since the nozzle pressure drop is always a small fraction of the dryer absolute pressure, it is adequate for calculation purposes to

132

replace P_j by P_{atm} in the above formula.

5.2.4 Total water removal rate

The total water removal rate is the sum of the impingement and conventional rates. The drying rate in conventional dryer sections increases mildly with steam pressure, averaging 15 kg/m^2-h for complete dryer sections in Canadian paper mills (Sayegh et al., 1987), but is much higher during the constant rate period: one may estimate it to be between 30 and 50 kg/m^2-h even at very low steam pressures (Kerr, 1989). In the latter part of a conventional dryer section where the paper is in the falling rate drying period, the drying rate is evidently significantly lower than 15 kg/m^2-h. The mass of steam consumed per unit mass water evaporated, κ, averages 1.5 in Canadian paper mills. With the basic constraint of the present analysis, that the steam exhausted from the impingement section is exactly consumed for drying in the conventional section, the water removal rate in the latter section is:

$$J_c = \frac{M_c}{\kappa} \tag{5.18}$$

where M_c is the sum of the steam generation in the impingement section, and the condensate addition streams for desuperheating.

Becker and Zakak (1985) indicate that the compression work is minimized by supersaturating the exhaust steam and compressing this wet steam in a screw compressor, so as to have saturated steam at the outlet. As this process is difficult to model, it will be assumed here that steam is brought to saturation in two desuperheaters, before and after the compressor, as shown on figure 5.4:
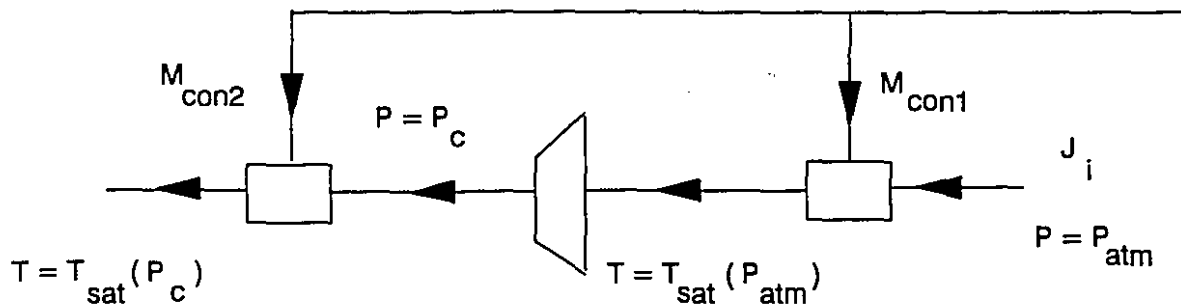
Figure 5.4 - Streams around the desuperheaters and compressor

The total water removal rate is given by:

$$J_t = J_i + J_c \tag{5.19}$$

which with equation 5.19 gives

$$J_t = J_i \left[1 + \frac{1}{\kappa} \left\{ 1 + \frac{M_{con1}}{J_i} + \frac{M_{con2}}{J_i} \right\} \right] \tag{5.20}$$

An energy balance on the first desuperheater gives:

$$\frac{M_{con1}}{J_i} = \frac{\bar{C}_{ps} (T_e - T_b)}{\Delta h_v} \tag{5.21}$$

The work per unit mass required to compress steam to the conventional pressure, P_c, is

$$w_c = \frac{\bar{C}_{ps} T_b}{\eta_c} \left[\left(\frac{P_c}{P_{atm}} \right)^{\frac{\gamma-1}{\gamma}} - 1 \right] \qquad (5.22)$$

A corresponding formula applies for the fan work w_f, in which case the exhaust pressure is $P_{atm} + \Delta P$, with ΔP obtained from (5.13). From (5.18), with $\gamma = 4/3$ for steam, the compressor exhaust temperature is

$$T_b \left\{ 1 + \frac{1}{\eta_c} \left[\left(\frac{P_c}{P_{atm}} \right)^{1/4} - 1 \right] \right\} \qquad (5.23)$$

An energy balance on the second desuperheater gives

$$\frac{M_{con2}}{J_1 + M_{con1}} = \frac{\bar{C}_{ps} \left[T_b \left\{ 1 + \frac{1}{\eta_c} \left[\left(\frac{P_c}{P_{atm}} \right)^{1/4} - 1 \right] \right\} - T_{sat, P_c} \right]}{\Delta h_v}$$

$$(5.24)$$

Now,

$$\frac{M_{con1} + M_{con2}}{J_1} = \frac{M_{con1}}{J_1} + \left[1 + \frac{M_{con1}}{J_1} \right] \left[\frac{M_{con2}}{J_1 + M_{con1}} \right] \qquad (5.25)$$

Substituting from (5.17), (5.20) and (5.21) into (5.16) gives:

$$J_t = J_i \left[1 + \frac{1}{\kappa} \left\{ 1 + \left[\frac{\bar{C}_{ps} (T_e - T_b)}{\Delta h_v} \right] + \left\{ 1 + \left[\frac{\bar{C}_{ps} (T_e - T_b)}{\Delta h_v} \right] \right\} \right. \right.$$

$$\left. \left. \ast \left\{ \frac{\bar{C}_{ps} \left[T_b \left\{ 1 + \frac{1}{\eta_c} \left[\left(\frac{P_c}{P_{atm}} \right)^{1/4} - 1 \right] \right\} - T_{sat, \, P_c} \right]}{\Delta h_v} \right\} \right\} \right]$$

(5.26)

5.2.5 Heat, work, and equivalent energy consumption

An energy balance on the control volume indicated by the dotted lines in figure 5.1 gives the heat consumption per unit mass of water evaporated in the complete cycle:

$$\frac{Q_i}{J_t} = \frac{M_J \left[\bar{C}_{ps}(T_J - T_e) - w_F \right]}{J_t}$$

(5.27)

The fan and compressor work consumption per unit water evaporated are:

$$\frac{W_F}{J_t} = \frac{M_J \, w_F}{J_t}$$

(5.28)

$$\frac{W_c}{J_t} = \frac{(J_1 + M_{con1}) \, w_c}{J_t} \qquad (5.29)$$

The total energy consumption per unit water evaporated is

$$E_t = \frac{Q_1 + W_F + W_c}{J_t} \qquad (5.30)$$

Finally, the equivalent energy consumption is

$$E_e = \frac{Q_1 + \varepsilon \, (W_F + W_c)}{J_t \; \Delta h_v} \qquad (5.31)$$

5.2.6 Simulation results

A computer program was written to solve the above equations for heat, work, total and equivalent energy consumption as a function of average impingement drying rate, with impinging jet temperature as a parameter. The program inputs are the dryer geometry (H, D, f), jet temperature and Reynolds number, moisture contents at the inlet of the conventional dryer section and at the outlet of the superheated steam impingement dryer, impingement drying rate, fan and compressor isentropic efficiencies, conventional dryer pressure, work-to-heat value ratio and conventional dryer steam consumption index κ. The sequence of calculations is illustrated in figure 5.5.

```
┌─────────────────────────────┐        ┌─────────────────────────────┐
│        FIXED INPUT          │        │       VARIABLE INPUT        │
│                             │        │                             │
│      Dryer geometry;        │        │   Jet temperature range;    │
│ Fan and compressor          │        │ Average impingement drying  │
│   efficiencies;             │        │        rate range.          │
│  Conventional dryer pressure│        │                             │
│    and performance index;   │        └─────────────────────────────┘
│  Work-to-heat value ratio;  │
│  Conventional dryer inlet and│
│  steam dryer exhaust moisture│        ┌──────────────┐
│         contents;           │        │ FUNCTION AND │
│       Basis weight.         │        │   VARIABLE   │
└─────────────────────────────┘        │  DEFINITION  │
                                       └──────────────┘
```

Set T_j, Re_j to lowest value in range

MAIN CALCULATION SEQUENCE:
X_{11}, $\bar{R}_1$, T_e, ΔP, W_f, W_c, Q_1

Increment T_j, Re_j

FINAL CALCULATION SEQUENCE
Q_1/J_t, W/J_t, E_t, E_e, fraction of drying done in steam impingement dryer

NO

Complete T_j, $\bar{R}_1$ range covered?

YES

OUTPUT
Print results to disk file

Figure 5.5 - Flowsheet of program for performance calculations on
combined steam impingement-conventional drying cycle
with fan circulation

138

A listing of the program for the present scheme and the two other cycles described in this chapter is included as appendix 5.

Heat, work and total energy consumption for conditions listed in table 5.2, and jet temperature T_j = 400 $^\circ$C, are shown in figure 5.6:

Dryer geometry	– Nozzle-to-web distance	H :	20 mm
	Nozzle diameter	D :	4 mm
	Open area ratio	f :	1.5 %

Moisture content at inlet of conventional dryer: X_l : 1.5

Moisture content at exhaust of steam impingement dryer: X_f : 0.08

Fan isentropic efficiency η_F : 0.7

Compressor isentropic efficiency η_C : 0.7

(Degueurce and Banquet, 1984)

Conventional dryer steam pressure P_c : 140 kPa abs.

Conventional dryer steam consumption index κ : 1.5 kg steam consumed / kg water evaporated

Table 5.2 – Conditions for simulation run of combined steam impingement-conventional dryer performance.
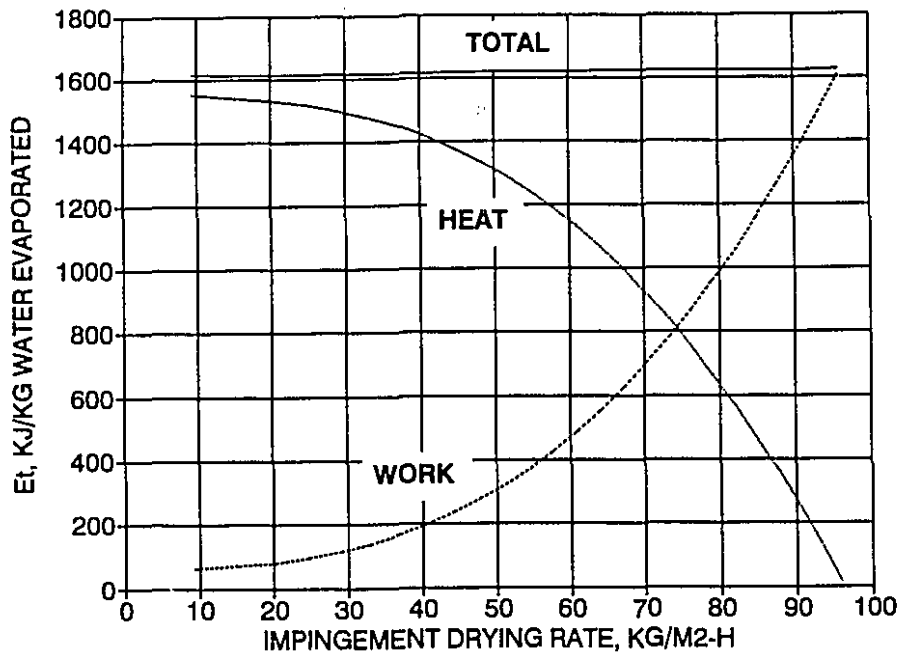
Figure 5.6 - Energy consumption for combined cycle with
circulation by fan: T_j = 400 °C

At low impingement drying rates, very little fan power is required to recirculate the steam through the impingement dryer. As the impingement drying rate increases with higher jet velocity, the steam temperature difference across the dryer decreases according to equation 5.15 and the fan supplies more of the total energy. The heat requirement of the superheater decreases accordingly, until a *limiting impingement drying rate* R_l is reached, where all of the energy is supplied by the fan. At this limit, the jet velocity is 240 m/s and the fan pressure boost is 14.7 kPa, and 54% of the total water removal is in the impingement dryer. The latter figure, computed by taking into account the additional steam generated in the desuperheaters, is close to the value $1/(1+1/\kappa)$ = 60% used as a first approximation to compute the

initial moisture content for impingement drying, thereby justifying the assumption that the fractional amount of liquid water used for desuperheating may be neglected in determining X_{11}. The limiting drying rate is the highest impingement drying rate which can be achieved at a given steam jet temperature for these conditions. This raises the possibility of designing a *heater-less* superheated steam drying cycle, which could be attractive in regions with low power cost due to the saving in eliminating the superheater.

Figure 5.7a shows the effect of average impingement drying rate on the equivalent energy consumption for the above conditions for $\varepsilon = 1.64$ (the ratio of electricity-to-natural gas price in Quebec), with jet temperature in the range $400\ ^{\circ}C \leq T_j \leq 600\ ^{\circ}C$. For high drying rate, $\bar{R}_1 > 70$ kg/m^2-h, the lowest equivalent energy consumption is obtained with the highest jet temperature, corresponding to the lowest jet Reynolds number. Average impingement drying rates of the order of 60 kg/m^2-h can be achieved with an equivalent energy consumption only about half the average value of 1.5 kg steam/ kg water evaporated for conventional dryers. These results demonstrate the potential of this cycle for retrofitting existing paper machines, or designing new ones, to achieve simultaneously higher drying rates and lower energy consumption.

Figure 5.7b shows results for the same case with $\varepsilon = 4.43$ (the ratio of electricity-to-natural gas prices in the United States). Equivalent energy consumption increases much faster with drying rate, eventually becoming higher than for conventional dryers because of the high cost of electricity relative to steam. With this model, performance curves can
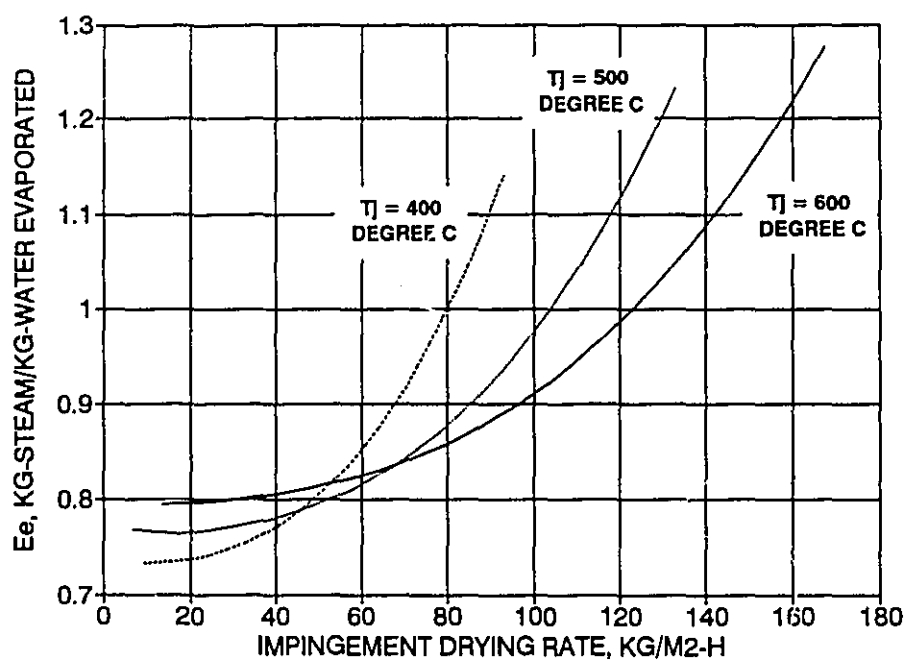
Figure 5.7a   Equivalent energy consumption for combined
cycle with circulation by fan; ε = 1.84
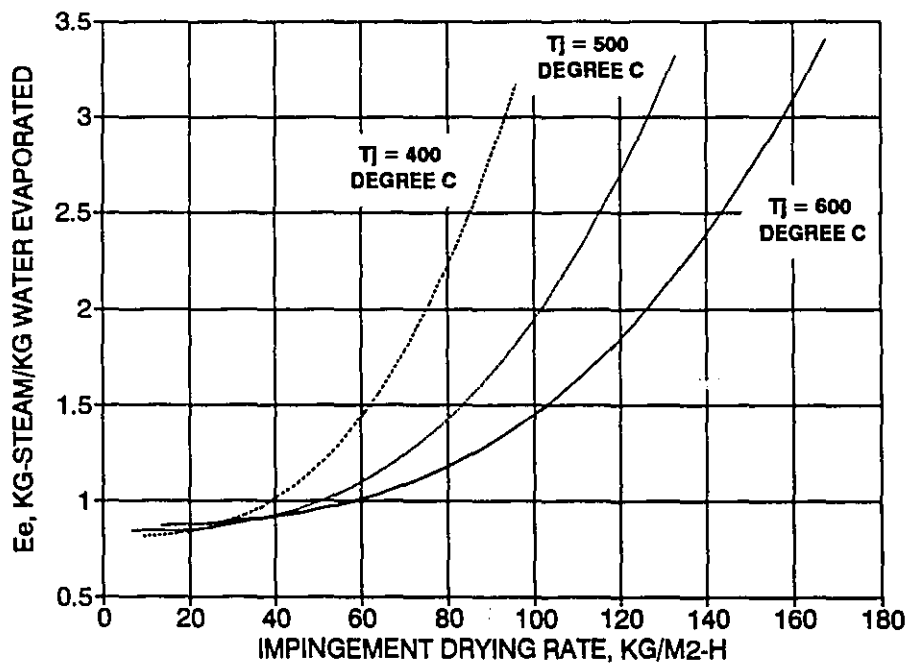
Figure 5.7b   Equivalent energy consumption for combined
cycle with circulation by fan; ε = 4.43

easily be obtained for the locally relevant value of the work-to-heat value ratio ε.

5.3 STEAM IMPINGEMENT-CONVENTIONAL CYCLE WITH RECIRCULATION BY THERMOCOMPRESSOR

5.3.1 Cycle description

The possibility of using a thermocompressor to boost the pressure of steam generated in a superheated steam paper dryer has been mentioned in numerous studies (Cui *et al.*, 1985, Beeby and Potter, 1986, Loo and Mujumdar, 1984) and used for the superheated steam Yankee dryer study of Thompson *et al.* (1991). In a thermocompressor, a high pressure motive stream is mixed with a low pressure induced stream and the combined stream is discharged at an intermediate pressure. Low cost and simplicity of maintenance make thermocompressors an attractive alternative to mechanical compressors. However, to obtain an appreciable pressure boost, the ratio of motive to induced mass flow rate must be high. Therefore, a particularly appropriate use of a thermocompressor here would be to supply the relatively low pressure boost required to recirculate steam around the impingement dryer circuit (figure 5.8a).
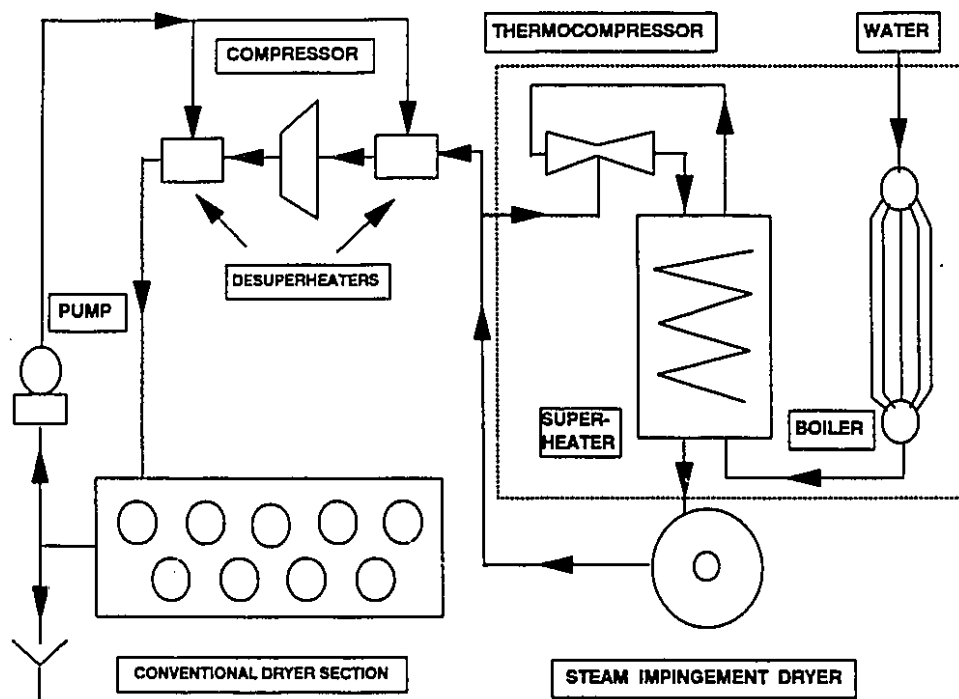
Figure 5.8a   Combined steam   impingement – conventional drying
cycle with recirculation by a thermocompressor

MOTIVE FLOW: M_{tm}, T_{tm}, P_{tm} EXHAUSTED FLOW: M_{te}, T_{te}, P_{te}

INDUCED FLOW: M_{ti}, T_{ti}, P_{ti}
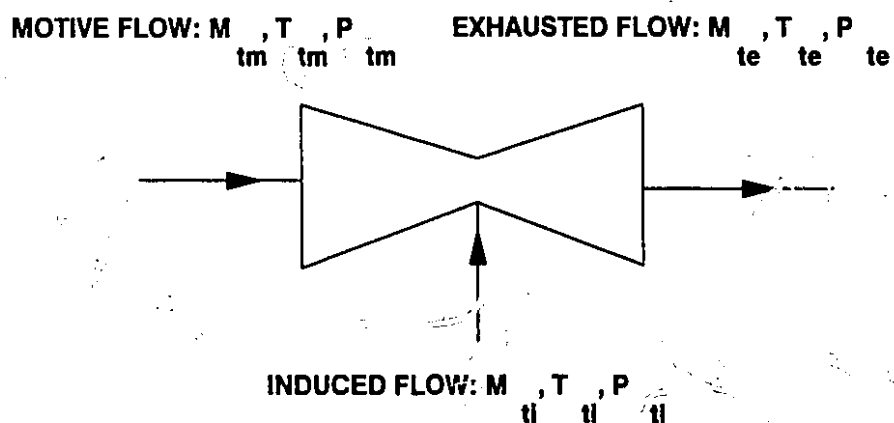
Figure 5.8b – Flows through a thermocompressor

144

As in the previous section, expressions for heat, work and equivalent energy consumption versus impingement drying rate will be derived for a combined superheated steam impingement-conventional drying cycle with circulation by a thermocompressor.

5.3.2 Thermocompressor performance

In a thermocompressor (figure 5.8b), motive steam with mass flow rate M_{Tm}, temperature T_{Tm} and pressure P_{Tm} drives induced steam with mass flow rate M_{Ti}, temperature T_{Ti} and pressure P_{Ti}. The exhausted steam has mass flow rate M_{Te}, temperature T_{Te} and pressure P_{Te}. The *thermocompressor efficiency* η_t is defined as the ratio of the work done by expanding the exhaust steam in an isentropic turbine between pressures P_{Te} and P_{Ti}, to that done by expanding the motive steam in an isentropic turbine between pressures P_{Tm} and P_{Ti}:

$$\eta_T \equiv \frac{M_{Te} \, \Delta h_{P_{Te} \rightarrow P_{Ti}}}{M_{Tm} \, \Delta h_{P_{Tm} \rightarrow P_{Ti}}} \tag{5.32}$$

An efficiency of 0.3 is typical of modern thermocompressors operating with a high ratio of induced-to-driving flow rate (Schmitt, 1978).

The work per unit mass, w, done by steam of initial temperature T expanded isentropically between arbitrary pressures P_1 and P_2 is

$$w = \bar{C}_{ps} \, T \left\{ 1 - \left[\frac{P_1}{P_2} \right]^{\frac{1-\gamma}{\gamma}} \right\} \tag{5.33}$$

Hence for steam ($\gamma = 4/3$), we have

$$\eta_T = \frac{M_{Te}\, T_{Te} \left\{ 1 - \left[\dfrac{P_{T1}}{P_{Te}} \right]^{1/4} \right\}}{M_{Tm}\, T_{Tm} \left\{ 1 - \left[\dfrac{P_{T1}}{P_{Tm}} \right]^{1/4} \right\}} \tag{5.34}$$

An energy balance for the adiabatic thermocompressor gives

$$M_{T1}\, T_{T1} + M_{Tm}\, T_{Tm} = (M_{T1} + M_{Tm})\, T_{Te} = M_{Te}\, T_{Te} \tag{5.35}$$

Substituting this into equation 5.34 and rearranging gives

$$\frac{M_{T1}}{M_{Tm}} = \frac{T_{Tm}}{T_{T1}} \left[\eta_T\; \frac{\left\{ 1 - \left[\dfrac{P_{T1}}{P_{Tm}} \right]^{1/4} \right\}}{\left\{ 1 - \left[\dfrac{P_{T1}}{P_{Te}} \right]^{1/4} \right\}} - 1 \right] \tag{5.36}$$

Since the thermocompressor motive steam must be produced in a separate boiler and recompressed for the conventional dryer section, it is desirable to use as little motive steam as possible. Equation 5.36 shows that this is achieved

i- by using a thermocompressor of the *highest efficiency* possible;

ii- by using motive steam of the *highest pressure* possible;

146

iii- by using motive steam of the *highest temperature* possible. Here, this can be accomplished by superheating the motive steam to the impinging jet temperature T_j, prior to injection in the thermocompressor. This superheating represents no additional heating requirement, as heat added at this level correspondingly reduces the heat to be supplied to the combined stream.

5.3.3 Heat consumption

In terms of the flow rates, temperatures and pressures in the present cycle, equation 5.36 can be written:

$$\frac{M_{T1}}{M_{Tm}} = \frac{M_j}{M_{Tm}} - 1 = \frac{T_j}{T_e} \left[\frac{\eta_T \left\{ 1 - \left[\dfrac{P_{atm}}{P_{Tm}}\right]^{1/4} \right\}}{\left\{ 1 - \left[\dfrac{P_{atm}}{P_j}\right]^{1/4} \right\}} - 1 \right] \quad (5.37)$$

An energy balance on the control volume indicated by the dotted lines in figure 5.8a gives

$$\Sigma Q = Q_b + Q_s = M_j h_j - M_{Tm} h_f - (M_j - M_{Tm}) h_e \quad (5.38)$$

$$\Sigma Q = M_j \bar{C}_{ps} (T_j - T_e) + M_{Tm} [\Delta h_v + \bar{C}_{ps} (T_e - T_{sat})]$$

$$(5.39)$$

$$= M_J \left[\bar{C}_{ps}(T_J - T_e) + \left[1 + \frac{T_J}{T_e} \left[\frac{\eta_T \left\{ 1 - \left[\frac{P_{atm}}{P_{Tm}} \right]^{1/4} \right\}}{\left\{ 1 - \left[\frac{P_{atm}}{P_J} \right]^{1/4} \right\}} - 1 \right] \right]^{-1} \right.$$

$$\left. \ast \; [\Delta h_v + \bar{C}_{ps}(T_e - T_{sat})] \right] \tag{5.40}$$

The relationships between T_J and T_e (equation 5.15) and between P_J and P_{atm} (equation 5.17), derived for the cycle with circulation by a fan, also apply here.

5.3.4 Total water removal rate

As previously, steam exhausted from the impingement dryer is desuperheated, compressed and desuperheated again for use in the conventional dryers. The total water removal rate is

$$J_t = J_1 + \frac{1}{\kappa} [J_1 + M_{Tm}] \left\{ 1 + \frac{M_{con1}}{J_1 + M_{Tm}} + \frac{M_{con2}}{J_1 + M_{Tm}} \right\} \tag{5.41}$$

Equations 5.20 through 5.24 for the desuperheater flow rates also apply in this case. Substituting the values in those equations into equation 5.41 gives

$$J_t = J_1 + \frac{J_1}{\kappa}\left[1 + \frac{M_{Tm}}{M_J}\frac{M_J}{J_1}\right]\left[1 + \left[\frac{\bar{C}_{ps}(T_e - T_b)}{\Delta h_v}\right] + \left\{1 + \left[\frac{\bar{C}_{ps}(T_e - T_b)}{\Delta h_v}\right]\right\}\right] \cdot$$

$$\left\{\frac{\bar{C}_{ps}\left[T_b\left\{1 + \frac{1}{\eta_c}\left[\left[\frac{P_c}{P_{atm}}\right]^{1/4} - 1\right]\right\} - T_{sat, P_c}\right]}{\Delta h_v}\right\}\right] \quad (5.42)$$

where the ratios M_{Tm}/M_J and M_J/J_1 are given by equations 5.37 and 5.12. For this cycle, the moisture content at the inlet of the steam impingement dryer must be determined iteratively, so as to have $(X_{11} - X_f)/(X_1 - X_f)$ equal to J_1/J_t.

5.3.5 Power consumption

While eliminating fan power consumption, circulation by thermocompressor increases compressor power by an amount proportional to the motive steam flow rate. The compressor power consumption is given by

$$W_c = J_1\left[1 + \frac{M_{Tm}}{M_J}\frac{M_J}{J_1}\right]\left[1 + \frac{\bar{C}_{ps}(T_e - T_b)}{\Delta h_v}\right]\frac{\bar{C}_{ps}T_b}{\eta_c}\left[\left(\frac{P_c}{P_{atm}}\right)^{1/4} - 1\right]$$

$$(5.43)$$

5.3.6 Simulation results

Specific heat and power consumptions Q_1/J_t and W_c/J_t, as well as equivalent energy consumption, were calculated for a motive steam pressure of 1135 kPa (150 p.s.i.g.), a thermocompressor efficiency $\eta_T = 0.3$, and other conditions as in table 5.2. Figures 5.9a and 5.9b show the equivalent energy consumption as a function of the average impingement drying rate, with temperature as a parameter, in the range $400 \leq T_J \leq 600$ °C, using work-to-heat value ratios for Québec ($\varepsilon = 1.64$) and the United States ($\varepsilon = 4.43$), respectively. Contrary to the previous cycle with circulation by a fan, the drying rate can be increased without limit by using ever greater quantities of externally-supplied motive steam. At drying rates higher than about 25 kg/m²-h, the energy consumption decreases substantially with increasing jet temperature, highlighting the importance of operating the dryer at the highest temperature possible. At a given jet temperature, as the drying rate increases with increasing jet velocity, a larger fraction of the steam exhausted to the conventional dryer section is thermocompressor motive steam. Hence most of the drying is done in the conventional dryer section, as shown on figure 5.9c, and the total equivalent energy consumption asymptotically approaches the value for the conventional dryer, 1.5 kg/kg, plus a small amount representing the compressor power.
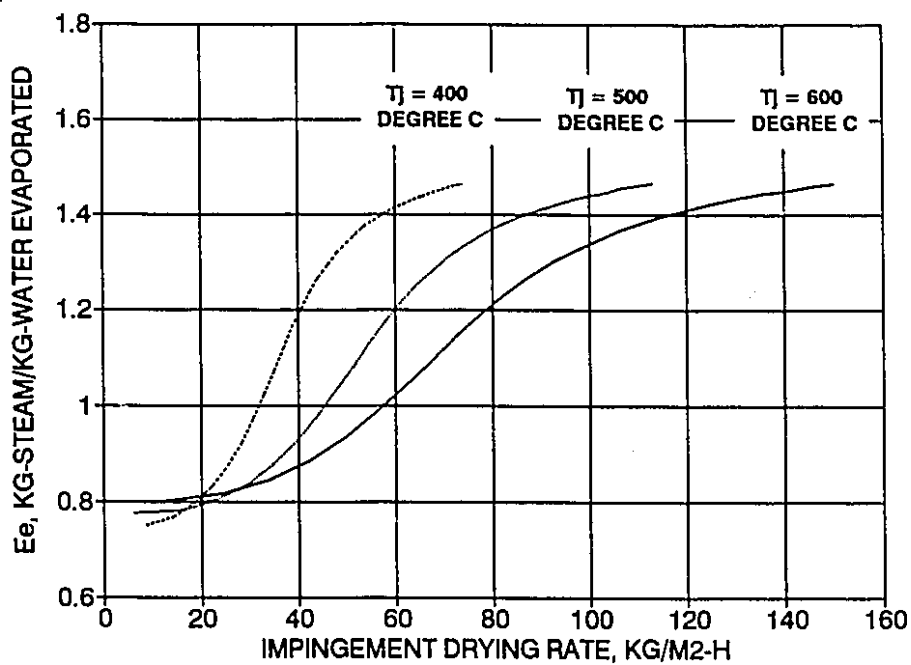
Figure 5.9a   Equivalent energy consumption for combined cycle with thermocompressor; ε = 1.64
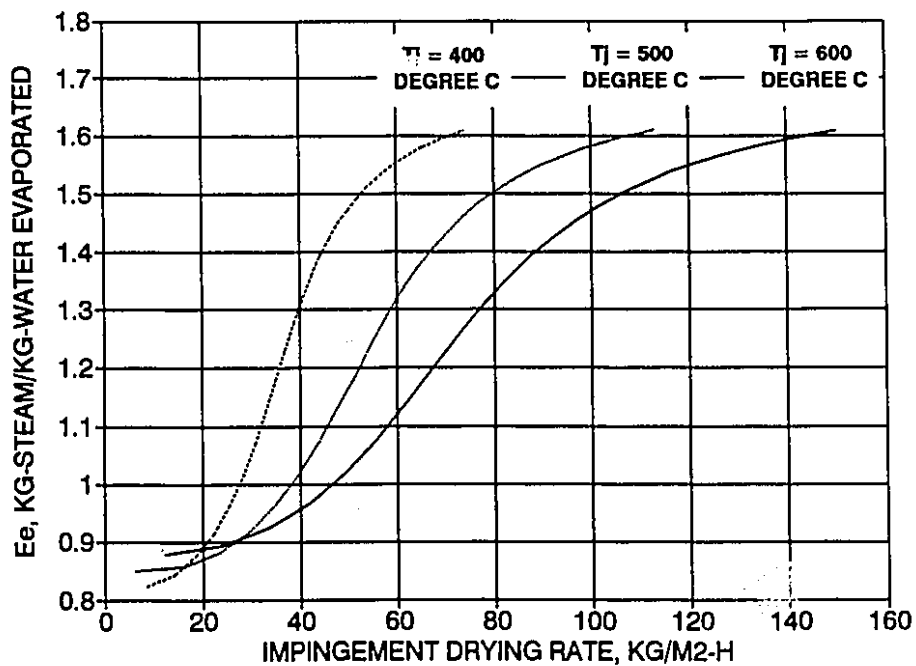
Figure 5.9b   Equivalent energy consumption for combined cycle with thermocompressor; ε = 4.43

151
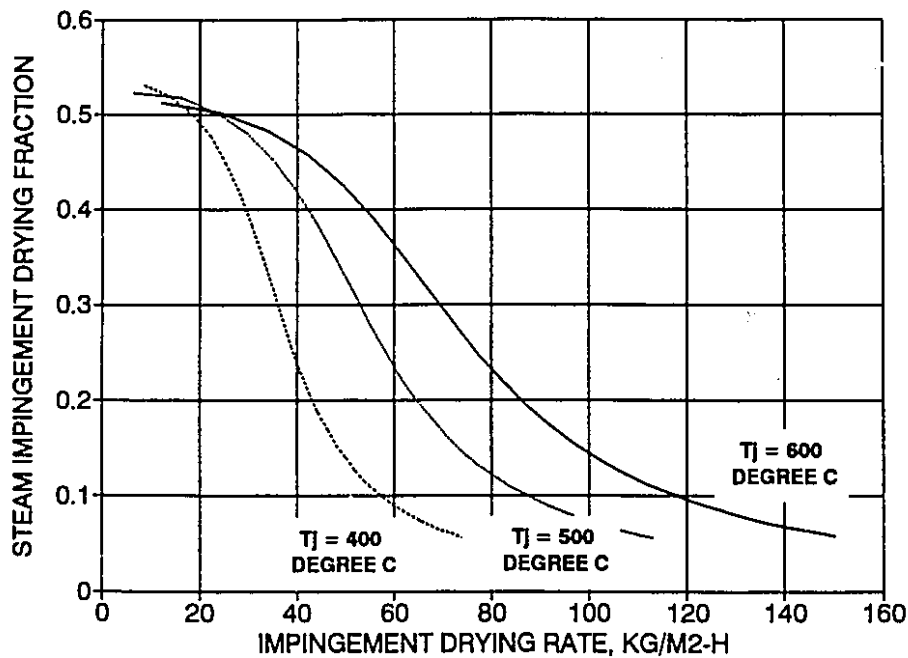
Figure 5.9c Fraction of drying done in steam impingement dryer
for combined cycle with steam recirculation by a
thermocompressor

5.3.7 Comparison of recirculation by fan or thermocompressor

Figure 5.10 shows a comparison of the performance of the two cycles
with recirculation by fan or by thermocompressor at T_J = 500 °C, a
typical operating temperature for modern impingement dryers. For
ε = 1.64, recirculation by fan is much more attractive in the drying
rate range of interest (say, $\bar{R}_1$> 60 kg/m^2-h). Because work costs only
slightly more than heat, it is not worthwhile to displace the fan work
by a comparatively large heat expenditure for the generation of
thermocompressor motive steam. The situation is quite different with
ε = 4.43, where the performance curves intersect at $\bar{R}_1$= 85 kg/m^2-h and
at larger drying rates, circulation by thermocompressor outperforms
circulation by fan. For very high impingement drying rate, the lower
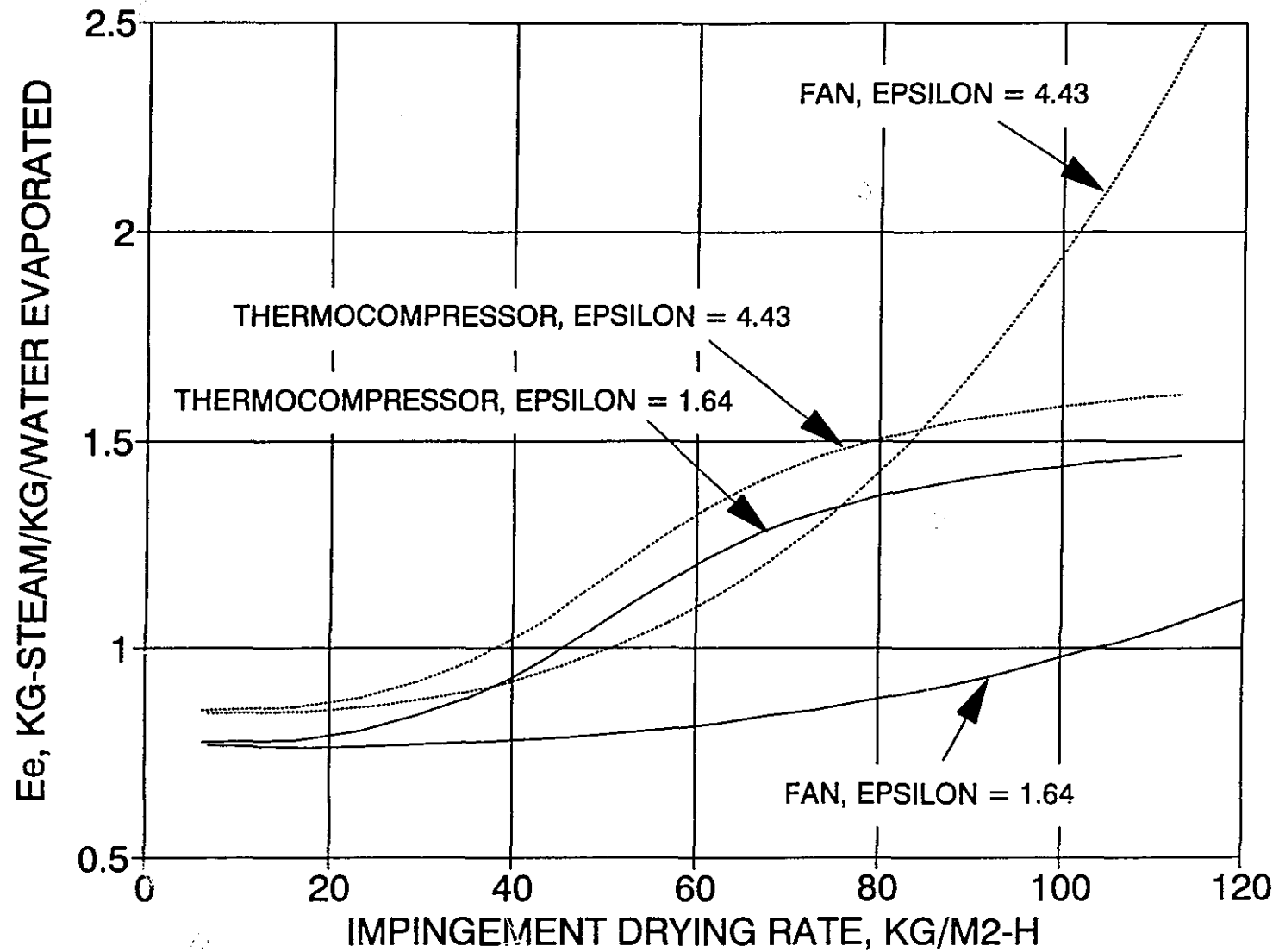
Figure 5.10 – Equivalent energy consumption: Recirculation by fan or thermocompressor; Tj = 500 degree C

energy consumption, along with the saving in capital and maintenance cost of the thermocompressor, indicate that this cycle is preferable to circulation by a fan in regions with high electricity cost. It should be noted, however, that at such high drying rates, the equivalent energy consumption is higher than that for the conventional process. In those cases, considerations other than energy consumption may determine the choice of means of recirculation.

5.4 COMBINED IMPINGEMENT-CONVENTIONAL DRYER WITH INTEGRATED OPEN-CYCLE HEAT PUMP

5.4.1 Cycle description

In the two cycles introduced so far, the energy of the steam exhausted from the steam dryer was recovered entirely by condensation in a conventional dryer section. Luthi (1981) proposed a cycle in which most of the latent heat of the exhausted steam is recovered in an open-cycle heat pump associated with the steam dryer, making it to a large extent independent of an external use of the steam generated. An embodiment of this cycle has been successfully implemented at the pilot-plant scale for clay drying in Great Britain (Heaton and Benstead, 1984).

Figure 5.11a is a schematic representation of this cycle and figure 5.11b shows the process on a temperature-entropy diagram. Superheated steam from a steam impingement dryer is split into a recirculating stream and an exhaust stream with a flow rate equal to the impingement drying rate. The compressed exhaust steam is condensed in a heat pump heat exchanger, thereby reheating the recirculating steam.

At low impingement drying rate, the fan adds very little energy to
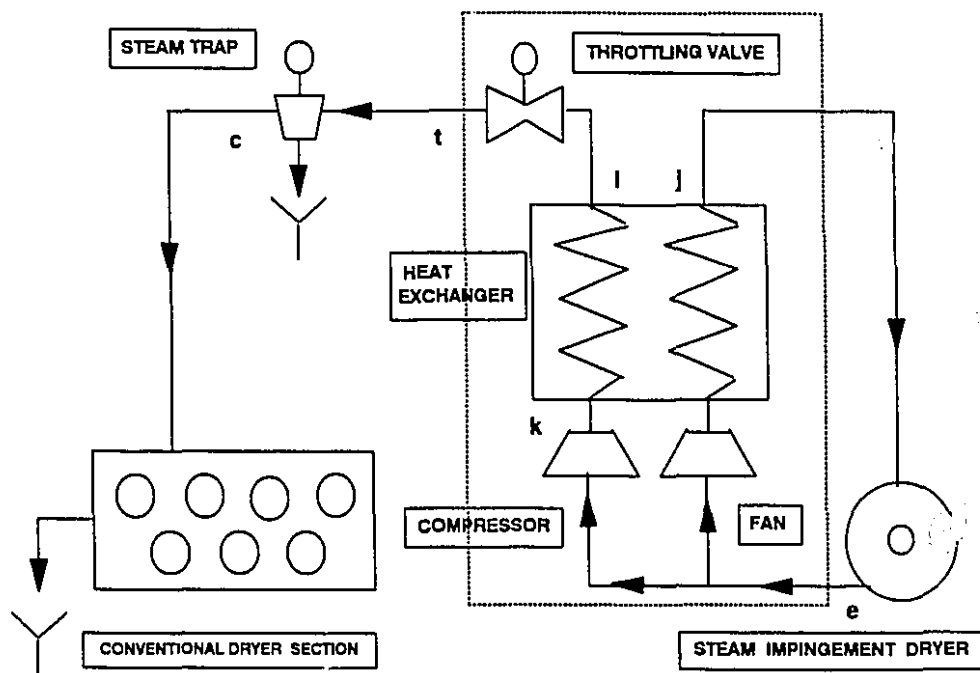
Figure 5.11a   Combined steam impingement-conventional
drying cycle with heat pump
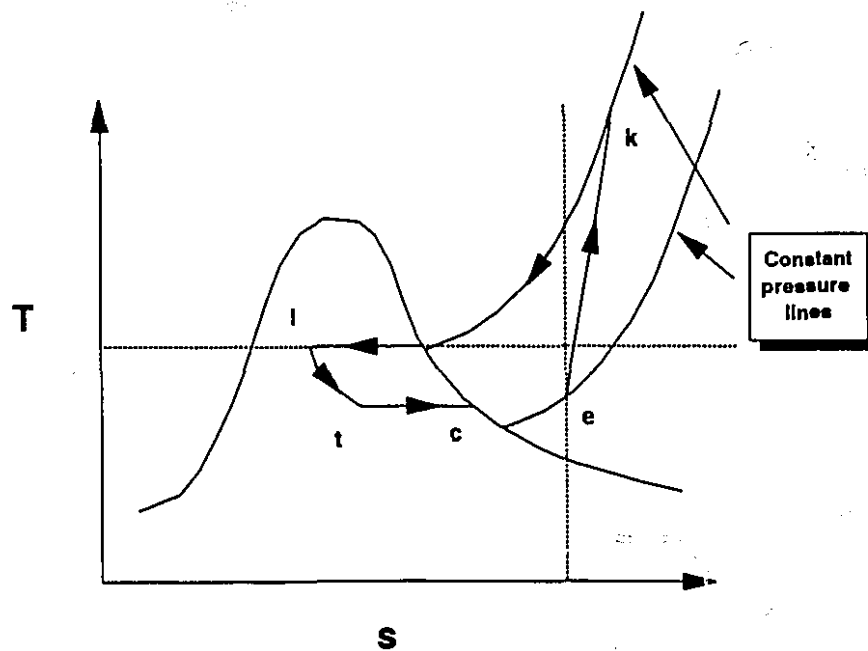
Figure 5.11b   Cycle representation on temperature-entropy diagram

the recirculated steam. As the dryer is a heat exchanger in which superheated steam M_j gives off sensible heat to evaporate water J_i, while in the heat pump exchanger, steam J_i gives up latent heat to reheat recirculating steam M_j, there is an inherent match between the heat removed in the dryer and that added in the exchanger. With increasing drying rate, however, the energy introduced with the fan becomes substantial, so that less heat needs to be transferred to the recirculating steam in the heat exchanger. Hence not all of the exhaust steam can be condensed, so that a condensate – steam mixture is discharged from the heat exchanger. After throttling to the pressure of the conventional dryer section and separation of the condensate in a steam trap, the remaining steam is condensed in a conventional dryer section.

5.4.2 Fan power

The fan work is

$$W_F = M_j \frac{\bar{C}_{ps} T_e}{\eta_F} \left[\left(\frac{P_j}{P_{atm}} \right)^{1/4} - 1 \right]$$
(5.44)

The relationships derived for the cycle with circulation by a fan between T_j and T_e (equation 5.15) and between P_j and P_{atm} (equation 5.17), also apply to this cycle.

5.4.3 Compressor power

The terminal temperature difference in the heat exchanger is very small (Blumberg, 1983) and may be taken as zero to a good approximation.

156

Therefore, the exhaust steam must be compressed to the saturation pressure corresponding to the impinging jet temperature. This constraint, in theory, limits the impinging jet temperature to somewhat less than the critical temperature of steam, 374.1 ^{o}C. In practice however, the highest obtainable steam pressure is probably about 15 atmospheres, corresponding to a saturation temperature of about 200 ^{o}C. Therefore, the maximum impinging jet temperature for this cycle will be only about 200 ^{o}C. The compressor work is

$$W_c = J_1 \frac{\bar{C}_{ps} T_e}{\eta_c} \left[\left(\frac{P_c}{P_{atm}} \right)^{1/4} - 1 \right] \qquad (5.45)$$

where $P_c = P_{sat}$ at T_j.

5.4.4 Heat exchanger outlet state and total water removal rate

The state of the steam after the throttling valve is determined from an energy balance on the control volume indicated by dotted lines in figure 5.11a:

$$W_F + W_c = M_j \, h_j + J_1 h_t - (M_j + J_1) h_e \qquad (5.46)$$

where h_t is the enthalpy at the exhaust of the throttling valve. Dividing by J_1, we have:

$$h_t = \frac{W_F + W_c - M_j \, \bar{C}_{ps}(T_j - T_e)}{J_1} + h_e \qquad (5.47)$$

With h_t determined, the steam quality x, the water vapor mass fraction
of the wet steam, is obtained from

$$x = \frac{h_t - h_f}{\Delta h_v} \qquad (5.48)$$

The saturated steam flow rate to the conventional dryer is

$$M_c = \bar{R}_1 \, x \qquad (5.49)$$

and the total water removal rate is

$$J_t = J_1 + J_c = J_1 + x \, J_1/\kappa = J_1 \, (1 + x/\kappa) \qquad (5.50)$$

Specific work consumption and total equivalent energy consumption
are obtained by dividing the work expressions (equations 5.44 and 5.45)
by this total water removal rate (equation 5.50). As for the cycle with
thermocompressor, the moisture content at the inlet of the steam
impingement dryer must be determined iteratively, so as to have
$(X_{1i}-X_f)/(X_i-X_f)$ equal to J_i/J_t.

5.4.5 Simulation results

Figures 5.12a and 5.12b show the performance characteristics
represented as a function of the average impingement drying rate, with
temperature as a parameter ($150 \leq T_j \leq 190$ °C), for $\varepsilon = 1.64$ and 4.43,
respectively. All other conditions are as given in table 5.2.
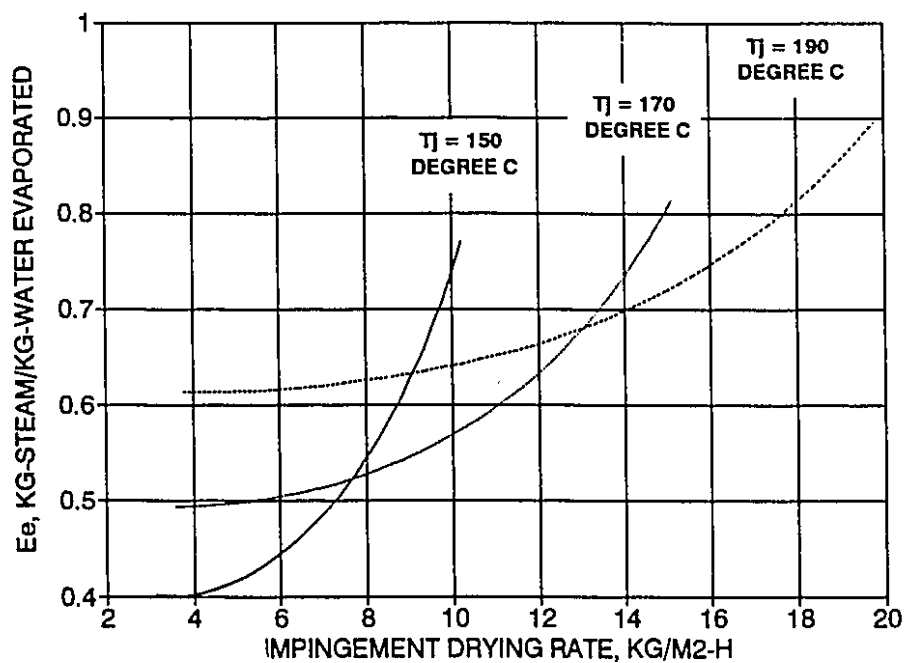
Figure 5.12a   Equivalent energy consumption for combined
cycle with heat pump; ε = 1.64
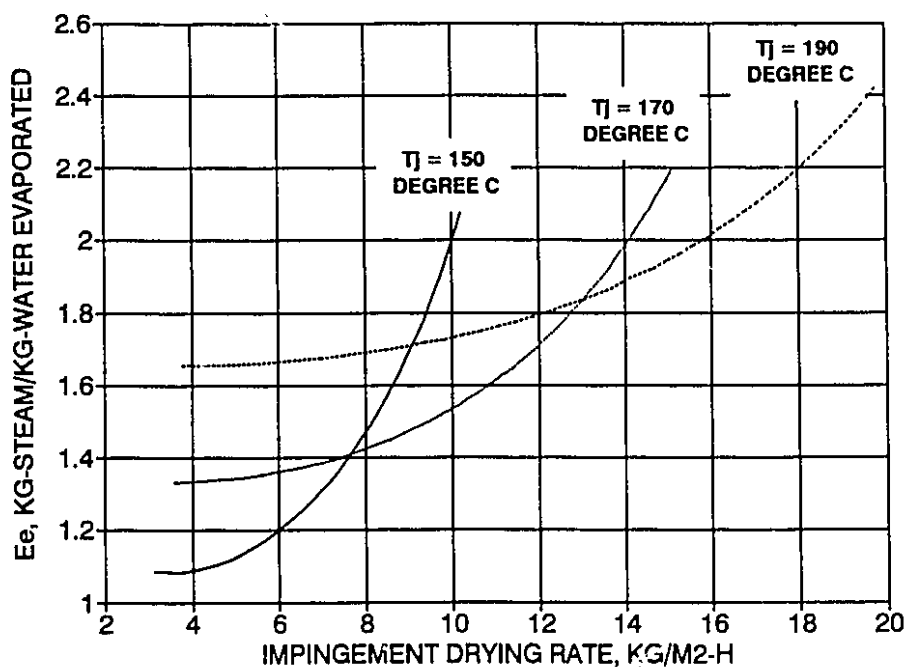
Figure 5.12b   Equivalent energy consumption for combined
cycle with heat pump; ε = 4.43

Since this cycle is closed, there corresponds to each inlet temperature a *limiting drying rate* at which all the energy to reheat the recirculating steam is supplied by the fan. In this limiting condition, no heat is transferred in the heat exchanger and the system performs similarly to the heaterless version of the cycle with recirculation by fan.

The highest impingement drying rate possible with this cycle is only 20 kg/m^2-h at T_j = 190 ^{o}C. In the upper range of achievable drying rates, energy consumption is minimized by using the highest impinging jet temperature possible, as for the two previous cycles. However, for equivalent energy consumption substantially less than that for conventional drying, 1.5 kg/kg, the range of impingement drying rates obtainable is so much lower than for either of the other two cycles that the heat pump cycle appears an unpromising option for industrial implementation.

5.5 CONCLUSION

Three self-contained cycles for implementing superheated steam impingement drying of paper have been analyzed in terms of an equivalent energy consumption, which takes into account the different values of heat and work energy. In all cycles, the equivalent energy consumption for a given jet temperature increases with increasing impingement drying rate, but for a given impingement drying rate, decreases with increasing superheat of the impingement steam.

With combined superheated steam - conventional drying employing a fan for impingement steam recirculation, the energy consumption is reduced by about half in regions of low electricity cost, by about one

160

third in regions of high electricity cost, compared to conventional drying. As impinging jet velocity is increased, a trade-off occurs, with impingement drying rate increasing (thereby reducing the size of the impingement dryer) but with the energy saving decreasing. At each impinging jet temperature there is a maximum drying rate corresponding to the energy for drying being entirely supplied by the fan. Building such a heater-less superheated steam impingement dryer could be advantageous in regions with low electricity cost.

Recirculation of the impingement steam by a thermocompressor eliminates the capital and power costs of a fan, but requires high pressure motive steam. The thermocompressor performance is improved by superheating the motive steam prior to injection into the thermocompressor. For all operating conditions giving an equivalent energy consumption better than that of a conventional dryer section, about $E_e = 1.5$, the equivalent energy consumption for superheated steam recirculation by a thermocompressor is higher than for recirculation by a fan. This difference becomes small for conditions giving impingement drying rates as high as 80 kg/m^2-h in regions of high electricity cost, $\varepsilon = 4.43$, in which case considerations other than equivalent energy consumption would determine the choice between a fan or a thermocompressor for steam recirculation. Thus the advantage of the fan would need to be balanced against the capital and maintenance cost advantage of the thermocompressor.

Combined steam impingement-conventional drying with an integrated open-cycle heat pump is limited to low impingement drying rates because the heat pump limits the impinging jet temperature to 200 $^\circ$C. The low drying rates that can be achieved make this cycle unsuitable for paper

drying.

The studi.: presented here provide a structure for analyzing alternative methods of using economically the steam generated by a superheated steam impingement dryer. The cycles presented are potentially attractive options for retrofitting existing paper machines, or designing new ones, to increase production capacity and reduce energy consumption. The choice of the means of recirculating the steam around the impingement dryer circuit, as well as the choice of impinging jet temperature and other operating conditions, must be made according to the specific conditions of the mill where implementation is being considered.

CHAPTER 6

CONCLUSIONS

6.1 CONTRIBUTIONS TO KNOWLEDGE

1- Characterization of drying of paper by impinging jets of superheated steam.

The complete moisture content - time history of a paper sheet drying under impinging jets of superheated steam was studied for the first time in an apparatus which closely simulates industrial conditions. It was found to be characterized by a short condensation period, a relatively long constant-rate drying period, and finally a falling-rate period where the drying rate decreases linearly with moisture content. Complete drying of paper (i.e. drying to well below the hygroscopic range) was achieved, even with steam jet superheats as low as 10 $^{\circ}$C.

2- Constant rate drying period in superheated steam impingement drying.

The constant drying rate was measured under superheated steam jets in the range $500 < Re_j \leq 12000$, $110 < T_j \leq 465$ $^{\circ}$C. It was found to be equal to the heat flux divided by the latent heat of evaporation of water. The heat flux is described by an expression adapted from Martin's (1977) correlation, with all transport properties evaluated at the jet conditions and using the property ratio $(T_j/T_b)^{-0.77}$ to account for the variation of fluid properties. The reduction of the heat transfer driving potential due to evaporation is adequately accounted for by the Couette flow approximation. The constant drying rate is independent of basis weight or pulp type. The evaporation front temperature was found

163

to be 100 °C throughout the constant rate period of steam drying. This is consistent with a derived expression, relating the temperature at the liquid side of a liquid-vapor interface to the evaporation rate.

3- Constant rate drying period in air impingement drying.

The constant drying rate was measured under impinging air jets in the range $2000 < Re_j \leq 8000$, $20 < T_j \leq 400$ °C. The constant drying rate in air drying was found to be given by an expression similar to that for steam drying, but with the property ratio $(T_j/T_{a.s.})^{-0.96}$ to account for the variation of fluid properties. For air drying, the evaporation front is at the adiabatic saturation temperature corresponding to the jet temperature. This confirms that the Lewis relation is valid in air impingement drying.

4- Inversion temperature

For equal mass fluxes of the drying fluid, steam drying is slower than air drying below an *inversion temperature* of 175 °C, and faster above. The constant drying rate is about twice as high in steam than in air for jet temperatures in the operating range of industrial impingement dryers (400 - 600 °C).

5- Specific blower power.

For equal drying rates, the blower power was found to be considerably lower for steam than for air at temperatures in the industrial range. At 500 °C, blower power with steam is only 15% of that with air. Thus large blower power savings are possible with superheated steam drying, in addition to the energy savings obtained by recycling the exhaust stream.

6- Equilibrium moisture content of paper in air.

A new, three parameter expression, was found to correlate all of

Prahl's (1968) measurements of the desorption equilibrium moisture content of kraft paper in the temperature range 20 °C - 80 °C. Using this expression, an exponential relationship between adsorption energy and moisture content was derived.

7- Equilibrium moisture content of paper in superheated steam.

For kraft paper, the equilibrium moisture content was measured to be practically zero at a steam temperature as low as 103 °C, i. e. the lowest that could be achieved and stably maintained. For paper made from a TMP pulp, the equilibrium moisture content decreases from 0.123 at 103 °C to practically zero at 109 °C. The measured values are much lower than those extrapolated from the correlation of Prahl's measurements.

8- Critical moisture content.

Both for air and for superheated steam, the critical moisture content was found not to be a constant material property, but to increase with the constant drying rate. This correlation is due to the coupling between the internal moisture transport and the external vapor transport resistances.

9- Slope of the falling rate period in steam drying.

The slope of the falling rate period increases with the constant drying rate in steam drying. This is due to the persistent influence of the external vapor transport resistance even after the onset of the falling rate period.

10- Correlation equations for complete drying of paper by impinging jets of superheated steam.

Correlation equations for the constant and falling rate periods of drying paper by impinging jets of superheated steam were developed. These equations agree generally well with experimental measurements

under a wide range of jet temperatures, flow rates, basis weight and type of paper. The results of this laboratory-scale investigation can therefore be applied with confidence for the design of an industrial superheated steam impingement dryer.

11- Combined cycles for implementing superheated steam drying of paper.

Two combined superheated steam impingement-conventional drying cycles were proposed: one steam recirculation by a fan, the other by a thermocompressor. For both cycles, the total equivalent energy consumption (expressed as equivalent kg steam / kg water evaporated) increases with increasing average steam impingement drying rate. The total equivalent energy consumption is generally lower with steam recirculation by a fan than by a thermocompressor, but the difference is small if the cost of electricity is high, relative to fuel. Substantial energy savings over the conventional dryer performance were found to be possible. In one embodiment of the cycle with fan circulation, a *heaterless* superheated steam drying cycle is obtained.

12- Cycle with integrated heat pump.

A previously suggested superheated steam drying cycle (Luthi, 1981) was shown to be of limited applicability to paper drying as the low maximum temperature that can be reached precludes achieving an average impingement drying rate higher than about 20 kg/m^2-h.

6.2 RECOMMENDATIONS FOR FUTURE STUDIES

1- Future experimentation with superheated steam impingement drying should provide for continuous measurement of sheet moisture content as drying proceeds. This can probably be achieved with an infrared moisture

sensor, so long as sufficient care is taken to reduce the contribution to infrared absorption of the steam in the path of the IR beam to and from the drying sheet.

2- As the conversion of Yankee tissue dryers to steam operation is an immediate potential application of superheated steam drying, drying of towel and tissue grade papers should be studied in greater detail.

3- A numerical study on the effect of the temperature dependence of fluid properties in simultaneous heat and mass transport under high-temperature impinging jets, patterned after the work of Chow and Chung (1983a, 1983b), should be done to verify the property ratio expressions $(T_j/T_b)^{-0.77}$ and $(T_j/T_{a.s.})^{-0.96}$ found to account for the effect of fluid property variations in steam and air impingement drying, respectively.

4- To better characterize the falling rate period and to determine limits to the industrial applicability of superheated steam impingement drying, the internal transport of moisture in paper drying intensely under impinging jets at high temperature should be studied. Experiments should be done to determine the transport equation and transport coefficients under such conditions.

5- As purity of the steam generated in superheated steam drying of paper is essential to recover its heat content, a pilot plant study should adress the question of the degradation of steam that comes into contact with moist paper. The effect of the infiltration of air into the steam cycle on steam condensibility, and of the evolution of corrosive non-condensibles from the paper sheet on steam corrosiveness should be measured; ways to minimize these effects should be developed.

167

REFERENCES

Al-Taleb, M., Hasan, M. and Mujumdar, A. S. (1987) Evaporation of Liquids From a Wet Stretching Surface into Air, Unsaturated Air and Superheated Solvents. Proc. 6th Int'l Drying Symposium, pp. 261-269.

Allander, C. G. (1961) TAPPI, vol. 44, pp. 332-337.

Ast, P. F. (1966) GE Test Report HV-ER-66-41.

Attwood, D. (1972) How Fiber-Water Relationships Affects Drying. In Gavelin, G., ed. Drying of Paper and Paperboard. Lockwood, New York, p. 2.

Becker, F. E. and Zakak, A. I. (1985) Recover Heat by Mechanical Vapor Recompression. Hydrocarbon Processing, May 1985, pp. 77-80.

Beeby, C. and Potter, O. E. (1986) Steam Drying In Drying '86, A. S. Mujumdar, ed., Hemisphere, pp. 41-58.

Blumberg, K. M. (1983) TMP Clean Steam Recovery For Paper Drying. TAPPI Journal, vol. 66, no. 6, pp. 69-70.

Brandon, C. E. (1981) Properties of Paper. In Casey, J. P., ed. Pulp and Paper Chemistry and Technology, 3rd ed., vol. 3, p. 1900. John Wiley, New York.

British Paper and Board Industry Federation (1978) Fiber-Water Interactions in Papermaking. Clowes and Sons, London.

Britt, K. W., ed. (1964) Handbook of Pulp & Paper Technology. Reinhold Publ. Co., New York.

Bulmer, M. G. (1979) Principles of Statistics. 2nd edition. Dover, New York, pp. 209-227.

Burgess, B. W., Chapman, S. M. and Seto, W. (1972a) The Papridryer Process. Part 1 - The Basic Concept and Laboratory Results. Pulp & Paper Mag. Canada, v. 73, no. 11, pp. 64-73.

Burgess, B. W., Seto, W., Koller, E. and Pye, I. T. (1972b) The Papridryer Process. Part 2 - Mill Trials. Pulp & Paper Mag. Canada, v. 73, no. 11, pp. 73-81.

Canadian Pulp and Paper Association (1950) Forming Handsheets for Physical Tests of Pulp. CPPA Standard C4, CPPA, Montreal, Canada.

Chance, J.L. (1974) Experimental Investigation of Air Impingement Heat Transfer under an Array of Impinging Jets. TAPPI, 57 (6), pp. 108-112.

Choudhury, W. U. and Chance, J. L. (1975) Energy Conservation in the Dryer by Vapor Compression. TAPPI, July 1975, pp. 98-101.

Chow, L. C. and Chung, J. N. (1983a) Evaporation of Water Into a Laminar Stream of Air and Superheated Steam. Int'l Journal of Heat and Mass Transfer, v. 26, no. 3, pp. 373-380.

Chow, L. C. and Chung, J. N. (1983b) Water Evaporation into a Turbulent Stream of Air, Humid Air or Superheated Steam. ASME paper 83-HT-2.

Chu, C. C., Finelt, S., Hoerrner, W., and Lin, M. S. (1959) Drying with Superheated Steam-Air Mixtures. Industrial and Engineering Chemistry, vol. 51, no. 3, pp. 275-280.

Chu, J. C., Lane, A. M. and Cronklin, D. (1953) Evaporation of Liquids Into Their Superheated Vapors. Industrial & Engineering Chemistry, v. 45, no. 7, pp. 1586-1591.

Crotogino, R.H. and Allenger, V.H. (1979) A Mathematical Model of the Papridryer Process. Transactions of the Technical Section of the CPPA, v. 80, no. 3.

Cui, W. K. and Mujumdar, A. S. (1984) A Novel Steam Jet And Double Effect Evaporation Dryer. In Drying '84, A. S. Mujumdar, ed., Hemisphere Publishing Co., pp. 468-479.

Cui, W. K., Douglas, W. J. M. and Mujumdar, A. S. (1985) Impingement Steam Drying of Paper. Drying Technology, v. 3, no. 2, pp. 307-320.

Das, D. (1982) Convective Heat Transfer under a Turbulent Impinging Slot Jet at Large Temperature Differences. M. Eng. Thesis, Dept. of Chemical Engineering, McGill University, Canada.

Das, D. Douglas, W. J. M. and Crotogino, R. H. (1985) Convective Heat Transfer Under a Turbulent Impinging Slot Jet at Large Temperature Differences. In Drying '85, A. S. Mujumdar, ed., Hemisphere, New York, pp. 354-359.

David, M. (1987) Exploratory Study of Properties of Superheated Steam Dried Paper. M. Eng. Thesis. Dept. of Chemical Engineering, McGill University, Montreal.

Degueurce, B. and Banquet, F. (1984) Use of Twin Screw Compressors For Steam Compression. 2nd Int'l Symposium on the large-scale applications of heat pumps, York, England, 25-27 September, 1984.

Dungler, J. (1952) Method for Drying Fibrous Sheet Material. U. S. Patent no. 2,590,849, 1 April, 1952.

Endo, A., Shishido, I., Suzuki, M. and Ohtani, S. (1977) Estimation of Critical Moisture Content. AIChE Symposium Series, v. 73, 163, pp. 57-62.

Faber, E.F., Heydenrych, M.D., Seppä, R.U.I. and Hicks, R.E. (1986) A Techno-Economic Comparison of Air and Steam Drying. In Drying '86, pp. 588-594, A.S. Mujumdar, ed., Hemisphere, New York.

Gardon, R. and Cobonpue, J. (1973) Int. Dev. in Heat Transfer, ASME, p. 454.

Gavelin, G. (1973) Drying of Paper and Paperboard, Lockwood, London.

Glaser, H. (1962) Chem.-Ing.-Tech., v. 34, no. 3, pp. 200-207.

Haji, M. and Chow, L. C. (1988) Experimental Measurement of Water Evaporation Rate Into Air and Superheated Steam. Journal of Heat Transfer, v. 110, pp. 237-242.

Han, T. S. and Ulmanen, U. (1958). Heat Transfer in Hot-Surface Drying of Paper. Tappi, v. 41, no. 4, pp. 185-188.

Hasan, M., Mujumdar, A. S. and Al-Taleb, M., (1986) Laminar Evaporation from Flat Surface into Unsaturated and Superheated Solvent Vapors. Proc. 5th Int'l Drying Symposium, pp. 604-616.

Hausbrand, E. (1908) Drying By Means Of Steam And Air. Scott, Greenwood & Son, London.

170

Heaton, A. V. and Benstead, R. (1984) Steam Recompression Drying. 2nd International Symposium on the Large Scale Applications of Heat Pumps, York, England, 25-27 September, 1984.

Hilgeroth, E. (1965) Chem. Ing.-Tech., v. 37, pp. 1264-1272.

Holman, J. P. (1976) Heat Transfer. 4th ed. McGraw-Hill, New York.

Kast, W., (1982) The Change of Heat Transfer and Mass Transfer Coefficients by Simultaneous Heat and Mass Transfer. Proceedings of the 2nd International Heat Transfer Conference, Munich, pp. 263-268. (FC47), F. R. G.

Kays, W. M. and Crawford, M. E. (1980) Convective Heat and Mass Transfer, 2nd edition. McGraw-Hill, New York.

Keey, R. B. (1978) Introduction to Industrial Drying Operations. Pergamon Press, London.

Kercher, D. M. and Tabakoff, W. J. (1969) Heat Transfer by a Square Array of Round Air Jets Impinging Perpendicular to a Flat Surface Including the Effect of Spent Air. J. of Eng. for Power, Trans. ASME, v. 92, Ser. A, no. 1.

Kerekes, R. J. (1980) A simple method for determining the thermal conductivity and contact resistance of paper. TAPPI, v. 63, no. 9.

Kerr B.(1989) Private communication with Dr. Bruce Kerr, Kruger Inc., Montreal.

Kershaw, T. N. (1980) Sheet Formation and Drying. In Pulp and Paper Chemistry and Chemical Technology, J. P. Casey, ed., John Wiley, New York, 3rd ed., p. 1009.

King, E. F. and Brater, B. W. (1963) Handbook of Hydraulics, 2nd edition.

Krötzsch, P. (1968) Chem.-Ing.-Tech., v. 40, no. 7, pp. 339-344.

Lee, P.F. and Hinds, J.A. (1981) Optimizing Dryer Performance. Modeling heat and mass transfer within a moist sheet of paper or board. TAPPI, v. 64, no. 12.

Lewis, W. K. (1922) The Evaporation of a Liquid Into a Gas. Mech. Eng., vol. 44, p. 455.

Lin, S. H. (1990) Moisture Absorption in Cellulosic Materials. Int. J. Engng. Sci., pp. 1151-56.

Lin, S. H. (1991) Moisture Desorption in Cellulosic Materials. In preparation for Int. J. Engng. Sci.

Lockwood-Post (1990) Lockwood-Post's Directory of the Pulp, Paper and Allied Trades, 1990. Miller Freeman, Publ., New York.

Loo, E. and Mujumdar, A.S. (1984) A Simulation Model for Combined Impingement and Through Drying Using Superheated Steam as the Drying Medium. Drying '84, A.S. Mujumdar, ed. Hemisphere, New York.

Luikov, A. V. (1978) Heat and Mass Transfer, 3rd ed.. Mir Publishers, Moscow.

Luthi, O. (1981) Paper Web Drying System and Process. U. S. Patent no. 4,242,808, 6 January 1981.

Maa, J. R. (1967) Evaporation Coefficient of Liquids. Industrial and Engineering Chemistry Fundamentals, vol. 6, no. 4, pp. 504-518.

Maa, J. R. (1970) Rates of Evaporation and Condensation between Pure Liquids and Their Own Vapors. Industrial and Engineering Chemistry Fundamentals, vol. 9, no. 2, 283-287.

Martin, H. (1977) Heat and Mass Transfer Between Impinging Gas Jets and Solid Surfaces. Adv. Heat Transfer, vol. 13, Academic Press, pp. 1-80.

McConnell, R. R. (1980) A Review of the State-of-the-art In Paper Drying. IPC Project 3394, report 1, the Institute of Paper Chemistry, Appleton, Wisc.

Mujumdar, A. S. (1987) Impingement Drying. In Handbook of Industrial Drying, A. S. Mujumdar, ed., Marcel Dekker, New York, pp. 461-474.

Nanri, Y. (1991) Dimensional Stability of Paper Dried by Superheated Steam. M. Eng. Thesis, Chemical Engineering Department, McGill University, Montréal.

Obot, N. T., Mujumdar, A. S. and Douglas, W. J. M. (1980) Design Correlations for Heat and Mass Transfer Under Various Turbulent Impinging Jet Configurations. In Drying '80, vol. 1, A. S. Mujumdar, ed. Hemisphere Publ. Corp., New York, pp. 388-402.

Patankar, R. S. (1980) Numerical Flow and Heat Transfer. McGraw-Hill, New-York.

Petersen, J. N. (1986) Analysis of Batch Drying Data Using SAS. Drying Technology, vol. 4, no. 3, pp. 319-330.

Poirier, D. J. and Sparkes, D. G. (1991) Impulse Drying on a Pilot Paper Machine. Proceedings of the Helsinki Symposium on Alternate Methods of Pulp and Paper Drying, Helsinki, Finland, June 4-7, 1991.

Poirier, N. (1991) Ph. D. Thesis, Dept. of Chemical Engineering, McGill University, Montreal.

Polat, O. (1989) Through-drying of Paper. Ph. D. Thesis, Chem. Eng. Department, McGill University, Montreal.

Polat, S. and Douglas, W. J. M. (1990) Heat Transfer under Multiple Slot Jets Impinging on a Permeable Moving Surface. A.I.Ch.E. Journal, v. 36, pp. 1370-1378.

Polat, S., Mujumdar, A. S. and Douglas, W. J. M. (1991a) Impingement Heat Transfer under a Confined Slot Jet. I. Effect of Surface Throughflow. Can. J. Chem. Eng., v. 69, pp. 266-273.

Polat, S., Mujumdar, A. S. and Douglas, W. J. M. (1991b) Impingement Heat Transfer under a Confined Slot Jet. II. Effect of Surface Motion and Throughflow. Can. J. Chem. Eng., v. 69, pp. 274-280.

Prahl, J.M. (1968) Thermodynamics of Paper Fiber and Water Mixtures, Ph. D. thesis, Harvard University.

Ramamurthy, P. (1991) Ph. D. Thesis, Chemical Engineering Department, McGill University.

Saad, N.R., Mujumdar, A.S. and Douglas, W.J.M. (1980) Heat Transfer under Multiple Turbulent Slot Jets Impinging on a Flat Plate. In Drying '80, 1, A.S. Mujumdar, ed., pp. 422-430, Hemisphere, New York.

Sayegh, N., Pikulik, I. I. and Simonsen, H. I. (1986) A Survey of Dryer Sections of Canadian Newsprint Machines. Part II. Energy Consumption and Drying Rate. Pulp & Paper Research Institute of Canada.

Schmitt, W. (1978) Ejectors. Von Karman Fluid Dynamics Institute.

Schrage, R. W., (1953) Theoretical Study of Interphase Mass Transfer. Columbia University Press, New York.

Sheikholeslami, R. (1990) Drying Hog Fuel in a Fixed Bed. Ph. D. Thesis, University of British Columbia, Vancouver, Canada.

Shibata, H. (1990) Drying Mechanisms of Sintered Spheres of Coarse Glass Beads in Superheated Steam. Ph. D. Thesis, Kyushu University, Japan.

Shishido, I., Suzuki, M. and Ohtani, S. (1985) Critical Moisture Content for Time-dependent Drying Conditions. In Drying '85, A. S. Mujumdar, ed., Hemisphere Publ. Co.

Sprague, C. H. (1985) High-Intensity Drying Processes. U. S. DOE Report DOE/CE/40738-T1.

Strumillo, C. and Kudra, T. (1986) Drying: Principles, Applications and Design. Gordon and Breach, New York, p. 73.

Stubbing, T. (1990) Airless Drying Process Saves Energy and Reduces Emissions. Paper Technology, June 1990, pp. 36-39.

Suzuki, M., Keey, R. B. and Maeda, S. (1977) On the Characteristic Drying Curve. AIChE Symposium Series, v. 73, 163, pp. 47-56.

Svensson, C. (1980) Steam Drying of Pulp. In Drying '80, vol. 2. A. S. Mujumdar, ed. Hemisphere, New York, pp. 301-307.

Svensson, C. (1981) Steam Drying of Hog Fuel. TAPPI, v. 64, no. 3, pp. 153-156.

Thompson, R., Belanger, P., Kerr, R. B. and Douglas, W. J. M. (1991) A Superheated Steam Dryer for Tissue Paper. Proceedings of the Helsinki Symposium on Alternate Methods of Pulp & Paper Drying, Helsinki, Finland, June 4-7, 1991.

Wenzel, L. and White, R. R. (1951) Drying Granular Solids In Superheated Steam. Industrial and Engineering Chemistry, v. 43, no. 8, pp. 1829-1837.

Wilkinson, L. (1989) SYSTAT, The System for Statistics. SYSTAT Corp., Evanston, Il.

Yoshida, T. and Hyodo, T. (1970): Evaporation of Water in Air, Humid Air and Superheated Steam, Ind. Engineering Chem. Process Des. Dev., 9, 207-214.

APPENDIX 1 - TOPICAL INVENTORY OF IMPINGEMENT DRYING EXPERIMENTS

------TOPIC--------	-----------------------------------EXPERIMENTAL CONDITIONS-----------------------------------					
	DRYING FLUID	PULP TYPE	BASIS WEIGHT G/M2	JET REYNOLDS NUMBER	JET TEMPERATURE DEG. C	FALLING RATE DATA OBTAINED? (YES/NO)
EFFECT OF TEMPERATURE ON THE CONSTANT DRYING RATE						
DRYING RATE	STEAM	TMP	48.8	2000	150	NO
VS. TEMPERATURE	STEAM	TMP	48.8	2000	250	YES
STEAM - TMP	STEAM	TMP	48.8	2000	350	YES
RE = 2000	STEAM	TMP	48.8	2000	450	NO
DRYING RATE	STEAM	KRAFT	60	2000	150	NO
VS. TEMPERATURE	STEAM	KRAFT	60	2000	175	NO
STEAM - KRAFT	STEAM	KRAFT	60	2000	200	NO
RE = 2000	STEAM	KRAFT	60	2000	225	NO
	STEAM	KRAFT	60	2000	300	NO
	STEAM	KRAFT	60	2000	350	NO
	STEAM	KRAFT	60	2000	400	NO
DRYING RATE	AIR	TMP	60	2197	20	NO
VS. TEMPERATURE	AIR	KRAFT	60	2286	100	NO
AIR - KRAFT	AIR	KRAFT	60	2433	125	NO
RE = 2000	AIR	KRAFT	60	2283	150	NO
	AIR	KRAFT	60	2501	175	NO
	AIR	KRAFT	60	2307	200	NO
	AIR	KRAFT	60	2613	225	NO
	AIR	KRAFT	60	2336	250	NO
	AIR	KRAFT	60	2733.5	300	NO
	AIR	KRAFT	60	2373	300	NO
	AIR	KRAFT	60	2414	350	NO
	AIR	KRAFT	60	2000	400	NO

DRYING RATE	AIR	KRAFT	60	4000	100	NO
VS. TEMPERATURE	AIR	KRAFT	60	4000	150	NO
AIR - KRAFT	AIR	KRAFT	60	4000	200	NO
RE = 4000	AIR	KRAFT	60	4000	250	NO
	AIR	KRAFT	60	4000	300	NO
	AIR	KRAFT	60	4000	350	NO

EFFECT OF JET REYNOLDS NUMBER ON THE CONSTANT DRYING RATE

DRYING RATE	STEAM	TISSUE	60	500	350	YES
VS. REYNOLDS NUMBER	STEAM	TISSUE	60	1000	350	YES
STEAM - TISSUE	STEAM	TISSUE	60	2000	350	YES
350 DEG. C	STEAM	TISSUE	60	4000	350	YES
DRYING RATE	STEAM	KRAFT	60	4000	150	NO
VS. REYNOLDS NUMBER	STEAM	KRAFT	60	4000	150	YES
STEAM - KRAFT	STEAM	KRAFT	60	6000	150	YES
150 DEG. C	STEAM	KRAFT	60	8000	150	YES
	STEAM	KRAFT	60	12000	150	YES
DRYING RATE	STEAM	KRAFT	60	500	350	YES
VS. REYNOLDS NUMBER	STEAM	KRAFT	60	1000	350	YES
STEAM - KRAFT	STEAM	KRAFT	60	1500	350	YES
350 DEG. C	STEAM	KRAFT	60	2000	350	YES
	STEAM	KRAFT	60	2000	350	YES
	STEAM	KRAFT	60	2500	350	NO
	STEAM	KRAFT	60	3000	350	YES
	STEAM	KRAFT	60	4000	350	NO
	STEAM	KRAFT	60	5000	350	NO
DRYING RATE	STEAM	TISSUE	35	500	350	YES
VS. REYNOLDS NUMBER	STEAM	TISSUE	35	2000	350	YES
STEAM - LIGHT TISSUE						
350 DEG. C						

EFFECT OF BASIS WEIGHT AND PULP TYPE ON THE CONSTANT DRYING RATE

EFFECT OF	STEAM	TISSUE	35	2000	350	YES
BASIS WEIGHT -	STEAM	TISSUE	100	2000	350	YES
TISSUE						
EFFECT OF	STEAM	KRAFT	60	2000	350	YES
BASIS WEIGHT -	STEAM	KRAFT	100	2000	350	YES
KRAFT						
EFFECT OF	STEAM	TMP	48.8	2000	425	YES
BASIS WEIGHT -	STEAM	TMP	60	2000	425	YES
TMP						
EFFECT OF	STEAM	TMP	48.8	2000	150	NO
PULP TYPE	STEAM	KRAFT	60	2000	150	NO
AND BASIS WEIGHT						

INVESTIGATION OF THE FALLING RATE PERIOD

FALLING RATE	AIR	KRAFT	60	2000	150	YES
PERIOD:	AIR	KRAFT	60	2000	250	YES
EFFECT OF	AIR	KRAFT	60	2000	350	YES
TEMPERATURE	AIR	KRAFT	60	2000	430	YES
IN AIR						
FALLING RATE	STEAM	KRAFT	60	2000	150	YES
PERIOD:	STEAM	KRAFT	60	2000	250	YES
EFFECT OF	STEAM	KRAFT	60	2000	350	YES
TEMPERATURE	STEAM	KRAFT	60	2000	350	YES
IN STEAM	STEAM	KRAFT	60	2000	435	YES

FALLING RATE	STEAM	KRAFT	30	2000	350	YES
PERIOD:	STEAM	KRAFT	60	2000	350	YES
EFFECT OF	STEAM	KRAFT	60	2000	350	YES
BASIS WEIGHT	STEAM	KRAFT	90	2000	350	YES
IN STEAM	STEAM	KRAFT	120	2000	350	YES
	STEAM	KRAFT	150	2000	350	YES

SPECIAL PURPOSE EXPERIMENTS

CONDENSATION AND DRYING WITHOUT PAPER	STEAM	NONE	0	2000	350	NO
AIR DRYING	AIR	TMP	60	2197	20	NO
AT ROOM TEMPERATURE	AIR	TMP	60	8000	20	YES
INVESTIGATION OF SCATTER IN FINAL MOISTURE CONTENT	STEAM	TMP	48.8	2000	350	YES
REPEATABILITY	STEAM	KRAFT	60	2000	350	YES
CHECK	STEAM	KRAFT	60	2000	350	YES
	STEAM	KRAFT	60	2000	350	YES
	STEAM	KRAFT	60	2000	350	YES

APPENDIX 2

ERROR ANALYSIS

A2.1 Accuracy of primary measurements.

Table A2.1 shows the estimated accuracy of primary measurements, i. e., elementary quantities directly measured by an instrument:

MEASUREMENT	ACCURACY	COMMENTS
SHEET TEMPERATURE	$\delta T_s = 0.5\ ^oC$	Based on calibration with ice and molten lead.
JET TEMPERATURE	$\delta T_j = 2.0\ ^oC$	Greater inaccuracy due to imperfection in temperature control loop.
NOZZLE-TO-WEB DISTANCE	$\delta H = 0.005$ m	Drying chamber machined in shop to close tolerances.
IMPINGEMENT SURFACE	$\delta A_i = 2 \times 10^{-6}\ m^2$	
OPEN-AREA RATIO	$\delta f = 0.0004$	
NOZZLE DIAMETER	$\delta D = 0.00001$ m	
RESIDENCE TIME	$\delta t = 0.02$ s	Computer clock accuracy = 0.01 s
DRYING CHAMBER PRESSURE	$\delta P = 0.5$ kPa	Pressure transducer manufacturer's data, checked by calibration.
VENTURI PRESSURE DROP	$\delta \Delta P = 0.1$ kPa	Based on three calibrations, section 2.4.
WEIGHT	$\delta W = 0.005$ g	Standard deviation of ten weighings of a standard weight.
SHEET DIAMETER	$\delta D_s = 0.0005$ m	
SHEET DRY WEIGHT	$\delta W_d / W_d = 0.03$	Based on measurements on 19 Kraft and 10 TMP sheets, table 2.2

Table A2.1 Accuracy of primary measurements.

A2.2 Accuracy of secondary measurements.

The accuracy of secondary measurements, i. e. quantities obtained by algebraic combinations of the primary measurements, is given by the general equation:

$$\delta f = \left[\sum_i \left(\frac{\partial f}{\partial x_i} \delta x_i \right)^2 \right]^{1/2} \qquad (A2.1)$$

Basis weight:

$$B = \frac{4 W_d}{\pi D_s^2} \qquad (A2.2)$$

$$\frac{\delta B}{B} = \left[\left(\frac{\delta W_d}{W_d} \right)^2 + \left(-2 \frac{\delta D_s}{D_s} \right)^2 \right]^{1/2} = 0.031 \qquad (A2.3)$$

Jet mass flow rate:

$$M_J = b \sqrt{\frac{M}{\mathbb{R}}} \sqrt{\frac{P \Delta P}{T_J}} \qquad (A2.4)$$

$$\frac{\delta M_J}{M_J} = \left[\left(\frac{\delta b}{b} \right)^2 + \left(\frac{1}{2} \frac{\delta P}{P} \right)^2 + \left(\frac{1}{2} \frac{\delta \Delta P}{\Delta P} \right)^2 + \left(-\frac{1}{2} \frac{\delta T}{\Delta T} \right)^2 \right]^{1/2} \qquad (A2.5)$$

$\delta M_J / M_J$ decreases with increasing flow rate and with increasing

temperature. For the typical conditions T_J = 350 $^{\circ}$C, Re_J = 2000 $(M_J = 8.86$ g/s$)$, $\delta M_J/M_J = 0.061$.

Jet Reynolds number:

$$Re_J = \frac{M_J D}{A_i f \mu_J} \qquad (A2.6)$$

Table A2.1 indicates that errors in D, A_i and f are very small compared to errors in M_J and μ_J; the former may therefore be neglected. Hence:

$$\frac{\delta Re_J}{Re_J} = \left[\left(\frac{\delta M_J}{M_J} \right)^2 + \left(\frac{-1}{\mu_J} \frac{\partial \mu_J}{\partial T_J} \delta T_J \right)^2 \right]^{1/2} \qquad (A2.7)$$

For the typical abovementioned conditions, $\delta Re_J / Re_J$ = 0.061.

Final moisture content:

$$X_f = \frac{\text{Wet sheet weight } (W_w) - \text{Dry sheet weight } (W_d)}{\text{Dry sheet weight } (W_d)} \qquad (A2.8)$$

True wet sheet weight = Weight of sample holder + lid + wet sheet (W_t)

  - Weight of sample holder + lid (W_{hl})

  ± Loss or gain of moisture due to unremovable condensation on lid and thermocouple leads, and vapor loss during transit towards balance (W_{lg}), estimated to be 0.025 g.

$$X_f = \frac{(W_t - W_{hl} \pm W_{lg}) - W_d}{W_d} = \frac{W_t - W_{hl} \pm W_{lg}}{W_d} - 1 \quad (A2.9)$$

$$\delta X_f = \left[\left(\frac{\delta W_t}{W_d} \right)^2 + \left(\frac{\delta W_{hl}}{W_d} \right)^2 + \left(\frac{\delta W_{lg}}{W_d} \right)^2 \right]^{1/2} \quad (A2.10)$$

With $W_d = 1.212$ g for $B = 60$ g/m^2, $\delta X_f = 0.021$.

A2.3 Accuracy of constant drying rates.

The constant drying rate was determined from linear regression on a series of n sets of X vs. t data. As the error in residence time is much smaller than that in final moisture content, only the latter must be considered. For such a procedure, the variance of the slope is given by (Bulmer, 1979):

$$\sigma^2 \left[\overline{\frac{dX}{dt}} \right] = \frac{\sigma^2 (X)}{\sum_n (t_i - \bar{t})^2} \quad (A2.11)$$

The variance increases with uncertainty in final moisture content, and decreases with the number of points from which the slope is determined. For the typical data set shown in table A2.2 (figure 4.13), with $\sigma^2 X = 4.6 \times 10^{-4}$ as determined above, the variance of the slope is found

X	t, s
1.926	5
1.432	7
1.135	8
1.364	8
1.046	9
0.651	10
0.85	10
0.65	10
0.823	10

Table A2.2 Sample moisture content – residence
time data for constant drying rate measurement.

to be

$$\sigma^2 \left[\overline{\frac{dX}{dt}} \right] = 1.90 \times 10^{-5} \qquad (A2.12)$$

With

$$R_c = -B \left[\overline{\frac{dX}{dt}} \right] \qquad (A2.13)$$

we obtain

$$\frac{\delta R_c}{R_c} = \left[\left(\frac{\delta B}{B} \right)^2 + \left(\frac{\delta \left[\overline{\frac{dX}{dt}} \right]}{\left[\overline{\frac{dX}{dt}} \right]} \right)^2 \right]^{1/2} = \qquad (A2.14)$$

$$\left[.031^2 + -0.019^2 \right]^{1/2} = 0.036$$

APPENDIX 3

HEAT LOSS THROUGH THE SAMPLE HOLDER

A3.1 Introduction

To simulate adiabatic behavior at the bottom of the sheet in our experiments, the sample holder consisted of a glass plate (thickness: 2.2 mm) glued to a thin stainless steel plate (thickness 1.2 mm). The bottom surface of the sample holder was at the top of the vacuum plenum chamber (ref. figure 2.1), containing stagnant drying fluid.

Adiabatic behavior was approached, but not perfectly achieved, with this setup. When the cool paper sheet/sample holder assembly is inserted in the drying chamber, heat flows from the impinging jets to the paper surface, and from the warming paper into the sample holder. Conduction into the sample holder reduces net heat transfer to the evaporation front, thus increasing the amount of condensation in steam drying, and reducing the drying rate in both steam and air drying. This situation is analogous to that encountered by Haji and Chow (1988) who found, in their measurement of evaporation rate into a turbulent stream of air or superheated steam, that conduction across the bottom of the evaporation pan affected the evaporation rate, especially in air drying.

Transient heat loss through the sample holder must be calculated to properly interpret the results of the experiments and to extrapolate adiabatic drying rates from the measured results. Thus the transient

heat conduction equation

$$\frac{1}{\alpha} \frac{\partial T}{\partial t} = \frac{\partial^2 T}{\partial x^2} \qquad \text{(A3.1)}$$

must be solved in the composite glass-steel sample holder, subject to the appropriate initial and boundary conditions.

A3.2 Sample holder heat loss calculation

The solution to the heat conduction equation was obtained by the finite difference technique. The calculation grid is illustrated in figure A3.1:
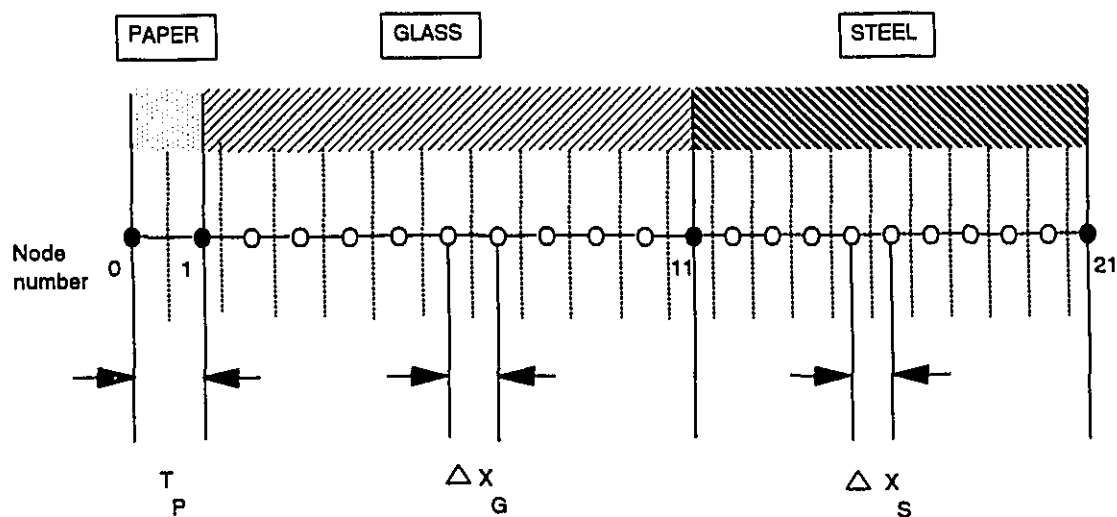
Figure A3.1. Calculation grid for finite difference solution of the heat conduction equation in the sample holder

The paper sheet was treated as a two-node system; the glass and steel plates each comprised ten equidistant points. The conductivity of moist paper was obtained from 4th order polynomial regression on the

data of Han and Ulmanen (1958) as presented in Gavelin (1972):

$X \leq 1.2$:

$$k_p = 0.06529 \left\{ \begin{array}{c} 1 - 0.75345 \ X + 10.60815 \ X^2 - 1.62953 \ X^3 \\ + 11.23522 X^4 - 9.59929 \ X^5 \end{array} \right\}$$

(A3.2)

$X > 1.2$

$k_p = 0.782 \quad (W/m^\circ C)$

Thermal properties of the glass and steel were obtained from Holman (1976). Interface resistances were neglected. The paper, glass and steel were assumed to be at 20 $^\circ$C initially.

For steam drying, since condensation droplets were observed on the bottom of the sample holder at the end of all experiments, the boundary condition $T = constant = T_b$ was imposed there. At the top, condensation was assumed to occur until the surface reaches 100 $^\circ$C and drying started from this point. For any surface temperature significantly below the boiling point, the kinetic expression for condensation rate, equation 3.12, has a value much higher than the impinging jet mass flux, which, therefore, limits the actual condensation rate. The condensation rate was therefore assumed to be equal to the jet mass flux. In addition to condensation, the paper surface receives heat by convection, according to the expression

$$\frac{Q}{A} = \frac{\Delta h_v \ F \ (H/D,f) \ k_j \ Pr_j^{0.42} \ Re_j^{2/3}}{D \ C_{ps,f}} \ ln \left\{ 1 + \frac{C_{ps,f} \ (T_j - T_s)}{\Delta h_v} \right\} \left\{ \begin{array}{c} property \\ ratio \end{array} \right\}$$

(A3.3)

where the property ratio is $(T_J/T_s)^{-0.77}$ for steam, $(T_J/T_s)^{-0.96}$ for air.

After drying has started, the net rate of heat transfer to the evaporation front is the convection flux minus the conduction flux through the bottom of the sheet.

For air drying, the bottom was assumed to be in natural convection with the stagnant air in the vacuum plenum chamber, with its temperature equal to the impinging jet temperature. The natural convection flux is (Holman, 1976)

$$Q_{n.c.} = 2.143 \ (T_J - T_s)^{5/4} \qquad (A3.4)$$

The net heat flux to the evaporation surface is the convection flux minus the conduction flux across the paper sheet.

The fully-implicit discretization equations were solved using the TDMA algorithm (Patankar, 1980). Two hundred time steps were used in the solution: the first 100 were very short ones (since temperatures are changing extremely fast at the beginning) and the next 100 were comparatively long ones. Results of a solution run obtained with comparatively long time increments (Δt_{short} = 0.1 sec., Δt_{long} = 1 sec.) agreed very well with those obtained using shorter increments (Δt_{short} = 0.01 sec., Δt_{long} = 0.1 sec.). All results appeared to be physically realistic. Heat flux into the glass and steel were calculated from Fourier's law at the boundaries. In addition, total heat transfer was calculated separately by integrating $\rho \ C_p \ \Delta T$ throughout the calculation domain. Cumulative heat transfer computed by the two methods agreed within 3%.

A3.3 Effect of sample holder heat loss in steam drying experiments

Figure A3.2 shows the evolution of the sample holder temperature profile, calculated for the representative case Re_j = 2000, T_j= 350 $^\circ$C, B = 60 g/m^2, X_1 = 1.6, t_p = 200 microns. The sample bottom temperature reaches 100 $^\circ$C gradually, owing to the buffering effect of the paper sheet. The temperature profile is much flatter in steel than in glass, owing to the higher diffusivity of steel.
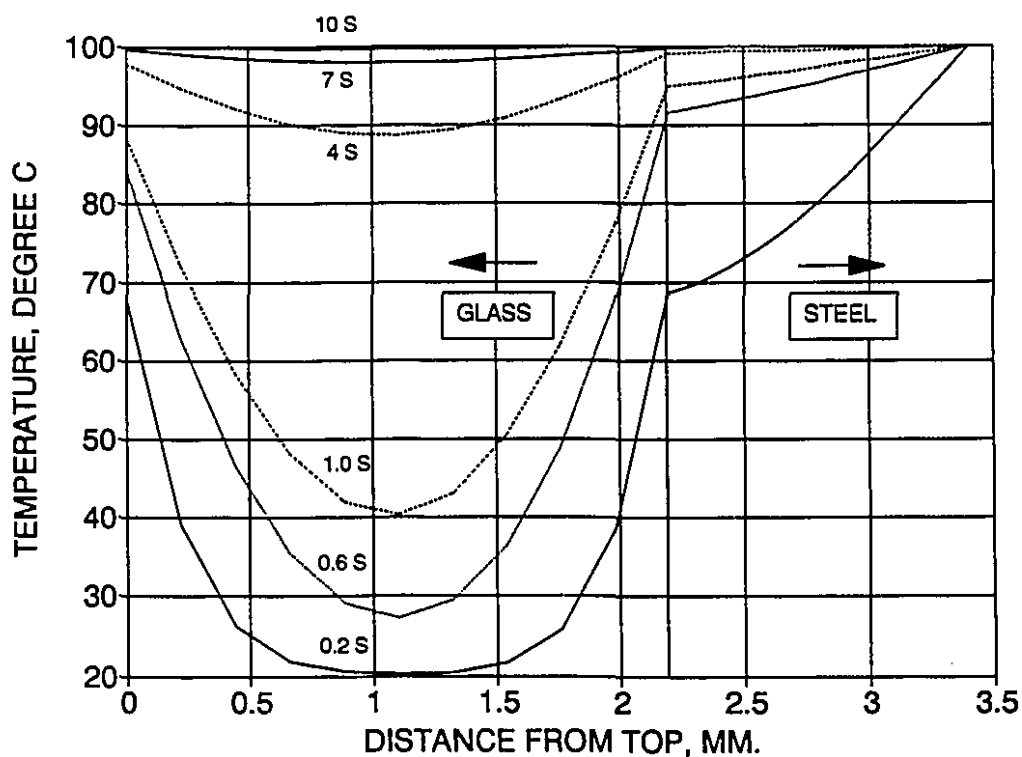
Figure A3.2   Sample holder temperature profile in steam drying experiments

Impinging jet heat flux, conduction flux through the bottom of the sheet and net heat flux are shown as fig. A3.3. In the early part of the condensation period, the evolution of the glass flux shows the
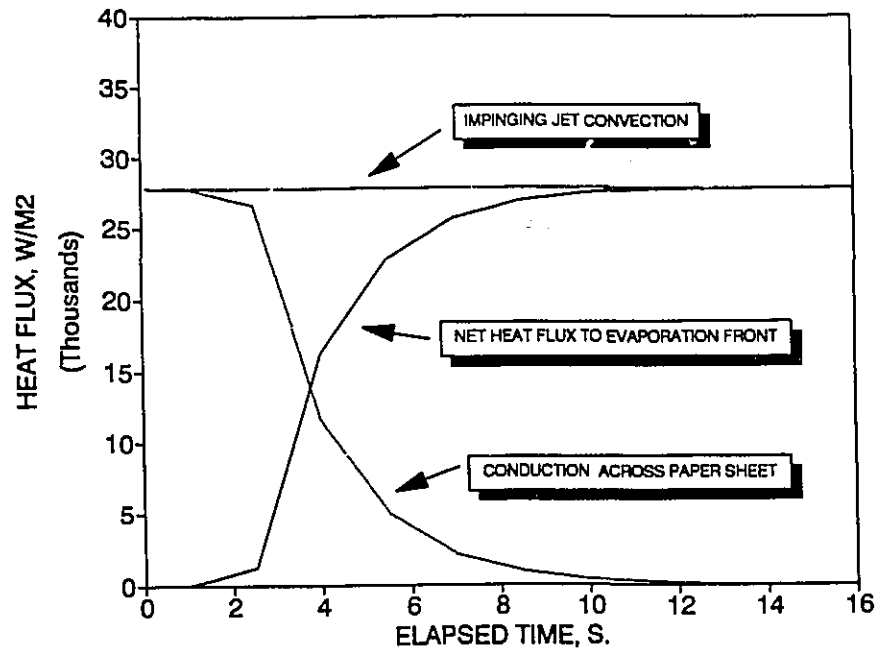
Figure A3.3   Heat fluxes in steam drying experiments

offsetting effects of the increase of the source (paper sample) and of the sink (glass) temperatures. When sheet temperature reaches 100 $^{\circ}$C, conduction heat flux starts to decrease monotonously.

The initially large conduction heat flux cools the sheet, explaining why more condensation occurs than the quantity expected on the basis of adiabatic mixing between the moist paper and the incoming steam. The latter quantity should depend solely on the initial moisture content and steam temperature, according to the equation

$$M_p h_p + M_s h_s = (M_p + M_s) h_{sat} \qquad (A3.5)$$

where M_p is the mass of the moist paper sheet;

h_p is the initial enthalpy of the moist paper sheet;

M_s is the mass of steam condensing on the paper sheet;

h_s is the enthalpy of the free stream;

h_{sat} is the enthalpy of the moist paper sheet at 100 $^{\circ}$C.

It is easily shown that this leads to

$$\Delta X = \frac{(C_{pf} + X_i \bar{C}_{pw})\,(T_b - T_{in})}{\Delta H_v + \bar{C}_{ps}\,(T_j - T_b)} \qquad (A3.6)$$

From the solution of this equation for $T_p = 20$ $^{\circ}$C and $X_i = 1.6$, represented on figure A3.4, a moisture content increase between
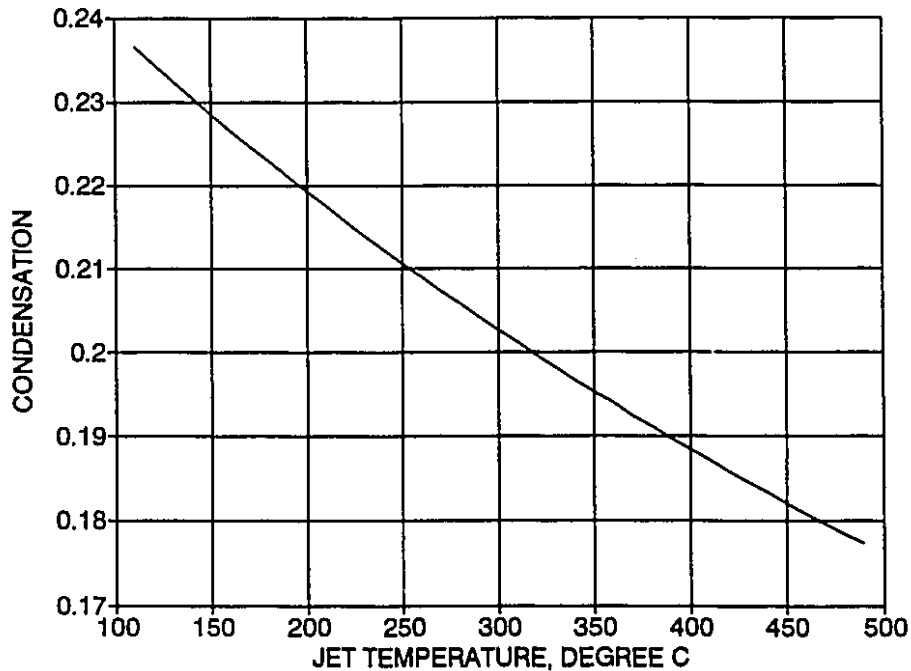
Figure A3.4 Expected condensation in steam drying experiments for $X_i = 1.6$, calculated on the basis of adiabatic mixing.

$\Delta X = 0.17$ and $\Delta X = 0.25$ should be expected. Yet condensation between $\Delta X = 1.0$ and 1.5 is observed in practice. The additional condensation is attributable to conduction at the beginning of the experiment, and would

not occur in a well-designed industrial steam impingement dryer.

In figure A3.5, the experimentally observed evolution of sample bottom temperature and moisture content are compared with predictions of this model. The time scale of the temperature rise, and the time scale and amount of condensation, are in good agreement with the model predictions.
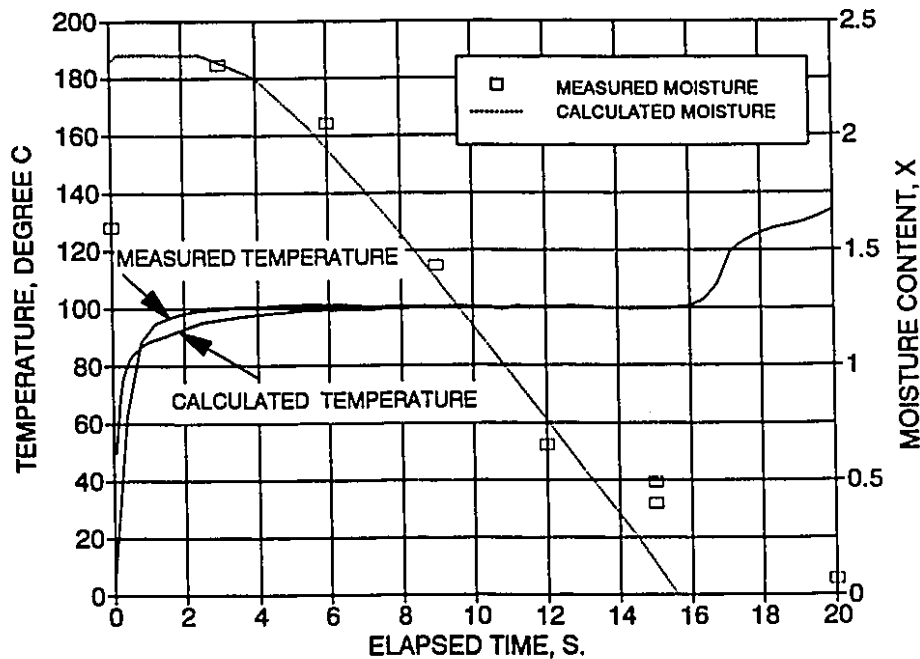
Figure A3.5 Observed and calculated temperature and moisture content
in steam drying experiments, for the case $T_j = 350\ °C$,
$Re_j = 2000$, $B = 60\ g/m^2$, $X_i = 1.6$, $t_p = 200$ microns.

A3.4 Effect of sample holder heat loss in air drying experiments

It was seen that sample holder heat loss results in substantial additional condensation in steam drying, but decreases rapidly as drying starts. In air drying, by contrast, drying starts immediately, i.e. before the temperature transient has had time to dissipate. Hence, relatively speaking, sample holder heat loss should decrease the drying

rate much more in air than in steam drying.

The evolution of sample holder temperature profile is shown in fig. A3.6 for the representative case $T_j = 350\ ^{\circ}C$, $Re_j = 2400$, $B = 48.8\ g/m^2$, $X_1 = 1.6$, $t_p = 150$ microns.
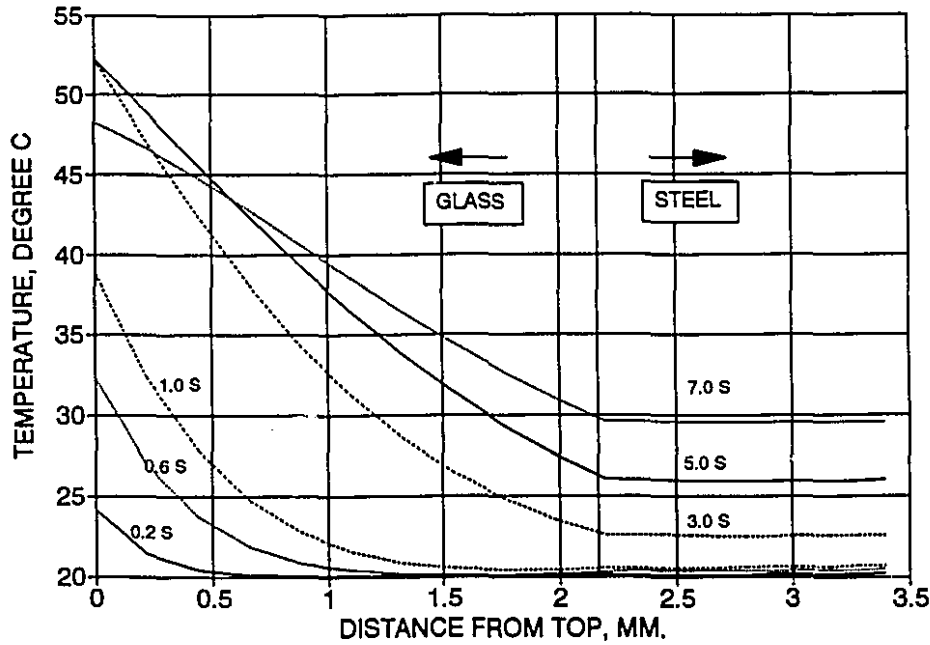
Figure A3.6   Sample holder temperature profile in air
drying experiments.

Steel temperature increases monotonously owing to the natural convection. Glass temperature profile is nearly parabolic, and after an initial increase, sample bottom temperature starts to decrease as the nearly dry paper sheet effectively insulates the sample holder (this point, however, probably occurs at a time when the model assumptions are no longer realistic).

Heat fluxes are shown as figure A3.7. Conduction heat flux is seen to be an important fraction of convection. The average conduction flux
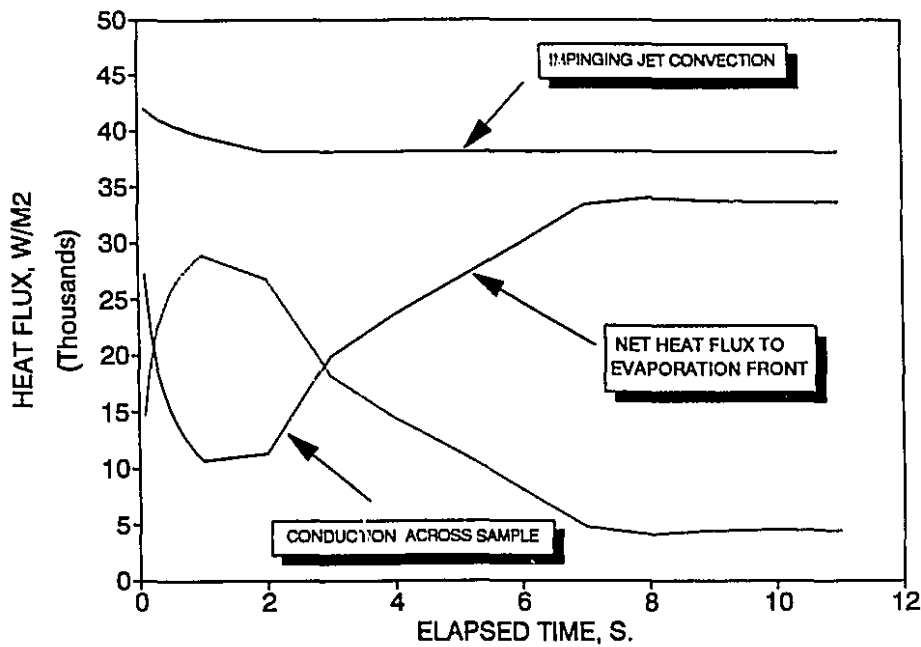
Figure A3.7   Heat fluxes in air drying experiments

in the period from 0 to 6 seconds,

$$\frac{\displaystyle\int_{t=0}^{t=6} Q_k \; dt}{\displaystyle\int_{t=0}^{t=6} dt} = 14 \; \text{kW/m}^2 \tag{A3.7}$$

is 36% of the convection heat flux. In figure A3.8, the experimentally observed evolution of sample bottom temperature and moisture content are compared with model prediction for the representative case. Sample holder heat loss is seen to reduce air drying rate by approximately

forty percent.
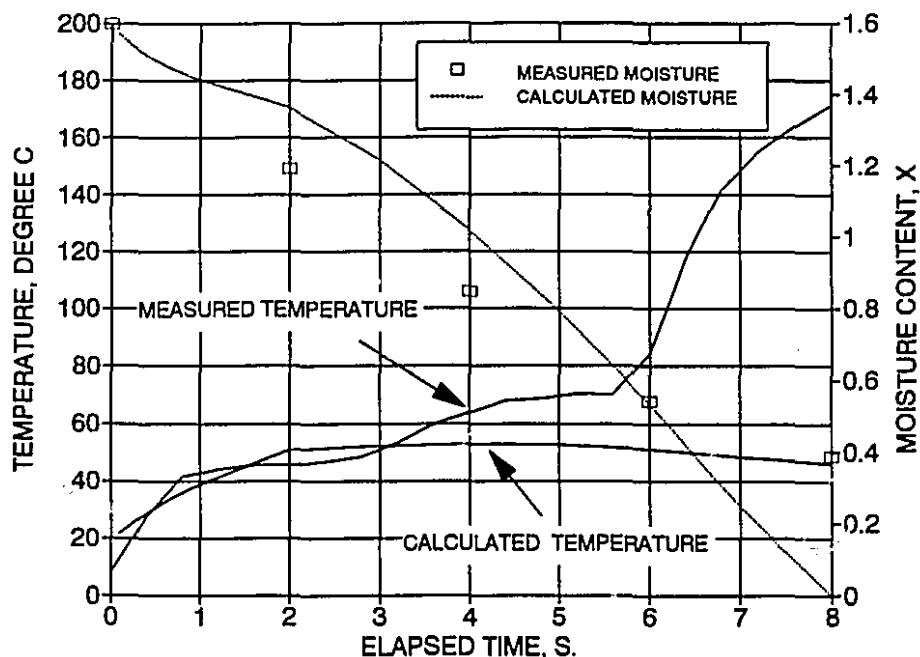
Figure A3.8   Observed and calculated temperature and moisture content
in air drying experiments, for the case $T_j = 350\ ^\circ C$,
$Re_j = 2400$, $B = 48.8\ g/m^2$, $X_1 = 1.6$, $t_p = 150$ microns.

A3.5 Constant drying rate correction factor

For steam drying, nearly all points used in computing the constant
drying rate were obtained in the range $1.5 \geq X \geq 0.4$. For the
representative case $T_j = 350\ ^\circ C$, $Re_j = 2000$, $B = 60\ g/m^2$, $X_1 = 1.6$,
$t_p = 200$ microns, the average conduction heat loss during this period is

$$\frac{\bar{Q}}{A} = \frac{\int_{X=1.5}^{X=0.4} H_f \, dt}{\int_{X=1.5}^{X=0.4} dt} = 0.39 \text{ kW/m}^2 \qquad \text{(A3.8)}$$

i. e. only 1.5 % of the convection heat flux. Hence the effect of conduction heat loss on the constant drying rate measurement may be safely neglected.

For air drying, a constant drying rate correction factor was calculated to take into account sample holder heat loss. The correction factor is defined as

$$\text{Correction factor} \equiv \frac{\text{Constant drying rate, according to model predictions}}{\text{Constant drying rate which would be measured in the absence of sample holder heat loss}} \qquad \text{(A3.9)}$$

The constant drying rate was evaluated between the initial and the critical moisture contents. Since the correction factor depends on initial moisture content, jet temperature and Reynolds number, and sheet thickness and basis weight, its value must be estimated separately for each set of conditions. In section 3.2.3, the corrected value of drying rate is calculated by multiplying the measured value by the constant drying rate correction factor. For the representative case $Re_j = 2000$, $B = 60$ g/m^2, $X_1 = 1.6$ and $t_p = 150$ microns, figure A3.9 shows the variation of correction factor with jet temperature.
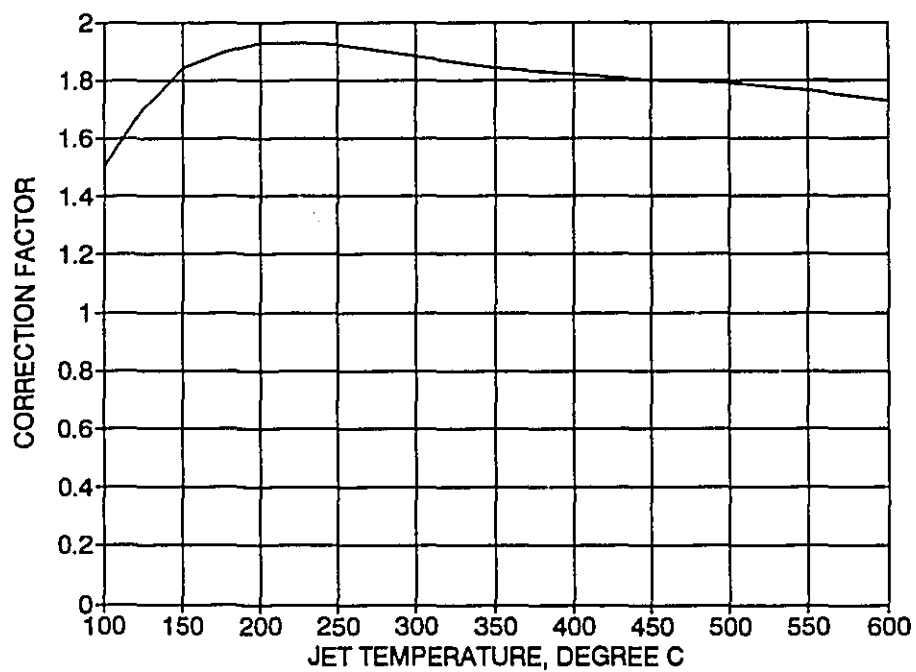
Figure A3.9 Constant drying rate correction factor
vs. jet temperature, for air impingement drying.

APPENDIX 4

FLUID PROPERTIES RELEVANT TO DRYING

```
'
'      MIXPROP.BAS - PROPERTIES OF AIR, STEAM AND AIR-STEAM
'      MIXTURES RELEVANT TO DRYING
'
'      WRITTEN IN QUICKBASIC 4.0 BY J.F. BOND, 24/5/90
'

'
'      1- VARIABLE AND FUNCTION DECLARATIONS
'


'      STEAM PROPERTIES

DECLARE FUNCTION SDEN! (T!)
DECLARE FUNCTION SCP! (T!)
DECLARE FUNCTION SMU! (T!)
DECLARE FUNCTION SCON! (T!)
DECLARE FUNCTION SPR! (T!)
DECLARE FUNCTION HFG! (T!)
DECLARE FUNCTION PSAT! (T!)
DECLARE FUNCTION TSATP! (P!)

'      AIR PROPERTIES

DECLARE FUNCTION ADEN! (T!)
DECLARE FUNCTION ACP! (T!)
DECLARE FUNCTION AMU! (T!)
DECLARE FUNCTION ACON! (T!)
DECLARE FUNCTION APR! (T!)

'      MIXTURE PROPERTIES

DECLARE FUNCTION MIXDEN! (TEMP!, SMF!)
DECLARE FUNCTION MIXCP! (TEMP!, SMF!)
DECLARE FUNCTION MIXMU! (TEMP!, SMF!)
DECLARE FUNCTION MIXCON! (TEMP!, SMF!)
DECLARE FUNCTION MIXPR! (TEMP!, SMF!)

'      BOUNDARY LAYER TEMPERATURES AND CONCENTRATIONS

DECLARE FUNCTION TWB! (T!)
DECLARE FUNCTION T13RD! (T!)
DECLARE FUNCTION TFILM! (T!)

DECLARE FUNCTION SMFWB! (T!)
DECLARE FUNCTION SMF13RD! (T!)
DECLARE FUNCTION SMFFILM! (T!)
```

```
'       EXPRESSIONS FOR TEMPERATURE-DEPENDENT PART OF DRYING RATE

DECLARE FUNCTION TDFFILM! (T!)
DECLARE FUNCTION TDF13RD! (T!)
DECLARE FUNCTION TDFWB! (T!)




COMMON SHARED AMW, SMW, PATM, SMF

AMW = 28.97                         ' MOLECULAR WEIGHT OF AIR
SMW = 18.015                        ' MOLECULAR WEIGHT OF WATER
PATM = 101.325                      ' ATMOSPHERIC PRESSURE, KPA


    '
    '         2- STEAM PROPERTIES ARE OUTPUT TO FILE AND SCREEN
    '



OPEN "C:STEAMP.PRN" FOR OUTPUT AS #1

PRINT #1, "                     PROPERTIES OF STEAM AT ATMOSPHERIC PRESSURE"
PRINT #1, " "
PRINT #1, "TEMPE-   DENSITY SPECIFIC  DYNAMIC    THERMAL       PRANDTL
HEAT OF"
PRINT #1, "RATURE            HEAT    VISCOSITY CONDUCTIVITY  NUMBER
EVAPORATION"
PRINT #1, "DEG. C   KG/M3   KJ/KG-K   10-6 PA-S 10-3 W/M-K    KJ/KG"
PRINT #1, " "
FOR T = 0 TO 100 STEP 10
PRINT #1, USING "#####"; T;
PRINT #1, USING "#######.###"; SDEN(T), SCP(T), SMU(T), SCON(T), SPR(T);
PRINT #1, USING "#########.#"; HFG(T)
NEXT T
PRINT #1, ; " "
FOR T = 150 TO 600 STEP 50
PRINT #1, USING "#####"; T;
PRINT #1, USING "#######.###"; SDEN(T), SCP(T), SMU(T), SCON(T), SPR(T);
IF T < 374 THEN
PRINT #1, USING "#########.#"; HFG(T)
ELSE PRINT #1, " "
END IF
NEXT T
CLOSE #1


CLS
LOCATE 1, 1
PRINT ; "                     PROPERTIES  OF  STEAM  AT  ATMOSPHERIC
PRESSURE"
```

```
PRINT ; " "
PRINT ; "TEMPE-    DENSITY  SPECIFIC   DYNAMIC    THERMAL        PRANDTI
HEAT OF"
PRINT ; "RATURE                HEAT     VISCOSITY  CONDUCTIVITY  NUMBER
EVAPORATION"
PRINT ; "DEG. C   KG/M3   KJ/KG-K    10-6 PA-S  10-3 W/M-K    KJ/KG"
PRINT ; " "
FOR T = 0 TO 100 STEP 20
PRINT USING "#####"; T;
PRINT USING "#######.###"; SDEN(T), SCP(T), SMU(T), SCON(T), SPR(T);
PRINT USING "#########.#"; HFG(T)
NEXT T
PRINT ; " "
FOR T = 150 TO 600 STEP 50
PRINT USING "#####"; T;
PRINT USING "#######.###"; SDEN(T), SCP(T), SMU(T), SCON(T), SPR(T);
IF T < 374 THEN
PRINT USING "#########.#"; HFG(T)
ELSE PRINT " "
END IF
NEXT T


'
'    3- AIR PROPERTIES ARE OUTPUT TO FILE AND SCREEN
'


OPEN "C:AIRP.PRN" FOR OUTPUT AS #1
PRINT #1, "                    PROPERTIES OF AIR AT ATMOSPHERIC PRESSURE
"
PRINT #1, " "
PRINT #1, "TEMPE-     DENSITY   SPECIFIC    DYNAMIC        THERMAL
PRANDTL"
PRINT #1, "RATURE               HEAT     VISCOSITY  CONDUCTIVITY  NUMBER
"
PRINT #1, "DEG. C     KG/M3      KJ/KG-K     10-6 PA-S   10-3 W/M-K
"
PRINT #1, " "
FOR T = 0 TO 100 STEP 10
PRINT #1, USING "#####"; T;
PRINT #1, USING "#######.###"; ADEN(T), ACP(T), AMU(T), ACON(T), APR(T)
NEXT T
PRINT #1, " "
FOR T = 150 TO 600 STEP 50
PRINT #1, USING "#####"; T;
PRINT #1, USING "#######.###"; ADEN(T), ACP(T), AMU(T), ACON(T), APR(T)
NEXT T

CLOSE #1
CLS
LOCATE 1, 1
PRINT ; "          PROPERTIES OF AIR AT ATMOSPHERIC PRESSURE          "
PRINT ; " "
```

```
PRINT ; "TEMPE-    DENSITY SPECIFIC   DYNAMIC     THERMAL       PRANDTL"
PRINT ; "RATURE             HEAT      VISCOSITY CONDUCTIVITY  NUMBER "
PRINT ; "DEG. C   KG/M3   KJ/KG-K    10-6 PA-S  10-3 W/M-K              "
PRINT ; " "
FOR T = 0 TO 100 STEP 20
PRINT USING "#####"; T;
PRINT USING "#######.###"; ADEN(T), ACP(T), AMU(T), ACON(T), APR(T)
NEXT T
PRINT ; " "
FOR T = 150 TO 600 STEP 50
PRINT USING "#####"; T;
PRINT USING "#######.###"; ADEN(T), ACP(T), AMU(T), ACON(T), APR(T)
NEXT T


'
'
'    4- MIXTURE PROPERTIES AT WET BULB (ADIABATIC SATURATION) CONDITIONS
'    ARE OUTPUT TO FILE AND SCREEN.
'




CLS
PRINT , "        MIXTURE PROPERTIES AT WET BULB CONDITIONS           "
PRINT , " "
PRINT "JET     W. B.    STEAM    AIR"
PRINT "TEMPE-    TEMPE-     MOLE       MOLE      DENSITY SPECIFIC DYNAMIC
THERMAL   PRANDTL"
PRINT "RATURE   RATURE    FRACT.    FRACT.                HEAT       VISC.
CONDUCT.   NUMBER "
PRINT "DEG. C  DEG. C                    KG/M3    KJ/KG-K  10-6 PA-S 10-3
W/M-K       "
PRINT , " "

FOR TJ = 20 TO 100 STEP 20
T = TWB(TJ)
SMF = SMFWB(TJ)
PRINT USING "###"; TJ;
PRINT USING "######.##"; T, SMF, (1 - SMF), MIXDEN(T, SMF), MIXCP(T,
SMF), MIXMU(T, SMF), MIXCON(T, SMF), MIXPR(T, SMF)
NEXT TJ

PRINT , " "

FOR TJ = 150 TO 600 STEP 50
T = TWB(TJ)
SMF = SMFWB(TJ)
PRINT USING "###"; TJ;
PRINT USING "######.##"; T, SMF, (1 - SMF), MIXDEN(T, SMF), MIXCP(T,
SMF), MIXMU(T, SMF), MIXCON(T, SMF), MIXPR(T, SMF)
NEXT TJ
```

```
OPEN "C:WBP.PRN" FOR OUTPUT AS #1
PRINT #1, "                      MIXTURE PROPERTIES AT WET BULB CONDITIONS"
PRINT #1, " "
PRINT #1, "JET      W. B.    STEAM    AIR"
PRINT #1, "TEMPE-   TEMPE-    MOLE     MOLE     DENSITY SPECIFIC DYNAMIC
THERMAL
 PRANDTL"
PRINT #1, "RATURE   RATURE   FRACT.   FRACT.            HEAT     VISC.
CONDUCT.
 NUMBER "
PRINT #1, "DEG. C  DEG. C                     KG/M3   KJ/KG-K  10-6 PA-S
10-3 W/M-K        "
PRINT #1, " "

FOR TJ = 20 TO 100 STEP 10
T = TWB(TJ)
SMF = SMFWB(TJ)
PRINT #1, USING "###"; TJ;
PRINT #1, USING "######.##"; T, SMF, (1 - SMF), MIXDEN(T, SMF), MIXCP(T,
SMF),
MIXMU(T, SMF), MIXCON(T, SMF), MIXPR(T, SMF)
NEXT TJ

PRINT #1, " "

FOR TJ = 150 TO 600 STEP 50
T = TWB(TJ)
SMF = SMFWB(TJ)
PRINT #1, USING "###"; TJ;
PRINT #1, USING "######.##"; T, SMF, (1 - SMF), MIXDEN(T, SMF), MIXCP(T,
SMF),
MIXMU(T, SMF), MIXCON(T, SMF), MIXPR(T, SMF)
NEXT TJ

CLOSE #1



'

'    5- MIXTURE PROPERTIES AT 1/3 REFERENCE CONDITIONS
'    ARE OUTPUT TO FILE AND SCREEN.
'




CLS
PRINT , "    MIXTURE PROPERTIES AT 1/3 REFERENCE CONDITIONS            "
PRINT , " "
PRINT "JET      1/3 RD   STEAM    AIR"
PRINT "TEMPE-   TEMPE-     MOLE     MOLE     DENSITY SPECIFIC DYNAMIC
THERMAL    PRANDTL"
PRINT "RATURE   RATURE    FRACT.   FRACT.             HEAT      VISC.
CONDUCT.  NUMBER "
```

```
PRINT "DEG. C  DEG. C                      KG/M3   KJ/KG-K  10-6 PA-S 10-3
W/M-K
         "
PRINT , " "

FOR TJ = 20 TO 100 STEP 20
T = T13RD(TJ)
SMF = SMF13RD(TJ)
PRINT USING "###"; TJ;
PRINT USING "######.##"; T, SMF, (1 - SMF), MIXDEN(T, SMF), MIXCP(T,
SMF), MIXMU(T, SMF), MIXCON(T, SMF), MIXPR(T, SMF)
NEXT TJ

PRINT , " "

FOR TJ = 150 TO 600 STEP 50
T = T13RD(TJ)
SMF = SMF13RD(TJ)
PRINT USING "###"; TJ;
PRINT USING "######.##"; T, SMF, (1 - SMF), MIXDEN(T, SMF), MIXCP(T,
SMF), MIXMU(T, SMF), MIXCON(T, SMF), MIXPR(T, SMF)
NEXT TJ


OPEN "C:13RDP.PRN" FOR OUTPUT AS #1
PRINT #1, "                         MIXTURE PROPERTIES AT 1/3 REFERENCE
CONDITIONS
         "
PRINT #1, " "
PRINT #1, "JET      1/3 RD    STEAM    AIR"
PRINT #1, "TEMPE-   TEMPE-     MOLE     MOLE    DENSITY SPECIFIC DYNAMIC
THERMAL
 PRANDTL"
PRINT #1, "RATURE   RATURE    FRACT.   FRACT.              HEAT      VISC.
CONDUCT.
 NUMBER "
PRINT #1, "DEG. C  DEG. C                      KG/M3    KJ/KG-K  10-6 PA-S
10-3 W/M-K        "
PRINT #1, " "

FOR TJ = 20 TO 100 STEP 10
T = T13RD(TJ)
SMF = SMF13RD(TJ)
PRINT #1, USING "###"; TJ;
PRINT #1, USING "######.##"; T, SMF, (1 - SMF), MIXDEN(T, SMF), MIXCP(T,
SMF),
MIXMU(T, SMF), MIXCON(T, SMF), MIXPR(T, SMF)
NEXT TJ

PRINT #1, " "

FOR TJ = 150 TO 600 STEP 50
T = T13RD(TJ)
SMF = SMF13RD(TJ)
```

```
        PRINT #1, USING "###"; TJ;
        PRINT #1, USING "######.##"; T, SMF, (1 - SMF), MIXDEN(T, SMF), MIXCP(T,
        SMF),
        MIXMU(T, SMF), MIXCON(T, SMF), MIXPR(T, SMF)
        NEXT TJ

        CLOSE #1


     '
     '     6- MIXTURE PROPERTIES AT FILM CONDITIONS
     '        ARE OUTPUT TO FILE AND SCREEN.
     '



        CLS
        PRINT , "     MIXTURE PROPERTIES AT FILM CONDITIONS              "
        PRINT , " "
        PRINT "JET       FILM      STEAM   AIR"
        PRINT "TEMPE-    TEMPE-      MOLE       MOLE      DENSITY SPECIFIC DYNAMIC
        THERMAL    PRANDTL"
        PRINT "RATURE    RATURE    FRACT.    FRACT.               HEAT      VISC.
        CONDUCT.  NUMBER "
        PRINT "DEG. C  DEG. C                    KG/M3   KJ/KG-K  10-6 PA-S 10-3
        W/M-K
             "
        PRINT , " "

        FOR TJ = 20 TO 100 STEP 20
        T = TFILM(TJ)
        SMF = SMFFILM(TJ)
        PRINT USING "###"; TJ;
        PRINT USING "######.##"; T, SMF, (1 - SMF), MIXDEN(T, SMF), MIXCP(T,
        SMF), MIXMU(T, SMF), MIXCON(T, SMF), MIXPR(T, SMF)
        NEXT TJ

        PRINT , " "

        FOR TJ = 150 TO 600 STEP 50
        T = TFILM(TJ)
        SMF = SMFFILM(TJ)
        PRINT USING "###"; TJ;
        PRINT USING "######.##"; T, SMF, (1 - SMF), MIXDEN(T, SMF), MIXCP(T,
        SMF), MIXMU(T, SMF), MIXCON(T, SMF), MIXPR(T, SMF)
        NEXT TJ


        OPEN "C:FILMP.PRN" FOR OUTPUT AS #1
        PRINT #1, "                          MIXTURE PROPERTIES AT FILM CONDITIONS
        "
        PRINT #1, " "
        PRINT #1, "JET       FILM      STEAM    AIR"
```

```
PRINT #1, "TEMPE-    TEMPE-    MOLE     MOLE    DENSITY SPECIFIC DYNAMIC
THERMAL
 PRANDTL"
PRINT #1, "RATURE   RATURE   FRACT.   FRACT.           HEAT    VISC.
CONDUCT.
 NUMBER "
PRINT #1, "DEG. C   DEG. C                    KG/M3   KJ/KG-K  10-6 PA-S
10-3 W/M-K        "
PRINT #1, " "

FOR TJ = 20 TO 100 STEP 10
T = TFILM(TJ)
SMF = SMFFILM(TJ)
PRINT #1, USING "###"; TJ;
PRINT #1, USING "######.##"; T, SMF, (1 - SMF), MIXDEN(T, SMF), MIXCP(T,
SMF),
MIXMU(T, SMF), MIXCON(T, SMF), MIXPR(T, SMF)
NEXT TJ

PRINT #1, " "

FOR TJ = 150 TO 600 STEP 50
T = TFILM(TJ)
SMF = SMFFILM(TJ)
PRINT #1, USING "###"; TJ;
PRINT #1, USING "######.##"; T, SMF, (1 - SMF), MIXDEN(T, SMF), MIXCP(T,
SMF),
MIXMU(T, SMF), MIXCON(T, SMF), MIXPR(T, SMF)
NEXT TJ

CLOSE #1


'FUNCTION DEFINITIONS


FUNCTION ACON! (T!)
'
'     THIS FUNCTION RETURNS THE CONDUCTIVITY OF AIR, IN
'     MW/M-DEG. C. IT IS TAKEN FROM HUANG & MUJUMDAR, DRYING '85, PP.
'     106-114.
'
VALUE = 1000 * (3.8793E-04 + 9.5425E-05 * (T + 273.2) - 3.0699E-08 * (T
+ 273.2) ^ 2)
ACON = VALUE
END FUNCTION

FUNCTION ACP! (T!)
'
'     POLYNOMIAL REGRESSION EQUATION FOR THE SPECIFIC HEAT CAPACITY OF
'     AIR (KJ/KG-DEG. C)TAKEN FROM Z. PAKOWSKI, HANDBOOK OF INDUSTRIAL
'     DRYING, A.S. MUJUMDAR, ED., 1987, PP. 915-932.
'
```

```
VALUE = .9774 + .0001124 * (T + 273.2) + 1.9035E-08 * (T + 273.2) ^ 2
ACP = VALUE
END FUNCTION

FUNCTION ADEN! (T!)
'
'     THIS FUNCTION RETURNS THE DENSITY OF AIR (KG/M3) AS A FUNCTION
'     OF THE TEMPERATURE. UNIVERSAL GAS CONSTANT: 8.3144 J/GMOLE-K,
'     MOLECULAR WEIGHT OF AIR: 28.97
VALUE = 353.048 / (T + 273.2)
ADEN = VALUE
END FUNCTION

FUNCTION AMU! (T!)
'
'     THIS FUNCTION RETURNS THE DYNAMIC VISCOSITY OF AIR (10-6 PA-SEC).
'     IT IS TAKEN FROM HUANG & MUJUMDAR, DRYING '87, PP. 106-114.
'
VALUE = 1000000! * (2.5641E-06 + 6.0198E-08 * (T + 273.2) - 2.3723E-11 *
(T + 273.2) ^ 2)
AMU = VALUE
END FUNCTION

FUNCTION APR! (T!)
'
'     THIS FUNCTION RETURNS THE PRANDTL NUMBER OF AIR. IT IS CALCULATED
'     FROM THE DEFINITION PR = MU * CP / K, USING THE FUNCTIONS DEFINED
'     IN THE PROGRAM.
'
VALUE = AMU!(T!) * ACP!(T!) / ACON!(T!)
APR! = VALUE
END FUNCTION

FUNCTION HFG! (T!)
'
'     THIS FUNCTION RETURNS THE ENTHALPY OF EVAPORATION OF WATER (KJ/KG)
'     AS A FUNCTION OF TEMPERATURE. IT IS TAKEN FROM REID, PRAUSNITZ &
'     POLING: THE PROPERTIES OF GASES & LIQUIDS, 4TH ED., NEW YORK, 1987,
'     P. 515.
'
VALUE = 2257! * (((1 - ((T + 273.2) / 647.3)) / .42353) ^ .38)
HFG = VALUE
END FUNCTION

FUNCTION MIXCON (T, SMF)
'
'         THIS FUNCTION RETURNS THERMAL CONDUCTIVITY (10-3 W/M-K) OF A
STEAM-AIR
'     MIXTURE WITH TEMPERATURE T AND STEAM MOLE FRACTION SMF. IT IS TAKEN
'     FROM REID, PRAUSNITZ & POLING: THE PROPERTIES OF GASES & LIQUIDS,
'     4TH ED., NEW YORK, 1987, P. 515.
'
CONWA = ((1 + (1.126 * SQR(SMU(T) / AMU(T)))) ^ 2) / 3.6022
CONAW = (SMW / AMW) * (AMU(T) / SMU(T)) * CONWA
```

```
VALUE = SCON(T) / (1 + ((1 - SMF) / SMF) * CONWA) + ACON(T) / (1 + (SMF
/ (1 -
SMF)) * CONAW)
MIXCON = VALUE
END FUNCTION


FUNCTION MIXCP (T, SMF)
'
'      THIS FUNCTION RETURNS THE SPECIFIC HEAT CAPACITY (KJ/KG-K)
'      OF A STEAM-AIR MIXTURE WITH TEMPERATURE T AND STEAM MOLE
'      FRACTION SMF.
'
SMASSF = (SMF * SMW) / ((SMF * SMW) + (1 - SMF) * AMW)
VALUE = SCP(T) * SMASSF + ACP(T) * (1 - SMASSF)
MIXCP = VALUE
END FUNCTION


FUNCTION MIXDEN (T, SMF)
'
'      THIS FUNCTION RETURNS THE DENSITY (KG/M3) OF A STEAM-AIR
'      MIXTURE WITH TEMPERATURE T AND STEAM MOLE FRACTION SMF.
'
VALUE = SDEN(T) * (SMF + ((1 - SMF) * AMW / SMW))
MIXDEN = VALUE
END FUNCTION


FUNCTION MIXMU (T, SMF)
'
'      THIS FUNCTION RETURNS THE VISCOSITY (10-6 PA-SEC) OF A STEAM-AIR
'      MIXTURE WITH TEMPERATURE T AND STEAM MOLE FRACTION SMF. IT IS TAKEN
'      FROM REID, PRAUSNITZ & POLING: THE PROPERTIES OF GASES & LIQUIDS,
'      4TH ED., NEW YORK, 1987, P. 407.
'
MUWA = ((1 + (1.126 * SQR(SMU(T) / AMU(T)))) ^ 2) / 3.6022
MUAW = (SMW / AMW) * (AMU(T) / SMU(T)) * MUWA
VALUE = SMU(T) / (1 + ((1 - SMF) / SMF) * MUWA) + AMU(T) / (1 + (SMF /
(1 - SMF)) * MUAW)
MIXMU = VALUE
END FUNCTION


FUNCTION MIXPR (T, SMF)
'
'      THIS FUNCTION RETURNS PRANDTL NUMBER OF A STEAM-AIR MIXTURE
'      WITH TEMPERATURE T AND STEAM MOLE FRACTION SMF.
'
VALUE = MIXMU(T, SMF) * MIXCP(T, SMF) / MIXCON(T, SMF)
MIXPR = VALUE
END FUNCTION


FUNCTION PSAT! (T!)
'
'      EXPONENTIAL REGRESSION FOR SATURATED STEAM PRESSURE (KPA) TAKEN
'      FROM Z. PAKOWSKI, HANDBOOK OF INDUSTRIAL DRYING, A.S. MUJUMDAR,
'      ED., 1987, PP. 915-932.
```

```
        '
        VALUE = EXP(23.1964 - (3816.44 / (T + 227.02))) / 1000
        PSAT = VALUE
        END FUNCTION


        FUNCTION SCON! (T!)
        '
        '     THIS FUNCTION RETURNS THE CONDUCTIVITY OF WATER VAPOR, IN
        '     MW/M-DEG. C. IT IS TAKEN FROM REID, PRAUSNITZ & POLING: THE
        '     PROPERTIES OF GASES & LIQUIDS, 4TH ED., NEW YORK, 1987, P. 515.
        '
        VALUE = 1000 * (.007341 - 1.013E-05 * (T + 273.2) + 1.801E-07 * ((T +
        273.2) ^
        2) - 9.1E-11 * (T + 273.2) ^ 3)
        SCON = VALUE
        END FUNCTION


        FUNCTION SCP! (T!)
        '
        '     POLYNOMIAL REGRESSION EQUATION FOR THE SPECIFIC HEAT CAPACITY OF
        '     WATER VAPOR (KJ/KG-DEG. C) TAKEN FROM Z. PAKOWSKI, HANDBOOK OF IN-
        '     DUSTRIAL DRYING, A.S. MUJUMDAR, ED., 1987, PP. 915.932
        '
        VALUE = 1.883 - 1.6737E-04 * (T + 273.2) + 8.4386E-07 * (T + 273.2) ^ 2
        - 2.6966E-10 * (T + 273.2) ^ 3
        SCP! = VALUE
        END FUNCTION


        FUNCTION SDEN! (T!)
        '
        '     THIS FUNCTION RETURNS THE DENSITY OF WATER VAPOR (KG/M3) AS A
        '         FUNCTION OF THE TEMPERATURE. UNIVERSAL GAS CONSTANT: 8.3144
        J/GMOLE-K,
        '     MOLECULAR WEIGHT OF WATER: 18.015.
        VALUE = 219.543 / (T + 273.2)
        SDEN = VALUE
        END FUNCTION


        FUNCTION SMF13RD (T)
        '
        '     THIS FUNCTION RETURNS THE STEAM MOLE FRACTION AT THE 1/3
        '     REFERENCE CONDITIONS.
        '
        VALUE = (2 / 3) * SMFWB(T)
        SMF13RD = VALUE
        END FUNCTION


        FUNCTION SMFFILM (T)
        '
        '     THIS FUNCTION RETURNS THE STEAM MOLE FRACTION AT THE
        '     FILM CONDITIONS.
        '
        VALUE = .5 * SMFWB(T)
        SMFFILM = VALUE
```

```
END FUNCTION

FUNCTION SMFWB! (T!)
'
'      THIS FUNCTION RETURNS THE STEAM MOLE FRACTION AT THE WET BULB
'      CONDITIONS.
'
VALUE = PSAT(TWB(T)) / PATM!
SMFWB = VALUE
END FUNCTION

FUNCTION SMU! (T!)
'
'      THIS FUNCTION RETURNS THE DYNAMIC VISCOSITY OF STEAM (10-6 PA-SEC).
'      IT IS TAKEN FROM LOO & MUJUMDAR, DRYING '84, PP. 264-282.
'
VALUE = 1000000! * (9.9354E-07 + 2.7067E-08 * (T + 273.2) + 8.8906E-12 *
((T +
273.2) ^ 2))
SMU = VALUE
END FUNCTION

FUNCTION SPR! (T!)
'
'      THIS FUNCTION RETURNS THE PRANDTL NUMBER OF STEAM. IT IS CALCULATED
'      FROM THE DEFINITION PR = MU * CP / K, USING THE FUNCTIONS DEFINED
'      IN THE PROGRAM.
'
VALUE = SMU!(T!) * SCP!(T!) / SCON!(T!)
SPR! = VALUE
END FUNCTION

FUNCTION T13RD (T)
'
'      THIS FUNCTION RETURNS THE 1/3 REFERENCE TEMPERATURE (DEG. C)
'      AS A FUNCTION OF THE DRY AIR TEMPERATURE.
'
VALUE = (2 / 3) * TWB(T) + (1 / 3) * T
T13RD = VALUE
END FUNCTION

FUNCTION TDF13RD (T)
'
'      THIS FUNCTION RETURNS THE TEMPERATURE-DEPENDENT DRYING RATE FACTOR
'          EVALUATED AT 1/3 REFERENCE CONDITIONS, AS A FUNCTION OF JET
TEMPERATURE.
'
CONDUCTANCE = .0036 * MIXCON(T13RD(T), SMF13RD(T)) * (MIXPR(T13RD(T),
SMF13RD(T)) ^ .42) / ACP(TFILM(T))
POTENTIAL = LOG(1 + (ACP(TFILM(T)) * (T - TWB(T)) / HFG(TWB(T))))
VALUE = CONDUCTANCE * POTENTIAL
TDF13RD = VALUE

END FUNCTION
```

```
FUNCTION TDFFILM (T)

'
'     THIS FUNCTION RETURNS THE TEMPERATURE-DEPENDENT DRYING RATE FACTOR
'     EVALUATED AT FILM CONDITIONS, AS A FUNCTION OF JET TEMPERATURE.
'
CONDUCTANCE = .0036 * MIXCON(TFILM(T), SMFFILM(T)) * (MIXPR(TFILM(T),
SMFFILM(T)) ^ .42) / ACP(TFILM(T))
POTENTIAL = LOG(1 + (ACP(TFILM(T)) * (T - TWB(T)) / HFG(TWB(T))))
VALUE = CONDUCTANCE * POTENTIAL
TDFFILM = VALUE

END FUNCTION

FUNCTION TDFWB (T)
'
'     THIS FUNCTION RETURNS THE TEMPERATURE-DEPENDENT DRYING RATE FACTOR
'     EVALUATED AT WET-BULB CONDITIONS, AS A FUNCTION OF JET TEMPERATURE.
'
CONDUCTANCE  =  .0036  *  MIXCON(TWB(T),  SMFWB(T))  *  (MIXPR(TWB(T),
SMFWB(T)) ^ .42) / ACP(TFILM(T))
POTENTIAL = LOG(1 + (ACP(TFILM(T)) * (T - TWB(T)) / HFG(TWB(T))))
VALUE = CONDUCTANCE * POTENTIAL
TDFWB = VALUE
END FUNCTION

FUNCTION TFILM (T)
'
'     THIS FUNCTION RETURNS THE FILM TEMPERATURE (DEG. C)
'     AS A FUNCTION OF THE DRY AIR TEMPERATURE.
'
VALUE = .5 * TWB(T) + .5 * T
TFILM = VALUE
END FUNCTION


FUNCTION TSATP! (P!)
'
'     THIS FUNCTION RETURNS THE SATURATION TEMPERATURE OF WATER VAPOR
'     (DEG. C) AT A GIVEN PRESSURE. IT IS THE INVERSE OF FUNCTION PSAT
'
VALUE = (3816.44 / (23.1964 - LOG(1000 * P))) - 227.02
TSATP = VALUE
END FUNCTION

FUNCTION TWB (T)
'
'        THIS  FUNCTION  RETURNS  THE  WET  BULB  (ADIABATIC  SATURATION)
TEMPERATURE
'     FOR DRY AIR AT ATMOSPHERIC PRESSURE (DEG. C). IT WAS OBTAINED FROM
'        POLYNOMIAL REGRESSION OF THE SOLUTION OF THE AIR-WATER ENTHALPY
BALANCE.
'
```

```
VALUE = -1.9249# + .459447# * T - 1.58036E-03 * (T ^ 2) + 2.7126E-06 *
(T ^ 3)
- 1.72402E-09 * (T ^ 4)
TWB = VALUE
END FUNCTION
```

TABLE A4.1 - PROPERTIES OF STEAM AT ATMOSPHERIC PRESSURE

TEMPE-RATURE DEG. C	DENSITY KG/M3	SPECIFIC HEAT KJ/KG-K	DYNAMIC VISCOSITY 10-6 PA-S	THERMAL CONDUCTIVITY 10-3 W/M-K	PRANDTL NUMBER	HEAT OF EVAPORATION KJ/KG
0	0.804	1.895	9.052	16.160	1.061	2540.0
10	0.775	1.897	9.372	16.850	1.055	2514.0
20	0.749	1.900	9.694	17.560	1.049	2487.5
30	0.724	1.902	10.018	18.290	1.042	2460.6
40	0.701	1.905	10.343	19.039	1.035	2433.1
50	0.679	1.908	10.670	19.808	1.028	2403.2
60	0.659	1.911	10.999	20.594	1.021	2376.7
70	0.640	1.914	11.330	21.399	1.013	2347.7
80	0.622	1.917	11.663	22.221	1.006	2318.1
90	0.604	1.921	11.997	23.060	0.999	2287.8
100	0.588	1.924	12.333	23.914	0.992	2256.8
150	0.519	1.943	14.041	28.412	0.960	2090.6
200	0.464	1.964	15.792	33.233	0.933	1899.3
250	0.420	1.988	17.589	38.308	0.913	1670.0
300	0.383	2.014	19.429	43.570	0.898	1372.9
350	0.352	2.041	21.315	48.950	0.889	895.9
400	0.326	2.070	23.244	54.379	0.885	
450	0.304	2.101	25.218	59.790	0.886	
500	0.284	2.133	27.237	65.115	0.892	
550	0.267	2.167	29.300	70.284	0.903	
600	0.251	2.201	31.407	75.230	0.919	

TABLE A4.2 - PROPERTIES OF AIR AT ATMOSPHERIC PRESSURE

TEMPE-RATURE DEG. C	DENSITY KG/M3	SPECIFIC HEAT KJ/KG-K	DYNAMIC VISCOSITY 10-6 PA-S	THERMAL CONDUCTIVITY 10-3 W/M-K	PRANDTL NUMBER
0	1.292	1.010	17.240	24.167	0.720
10	1.247	1.011	17.710	24.950	0.717
20	1.204	1.012	18.175	25.727	0.715
30	1.164	1.013	18.635	26.499	0.713
40	1.127	1.014	19.091	27.264	0.710
50	1.092	1.016	19.542	28.023	0.708
60	1.060	1.017	19.988	28.775	0.706
70	1.029	1.018	20.430	29.522	0.705
80	1.000	1.019	20.867	30.262	0.703
90	0.972	1.021	21.299	30.997	0.701
100	0.946	1.022	21.726	31.725	0.700
150	0.834	1.028	23.791	35.274	0.694
200	0.746	1.035	25.738	38.669	0.689
250	0.675	1.041	27.566	41.911	0.685
300	0.616	1.048	29.275	44.999	0.682
350	0.567	1.055	30.866	47.934	0.679
400	0.524	1.062	32.338	50.715	0.677
450	0.488	1.069	33.692	53.343	0.675
500	0.457	1.076	34.927	55.818	0.673
550	0.429	1.083	36.043	58.138	0.671
600	0.404	1.090	37.041	60.306	0.670

TABLE A4.3 - MIXTURE PROPERTIES AT WET BULB CONDITIONS

JET TEMPE- RATURE DEG. C	W. B. TEMPE- RATURE DEG. C	STEAM MOLE FRACT.	AIR MOLE FRACT.	DENSITY KG/M3	SPECIFIC HEAT KJ/KG-K	DYNAMIC VISC. 10-6 PA-S	THERMAL CONDUCT. 10-3 W/M-K	PRANDTL NUMBER
20	6.65	0.01	0.99	1.26	1.02	17.47	24.61	0.72
30	10.51	0.01	0.99	1.24	1.02	17.62	24.88	0.72
40	14.09	0.02	0.98	1.22	1.02	17.76	25.13	0.72
50	17.42	0.02	0.98	1.21	1.02	17.88	25.36	0.72
60	20.52	0.02	0.98	1.19	1.03	17.99	25.56	0.72
70	23.38	0.03	0.97	1.18	1.03	18.08	25.75	0.72
80	26.03	0.03	0.97	1.17	1.03	18.15	25.91	0.72
90	28.49	0.04	0.96	1.15	1.03	18.22	26.06	0.72
100	30.76	0.04	0.96	1.14	1.04	18.27	26.18	0.72
150	39.72	0.07	0.93	1.10	1.06	18.42	26.63	0.73
200	45.69	0.10	0.90	1.07	1.07	18.45	26.87	0.74
250	49.81	0.12	0.88	1.04	1.09	18.42	26.99	0.74
300	52.95	0.14	0.86	1.02	1.10	18.37	27.06	0.75
350	55.72	0.16	0.84	1.01	1.11	18.31	27.11	0.75
400	58.47	0.18	0.82	0.99	1.13	18.22	27.13	0.76
450	61.29	0.21	0.79	0.97	1.14	18.11	27.13	0.76
500	64.03	0.24	0.76	0.95	1.16	17.97	27.12	0.77
550	66.26	0.26	0.74	0.94	1.18	17.83	27.08	0.78
600	67.30	0.27	0.73	0.93	1.19	17.76	27.06	0.78

TABLE A4.4 - MIXTURE PROPERTIES AT 1/3 REFERENCE CONDITIONS

JET TEMPE-RATURE DEG. C	1/3 RD TEMPE-RATURE DEG. C	STEAM MOLE FRACT.	AIR MOLE FRACT.	DENSITY KG/M3	SPECIFIC HEAT KJ/KG-K	DYNAMIC VISC. 10-6 PA-S	THERMAL CONDUCT. 10-3 W/M-K	PRANDTL NUMBER
20	11.10	0.01	0.99	1.24	1.01	17.70	24.98	0.72
30	17.01	0.01	0.99	1.21	1.02	17.96	25.42	0.72
40	22.73	0.01	0.99	1.19	1.02	18.21	25.85	0.72
50	28.28	0.01	0.99	1.17	1.02	18.44	26.26	0.72
60	33.68	0.02	0.98	1.14	1.02	18.66	26.65	0.72
70	38.92	0.02	0.98	1.12	1.02	18.87	27.02	0.72
80	44.02	0.02	0.98	1.10	1.03	19.07	27.38	0.72
90	48.99	0.03	0.97	1.09	1.03	19.26	27.73	0.72
100	53.84	0.03	0.97	1.07	1.03	19.44	28.07	0.72
150	76.48	0.05	0.95	0.99	1.05	20.26	29.61	0.72
200	97.13	0.07	0.93	0.93	1.06	20.98	31.01	0.72
250	116.54	0.08	0.92	0.88	1.07	21.65	32.32	0.72
300	135.30	0.09	0.91	0.83	1.08	22.29	33.60	0.72
350	153.81	0.11	0.89	0.79	1.09	22.91	34.85	0.72
400	172.31	0.12	0.88	0.76	1.10	23.49	36.10	0.72
450	190.86	0.14	0.86	0.72	1.12	24.05	37.34	0.72
500	209.35	0.16	0.84	0.69	1.13	24.57	38.58	0.72
550	227.51	0.17	0.83	0.66	1.15	25.09	39.81	0.72
600	244.87	0.18	0.82	0.63	1.16	25.65	41.03	0.72

TABLE A4.5 - MIXTURE PROPERTIES AT FILM CONDITIONS

JET TEMPE- RATURE DEG. C	FILM TEMPE- RATURE DEG. C	STEAM MOLE FRACT.	AIR MOLE FRACT.	DENSITY KG/M3	SPECIFIC HEAT KJ/KG-K	DYNAMIC VISC. 10-6 PA-S	THERMAL CONDUCT. 10-3 W/M-K	PRANDTL NUMBER
20	13.33	0.00	1.00	1.23	1.01	17.82	25.17	0.72
30	20.25	0.01	0.99	1.20	1.02	18.13	25.69	0.72
40	27.05	0.01	0.99	1.17	1.02	18.43	26.20	0.72
50	33.71	0.01	0.99	1.15	1.02	18.72	26.70	0.71
60	40.26	0.01	0.99	1.12	1.02	18.99	27.18	0.71
70	46.69	0.01	0.99	1.10	1.02	19.26	27.65	0.71
80	53.02	0.02	0.98	1.08	1.03	19.52	28.11	0.71
90	59.24	0.02	0.98	1.05	1.03	19.78	28.56	0.71
100	65.38	0.02	0.98	1.03	1.03	20.02	29.00	0.71
150	94.86	0.04	0.96	0.95	1.04	21.17	31.07	0.71
200	122.85	0.05	0.95	0.87	1.05	22.21	33.01	0.71
250	149.91	0.06	0.94	0.82	1.06	23.20	34.88	0.71
300	176.48	0.07	0.93	0.76	1.07	24.16	36.69	0.71
350	202.86	0.08	0.92	0.72	1.08	25.07	38.48	0.71
400	229.23	0.09	0.91	0.68	1.09	25.95	40.25	0.71
450	255.65	0.10	0.90	0.64	1.11	26.79	42.01	0.71
500	282.02	0.12	0.88	0.61	1.12	27.59	43.75	0.71
550	308.13	0.13	0.87	0.58	1.13	28.37	45.48	0.71
600	333.65	0.14	0.86	0.55	1.14	29.16	47.15	0.71

APPENDIX 5

PERFORMANCE CALCULATIONS FOR SUPERHEATED STEAM DRYING CYCLES

```
'
'     CYCLES.BAS - PERFORMANCE CALCULATIONS ON
'     SUPERHEATED STEAM DRYING CYCLES
'     WRITTEN IN QUICKBASIC 4.0 BY J. F. BOND
'     THIS VERSION LAST MODIFIED 9/9/91

'     THIS PROGRAM CALCULATES ENERGY CONSUMPTION VS. IMPINGEMENT DRYING
'     RATE FOR THREE COMBINED SUPERHEATED STEAM IMPINGEMENT-CONVENTIONAL
'     DRYING CYCLES:
'
'     1- IMPINGEMENT-CONVENTIONAL DRYING WITH RECIRCULATION BY FAN
'     2- IMPINGEMENT-CONVENTIONAL DRYING WITH RECIRCULATION BY THERMO-
'        COMPRESSOR;
'     3- PURE IMPINGEMENT DRYING WITH OPEN-CYCLE HEAT PUMP (LUTHI'S FIRST
'        CYCLE).'

'     THE PROGRAM COMPRISES FOUR SECTIONS:

'     A- FUNCTION AND VARIABLE DECLARATION;
'     B- INPUT AND PRELIMINARY CALCULATIONS;
'     C- MAIN CALCULATION SEQUENCE;
'     D- EXPORTING OF RESULTS.

'     A- FUNCTION AND VARIABLE DECLARATION


'     FLUID PROPERTIES


DECLARE FUNCTION CP (T)
DECLARE FUNCTION SDEN (T)
DECLARE FUNCTION CON (T)
DECLARE FUNCTION MU (T)
DECLARE FUNCTION TSATP (P)
DECLARE FUNCTION PSAT! (T!)


'     DRYING RATE EQUATIONS


DECLARE FUNCTION RIC (M, XII, XF, R, X)
'AVERAGE DRYING RATE FOR DRYING BEGINNING IN THE CONSTANT RATE PERIOD
DECLARE FUNCTION RIF (M, XII, XF, R, X)
'AVERAGE DRYING RATE FOR DRYING ENTIRELY WITHIN FALLING RATE PERIOD

DEFSNG A-Z
DIM RESULTSM(10, 500)
DIM RESULTST(10, 500)
DIM RESULTSL(10, 500)
```

```
DHV = 2258.1              'ENTHALPY OF EVAPORATION OF WATER, KJ/KG
TB = 100                  'ATMOSPHERIC BOILING POINT OF WATER, DEG. C
PATM = 101.325            'ATMOSPHERIC PRESSURE, KPA
RS = 461.495             'GAS CONSTANT FOR STEAM, N-M/KG-DEG. C.
CD = .8                   'NOZZLE DISCHARGE COEFFICIENT
CL = 4.2                  'SPECIFIC HEAT OF LIQUID WATER, KJ/KG-DEG. C


' B-  INPUT AND PRELIMINARY CALCULATIONS



' OPERATING CONDITIONS ARE READ FROM A FILE AND MODIFIED AS REQUIRED


OPEN "C:\QUICKBAS\CYCLES.DTA" FOR INPUT AS #1
INPUT #1, HM, DM, FM, TJLOM, TJHIM, TJSTM, TJLOT, TJHIT, TJSTT, TJLOL,
TJHIL, TJSTL, RILOM, RIHIM, RILOT, RIHIT, RILOL, RIHIL, ETAF, ETAC,
ETAT, PMOT, PC, EPSILON, KAPPA, XIC, XF, B
CLOSE #1

DISPLAY:
CLS
PRINT "       CYCLES.BAS -  OPERATING CONDITIONS AND PARAMETERS            "
PRINT
PRINT
PRINT "DRYER GEOMETRY: NOZZLE-TO-WEB DISTANCE:", HM, "MM"
PRINT "                NOZZLE DIAMETER:        ", DM, "MM"
PRINT "                OPEN AREA RATIO:        ", FM, "%"
PRINT
PRINT "JET TEMPERATURE AND DRYING RATE RANGE"
PRINT
PRINT "TEMPERATURES (DEG. C):      LOWEST     HIGHEST    INCREMENT SIZE "
PRINT "MECH. COMPRESSION", TJLOM, TJHIM, TJSTM
PRINT "THERMOCOMPRESSION", TJLOT, TJHIT, TJSTT
PRINT "LUTHI'S CYCLE    ", TJLOL, TJHIL, TJSTL
PRINT
PRINT "DRYING RATES (KG/M2-HR):    LOWEST     HIGHEST  "
PRINT "MECH. COMPRESSION", RILOM, RIHIM
PRINT "THERMOCOMPRESSION", RILOT, RIHIT
PRINT "LUTHI'S CYCLE    ", RILOL, RIHIL
PRINT
PRINT
INPUT ; "PRESS ENTER TO SEE REMAINING CONDITIONS", REPLY
CLS
PRINT
PRINT
PRINT "FAN ISENTROPIC EFFICIENCY:               ", ETAF
PRINT "COMPRESSOR ISENTROPIC EFFICIENCY:      ", ETAC
PRINT "THERMOCOMPRESSOR EFFICIENCY:           ", ETAT
PRINT "THERMOCOMPRESSOR MOTIVE STEAM PRESSURE:", PMOT, "KPA ABS."
PRINT "CONVENTIONAL DRYER PRESSURE:      ", PC, "KPA ABS."
```

```
PRINT "WORK-TO-HEAT VALUE RATIO:            ", EPSILON
PRINT "STEAM CONSUMPTION INDEX:             ", KAPPA, "KG/KG"
PRINT
PRINT "CONVENTIONAL DRYER INLET MOISTURE CONTENT:   ", XIC
PRINT "IMPINGEMENT DRYER FINAL MOISTURE CONTENT:    ", XF
PRINT
PRINT "SHEET BASIS WEIGHT:                  ", B, "G/M2"
PRINT
PRINT
INPUT "DO YOU WISH TO MAKE ANY CHANGES (Y/N)?", ANSWER$
IF (ANSWER$ = "Y" OR ANSWER$ = "y") THEN GOTO CHANGES ELSE GOTO PRELIM

CHANGES:
CLS

PRINT "ENTER NEW VALUES; PRESS ENTER TO LEAVE CONDITION UNCHANGED"
PRINT
PRINT "("; HM; ")          ";
INPUT "NOZZLE-TO-WEB SPACING (MM.): ", TEMP$
IF (TEMP$ <> "") THEN HM = VAL(TEMP$)
PRINT "("; DM; ")          ";
INPUT "NOZZLE DIAMETER (MM.):", TEMP$
IF (TEMP$ <> "") THEN DM = VAL(TEMP$)
PRINT "("; FM; ")          ";
INPUT "OPEN-AREA RATIO (%):", TEMP$
IF (TEMP$ <> "") THEN FM = VAL(TEMP$)
PRINT "("; TJLOM; ")        ";
INPUT "MECH. COMPRESSION LOWEST TEMPERATURE (DEG. C):", TEMP$
IF (TEMP$ <> "") THEN TJLOM = VAL(TEMP$)
PRINT "("; TJHIM; ")        ";
INPUT "MECH. COMPRESSION HIGHEST TEMPERATURE (DEG. C):", TEMP$
IF (TEMP$ <> "") THEN TJHIM = VAL(TEMP$)
PRINT "("; TJSTM; ")        ";
INPUT "MECH. COMPRESSION TEMPERATURE STEP(DEG. C):", TEMP$
IF (TEMP$ <> "") THEN TJSTM = VAL(TEMP$)
PRINT "("; TJLOT; ")        ";
INPUT "THERMOCOMPRESSION LOWEST TEMPERATURE (DEG. C):", TEMP$
IF (TEMP$ <> "") THEN TJLOT = VAL(TEMP$)
PRINT "("; TJHIT; ")        ";
INPUT "THERMOCOMPRESSION HIGHEST TEMPERATURE (DEG. C):", TEMP$
IF (TEMP$ <> "") THEN TJHIT = VAL(TEMP$)
PRINT "("; TJSTT; ")        ";
INPUT "THERMOCOMPRESSION TEMPERATURE STEP(DEG. C):", TEMP$
IF (TEMP$ <> "") THEN TJSTT = VAL(TEMP$)
PRINT "("; TJLOL; ")        ";
INPUT "LUTHI'S CYCLE LOWEST TEMPERATURE (DEG. C):", TEMP$
IF (TEMP$ <> "") THEN TJLOL = VAL(TEMP$)
PRINT "("; TJHIL; ")        ";
INPUT "LUTHI'S CYCLE HIGHEST TEMPERATURE (DEG. C):", TEMP$
IF (TEMP$ <> "") THEN TJHIL = VAL(TEMP$)
PRINT "("; TJSTL; ")        ";
INPUT "LUTHI'S CYCLE TEMPERATURE STEP (DEG. C):", TEMP$
IF (TEMP$ <> "") THEN TJSTL = VAL(TEMP$)
PRINT "("; RILOM; ")        ";
```

```
INPUT "MECH. COMPRESSION LOWEST DRYING RATE (KG/M2-HR):", TEMP$
IF (TEMP$ <> "") THEN RILOM = VAL(TEMP$)
PRINT "("; RIHIM; ")          ";
INPUT "MECH. COMPRESSION HIGHEST DRYING RATE (KG/M2-HR):", TEMP$
IF (TEMP$ <> "") THEN RIHIM = VAL(TEMP$)
PRINT "("; RILOT; ")          ";
INPUT "THERMOCOMPRESSION LOWEST DRYING RATE (KG/M2-HR):", TEMP$
IF (TEMP$ <> "") THEN RILOT = VAL(TEMP$)
PRINT "("; RIHIT; ")          ";
INPUT "THERMOCOMPRESSION HIGHEST DRYING RATE (KG/M2-HR):", TEMP$
IF (TEMP$ <> "") THEN RIHIT = VAL(TEMP$)
PRINT "("; RILOL; ")          ";
INPUT "LUTHI'S CYCLE LOWEST DRYING RATE (KG/M2-HR):", TEMP$
IF (TEMP$ <> "") THEN RILOL = VAL(TEMP$)
PRINT "("; RIHIL; ")          ";
INPUT "LUTHI'S CYCLE HIGHEST DRYING RATE (KG/M2-HR):", TEMP$
IF (TEMP$ <> "") THEN RIHIL = VAL(TEMP$)
PRINT "("; ETAF; ")          ";
INPUT "FAN ISENTROPIC EFFICIENCY:", TEMP$
IF (TEMP$ <> "") THEN ETAF = VAL(TEMP$)
PRINT "("; ETAC; ")          ";
INPUT "COMPRESSOR ISENTROPIC EFFICIENCY:", TEMP$
IF (TEMP$ <> "") THEN ETAC = VAL(TEMP$)
PRINT "("; ETAT; ")          ";
INPUT "THERMOCOMPRESSOR EFFICIENCY:", TEMP$
IF (TEMP$ <> "") THEN ETAT = VAL(TEMP$)
PRINT "("; PMOT; ")          ";
INPUT "THERMOCOMPRESSOR MOTIVE STEAM PRESSURE (KPA ABS.):", TEMP$
IF (TEMP$ <> "") THEN PMOT = VAL(TEMP$)
PRINT "("; PC; ")          ";
INPUT "CONVENTIONAL DRYER PRESSURE (KPA ABS.):", TEMP$
IF (TEMP$ <> "") THEN PC = VAL(TEMP$)
PRINT "("; EPSILON; ")          ";
INPUT "WORK-TO-HEAT VALUE RATIO:", TEMP$
IF (TEMP$ <> "") THEN EPSILON = VAL(TEMP$)
PRINT "("; KAPPA; ")          ";
PRINT "KG-STEAM/KG-WATER EVAPORATED"
INPUT "IN CONVENTIONAL DRYER SECTION:", TEMP$
IF (TEMP$ <> "") THEN KAPPA = VAL(TEMP$)
PRINT "("; XIC; ")      ";
INPUT "CONVENTIONAL DRYER INLET MOISTURE CONTENT:", TEMP$
IF (TEMP$ <> "") THEN XIC = VAL(TEMP$)
PRINT "("; XF; ")      ";
INPUT "IMPINGEMENT DRYER FINAL MOISTURE CONTENT:", TEMP$
IF (TEMP$ <> "") THEN XF = VAL(TEMP$)
PRINT "("; B; ")      ";
INPUT "SHEET BASIS WEIGHT, G/M2:", TEMP$
IF (TEMP$ <> "") THEN B = VAL(TEMP$)


OPEN "C:\QUICKBAS\CYCLES.DTA" FOR OUTPUT AS #1
WRITE #1, HM, DM, FM, TJLOM, TJHIM, TJSTM, TJLOT, TJHIT, TJSTT, TJLOL,
TJHIL, TJSTL, RILOM, RIHIM, RILOT, RIHIT, RILOL, RIHIL, ETAF, ETAC,
ETAT, PMOT, PC, EPSILON, KAPPA, XIC, XF, B
```

```
CLOSE #1

GOTO DISPLAY

PRELIM:


'    PRELIMINARY CALCULATIONS


H = HM / 1000              'CONVERSION TO METERS
D = DM / 1000
F = FM / 100               'CONVERSION TO FRACTION
FGEO = (((1 + (((H / D) * SQR(F) / .6) ^ 6)) ^ -.05) * SQR(F) * (1 - 2.2
* SQR(F))) / (1 + .2 * ((H / D) - 6) * SQR(F))
'GEOMETRICAL HEAT TRANSFER COEFFICIENT
MPC = 1 - (PATM / PMOT) ^ .25      'MOTIVE POWER COEFFICIENT



'    C- MAIN CALCULATION SEQUENCE



'    C1- IMPINGEMENT-CONVENTIONAL DRYING WITH RECIRCULATION BY FAN

'    SEQUENCE OF CALCULATIONS:

'    -JET MASS FLOW RATE AND VELOCITY
'    -INITIAL MOISTURE CONTENT FOR IMPINGEMENT STEAM DRYING
'    -AVERAGE IMPINGEMENT DRYING RATE
'    -OUTLET TEMPERATURE TE
'    -DRYER PRESSURE DROP AND FAN EXHAUST PRESSURE PF
'    -TOTAL WATER REMOVAL RATE JT
'    -FAN WORK WF
'    -COMPRESSOR WORK WC
'    -HEAT CONSUMPTION QI
'    -SPECIFIC VALUES:   -QI/JT
'                        -W/JT
'                        -TOTAL ENERGY ET/JT
'                        -TOTAL EQUIVALENT ENERGY EE/JT
'


'        NOTE: THE IMPINGEMENT DRYER AREA IS TAKEN TO BE 1 SQUARE METER
'        THIS SIMPLIFIES CALCULATIONS, AS JI = RI


ROW% = 1
COLUMN% = 1

FOR TJ = TJLOM TO TJHIM STEP TJSTM

FOR REJ = 500 TO 100000 STEP 500
```

```
'     JET MASS FLOW RATE (KG/H) AND VELOCITY (M/S)


MJ = 3600 * F * MU(TJ) * REJ / D
UJ = (MU(TJ) * REJ) / (SDEN(TJ) * D)


'     INITIAL MOISTURE CONTENT FOR IMPINGEMENT STEAM DRYING
'     AND AVERAGE IMPINGEMENT DRYING RATE (KG/M2-H)


XII = XF + (1 / (1 + (1 / KAPPA))) * (XIC - XF)
RC = 3.6 * CON(TJ) * (((TJ + 273.2) / (TB + 273.2)) ^ -.77) * (FGEO / D)
* (REJ ^ .66667) * LOG(1 + (CP((TJ + TB) / 2) * (TJ - TB) / DHV)) /
CP((TJ + TB) / 2)
XC = .373 * (RC ^ .265)
M = 3.028 * (RC ^ .495) * (B ^ .198)


RF = RC + 3.028 * (RC ^ .495) * (B ^ .198) * (XF - .373 * (RC ^ .265))
IF (RF <= 0) THEN GOTO REJINCM           'PROVISION FOR RF>0

IF (XII > XC) THEN RI = RIC(M, XII, XF, RC, XC) ELSE RI = RIF(M, XII,
XF, RC, XC)
JI = RI
IF (RI < RILOM) THEN GOTO REJINCM
IF (RI > RIHIM) THEN GOTO TJINCM



'     OUTLET TEMPERATURE TE (DEG. C)


ALPHA = (RI * D) / (3600 * F * MU(TJ) * REJ)
TE = (1 / (1 + ALPHA)) * (TJ + ALPHA * (TB - (DHV / CP((TJ + TB) / 2))))



'     FAN EXHAUST PRESSURE PF (KPA ABS.)


DELTAP = .0000005 * ((MU(TJ) / (CD * D)) ^ 2) * RS * (TJ + 273.2) * (REJ
^ 2) / PATM
PF = PATM + DELTAP



'     TOTAL WATER REMOVAL RATE JT (KG/H)


TEMP1 = CP((TB + TSATP(PC)) / 2) / DHV
TEMP2 = (TB + 273.2) * (1 + (1 / ETAC) * ((PC / PATM) ^ .25 - 1)) -
(TSATP(PC) + 273.2)
```

```
TEMP3 = TEMP1 * TEMP2
TEMP4 = CP((TE + TB) / 2) * (TE - TB) / DHV
JT = JI * (1 + (1 / KAPPA) * (1 + TEMP4 + (1 + TEMP4) * TEMP3))


'    FAN WORK WF (KJ/H)

WF = (MJ * CP(TE) * (TE + 273.2) / ETAF) * ((PF / PATM) ^ .25 - 1)


'    COMPRESSOR WORK WC (KJ/H)

WC = JI * (1 + TEMP4) * CP(TB) * ((TB + 273.2) / ETAC) * ((PC / PATM) ^
.25 - 1)


'    HEAT CONSUMPTION QI (KJ/H)


QI = MJ * CP((TJ + TE) / 2) * (TJ - TE) - WF


'    PROVISION FOR POSITIVE HEAT CONSUMPTION


IF (QI < 0) THEN GOTO TJINCM


'    SPECIFIC HEAT (KJ/KG), WORK (KJ/KG), TOTAL (KJ/KG) AND EQUIVALENT
'    (KG/KG) ENERGY CONSUMPTION

RESULTSM(1, ROW%) = TJ
RESULTSM(2, ROW%) = UJ
RESULTSM(3, ROW%) = DELTAP
RESULTSM(4, ROW%) = JI
RESULTSM(5, ROW%) = JT
RESULTSM(6, ROW%) = QI / JT
RESULTSM(7, ROW%) = (WF + WC) / JT
RESULTSM(8, ROW%) = (QI + WF + WC) / JT
RESULTSM(9, ROW%) = (QI + EPSILON * (WF + WC)) / (JT * DHV)

ROW% = ROW% + 1


REJINCM:
NEXT REJ

TJINCM:
NEXT TJ

LR% = ROW% - 1
```

```
'       RESULTS PRINTING SECTION


CLS
PRINT "                              RESULTS           "
PRINT
PRINT "   TJ     UJ    DELTAP     JI     JT     HEAT    WORK     TOTAL
EQUV."
PRINT "  DEG.C   M/S    KPA      KG/H   KG/H   KJ/KG   KJ/KG    KJ/KG
KG/KG."
PRINT
FOR ROW% = 1 TO LR%
PRINT  USING  "#####.##";  RESULTSM(1,  ROW%);  RESULTSM(2,  ROW%),
RESULTSM(3,  ROW%),  RESULTSM(4,  ROW%),  RESULTSM(5,  ROW%),  RESULTSM(6,
ROW%), RESULTSM(7, ROW%), RESULTSM(8, ROW%), RESULTSM(9, ROW%)

NEXT ROW%



'     RESULTS EXPORT SECTION


OPEN "C:\JFBOND\SWIFT\CYCRES1.PRN" FOR OUTPUT AS #1

PRINT #1, "   CYCLES.BAS -  OPERATING CONDITIONS AND PARAMETERS   "
PRINT #1,
PRINT #1, "DRYER GEOMETRY:    NOZZLE-TO-WEB SPACING: ", HM, "MM."
PRINT #1, "                   NOZZLE DIAMETER:", DM, "MM."
PRINT #1, "                   OPEN-AREA RATIO:", FM, "%"
PRINT #1,
PRINT #1, "TEMPERATURES (DEG. C):  LOWEST  HIGHEST   INCREMENT SIZE "
PRINT #1, "MECH. COMPRESSION", TJLOM, TJHIM, TJSTM
PRINT #1, "THERMOCOMPRESSION", TJLOT, TJHIT, TJSTT
PRINT #1, "LUTHI'S          ", TJLOL, TJHIL, TJSTL
PRINT #1,
PRINT #1, "DRYING RATES (KG/M2-HR):    LOWEST      HIGHEST    "
PRINT #1, "MECH. COMPRESSION", RILOM, RIHIM
PRINT #1, "THERMOCOMPRESSION", RILOT, RIHIT
PRINT #1, "LUTHI'S          ", RILOL, RIHIL
PRINT #1,
PRINT #1, "FAN ISENTROPIC EFFICIENCY:      ", ETAF
PRINT #1, "COMPRESSOR ISENTROPIC EFFICIENCY:", ETAC
PRINT #1, "THERMOCOMPRESSOR EFFICIENCY:    ", ETAT
PRINT #1, "CONVENTIONAL DRYER PRESSURE:    ", PC, "KPA ABS."
PRINT #1, "WORK-TO-HEAT VALUE RATIO:       ", EPSILON
PRINT #1, "KG-STEAM/KG WATER EVAP. IN CON- ", KAPPA
PRINT #1, "VENTIONAL DRYER SECTION         "
PRINT #1, "CONVENTIONAL DRYER INLET MOISTURE CONTENT:  ", XIC
PRINT #1, "IMPINGEMENT DRYER FINAL MOISTURE CONTENT:   ", XF
PRINT #1, "SHEET BASIS WEIGHT:             ", B, "G/M2"
PRINT #1, "                               RESULTS         "
```

```
PRINT #1,
PRINT #1, "      TJ      UJ     DELTAP      JI       JT      HEAT     WORK
TOTAL      EQUV."
PRINT #1, "    DEG.C    M/S      KPA      KG/H     KG/H    KJ/KG    KJ/KG
KJ/KG    KG/KG."
PRINT #1,
CLOSE #1

OPEN "C:\JFBOND\SWIFT\CYCM.PRN" FOR OUTPUT AS #1

FOR ROW% = 1 TO LR%
PRINT #1, RESULTSM(1, ROW%); RESULTSM(2, ROW%); RESULTSM(3, ROW%);
RESULTSM(4, ROW%); RESULTSM(5, ROW%); RESULTSM(6, ROW%); RESULTSM(7,
ROW%); RESULTSM(8, ROW%); RESULTSM(9, ROW%)
NEXT ROW%

CLOSE #1




'     C2- IMPINGEMENT-CONVENTIONAL DRYING WITH RECIRCULATION BY
'          THERMOCOMPRESSOR


'     SEQUENCE OF CALCULATIONS:
'
'     -JET MASS FLOW RATE AND VELOCITY
'     -INITIAL MOISTURE CONTENT FOR IMPINGEMENT STEAM DRYING
'     -AVERAGE IMPINGEMENT DRYING RATE
'     -OUTLET TEMPERATURE TE
'     -DRYER PRESSURE DROP AND THERMOCOMPRESSOR EXHAUST PRESSURE PJ
'     -THERMOCOMPRESSOR MOTIVE STEAM FLOW RATE MTM
'     -TOTAL WATER REMOVAL RATE JT
'     -COMPRESSOR WORK WC
'     -HEAT CONSUMPTION QI
'     -SPECIFIC VALUES:    -QI/JT
'                          -W/JT
'                          -TOTAL ENERGY ET/JT
'                          -TOTAL EQUIVALENT ENERGY EE/JT



'     NOTE: THE IMPINGEMENT DRYER AREA IS TAKEN TO BE 1 SQUARE METER
'     THIS SIMPLIFIES CALCULATIONS, AS JI = RI


ROW% = 1
COLUMN% = 1



'     NOTE: FOR THE CYCLE WITH THERMOCOMPRESSOR, XII MUST BE DETERMINED
```

```
'      ITERATIVELY BECAUSE OF THE COUPLING BETWEEN IMPINGING JET AND
'      THERMOCOMPRESSOR MOTIVE MASS FLOW RATES.


XII = XF + (1 / (1 + (1 / KAPPA))) * (XIC - XF)   'INITIAL GUESS FOR XII


FOR TJ = TJLOT TO TJHIT STEP TJSTT

FOR REJ = 500 TO 100000 STEP 500



'      JET MASS FLOW RATE (KG/H) AND VELOCITY (M/S)


MJ = 3600 * F * MU(TJ) * REJ / D
UJ = (MU(TJ) * REJ) / (SDEN(TJ) * D)


'      INITIAL MOISTURE CONTENT FOR IMPINGEMENT STEAM DRYING
'      AND AVERAGE IMPINGEMENT DRYING RATE (KG/M2-H)



RATECALC:

RC = 3.6 * CON(TJ) * (((TJ + 273.2) / (TB + 273.2)) ^ -.77) * (FGEO / D)
* (REJ ^ .66667) * LOG(1 + (CP((TJ + TB) / 2) * (TJ - TB) / DHV)) /
CP((TJ + TB) / 2)
XC = .373 * (RC ^ .265)
M = 3.028 * (RC ^ .495) * (B ^ .198)


RF = RC + 3.028 * (RC ^ .495) * (B ^ .198) * (XF - .373 * (RC ^ .265))
IF (RF <= 0) THEN GOTO REJINCT            'PROVISION FOR RF>0

IF (XII > XC) THEN RI = RIC(M, XII, XF, RC, XC) ELSE RI = RIF(M, XII,
XF, RC, XC)
JI = RI
IF (RI < RILOT) THEN GOTO REJINCT
IF (RI > RIHIT) THEN GOTO TJINCT



'      OUTLET TEMPERATURE TE (DEG. C)


ALPHA = (RI * D) / (3600 * F * MU(TJ) * REJ)
TE = (1 / (1 + ALPHA)) * (TJ + ALPHA * (TB - (DHV / CP((TJ + TB) / 2))))
```

'   DRYER PRESSURE DROP AND THERMOCOMPRESSOR EXHAUST PRESSURE PJ (KPA)

DELTAP = .0000005 * ((MU(TJ) / (CD * D)) ^ 2) * RS * (TJ + 273.2) * (REJ
^ 2) / PATM
PJ = PATM + DELTAP

'   THERMOCOMPRESSOR MOTIVE STEAM FLOW RATE MTM (KG/H)

QRATIO = ((TJ + 273.2) / (TE + 273.2)) * ((ETAT * MPC) / (1 - (PATM /
PJ) ^ .25) - 1)
MTM = MJ / (QRATIO + 1)

'   TOTAL WATER REMOVAL RATE JT (KG/H)

TEMP1 = CP((TB + TSATP(PC)) / 2) / DHV
TEMP2 = (TB + 273.2) * (1 + (1 / ETAC) * ((PC / PATM) ^ .25 - 1)) -
(TSATP(PC) + 273.2)
TEMP3 = TEMP1 * TEMP2
TEMP4 = CP((TE + TB) / 2) * (TE - TB) / DHV
JT = JI + (1 / KAPPA) * (JI + MTM) * (1 + TEMP4 + (1 + TEMP4) * TEMP3)

'   COMPRESSOR WORK WC (KJ/H)

WC = (JI + MTM) * (1 + TEMP4) * CP(TB) * ((TB + 273.2) / ETAC) * ((PC /
PATM) ^ .25 - 1)

'   HEAT CONSUMPTION QI (KJ/H)

QI = MJ * CP((TJ + TE) / 2) * (TJ - TE) + MTM * (DHV + CP((TB + TE) / 2)
* (TE - TB))

'   ITERATION OF XII

IF (((XF + (JT / JI) * (XII - XF)) - XIC) > .01) THEN
XII = XII - .001
IF (XII > (2 * XF)) GOTO RATECALC ELSE GOTO TJINCT
END IF

IF (((XF + (JT / JI) * (XII - XF)) - XIC) < -.01) THEN
XII = XII + .001
IF (XII > (2 * XF)) GOTO RATECALC ELSE GOTO TJINCT
END IF

```
'     SPECIFIC HEAT (KJ/KG), WORK (KJ/KG), TOTAL (KJ/KG) AND
'     EQUIVALENT (KG/KG) ENERGY CONSUMPTION


RESULTST(1, ROW%) = TJ
RESULTST(2, ROW%) = UJ
RESULTST(3, ROW%) = DELTAP
RESULTST(4, ROW%) = JI
RESULTST(5, ROW%) = JT
RESULTST(6, ROW%) = QI / JT
RESULTST(7, ROW%) = WC / JT
RESULTST(8, ROW%) = (QI + WC) / JT
RESULTST(9, ROW%) = (QI + EPSILON * WC) / (JT * DHV)


ROW% = ROW% + 1


REJINCT:
NEXT REJ

TJINCT:
NEXT TJ

LR% = ROW% - 1



'     RESULTS PRINTING SECTION



CLS
PRINT "                             RESULTS          "
PRINT
PRINT "   TJ      UJ     DELTAP     JI      JT     HEAT     WORK     TOTAL
EQUV."
PRINT "  DEG.C   M/S     KPA      KG/H    KG/H    KJ/KG    KJ/KG    KJ/KG
KG/KG."
PRINT
FOR ROW% = 1 TO LR%
PRINT USING "#####.##"; RESULTST(1, ROW%); RESULTST(2, ROW%),
RESULTST(3, ROW%), RESULTST(4, ROW%), RESULTST(5, ROW%), RESULTST(6,
ROW%), RESULTST(7, ROW%), RESULTST(8, ROW%), RESULTST(9, ROW%)

NEXT ROW%



'     RESULTS EXPORT SECTION


OPEN "C:\JFBOND\SWIFT\CYCT.PRN" FOR OUTPUT AS #1
```

```
FOR ROW% = 1 TO LR%
PRINT #1, RESULTST(1, ROW%); RESULTST(2, ROW%); RESULTST(3, ROW%);
RESULTST(4, ROW%); RESULTST(5, ROW%); RESULTST(6, ROW%); RESULTST(7,
ROW%); RESULTST(8, ROW%); RESULTST(9, ROW%)

NEXT ROW%

CLOSE #1


'    C3- PURE IMPINGEMENT DRYING WITH OPEN-CYCLE HEAT PUMP (LUTHI'S FIRST
'    CYCLE).



'    SEQUENCE OF CALCULATIONS:


'       -JET MASS FLOW RATE AND VELOCITY
'       -INITIAL MOISTURE CONTENT FOR IMPINGEMENT STEAM DRYING
'       -AVERAGE IMPINGEMENT DRYING RATE
'       -OUTLET TEMPERATURE TE
'       -DRYER PRESSURE DROP AND FAN EXHAUST PRESSURE PF
'       -FAN WORK WF
'       -COMPRESSOR WORK WC
'       -TOTAL WATER REMOVAL RATE JT
'       -HEAT CONSUMPTION QI
'       -SPECIFIC VALUES:   -QI/JT
'                           -W/JT
'                           -TOTAL ENERGY ET/JT
'                           -TOTAL EQUIVALENT ENERGY EE/JT
'


'    NOTE: THE IMPINGEMENT DRYER AREA IS TAKEN TO BE 1 SQUARE METER
'    THIS SIMPLIFIES CALCULATIONS, AS JI = RI


ROW% = 1
COLUMN% = 1


'    NOTE: FOR THIS CYCLE, XII MUST BE DETERMINED ITERATIVELY
'    BECAUSE OF THE COUPLING BETWEEN IMPINGING JET MASS FLOW
'    RATE AND HEAT EXCHANGER OUTLET STATE.


XII = XIC                          'INITIAL GUESS FOR XII


FOR TJ = TJLOL TO TJHIL STEP TJSTL

FOR REJ = 200 TO 10000 STEP 200
```

```
'        JET MASS FLOW RATE (KG/H) AND VELOCITY (M/S)


MJ = 3600 * F * MU(TJ) * REJ / D
UJ = (MU(TJ) * REJ) / (SDEN(TJ) * D)


'        INITIAL MOISTURE CONTENT FOR IMPINGEMENT STEAM DRYING
'        AND AVERAGE IMPINGEMENT DRYING RATE (KG/M2-H)


RATECALCL:

RC = 3.6 * CON(TJ) * (((TJ + 273.2) / (TB + 273.2)) ^ -.77) * (FGEO / D)
* (REJ ^ .66667) * LOG(1 + (CP((TJ + TB) / 2) * (TJ - TB) / DHV)) /
CP((TJ + TB) / 2)
XC = .373 * (RC ^ .265)
M = 3.028 * (RC ^ .495) * (B ^ .198)


RF = RC + 3.028 * (RC ^ .495) * (B ^ .198) * (XF - .373 * (RC ^ .265))
IF (RF <= 0) THEN GOTO REJINCL            'PROVISION FOR RF>0

IF (XII > XC) THEN RI = RIC(M, XII, XF, RC, XC) ELSE RI = RIF(M, XII,
XF, RC, XC)
JI = RI
IF (RI < RILOL) THEN GOTO REJINCL
IF (RI > RIHIL) THEN GOTO TJINCL



'        OUTLET TEMPERATURE TE (DEG. C)


ALPHA = (RI * D) / (3600 * F * MU(TJ) * REJ)
TE = (1 / (1 + ALPHA)) * (TJ + ALPHA * (TB - (DHV / CP((TJ + TB) / 2))))



'        FAN EXHAUST PRESSURE PF (KPA ABS.)


DELTAP = .0000005 * ((MU(TJ) / (CD * D)) ^ 2) * RS * (TJ + 273.2) * (REJ
^ 2) / PATM
PF = PATM + DELTAP


'        FAN WORK WF (KJ/H)


WF = (MJ * CP(TE) * (TE + 273.2) / ETAF) * ((PF / PATM) ^ .25 - 1)
```

```
'     COMPRESSOR WORK WC (KJ/H)


WC = JI * CP(TE) * ((TE + 273.2) / ETAC) * ((PSAT(TJ) / PATM) ^ .25 - 1)




'     TOTAL WATER REMOVAL RATE JT (KG/H)


HT = ((WF + WC - (MJ * CP((TJ + TE) / 2) * (TJ - TE))) / JI) + (DHV +
CP((TB + TE) / 2) * (TE - TB))
QUAL = (HT - (CL * (TSATP(PC) - TB))) / DHV
JT = JI * (1 + QUAL / KAPPA)




'     ITERATION OF XII


IF (((XF + (JT / JI) * (XII - XF)) - XIC) > .01) THEN
XII = XII - .001
IF (XII > (2 * XF)) GOTO RATECALCL ELSE GOTO TJINCL
END IF

IF (((XF + (JT / JI) * (XII - XF)) - XIC) < -.01) THEN
XII = XII + .001
IF (XII > (2 * XF)) GOTO RATECALCL ELSE GOTO TJINCL
END IF




'     SPECIFIC HEAT (KJ/KG), WORK (KJ/KG), TOTAL (KJ/KG) AND EQUIVALENT
'     (KG/KG) ENERGY CONSUMPTION


RESULTSL(1, ROW%) = TJ
RESULTSL(2, ROW%) = UJ
RESULTSL(3, ROW%) = DELTAP
RESULTSL(4, ROW%) = JI
RESULTSL(5, ROW%) = JT
RESULTSL(6, ROW%) = WF / JT
RESULTSL(7, ROW%) = WC / JT
RESULTSL(8, ROW%) = EPSILON * (WF + WC) / (JT * DHV)
RESULTSL(9, ROW%) = QUAL




ROW% = ROW% + 1

IF (QUAL > 1) THEN GOTO TJINCL              'PROVISION FOR QUALITY < 1
```

```
REJINCL:
NEXT REJ

TJINCL:
NEXT TJ

LR% = ROW% - 1


'      RESULTS PRINTING SECTION


CLS
PRINT "                              RESULTS          "
PRINT
PRINT "    TJ      UJ     DELTAP      JI     JT    WF/JT    WC/JT      EQUV.
QUALITY"
PRINT
FOR ROW% = 1 TO LR%
PRINT  ;  USING  "#####.##";  RESULTSL(1,  ROW%);  RESULTSL(2,  ROW%);
RESULTSL(3,  ROW%);  RESULTSL(4,  ROW%);  RESULTSL(5,  ROW%);  RESULTSL(6,
ROW%); RESULTSL(7, ROW%), RESULTSL(8, ROW%), RESULTSL(9, ROW%)

NEXT ROW%


'      RESULTS EXPORT SECTION


OPEN "C:\JFBOND\SWIFT\CYCL.PRN" FOR OUTPUT AS #1

FOR ROW% = 1 TO LR%

PRINT  #1,  RESULTSL(1,  ROW%);  RESULTSL(2,  ROW%);  RESULTSL(3,  ROW%);
RESULTSL(4,  ROW%);  RESULTSL(5,  ROW%);  RESULTSL(6,  ROW%);  RESULTSL(7,
ROW%); RESULTSL(8, ROW%); RESULTSL(9, ROW%)

NEXT ROW%
CLOSE #1

END


FUNCTION RIC (M, XII, XF, RC, XC)


'      THIS FUNCTION RETURNS THE AVERAGE IMPINGEMENT DRYING RATE, KG/M2-H,
'      FOR DRYING BEGINNING IN THE CONSTANT RATE PERIOD AND ENDING WITHIN
'      THE FALLING RATE PERIOD. THE INPUTS ARE THE SLOPE OF THE FALLING
'      RATE,  THE  INITIAL  AND  FINAL  MOISTURE  CONTENTS  FOR  IMPINGEMENT
'      DRYING, THE CONSTANT DRYING RATE AND THE CRITICAL MOISTURE CONTENT.
'
```

```
VALUE = (XII - XF) / (((XII - XC) / RC) - (1 / M) * LOG((1 + (M / RC) *
(XF - XC))))
RIC = VALUE

END FUNCTION

FUNCTION RIF (M, XII, XF, RC, XC)


'       THIS FUNCTION RETURNS THE AVERAGE IMPINGEMENT DRYING RATE, KG/M2-H,
'       FOR DRYING ENTIRELY WITHIN THE FALLING RATE PERIOD. THE INPUTS ARE
'       THE SLOPE OF THE FALLING RATE, THE INITIAL AND FINAL MOISTURE CON-
'       TENTS FOR IMPINGEMENT DRYING, THE CONSTANT DRYING RATE AND THE CRI-
'       TICAL MOISTURE CONTENT.


VALUE = (-M * (XII - XF)) / LOG((1 + (M / RC) * (XF - XC)) / (1 + (M /
RC) * (XII - XC)))
RIF = VALUE

END FUNCTION



'       STEAM PROPERTY FUNCTION DEFINITIONS ARE GIVEN IN APPENDIX 4
```